



HAL
open science

Alternatives to “native human islets” for research in vitro and in vivo: pseudo-islets and pancreatic endocrine cells from pluripotent stem cells – the role of progerin in differentiation and maturation

Alix Vaissié

► **To cite this version:**

Alix Vaissié. Alternatives to “native human islets” for research in vitro and in vivo: pseudo-islets and pancreatic endocrine cells from pluripotent stem cells – the role of progerin in differentiation and maturation. Human health and pathology. Université de Lille, 2019. English. NNT : 2019LILUS035 . tel-03934961

HAL Id: tel-03934961

<https://theses.hal.science/tel-03934961v1>

Submitted on 11 Jan 2023

HAL is a multi-disciplinary open access archive for the deposit and dissemination of scientific research documents, whether they are published or not. The documents may come from teaching and research institutions in France or abroad, or from public or private research centers.

L'archive ouverte pluridisciplinaire **HAL**, est destinée au dépôt et à la diffusion de documents scientifiques de niveau recherche, publiés ou non, émanant des établissements d'enseignement et de recherche français ou étrangers, des laboratoires publics ou privés.



Université
de Lille

Ecole Doctorale Biologie-Santé (446)

Laboratoire U1190 – Recherche Translationnelle sur le Diabète

**Alternatives to “native human islets” for research *in vitro* and *in vivo*:
pseudo-islets and pancreatic endocrine cells from pluripotent stem cells – the
role of progerin in differentiation and maturation**

Par Alix Vaissié

Thèse de doctorat de Biologie Cellulaire

Présentée et soutenue publiquement le 17 décembre 2019

Devant un jury composé de :

Prof. Ibrahim Yakoub-Agha	Université de Lille – CHU de Lille	Président du jury
Dr. Valérie Schreiber	CNRS - Université de Strasbourg	Rapporteur
Dr. Xavier Nissan	I-STEM - Université Paris Saclay	Rapporteur
Dr. Maria Cristina Nostro	McEwen Stem Cell Institute - University of Toronto	Examineur
Dr. Olivier Pluquet	Institut Pasteur de Lille – Université de Lille	Examineur
Prof. Julie Kerr-Conte	Université de Lille	Directeur de thèse

Remerciements

A Madame le Docteur Valérie Schreiber,

Vous me faites l'honneur d'accepter de faire partie du Jury de cette thèse. Soyez assurée de mon profond respect et de ma reconnaissance

A Monsieur le Docteur Xavier Nissan,

Merci d'avoir accepté de juger ce travail et de nous avoir fait confiance avec votre matériel précieux et vos conseils. Veuillez accepter mes sincères remerciements et soyez assuré de mon profond respect.

A Monsieur le Docteur Olivier Pluquet,

Vous me faites l'honneur de juger ce travail. Veuillez recevoir mes remerciements pour votre disponibilité et vos conseils. Soyez assuré de ma profonde gratitude.

To Doctor Maria Cristina Nostro,

My warmest thanks for judging this thesis. I would like to express you my gratitude for your support and encouragement throughout the course of my PhD and also for all the time you had for me during my stay in Toronto.

A Madame le Professeur Julie Kerr-Conte,

Je vous remercie d'avoir dirigé ce travail. Merci pour vos encouragements et votre soutien durant cette thèse. Soyez assurée de ma plus profonde gratitude et de tout mon respect.

Au terme de ce travail, je tiens également à remercier :

L'Agence Régionale de Santé, EGID et le CHU de Lille d'avoir financé mes années de thèse et ainsi de m'avoir permis de réaliser ce projet.

L'équipe du laboratoire U1190 : le Professeur François Pattou, directeur du laboratoire U1190, de m'y avoir accueillie. Un grand merci à Julien Thevenet, Nathalie Dellaleau, Gianni Pasquetti, Anaïs Coddeville, Valéry Gmyr, Matthias Huyghe et Ericka Moerman pour votre aide dans la réalisation de différents protocoles et à Amanda Elledge pour l'anglais. Et tous les autres membres pour votre soutien et gentillesse. Merci à mes deux colocataires de bureau : Lorea Zubiaga et Mikael Chetboun de m'avoir supportée pendant la rédaction de ce manuscrit. Merci à Chiara Saponaro pour ton aide et ton soutien tout au long de cette thèse. Asante sana simba Kussi.

The Nostro Lab members: a huge thanks to Farida Sarangi for everything you taught me, to Frankie Poon for the flow cytometry experiments and methodology to interpret them, to Yasaman Aghazadeh and Adriana Migliorini for your help and support. All the lab members for your welcome and kindness, thanks to you it was a very pleasant and memorable experience.

Mes amis : nul besoin de vous citer. Merci d'avoir été toujours présents et désolée de l'avoir été un peu moins ces derniers temps. Promis, on se rattrapera ! Mention spéciale pour le dernier arrivé dans la bande, Auguste.

Mes parents : pour votre amour et votre soutien indéfectible tout au long de ces années.

Mon frère : pour toujours savoir quoi dire quand ça ne va pas, merci d'avoir toujours été présent.

Mes grands-parents : je vous serai éternellement reconnaissante pour votre présence et votre soutien de chaque instant.

Table of contents

Abstract	9
Résumé	11
Abbreviation list	13
Figures list	17
Table list	21
Chapter 1: Introduction	23
1. Background	25
2. Limitation of the use of human islets for research	31
3. Pseudo-islets	32
4. Embryogenesis and early pancreas development	38
5. Stem cells & pluripotent stem cells	42
1) Embryonic stem cell (ESC)	43
2) Induced pluripotent stem cells	45
3) Pluripotent stem cell applications	49
6. Stem-cell derived pancreatic endocrine cells	53
7. Factors associated with the maturation of pancreatic β cells	58
8. Directing aging using progerin	60
9. Hutchinson-Gilford Progeria Syndrome	62
10. Objectives	66
Chapter 2: Materiel & Methods	69
1. Materials	71
1) Human pluripotent cell lines	71
2) Human islets	71

3) Human fibroblasts	72
4) Cell culture	72
5) Molecular biology	74
6) Immunohistochemistry	75
7) Flow cytometry (FCM)	76
8) Fluorescence activated cell sorting (FACS)	77
9) Perifusion	77
10) Mice	77
11) ELISA	77
12) Software	77
13) Microscopes and devices	78
2. Methods	78
1. Cell culture	78
2. Perifusion of human islets	82
3. Molecular biology	82
4. Immunohistochemistry	84
5. Flow Cytometry and Fluorescence Activated Cell Separation	84
6. Mice	86
7. ELISA	87
8. Statistics	87
Chapter 3: Pseudo-islets	89
1. In vitro	92
2. In vivo	94
Chapter 4: Human pluripotent stem cell differentiation - Reproduction and optimization of published protocols	99
1. First generation differentiation protocol according to the Odorico 2012 protocol	102

2.	Future strategies for the generation of pancreatic progenitors with iPS DF19.9 cells using second generation protocols following cancellation of H1 authorization.....	107
1)	Making definitive endoderm with the Rezaia 2014 protocol and SD Kit (stage 1 cells)	108
2)	Making pancreatic progenitor using the Rezaia 2014 protocol and SD Kit (stage 4 cells)	111
3)	Making maturing β -like cell using the Rezaia 2014 protocol and SD Kit (stage 7 cells)	114
3.	H1 new authorization – Dec 2017.....	117
1)	Optimization of definitive endoderm differentiation	118
2)	Optimization of pancreatic progenitor differentiation	119
4.	iPS Progeria.....	124
1)	Optimization of definitive endoderm differentiation.	125
2)	Optimization of pancreatic progenitor differentiation	130
Chapter 5: Using progerin to induce aging in cells derived from pluripotent stem cells.....		133
1.	Progerin expression during differentiation of pluripotent stem cells	137
2.	Progerin inducing maturation.....	139
3.	Progerin inducing aging	147
Chapter 6: Discussion.....		155
Chapter 7:General conclusion		167
Annexes		170
Bibliography		177

Abstract

Introduction: The use of human islets of Langerhans is the gold standard for research, both for physiological research and for the development of new therapeutic molecules for the treatment of type 2 diabetes. The demand of human islets for research projects is constantly growing however, the availability is limited and different islet preparations show significant variability between human pancreata.

Objectives: The main objective of this thesis was to propose an alternative to native human islets that can provide homogeneous and abundant pancreatic islets for research. To do this, we had two main objectives: 1) the production of controlled diameter pseudo-islets from human pancreata, and the evaluation of their function *in vitro* and *in vivo* compared to their native islet counterparts; 2) the optimization of the production of pancreatic endocrine cells from different pluripotent stem cell lines and evaluation of the impact of progerin on the differentiation and maturation of the cells produced. Pluripotent stem cells from healthy donors (H1, WiCell) and from patients affected with accelerated aging disease Progeria (HGPS, iStem).

Material and Methods: The pseudo-islets were formed in clinical islet medium (CMRL 1066 human albumin, insulin) 7 days using the 5D Sphericalplate (Kugelmeiers) and compared to the native islets D1 (day 1) and D7 (day 7) from the same donor.

The differentiation of pluripotent stem cells (iPS DF19.9, H1 and iPS HGPS cells) was optimized using different protocols: the Rezia protocol, the SD Kit (StemCell Technologies) and the Nostro protocol. For *in vitro* maturation gene expression among different cell lines was evaluated by qPCR. Protein expression was assessed by immunofluorescence technique and Flow cytometry analysis (EGID).

For *in vivo* maturation, after transplantation under the kidney capsule of immunodeficient mice, blood glucose and human c-peptide measurements were assessed as well as metabolic test such as IPGTT were performed.

Results: The pseudo-islets (n=4) generated in clinical islet medium secreted significantly less insulin *in vitro* than the native islets at D1 but with no significant difference from the native islets at D7. In both groups at D7, a significant decrease in intracellular insulin was observed compared

to native islets at D1. *In vivo*, the native islets at D1 secrete significantly more human c-peptide than the native islets at D7, while the difference is not significant between the native islets at D1 and the pseudo-islets at D7. In addition, morphometric analysis of the grafts revealed that the pseudo-islets tend to have more glucagon positive cells than the other two groups.

Optimization of the differentiation of pluripotent stem cells allowed us to obtain more than 95% endoderm for H1 cells and 80% for iPS HGPS cells. For both lines, we generated 95% of pancreatic progenitor cells. The comparison of maturation genes revealed that progerin lead to a slight increase of cell maturation in the iPS HGPS group compared to H1 cells. However, no differences in *in vivo* function was observed. Age-related markers (53BP1, IGF1r, p16 and yH2AX) which validated in a pancreas from an elderly donor and an insulinoma. We identified yH2AX after 6 months transplantation of H1-grafts in endocrine and non-endocrine cells, while the expression in iPS HGPS-grafts appeared in the majority of cells, which had various shape of nuclei

Conclusion: This work provided positive results in terms of functional pseudo-islets and stem cells derived pancreatic endocrine cells. However, they remain preliminary and further studies must be conducted to provide realistic alternatives to native human islets for research.

Résumé

Introduction : L'utilisation des îlots humains de Langerhans est la référence pour la recherche, tant physiologique que pour le développement de nouvelles molécules thérapeutiques pour le traitement du diabète de type 2. La demande d'îlots de Langerhans humains pour des projets de recherche est en constante augmentation, cependant, la disponibilité est limitée et les différentes préparations d'îlots de Langerhans révèlent une grande variabilité entre elles.

Objectifs : L'objectif principal de cette thèse était de proposer une alternative aux îlots de Langerhans humains natifs qui permettrait d'obtenir des îlots pancréatiques homogènes et en quantité abondante pour les projets de recherche.

Pour ce faire, nous avons deux objectifs principaux : 1) la production de pseudo-îlots de diamètre contrôlé à partir de pancréas humain, et l'évaluation de leur fonction *in vitro* et *in vivo* par rapport à leurs équivalents îlots natifs ; 2) l'optimisation de la production de cellules endocrines pancréatiques à partir de différentes lignées de cellules souches pluripotentes et l'évaluation des effets de la progérine sur la différenciation et la maturation des cellules produites. Les cellules souches pluripotentes utilisées provenaient de donneurs sains (H1, WiCell) et de patients atteints de Progeria (HGPS, iStem).

Matériel et méthodes : Les pseudo-îlots ont été formés dans un milieu d'îlots clinique (CMRL 1066 albumine humaine, insuline) pendant 7 jours en utilisant les Sphericalplate 5D (Kulgelmeiers) et comparés aux îlots natifs J1 (jour 1) et J7 (jour 7) du même donneur.

La différenciation des cellules souches pluripotentes (cellules iPS DF19.9, H1 et iPS HGPS) a été optimisée par différents protocoles : le protocole ReZania, le SD Kit (StemCell Technologies) et le protocole Nostro. L'expression des gènes de maturation *in vitro* entre différentes lignées cellulaires a été évaluée par qPCR. L'expression des protéines a été évaluée par immunofluorescence et par cytométrie en flux (plateforme EGID).

Pour la maturation *in vivo*, après la transplantation sous la capsule rénale de souris immunodéficientes, des mesures de glycémie et de c-peptide humain ont été effectuées, ainsi que des tests métaboliques comme l'ipGTT.

Résultats : Les pseudo-îlots (n=4) générés ont sécrété significativement moins d'insuline *in vitro* que les îlots natifs à J1 mais sans différence significative avec les îlots natifs à J7. Dans les deux groupes à J7, on a observé une diminution significative de l'insuline intracellulaire comparativement aux îlots natifs à J1. *In vivo*, les îlots natifs à J1 sécrètent significativement plus de c-peptide humain que les îlots natifs à J7, alors que la différence n'est pas significative entre les îlots natifs à J1 et les pseudo-îlots à J7. De plus, l'analyse morphométrique des greffons a révélé que les pseudo-îlots ont tendance à avoir plus de cellules glucagon-positives que les deux autres groupes.

L'optimisation de la différenciation des cellules souches pluripotentes a permis d'obtenir plus de 95% d'endoderme pour les cellules H1 et 80% pour les cellules iPS HGPS. Pour les deux lignées, nous avons généré 95 % de progéniteurs pancréatiques. La comparaison des gènes de maturation a révélé que la progérine conduisait à une légère augmentation de la maturation cellulaire dans le groupe iPS HGPS par rapport aux cellules H1. Des marqueurs liés à l'âge (53BP1, IGF1r et γ H2AX) ont été validés dans un pancréas provenant d'un donneur âgé et un insulinome. Cependant, aucune différence de la fonctionnalité *in vivo* n'a été observée. Six mois post transplantation, nous avons identifié γ H2AX dans des cellules endocrines et non endocrine des greffons H1 alors que dans les greffons HGPS, nous l'avons observé dans une plus vaste proportion de cellules présentant différentes formes de noyaux.

Conclusion : Ces travaux ont donné des résultats positifs : pseudo-îlots fonctionnels et de cellules souches dérivées de cellules endocrines pancréatiques. Toutefois, ces travaux demeurent préliminaires et d'autres études doivent être menées pour fournir des alternatives réalistes aux îlots de Langerhans humains natifs à des fins de recherche.

Abbreviation list

3D	3 Dimensions
53BP1	tumor suppressor p53-binding protein
yH2AX	Histone A family member X
ABM	Agence de la Biomédecine
BMI	Body Mass Index
BMP	Bone Morphogeneic Protein
BSA	Bovin Serum Albumin
Chromo A	Chromogranin A
CHGA	Chromogranin A
CK19	Cytokeratin 19
CMRL media	Connaught Medical Research Laboratories
CXCR4	C-X-C chemokine receptor type 4
D1	Day 1
D7	Day 7
DMEM	Dulbecco's Modified Eagle Medium
DMEM/F-12	Dulbecco's Modified Eagle Medium: Nutrient F-12
DMSO	Dimethyl sulfoxide
EDTA	Ethylenediaminetetraacetic acid
EGF	Epidermal Growth Factor
FACS	Fluorescent Activated Cell sorting
FGF	Fibroblast Growth Facor
FOXA2	Forkhead box protein A2 also known as Hepatocyte nuclear factor 3a (HNF3a)
FSC	Forward Scatter
G3	Glucose 3mM
G15	Glucose 15mM
GCG	Glucagon
H1	Human embryonic stem cell H1
HbA1c	Glycated Hemoglobin

hESC	human Embryonic Stem Cell
HEPES	(4-(2-hydroxyethyl)-1-piperazineethanesulfonic acid
HGPS	Hutchinson Gilford Progeria Syndrom
HAS	Human Serum Albumine
IEQ	Islet Equivalent
IGF1r	Insulin-like Growth Factor 1
IMDM	Iscove's Modified Dulbecco's Medium
INS	Insulin
ipGTT	intraperitoneal Glucose Tolerance Test
iPS	induced Pluripotent Stem (cell)
Klf4	Krüppel-like transcription factor 4
LMNA	Lamin A
LAM A	Lamin A
LAM C	Lamin C
LAM A/C	Lamin A/C
MafA	Musculoaponeurotic fibrosarcoma oncogene family A
MafB	Musculoaponeurotic fibrosarcoma oncogene family B
MEOX2/GAX	Mesenchyme Homeobox 2/ Growth Arrest-specific Homeobox
MTG	1-Thioglycerol
NeuroD1	Neurogenic differentiation 1
NGN3	Neurogenin 3
NKX6.1	Homeobox protein NKX6.1
Oct3/4	Octamer-binding transcription factor
PDX1	Pancreatic and Duodenal Homeobox 1
PMO	Phosphorodiamidate Morpholino Oligomers
RA	Retinoic Acid
S4	Stage 4
S7	Stage 7
SD Kit	STEMDiff kit (STEMCell Tehnologies)
SOPF	Specific and Opportunistic Pathogen Free
SOX2	SRY-box 2

SSC	Side Scatter
T1D	Type 1 Diabetes
T2D	Type 2 Diabetes
T3	Triiodothyronin
TGFb	Transforming Growth Factor beta
UW	University of Wisconsin
U of T	University of Toronto

Figures list

- Figure 1: Blood glucose (mg/dL and mM) and insulin levels (μ UI/mL and pM) during 24 hours from 14 healthy adult individuals
- Figure 2: Glycated hemoglobin (percent) between patients treated by conventional or intensive insulin therapy
- Figure 3: Continuous glucose monitoring for 5 consecutive days of a child with T1D before and after treatment by ‘artificial pancreas’
- Figure 4: Graphical overview showing the all relevant steps from islet isolation from the donor until the islet transplantation into the recipient
- Figure 5: Representative image of a human pancreatic islets from one donor stained with dithizone to assess the purity of the preparation
- Figure 6: Continuous glucose monitoring of a T1D patient before and after islet transplantation
- Figure 7: Graph depicts the loss of β cell mass from donor islet isolation until the islets are grafted into the recipient
- Figure 8: A dynamic perfusion system was used to determine insulin secretion of human islet preparations in response to changing glucose concentrations (3mM, 15mM, 3mM)
- Figure 9: Schematic representation of the 3D Select TM process to generate standardized islet microtissues
- Figure 10: Glucose-stimulated insulin secretion (GSIS) profile and insulin content of intact native islets compared to pseudo-islets.
- Figure 11: Islets and pseudo-islets architecture and cellular composition.
- Figure 12: Pancreatic cell lineage determination during pancreas organogenesis
- Figure 13: Immunocytochemical staining of the endocrine marker synaptophysin (in black) on a fetal pancreas at 16 weeks of gestation shows single cell or small endocrine cell aggregates in direct contact with pancreatic duct (D)
- Figure 14: Similarities and differences during pancreas morphogenesis in mouse (top) and Human (bottom).
- Figure 15: Sources of pluripotent stem cells: pluripotent stem cells are hallmarked by self-renewal capacity and differentiation in cells of all the three germ layers (ectoderm, mesoderm, endoderm)
- Figure 16: Representative image of an embryonic stem cell (H1) cultured in m-TeSR.
- Figure 17: Possible application for pluripotent stem cells in research and for clinical treatment strategy
- Figure 18: (A) Insulin and glucagon polyhormonal cells, pluripotent stem cell derived insulin and glucagon positive cells are ARX positive (B) and NKX6.1 negative (C).....
- Figure 19: Overview of lineage segregation in human pancreatic development.....
- Figure 20: Overview of human pluripotent stem cells (hPSC) step-wise differentiation towards β cells. Different differentiation stages from pluripotent stem cell towards stage 7.

Figure 21: Inducing cellular aging in hPSC-derived lineages

Figure 22: Age-associated changes induced by progerin overexpression in iPSC-mDA Neurons derived from young and old donors

Figure 23: Schematic overview of the biogenesis of lamin A and progerin

Figure 24: Representative immunofluorescent image of HGPS cells: progerin (red) and human DNA (blue) showing nuclei deformation with high level of progerin (left) compared to low level of progerin (right)

Figure 25: Similarities and differences between HGPS (left) and physiological aging

Figure 26: Strategy gating flowchart.....

Figure 27: Glycemia, human c-peptide and human c-peptide divided by glycemia during glucose challenge (3g/kg) in normoglycemic nude mice with a human islet transplant under the kidney capsule.....

Figure 28: Overview of pseudo-islets experiments.....

Figure 29: Dynamic insulin secretion by perfusion in response to glucose variations.....

Figure 30: Insulin content of native human islets at D1 and D7 and pseudo-islets at D7

Figure 31: In vivo function of D1 native human islets, D7 native islets and pseudo-islets.

Figure 32: Morphometric analysis of grafted native human islets D1, D7 and pseudo-islets.....

Figure 33: Correlation of glucose-stimulated insulin secretion between native human islets and pseudo-islets

Figure 34: Timeline of stem cell differentiation at U1190, Lille.....

Figure 35: Overview of applied differentiation protocols from 2012 to 2015.....

Figure 36: Phenotype of H1 cells stage 1-4 during differentiation with the Odorico protocol.....

Figure 37: In vivo evaluation of engrafted stage 4-H1 cells differentiated according to the Odorico protocol.....

Figure 38: Overview of differentiation protocol applied with iPS DF19.9 cells.....

Figure 39: CXCR4 and FOXA2 gene and protein expression from iPS DF19.9-derived cells at differentiation stage 1 with SD Kit compared to the Rezanja protocol.....

Figure 40: Stage 4 cells generated using the Rezanja protocol or SD Kit with iPS DF19.9 cells – in vitro evaluation.....

Figure 41: Stage 4 cells generated with iPS DF19.9 cells using SD Kit - In vivo evaluation.....

Figure 42: iPS DF19.9 cells at stage 7 using SD Kit + Rezanja or Rezanja alone - in vitro evaluation.....

Figure 43: Stage 7 cells generated using the Rezanja protocol or SD Kit with iPS DF19.9 cells engrafted under the kidney capsule – in vivo evaluation.....

Figure 44: Overview of applied differentiation protocols with H1 cells.....

Figure 45: Stage 1 cells generated using SD Kit with H1 cells optimized in Toronto.....

Figure 46: Stage 4 cells generated using SD Kit with H1 cells – FACS quantification of pancreatic progenitors.....

Figure 47: Stage 4 cells generated using the Nostro protocol with H1 cells – FACS quantification of endoderm formation.

Figure 48: Stage 4 cells generated by using the Nostro protocol with H1 cells – in vitro evaluation.

Figure 49: In vivo evaluation of stage 4 cells generated with H1 cells using SD Kit and the Nostro protocol over 4 months (n=8 mice).

Figure 50: Dynamic GSIS by perfusion of explanted H1-derived S4 cells grafts, 6 months after transplant (black) and an explant human islet graft (control, red).

Figure 52: Stage 1 cells generated using SD Kit or the Rezanja protocol with patient specific iPS HGPS cells – Definitive endoderm quantification.

Figure 53: Stage 1 cells generated using the Rezanja protocol with patient specific iPS HGPS cells – FACS sorting on CXCR4/C-Kit.

Figure 54: Stage 1 cells generated using a SD Kit (Nostro adaptation) with patient specific iPS HGPS AG1972– Definitive endoderm quantification.

Figure 55: Stage 4 cells generated using the Nostro protocol with patient specific iPS HGPS AG1972 cells – FACS quantification of pancreatic progenitor.

Figure 56: Stage 4 cells generated using the Nostro protocol with patient specific iPS HGPS AG1972- in vitro evaluation.

Figure 57: Fasting human c-peptide levels (ng/L) measured over 4 months (n=8 mice).

Figure 58: Overview of the objectives of using progeria to induce aging in cells derived from pluripotent cells.

Figure 59: Gene expression profile of Progerin, Lamin A and Lamin C was determined in fibroblasts from patients with HGPS-Progeria (Fibro HGPS – AG1972), undifferentiated iPS HGPS cells (dedifferentiated from Fibro HGPS – AG1972), S4 cells generated from iPS HGPS or H1 cells and human islets by Taqman qPCR.

Figure 60: MAFa, MAFb, NeuroD1 and Urocortin 3 expression in iPS HGPS (AG1972) and H1- derived cells at stage 4 and human islets.

Figure 61: Human c-peptide secretion of differentiated H1 or iPS HGPS cells 4 months after transplantation.

Figure 62: Representative image of a trichrome staining showing duct (top) and endocrine like structure (bottom) in human pancreas (left panel) and iPS HGPS graft 5 months post-transplantation (right panel). ..

Figure 63: Immunofluorescent staining of graft of iPS HGPS-derived stage 4 cells, harvested 6 months after transplantation (Expt 68) for chromogranin A endocrine (Chromo A, red) and CK19 epithelium (green)

Figure 64: Immunofluorescent staining of graft of H1-derived stage 4 cells, harvested 6 months after transplantation (Expt 73) for chromogranin A (Chromo A, red) and DAPI (blue).....

Figure 65: Representative immunofluorescent image for progerin, lamin A and chromogranin A.....

Figure 66: Progerin (red), human nuclei (green) and DAPI (blue) staining in iPS HGPS graft versus H1 graft.

Figure 67: Representative immunofluorescent images for progerin in iPS HGPS-derived stage 4 cells graft, in a teratoma like structure harvested 6 months after transplantation (Expt 68).....

Figure 68: Validation of aging markers on 70-year-old pancreas (H1066) and an insulinoma. 53BP1, yH2AX, IGF1r (green) were co-stained with pan-endocrine marker chromogranin A (red) in the pancreas of a 70-year-old donor (H1066) and in an insulinoma (benign tumor composed of immature cells).....

Figure 69: Immunofluorescent staining of graft of H1-derived stage 4 cells, harvested 6 months after transplantation (Expt 73) for chromogranin A (Chromo A, red) and yH2AX (green).....

Figure 70: Immunofluorescent staining of graft of iPS HGPS-derived stage 4 cells, harvested 6 months after transplantation (Expt 68) for chromogranin A (Chromo A, red) and yH2AX (green).....

Table list

Table 1: Number of islet isolation, number of IEQ used for internal and external research (U1190 – unpublished data)	30
Table 2: Different methodology and timing to obtain pseudo-islets from pig, dog, rodent and human native islets.	33
Table 3: Advantages and limitations of native human β -cell, stem cell-derived β -cell and EndoC- β H-cell (Scharfmann et al. 2019).	37
Table 4: Advantages and disadvantages of published delivery methods used for reprogramming (Brouwer et al. 2016; Takahashi and Yamanaka 2016; Karagiannis et al. 2019).	46
Table 5: Evaluation of reprogramming factors capable of reprogramming human cells. EMT: epithelial to mesenchymal transition. MET: mesenchymal to epithelial transition. (Brouwer et al. 2016; Omole and Fakoya 2018).	47
Table 6: Clinical trials with embryonic stem cell-derived cells	52
Table 7: Clinical trials with induced pluripotent stem cell-derived cells	52
Table 8: Characteristics of published pancreatic β -like cell differentiation protocols.	57
Table 9: Islet donor characteristics for pseudo-islets experiments.	72
Table 10: Acronyms used in differentiation protocols	81
Table 11: Summary of optimized experiments with H1 and IPS HGPS cells	135

Chapter 1: Introduction

1. Background

The World Health Organization defines diabetes as a chronic disease that occurs when the pancreas does not secrete enough insulin or when the body is unable to effectively use the produced insulin. This leads to chronic fasting hyperglycemia ($\geq 7\text{mM}$) resulting in severe microvascular (retinopathy, neuropathy, nephropathy) and macrovascular complications (cardiovascular disorders). The management of diabetes and its complications represents therefore a considerable socioeconomic burden for society. Indeed, the International Diabetes federation has identified 425 million diabetics worldwide and estimates that there will be 629 million by 2045, representing a 48% increase in diabetes prevalence (Cho et al. 2018).

Blood glucose is tightly regulated (Figure 1) by the release of hormones by the pancreatic islets of Langerhans in a precise range of normal values (3,0 to 7,8 mM) throughout the day.

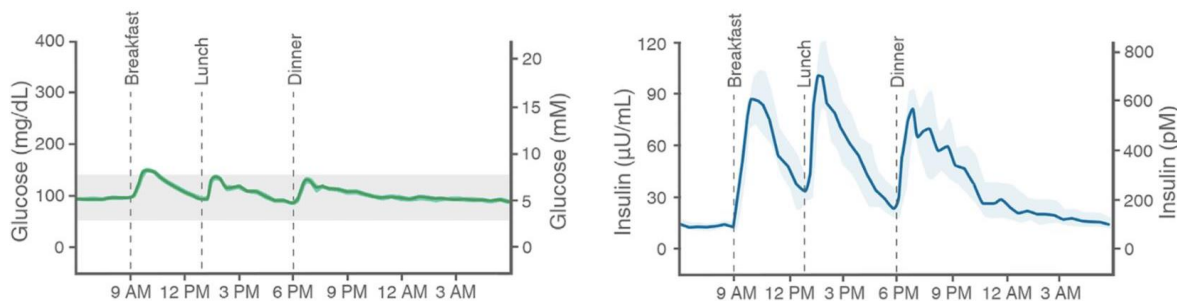


Figure 1: Blood glucose (mg/dL and mM) and insulin levels ($\mu\text{U/mL}$ and pM) during 24 hours from 14 healthy adult individuals. Lines represent the means and shading the SEM (Latres et al. 2019).

There are mainly two forms of diabetes, type 1 diabetes (T1D) and type 2 diabetes (T2D) that differ in their etiology. While T1D is based on autoimmune destruction of β cells causing an absolute insulin deficiency, T2D is characterized by progressive insulin secretion impairment and insulin resistance (Atkinson et al. 2011; Holman et al. 2015; You and Henneberg 2016; American Diabetes Association 2019). Since its discovery by F. Banting and C. Best in 1921 (Nobel Prize in Physiology or Medicine in 1923 to F. Banting & J. Macleod, University of Toronto), daily insulin injection remains the treatment for T1D. The exogenous supply of insulin mimics normal kinetics of insulin secretion during the day in order to maintain blood glucose levels in physiological values (Polonsky et al. 1988). Development of short- and long-acting analogues enable most of the patients to achieve this goal (Mathieu et al. 2017).

The US funded Diabetes Control and Complications Trials (DCCT) sought to determine if achieving near normal glucose levels would ameliorate the long-term complications (eye, kidneys, nerve disease) of diabetes. T1D patients (n=1441) were divided in two groups, ‘conventional’ (1 or 2 insulin injections per day) or ‘intensive’ (3 or more insulin injections per day) insulin regimen where patients achieved respectively a mean of 7.2% and 9.1% HbA1c which reflect glycemic equilibrium over 3 months. After 6.5 years follow-up, the risk of developing retinopathy, nephropathy, neuropathy and macrovascular complications was reduced by 76%, 34%, 69% and 34% respectively in the intensive group (Diabetes Control and Complications Trial Research Group et al. 1993). In a subsequent study the Epidemiology and Diabetes Interventions and Complications (EDIC) study 93% of patients in the DCCT study were followed over 30 years after training the patients in the conventional group how to better control their glycemia. Although both groups subsequently had similar (Figure 2) HbA1c levels of 8%, patients who originally had ‘intensive’ insulin therapy had a >30% reduced risk of complications (Diabetes Control and Complications Trial (DCCT)/Epidemiology of Diabetes Interventions and Complications (EDIC) Study Research Group 2016).

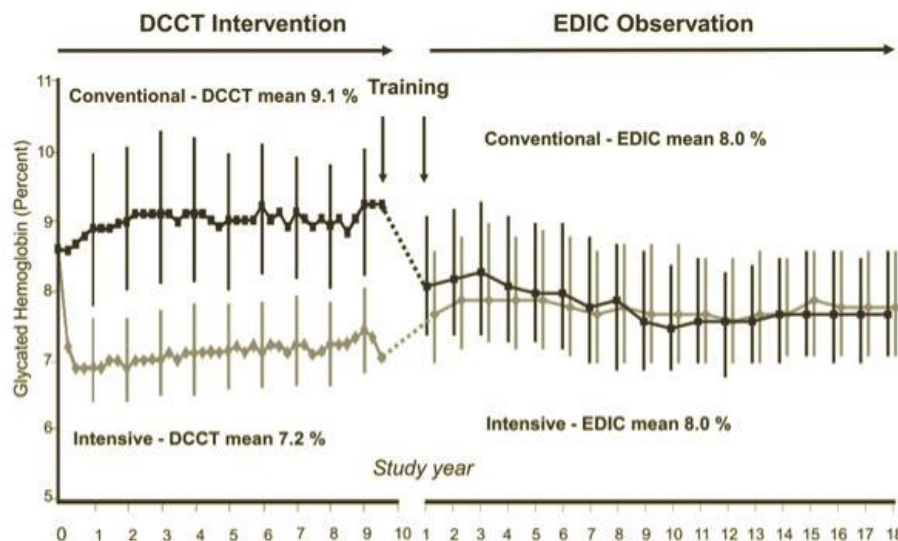


Figure 2: Glycated hemoglobin (percent) between patients treated by conventional or intensive insulin therapy (Nathan 2014).

This long-term effect on diabetes complications is attributed to the “metabolic memory” theory (Nathan et al. 2003, 2005; Holman et al. 2008). However, there are several side effects associated with the use of insulin, the most severe of which are severe hypoglycemia episodes, which require third party intervention and are life-threatening. In the DCCT study, severe hypoglycemia episodes

were 3 times more frequent in the ‘intensive’ insulin regimen group compared to ‘conventional’ therapy group (Diabetes Control and Complications Trial Research Group et al. 1993). Treatments achieving improved glycemic equilibrium like islet transplantation may have a long-term effect on diabetes complications.

‘Closed-loop system’ or ‘artificial pancreas’ are devices coupling insulin pump to a continuous glucose monitoring system (CGMS) in order to deliver insulin in response to measured glucose variations. Such devices improve glucose control as shown in Figure 3.

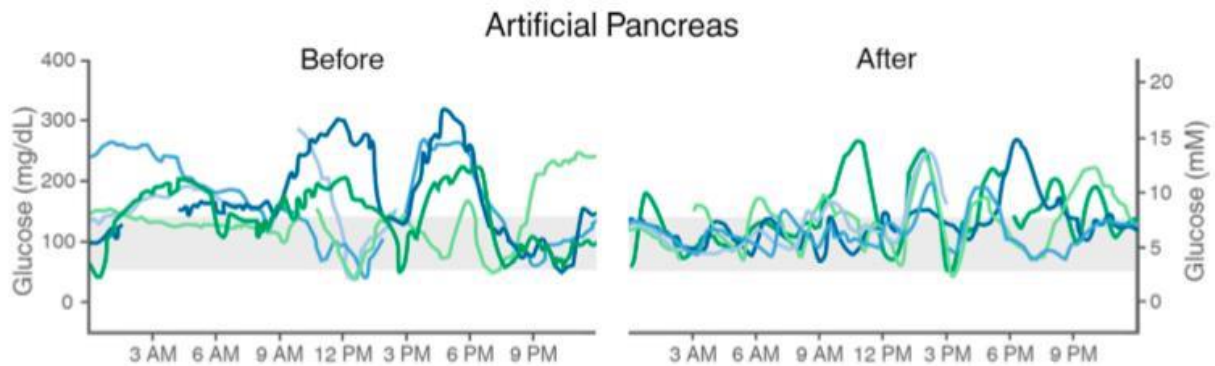


Figure 3: Continuous glucose monitoring for 5 consecutive days of a child with T1D before and after treatment by ‘artificial pancreas’ (Latres et al. 2019).

Next generation ‘artificial pancreas’ systems under evaluation are bi-hormonal (insulin and glucagon) systems, which also prevents hypoglycemic episodes by secreting glucagon in response to low blood glucose level. Beside its attractive treatment potential for T1D patients this technology has some limitations. Indeed, CGMS measures glucose from the interstitial fluid and not directly from the blood, there is, therefore, a lag time for the interstitial fluid glucose levels to reflect blood glucose levels. Lag time can vary from 5 to 10 minutes (Basu et al. 2013; Allen and Gupta 2019). Furthermore, such devices cost around 10 000 USD and some patients refuse to wear a device at all times.

Despite evident progress, about 1% of all T1D patients have difficulty in equilibrating their glycemia, even with modern devices, and suffer from severe debilitating hypoglycemic unawareness. In those cases, the benefit/risk ratio of transplantation and lifetime immunosuppressive treatment is in favor of β cell replacement therapy in the form of a pancreas transplantation, islet or β cell transplantation.

Pancreas transplantation is often done simultaneously (SPK) or after kidney (PAK) transplantation although it can be transplanted alone (PTA). Study at 10 years post-transplantation, reported more

than 80% (SPK) and 60% (PTA) insulin independence at 10 years (Gruessner and Gruessner 2012; Lombardo et al. 2017).

Islet transplantation is a less invasive validated treatment for severe forms of T1D. Islet transplantation can be performed alone or after kidney graft in T1D patients with severe hypoglycemic unawareness (Vantighem et al. 2019b). The Collaborative Islet Transplant Registry (CITR) reported 1 086 T1D recipients between 1999-2015 (10th annual CITR report 2017). Islet isolation (Figure 4) starts with the removal pancreas harvested from brain-deceased donors in France, or from cardiorespiratory-deceased donors in other countries. The pancreas is digested using an enzyme (collagenase) and a Ricordi digestion chamber. The endocrine and exocrine tissues are then separated and the islets are then purified (Figure 5). If the obtained islets meet the release criteria (number of islet equivalent (IEQ) > 200 000), they are then injected intraportally to the recipient via a mesenteric vein. The same T1D patient will need 2-3 islet preparation in order to reach the goal of 10000 IEQ/kg recipient bodyweight (Vantighem et al. 2019b).

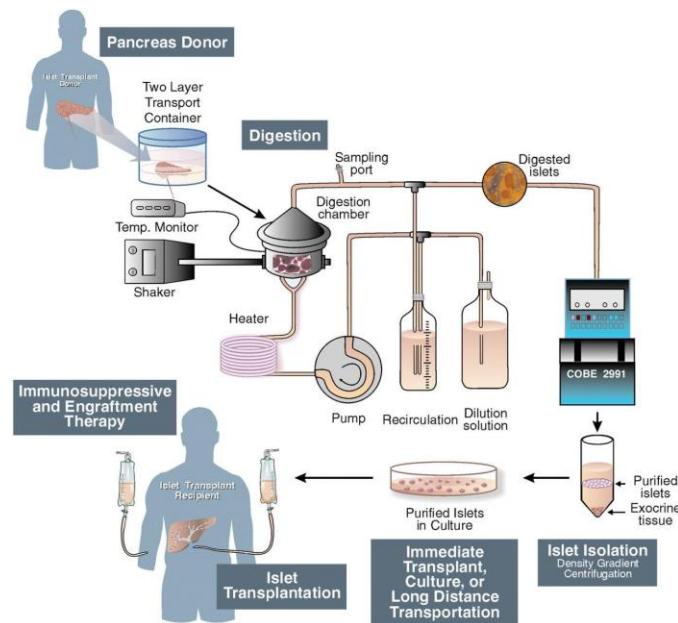


Figure 4: Graphical overview showing the all relevant steps from islet isolation from the donor until the islet transplantation into the recipient (Merani and Shapiro 2006).

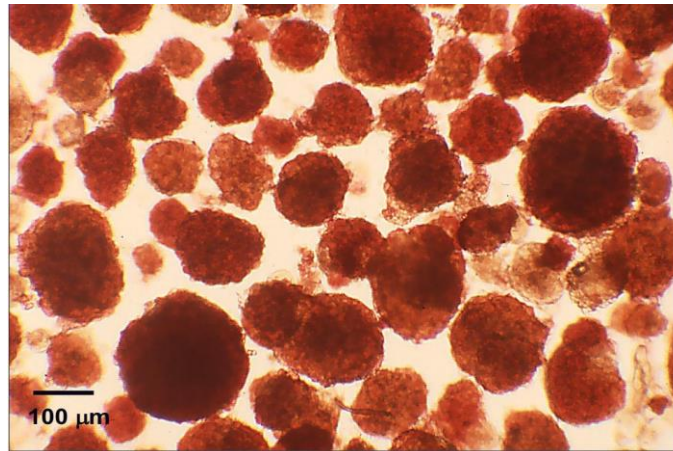


Figure 5: Representative image of a human pancreatic islets from one donor stained with dithizone to assess the purity of the preparation. Scale bar =100μm

Figure 6 shows the CGMS profile of a T1D patient over the day with the frequent hypo and hyperglycemic periods which were corrected after ectopic islet cell transplantation. Cell therapy can be a very effective treatment option to restore endogenous insulin secretion for severe forms of diabetes. The U1190 laboratory has been producing islets for clinical transplantation since 2003 and it is currently participating to its 5th clinical trial. The clinical results of the U1190 laboratory at 10 years after islet transplantation show that 28% of the patients are insulin independent (Vantghem et al. 2019b, 2019a).

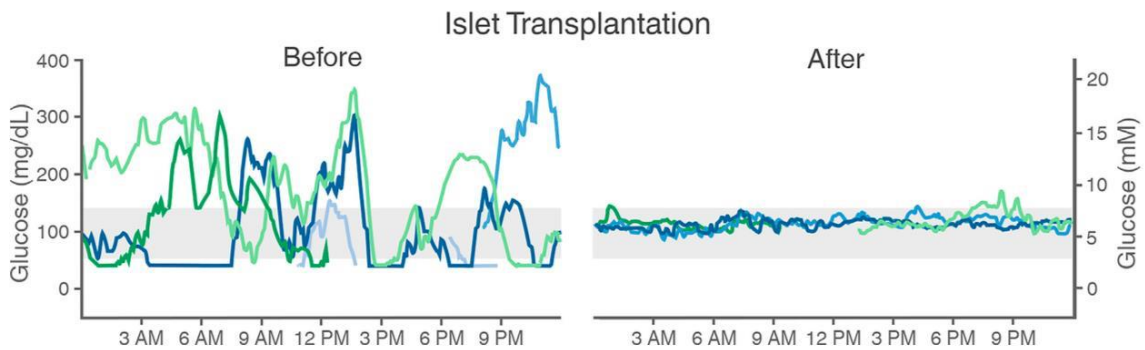


Figure 6: Continuous glucose monitoring of a T1D patient before and after islet transplantation (Latres et al. 2019).

The current islet isolation protocol requires improvement. Indeed, we estimate the loss of β cell mass at approximately 50% after islet isolation (Figure 7, red square) and only 40% of pancreases reach the 200 000 IEQ release criteria.

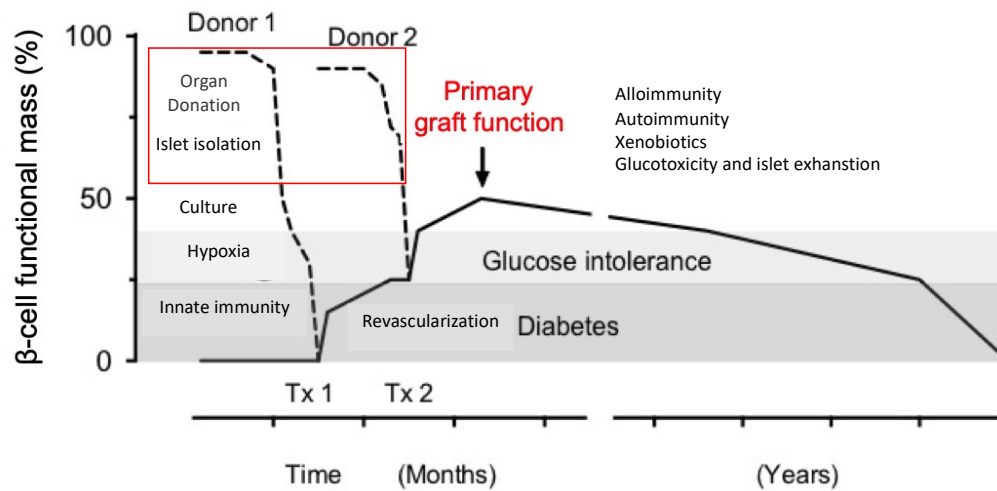


Figure 7: Graph depicts the loss of β cell mass from donor islet isolation until the islets are grafted into the recipient. Tx: Transplantation (F. Pattou unpublished).

When islets cannot be used for clinical purposes and the family has granted consent for scientific use, they are released for research use. Table 1 shows the numbers of islet isolation, IEQ used for internal research and IEQ used for external research per year from 2012 to 2018. Our laboratory uses human islets for research in the context of the physiology of human islets of Langerhans and glucose transporters (Bonner et al. 2015; Saponaro et al. 2019), and their adaptive capacities to obesogenic environment (Gargani et al. 2013). The U1190 laboratory, with its 25 years of expertise, sends human islets for research to many scientific collaborators within Europe and throughout the world.

Table 1: Number of islet isolation, number of IEQ used for internal and external research (U1190 – unpublished data)

	2012	2013	2014	2015	2016	2017	2018
Number of isolation	53	54	69	61	53	52	50
Number of IEQ used for internal research	1 330 603	856 474	878 377	712 928	486 160	586 667	300 200
Number of IEQ used for external research	421 384	606 773	906 553	853 386	715 614	1 261 130	922 900

Most of the basic research published on diabetes is based on rodent models. The possibility of using human islets of Langerhans is a considerable asset to confirm or refute these results and this is increasingly requested by editors and peer review committees (Kulkarni and Stewart 2014; Nano et al. 2015). The heterogeneity and quality of human islets for research has been recently underlined (Hart and Powers 2019; Nano et al. 2019) and an obligatory checklist has been adopted to report specific characteristics of human islet preparations, harvesting data including cold ischemia time, culture duration, viability, and functional glucose stimulated insulin secretion tests (Annexe 1). The goal is to ensure the transparency of the data in terms of donor information but also about quality and functionality of the human islets used for research.

2. Limitation of the use of human islets for research

The use of human islets of Langerhans is the gold standard for research, both for physiological research and for the development of new therapeutic molecules. However, human pancreatic islets are very heterogeneous. Within the same preparation of human islets, islets are highly variable in size, and insulin secretion from islets of Langerhans in response to glucose or pharmacological compounds is variable between different donors (Henquin 2018; Nasteska and Hodson 2018; Dominguez-Gutierrez et al. 2019; Dybala and Hara 2019). In the U1190 laboratory, more than 1000 human pancreases have been isolated. Each human islet preparation is assessed for insulin secretion in response to glucose whereby 400 IEQ (standardized unit of Islets EQuivalent to 150 microns in diameter) are placed in each perfusion chamber. The dynamics of insulin secretion of ten consecutive human islet preparations, assessed by perfusion, shows the typical physiological insulin secretion profiles (Figure 8): basal secretion at 3mM glucose, then a peak of secretion (first phase) followed by a plateau (second phase) at 15mM and, finally, a return to basal secretion when glucose is switched back to 3mM glucose. However, secretion is highly heterogeneous between donors. One of the reason for the observed islet heterogeneity has been attributed to phenotypic and clinical characteristics of donors such as sex, BMI, HbA1c, cause of death or number of days spent in intensive care unit (Henquin 2018).

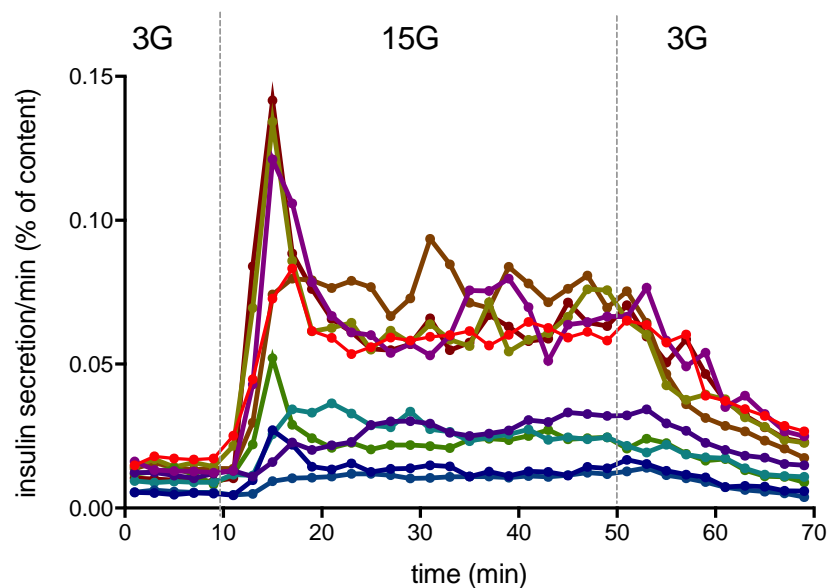


Figure 8: A dynamic perfusion system was used to determine insulin secretion of human islet preparations in response to changing glucose concentrations (3mM, 15mM, 3mM). Islets were incubated in 3mM glucose for 1 hour prior to experimentation to equilibrate basal secretion. The secretion pattern of each donor is represented with a different color. Insulin secretion was normalized to the percentage of insulin content (U1190 unpublished data).

In addition to functional differences, the expression of key transcription factors (PDX1, NKX6.1, MAFA) in human islets that have been isolated and cultured *ex vivo* (Teo et al. 2018) varied considerably from 0 to 47% of the human islet cells.

Despite their heterogeneity, human pancreatic islets remained the ‘gold standard’ and there is, therefore, a considerable demand of human islets for research (Nano et al. 2015). However, no evident increase in their availability have been observed. As a consequence, the scientific community is seeking alternatives to "native" human islets (Nano et al. 2019).

3. Pseudo-islets

Pseudo-islets were first described in the dog model by D.W. Scharp in the 80’s (Britt et al. 1981) as a new approach in the struggle to mass isolate the elusive islet. After complete digestion of the pancreas, purified individual endocrine cells underwent a steady rotational culture for 8 days, in order to obtain solid aggregates that could survive 4 weeks in culture. Intact pancreatic islets are routinely used to produce uniform diameter pseudo-islets. Different techniques for the production of pseudo-islets have been published mainly in humans, mice and dogs: rotation rotational culture

(Britt et al. 1981; Ju et al. 2013; Yu et al. 2018), spontaneous reaggregation (Schröder et al. 1983; Hopcroft et al. 1985; Halban et al. 1987), hanging drops (Cavallari et al. 2007; Pathak et al. 2017; Zuellig et al. 2017), micromolds or microwells (Ramachandran et al. 2014; Hilderink et al. 2015). Numerous commercial plates are now available (5D Sphericalplate, Ezsphere, PrimeSurface 3D). The number of cells seeded per well determines the diameter of the pseudo-islets. Pseudo-islet formation requires 3 to 8 days (Table 2).

Table 2: Different methodology and timing to obtain pseudo-islets from pig, dog, rodent and human native islets.

Source	Method	Time (days)	Reference
Pig/Dog	Spontaneous reaggregation + rotation	7	(Britt et al. 1981)
Rodent	Spontaneous reaggregation	4-6	(Schröder et al. 1983)
	Spontaneous reaggregation	3-4	(Hopcroft et al. 1985)
	Spontaneous reaggregation	5-6	(Halban et al. 1987)
	Hanging Drop	5-8	(Cavallari et al. 2007)
	Spontaneous reaggregation + shaking	1	(Ju et al. 2013)
	Agarose microwells	6-7	(Ramachandran et al. 2014)
	Agarose microwells	7	(Ichihara et al. 2016)
	Hanging Drop	5	(Pathak et al. 2017)
	Hanging Drop	4-6	(Zuellig et al. 2017)
Human	Microtissues	-	InSphero
	Agarose microwells + rotation	3-5	(Ramachandran et al. 2014)
	Agarose microwells	7	(Hilderink et al. 2015)
	Hanging Drop	4-6	(Zuellig et al. 2017)
	Centrifugal Forced Aggregation	2-3	(Yu et al. 2018)

The company InSphero provides pseudo-islets for research to academia and industry formed as described in Figure 9.

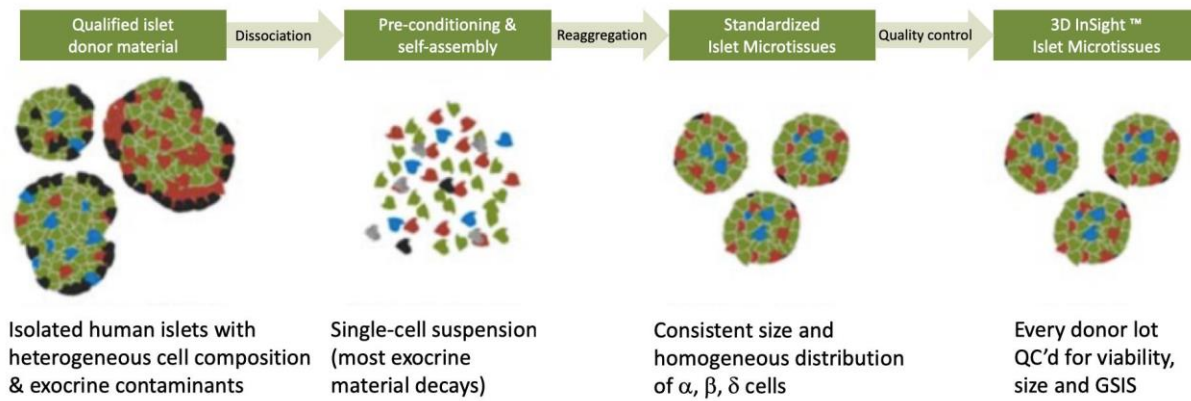


Figure 9: Schematic representation of the 3D Select™ process to generate standardized islet microtissues. A heterogeneous fraction of isolated human islets is dissociated to obtain a single cell suspension. Pancreatic cells are reaggregate to achieve pseudo-islets with uniform size and cellular composition. Each preparation is assessed for viability and glucose-stimulated insulin secretion. Exocrine contaminant cells are not incorporated into nascent islet microtissues and decay (from <http://www.insphero.com>).

“3D InSight™ Islet Microtissues are uniform, functionally robust, and long-lived primary islets designed for high-throughput study of pancreatic islet function, regeneration, and preservation. The uniform size and cellular composition, and the functionality of islet microtissues minimizes intra-assay and intra-donor variability associated with native islets. Moreover, the improved viability in culture enables assessment of long-term compound effects and disease modeling.” <http://www.insphero.com>

Although the method is not new, pseudo-islet technology is generating renewed interest from the islet transplant community in particular due to a claim from the team in Zürich that islet size influence graft islet outcome. Immediately after transplantation and before revascularization, islets are hypoxic in the portal blood and get oxygen mainly by diffusion (Lehmann et al. 2007). Logically, smaller islets should outperform larger ones in this setting. Indeed, small islets showed improved survival rates under normoxic and hypoxic conditions compared to larger diameter islets, and superior insulin secretion capacity (Figure 10 A-D) and content (Figure 10 E).

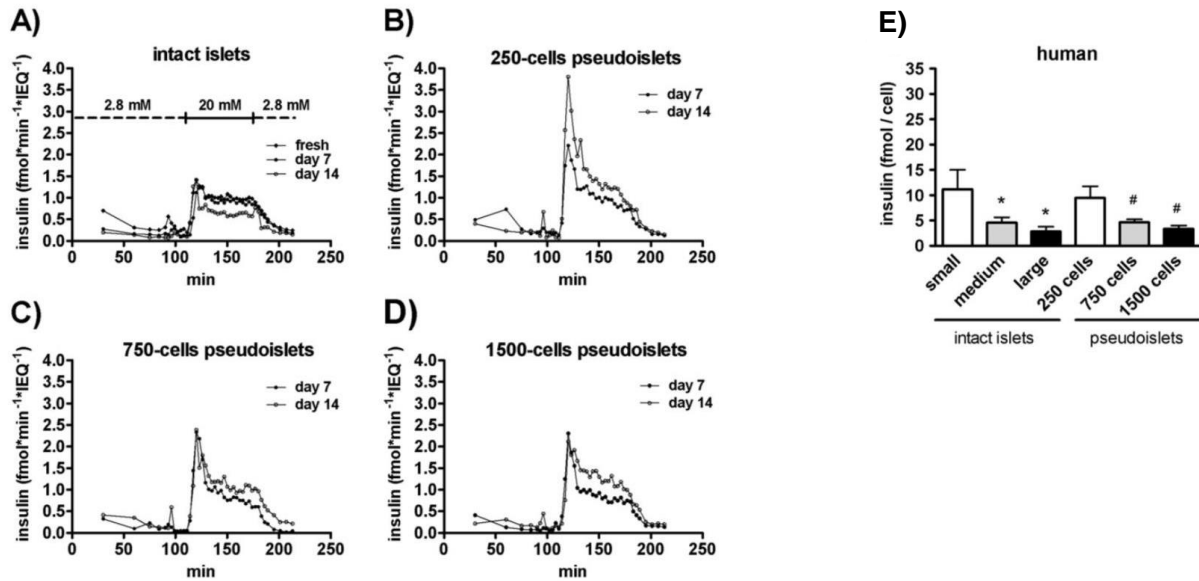


Figure 10: Glucose-stimulated insulin secretion (GSIS) profile and insulin content of intact native islets compared to pseudo-islets. Insulin secretion profiles from perfusion assays of intact native human islets (A), pseudo-islets after 7 and 14 days in culture composed of 250 cells (B), 750 cells (C) and 1500 cells (D). Data were normalized to total islet volume and per condition n=100 islets were used. (E) The total insulin content was expressed per cell from intact native human islets of different sizes or pseudo-islets (250, 750 and 1500 cells). Data are expressed as mean \pm SEM (Zuellig et al. 2017).

Pseudo-islets show similar endocrine cell distribution as native islets both in the pancreas and after isolation (Figure 11) with some reports of slightly increased glucagon in pseudo-islets. Likewise, pseudo-islets of small diameter (< 100 μ m) also show higher viability (Ramachandran et al. 2014), improved glucose-stimulated insulin secretion, increased tolerance to hypoxia and improved function and vascularization after transplantation in rodents (Yu et al. 2018).

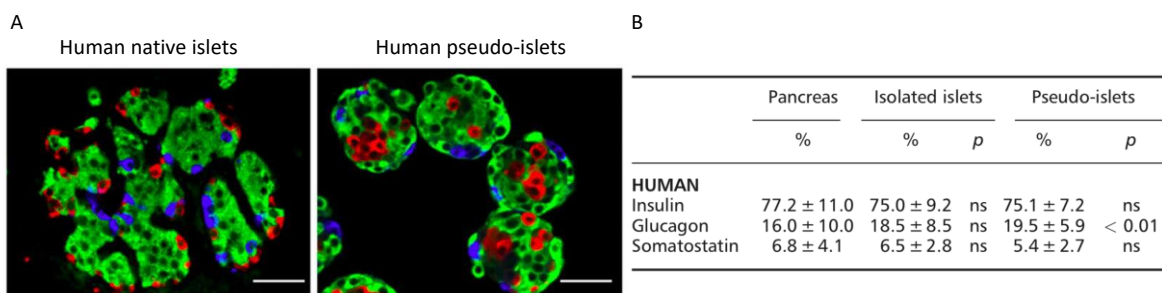


Figure 11: Islets and pseudo-islets architecture and cellular composition. (A) Immunofluorescent staining of insulin (green), glucagon (red) and somatostatin (blue), scale bar = 50 μ m. (B) Relative abundance of hormone-expressing cells. Data are expressed as mean \pm SD (Zuellig et al. 2017).

Altogether, pseudo-islets technology allows the production of islets of a constant diameter in order to reduce heterogeneity, improve function, resistance to hypoxia and enhance vascularization post transplantation (Yu et al. 2018). For these above mentioned reasons pseudo-islets are gearing up for clinical transplantation in North America (Yu et al. 2018) and in Europe (Lebreton et al. 2019).

However, cell therapy with pseudo-islets requires native human islets as starting material or human pancreases and is, therefore, like islet transplantation affected by the scarcity of pancreatic tissue available (2000 organs/year in France). In 2011, Dr. P Ravassard and Dr. R Scharfmann published a long awaited functional human pancreatic β cell line, EndoC- β H1 cells which expressed β -cell specific markers, resembled native β -cells in their expression of specific and epigenetic markers and secreted insulin in response to a glucose stimulation (Ravassard et al. 2011; Lawlor et al. 2019). This human β cell line has the advantage of being readily available and has been used worldwide since 2011 as a surrogate to native human β -cells for research purpose. Nevertheless, EndoC- β H1 cannot be used for cell therapy neither to study β -cell development. A recent review (Table 3) highlights the advantages and limitations of the the EndoC- β H1 cells compared to native human islets and pluripotent stem cell-derived β cells.

Table 3: Advantages and limitations of native human β -cell, stem cell-derived β -cell and EndoC- β H-cell (Scharfmann et al. 2019).

	Primary human β cells	Stem cell-derived β cells	EndoC- β H cell lines
Convenience and ease of use			
Accessibility and abundance	Limited number of donor organs; limited number of islet isolation centers; shipment is needed	In-house production is complex and requires a high level of expertise; large-scale culture is possible	In-house propagation requires a moderate level of expertise; large-scale culture is possible
Costs	Human islet isolation: very high cost; commercial islets: very high cost	In-house production: high cost	Propagation: low cost
Care and propagation of the cells	Relatively easy, but lifespan of the cells is limited; propagation impossible (no cell division)	Differentiation process is labor-intensive and requires major expertise (starting from frozen stock of endocrine progenitor cells reduces this difficulty); propagation and expansion to large cell numbers is possible	Cell care is relatively easy; propagation and expansion to large cell numbers is relatively easy (doubling time is approximately 7 days)
Cryopreservation	Very difficult; limited cell recovery	Well suited for cryopreservation and future expansion or differentiation	Well suited for cryopreservation and future expansion
Consistency and reproducibility	Donor-to-donor variability (genetic, functional); dependence on cold/warm ischemia time; shipment affects quality	Protocol- and batch-dependent; fluctuation in differentiation efficiency and maturational state of the β -like cells	Robust
Safety risks	Standard biosafety recommendations; donors are tested for specific human pathogens to limit the likelihood that cells are contaminated	Standard biosafety recommendations; cells are free of adventitious contaminating pathogens	Standard biosafety recommendations; cells are infected by a xenotropic retrovirus, but good laboratory practice avoids pathogen propagation (141)
Authentication	No drift since no propagation	Genetic authenticity profiles (STR, SNP, or HLA patterns) of many pluripotent stem cell lines are available	Genetic authenticity profiles (STR) of the EndoC- β H cell lines are available
Dependence on external provider	High	Low	Low
Proximity to native β cells			
Differentiation state and functional maturation	Gold standard	Protocol-dependent, but recent advances are promising and are approaching strong resemblance to primary human β cells	Strong resemblance to primary human β cells, although functional maturation remains suboptimal; maturation can be further improved by reversing of immortalization
Endocrine and β cell purity	Variable endocrine purity of islet preparations; study of pure β cells is difficult	Differentiation efficiency has greatly advanced; β cell purity can be further enhanced using FACS	Pure <i>INS</i> -expressing cells; some expression of SST
Chromosomal aberrations	Diploid	Diploid	Pseudodiploid
Contribution to current knowledge on β cells	Most contributions to the field	Increasing number of contributions	Starting to contribute
Versatility and study area			
β Cell function	Fresh islets are the gold standard, but culture and shipment often impair function and increase variability; persistence of paracrine effects mimics islet function better than isolated β cells	Batch-dependent variation in function, with good batches approaching the functionality of primary human islets	Robust performance in functional assays, with strong resemblance to primary human islets in terms of glucose- and incretin-stimulated insulin secretion
Diabetes modeling	Source: islets from diabetic or healthy donors; mini-organ: partial preservation of the interaction between different islet cell types	Source: iPSC-derived β cells from diabetic or healthy donors (nondiabetic source in case of ESC-derived β cells); mini-organ: efforts ongoing for reaggregation of differentiated α - and β -like cells	Source: nondiabetic; mini-organ: efforts ongoing for production of α and δ cell lines
Pharmacological and toxicology screening	Useful, but difficult because of variability and limited material	Useful	Useful
Cell therapy	Used in clinical practice	Studied in clinical trials	Not suitable, mainly because of tumoral properties
β Cell development	Not suitable	Useful	Not suitable
Genetic modification	Transfection and transduction	Transfection and transduction; CRISPR/Cas gene editing	Transfection and transduction; CRISPR/Cas gene editing, theoretically possible and under way in several laboratories

ESC, embryonic stem cell; iPSC, induced pluripotent stem cell; SNP single-nucleotide polymorphism; STR, short tandem repeat.

4. Embryogenesis and early pancreas development

Considerable efforts have been made to develop protocols for the differentiation of pluripotent stem cells to mature endocrine cells. To do this, it's important to understand the mechanisms of embryogenesis and identify the factors that are involved in the pancreas organogenesis, in order to mimic these pathways *in vitro*.

The oocyte begins its first segmentation to form the morula, which is composed of about thirty cells. The cells tighten together and then flatten to form an internal cell mass, giving place to a cavity, which is the blastocyst stage. Then, the cells of the internal cell mass shape themselves to form the ectoderm and mesoderm, which during gastrulation will form the mesoderm and endoderm (Lu et al. 2001; Shook and Keller 2003). It has been shown that Nodal, a member of the TGF β family signaling pathway, is necessary and sufficient to induce the formation of the endoderm and mesoderm (McCracken and Wells 2012). Nodal allows the gastrulation and formation of the mesoderm, as well as the separation of the endoderm (high Nodal) and the mesoderm (low Nodal).

Subsequently, the cells of the endoderm will differentiate into the respiratory and digestive tract, the thyroid, thymus, lungs, liver and pancreas. The cells of the mesoderm will give rise to muscle, bone and blood vessels, while those of the ectoderm will form the epidermis and nervous system. The endoderm acquires an antero-posterior pattern; several pathways activated by signaling factors such as wingless-related integration site (Wnt), fibroblast growth factor (FGF), Bone morphogenic protein (BMP) and retinoic acid (RA) have a posteriorizing effect (Tiso et al. 2002; Dessimoz et al. 2006; McLin et al. 2007; Bayha et al. 2009). This antero-posteriori identity is associated with cell morphogenesis events to form the primitive gut tube and induce pancreatic organogenesis (Lawson et al. 1986; Tremblay and Zaret 2005). Dorsal and ventral buds fuse together to form the pancreas (Slack 1995; Polak et al. 2000; Jennings et al. 2013, 2017). The cells of the posterior foregut will give rise to PDX1 positive multipotent progenitor cells (Wells and Melton 2000) which will be able to differentiate into endocrine or exocrine cells (Gu et al. 2002). Under high or low Notch signaling, multipotent progenitors will differentiate into trunk (bipotent cells) or tip (unipotent) cells (Zhou et al. 2007), respectively. Tip cells will give rise to acinus while trunk cells will give rise, to duct or endocrine cells, under high or low Notch signaling respectively. Trunk cells express neurogenin 3 (NGN3), which is a pro-endocrine gene (Gu et al. 2002; Salisbury et al. 2014) whose expression is detected in two waves during mouse embryogenesis (Villasenor et al. 2008). In the first wave, known as first transition, mainly α cells are generated at high NGN3

levels while during the second transition, NGN3 allows the differentiation into all endocrine cells including β cells (Figure 12) (Johansson et al. 2007).

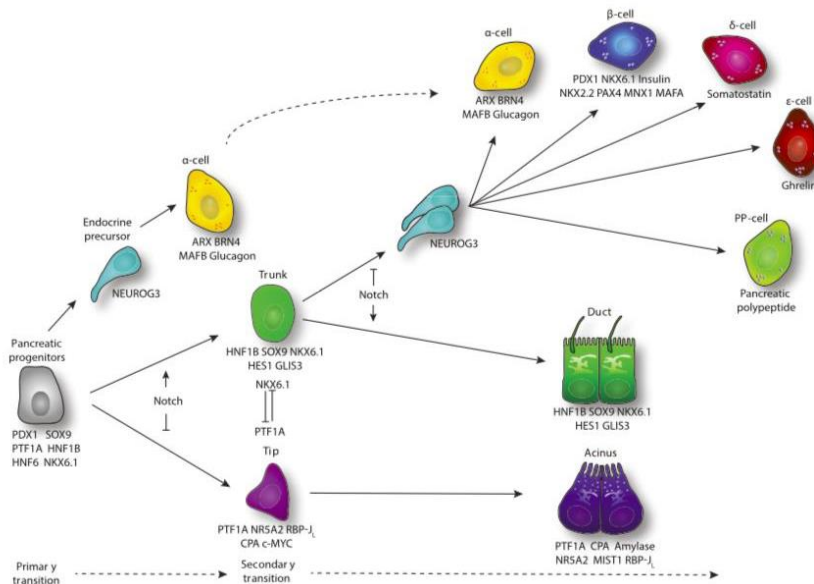


Figure 12: Pancreatic cell lineage determination during pancreas organogenesis (Larsen and Grapin-Botton 2017).

After cell differentiation, endocrine cells migrate to the surrounding mesenchyme and form the islets of Langerhans, composed of α , β , δ , ϵ and PP cells which produce glucagon, insulin, somatostatin, ghrelin and pancreatic polypeptides respectively.

Pancreatic islet neogenesis from ducts occurs in human fetal pancreas (Figure 13). Further differentiation and rearrangement of the endocrine cells in the islets will occur until adulthood (Jeon et al. 2009).

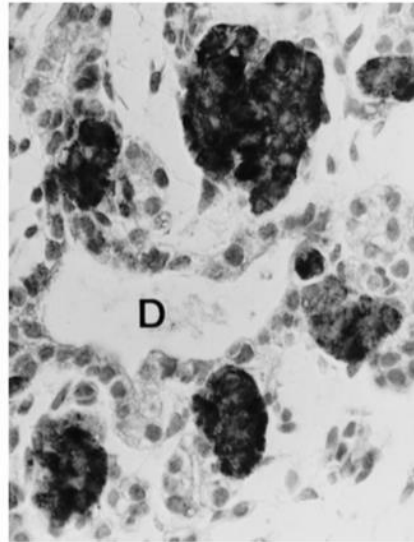


Figure 13: Immunocytochemical staining of the endocrine marker synaptophysin (in black) on a fetal pancreas at 16 weeks of gestation shows single cell or small endocrine cell aggregates in direct contact with pancreatic duct (D) (Rooman et al. 1997).

Most of the knowledge on embryogenesis and pancreatic organogenesis is from murine models due to scarcity of human fetal samples (Jennings et al. 2013; Nair and Hebrok 2015). Recapitulating murine embryogenesis in human pluripotent stem cell lines may not be optimal since some signaling pathways are well conserved between the mouse and humans but others diverge. This knowledge is used as a starting point for the development of new protocols for the differentiation of human pluripotent stem cells to endocrine β cells *in vitro*. Figure 14 highlights the similarities and differences between human and mouse pancreas morphogenesis (Nair and Hebrok 2015).

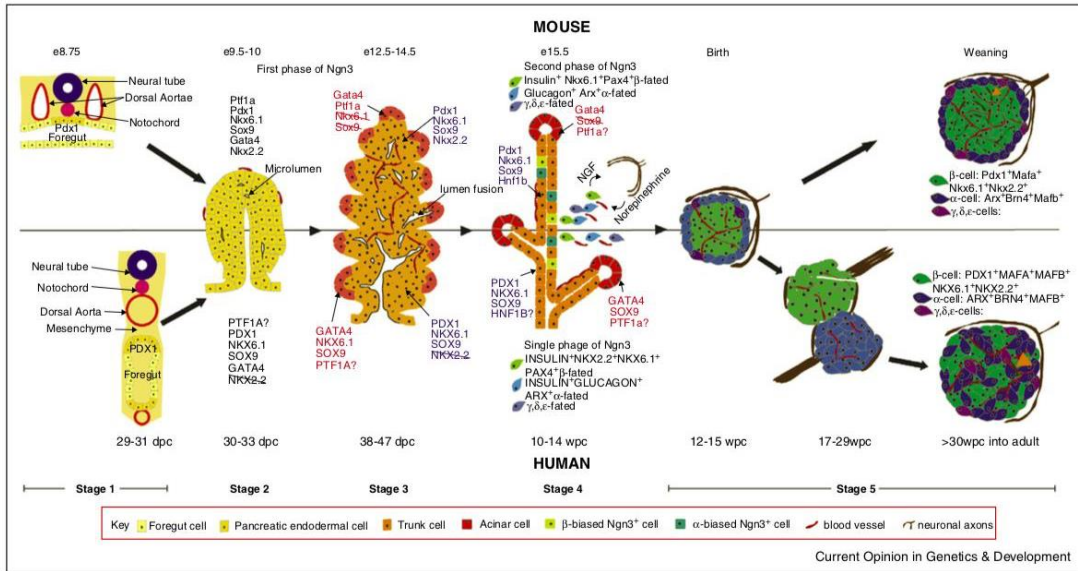


Figure 14: Similarities and differences during pancreas morphogenesis in mouse (top) and Human (bottom). e: embryonic day, dpc: day post conception, wpc: week post conception (Nair and Hebrok 2015).

5. Stem cells & pluripotent stem cells

First described by Auguste Weissman in 1883, in contrast to terminally differentiated somatic cells, stem cells harbor a high grade of plasticity in order to differentiate in various cell types (pluripotency) and display self-renewal properties.

Pluripotency is the ability of a cell to differentiate into the three embryonic germ layers. Pluripotency is a temporal state observed during embryogenesis and can be artificially maintained during *in vitro* culture by specific culture media. Indeed, components in culture medium allow to promote self-renewal while inhibiting differentiation (Li and Belmonte 2017; Smith 2017; Akberdin et al. 2018).

In contrast to most *in vitro* cultured somatic cells that have a finite number of cell division (Hayflick limit <80), stem cells are capable of extensive proliferation (self-renewal) (> 160) without evidence of oncogenic transformation or senescence (Zeng 2007). Self-renewal is achieved by symmetrical cell division, one stem cell to divide into two daughter cells, at least one of which remains undifferentiated. Thus, stem cells are constantly renewed which allows access to an unlimited cell reservoir (Zeng and Rao 2007).

Stem cells have the ability to differentiate into different cell types (plasticity). While differentiating, the cells become more and more specialized. The mature cells will be able to function as a tissue or organ. Stem cells may be able to generate several types of differentiated cells. Once the progenitor is engaged in a path of differentiation, it loses the ability to self-renew. Pluripotency can be demonstrated *in vivo* by the formation of teratoma composed of cells from the three embryonic germ layers after transplantation in immunodeficient mice (Thomson et al. 1998). Stem cells are characterized by a high nucleo-cytoplasmic ratio and form colonies when cultured *in vitro*. There are different sources of pluripotent stem cells, embryonic stem cells from the inner cell mass of the blastocyst or induced-pluripotent stem cell “iPS” generated from somatic cells (Figure 15).

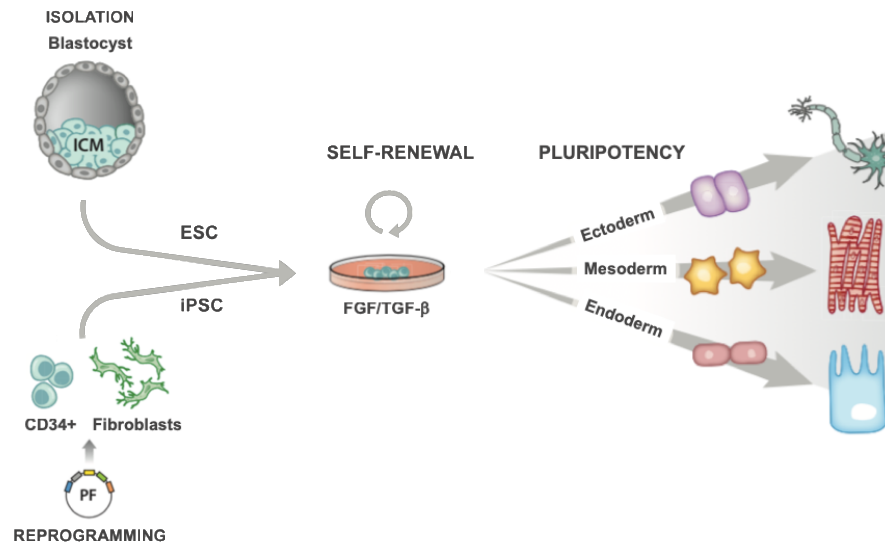


Figure 15: Sources of pluripotent stem cells: pluripotent stem cells are hallmarked by self-renewal capacity and differentiation in cells of all the three germ layers (ectoderm, mesoderm, endoderm) (Grandy et al. 2019).

1) Embryonic stem cell (ESC)

The development of a new organism begins with the zygote resulting from the fusion of a male and a female gamete. The zygote is composed of totipotent cells that have the potential for self-renewal and the ability to differentiate into all cells of the organism. During differentiation, cells gradually specialize into pluripotent, multipotent and unipotent cells to result in a fully differentiated cell state. Totipotent stem cells are cells at the morula stage. They are able to differentiate in all cell types of an organism as well as embryonic appendages (Jaenisch and Young 2008). Pluripotent stem cells can differentiate into one of the three embryonic layers (endoderm, mesoderm, ectoderm) and lead to all the cell types of an organism. Contrary to totipotent stem cells, they do not differentiate and produce embryonic appendages. There are different types of pluripotent stem cells: embryonic stem cells and induced pluripotent stem cells. Multipotent stem cells are restricted in their differentiation potential within a tissue or lineage (Young et al. 2004). They maintain tissue homeostasis by differentiating into the different cell types of this tissue, such as hematopoietic stem cells that have the potential to reconstitute hematopoiesis. Unipotent stem cells are only able to differentiate into a single cell type such as endothelial progenitor cells

Embryonic stem (Figure 16) cells are generated from pluripotent stem cells present in the blastocyst stage within the inner cell mass. They were first characterized in mice by Evans and Martin in 1981

(Evans and Kaufman 1981; Martin 1981) and then in humans by Thomson 1998 (Thomson et al. 1998). Evans et al. showed that inner cellular mass cells (ECM) could be cultured *in vitro* while maintaining their pluripotency capacity for years in culture (Rosler et al. 2004).

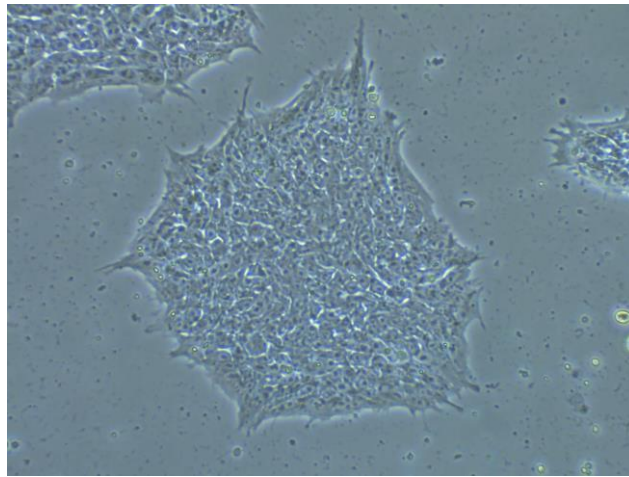


Figure 16: Representative image of an embryonic stem cell (H1) cultured in m-TeSR.

Derivation methods:

There are different methods of embryonic stem cells derivation: isolation from the inner cell mass of the blastocyst, nuclear transfer and cell fusion.

Most of the embryonic stem cell lines used today are obtained by isolating, dissociating and culturing cells from the blastocyst's inner cell mass as described by Thomson. However, this requires the use of supernumerary human embryos initially produced as part of medical assisted procreation and obtained by *in vitro* fertilization, then donated to research with the informed consent of parents. In France, embryonic stem cells are subject to a strict regulatory framework (Law 2013-715). Research using embryonic stem cells must be authorized by a nominative derogation (Annexe 2) issued by the French Biomedical Agency (ABM). Major progress was made in 2013 where a non-destructive single cell biopsy of the inner cell mass at the blastocyst stage was performed (DPMAregister DDE 10 2004 062 184.5) (Dittrich et al. 2015).

Nuclear transfer consists of removing the nucleus from a somatic cell and introducing it into the cytoplasm of an enucleated oocyte. This technique resulted in the birth of the Dolly sheep in 1997. In 2013, the nuclear transfer was carried out from human cells, thus making it possible to generate human blastocysts called NT-ESC (Nuclear Transfert-Embryonic Stem Cells) (Tachibana et al. 2013). This technique makes it possible to obtain embryonic stem cells specific to a patient and to model some genetic disease. Although nuclear transfer does not require the destruction of embryos, the use of human oocytes also presents ethical problems.

Cell fusion is the fusion of a somatic cell with an embryonic stem cell resulting in the formation of a tetraploid hybrid stem cell. This technique has made it possible to highlight the ability of embryonic stem cells to reprogram the nucleus of a somatic cell.

2) Induced pluripotent stem cells

Described in 2006 by Prof. Yamanaka and awarded the Nobel Prize for Medicine and Physiology in 2012, induced Pluripotent Stem cells (iPSC) are reprogrammed mature adult cells back to an pluripotent state using reprogramming factors. The generated cells are genetically identical to the donor's cells, and highly similar to embryonic stem cells in terms of morphology, proliferation and self-renewal capacity and cell differentiation capacity in cells from the three embryonic layers. Yamanaka et al. identify 4 reprogramming factors by screening 24 factors, previously observed in mouse embryonic fibroblast, enabling the reprogramming of mouse fibroblasts (Takahashi and Yamanaka 2006) and human fibroblasts (Takahashi et al. 2007) using a retroviral transduction.

Since then, many cell types have been reprogrammed. Starting cells that can be obtained easily and without invasive procedures and cells sensitive to reprogramming are favored. Most of the reprogrammed cells are cells from mesodermal origin: fibroblasts (Takahashi et al. 2007), hematopoietic lineage (Giorgetti et al. 2009; Loh et al. 2009; Kunisato et al. 2011) or adipose cells (Qu et al. 2012). iPSCs have also been generated from cells derived from ectoderm: keratinocytes (Aasen et al. 2008), neural progenitors (Kim et al. 2009b), or melanocytes (Utikal et al. 2009) and from cells derived from endoderm: hepatocytes (Liu et al. 2010) or pancreatic β cells (Bar-Nur et al. 2011).

The 4 stemness transcription factors also known as Yamanaka cocktail are Oct 3/4 (Octamer-binding transcription factor 3/4, also known as POU5F1), Sox2 (SRX-box 2), Klf4 (Krüppel-like transcription factor 4), and c-Myc. Oct3/4 is exclusively expressed in embryonic stem cells and primordial germ cell and is crucial for in vitro and in vivo pluripotency (Schöler et al. 1989; Nichols et al. 1998). Sox2 expression is required for maintenance of pluripotency of epiblast cells and regulate OCT3/4 in mouse ESC (Avilion et al. 2003; Masui et al. 2007). Oct3/4 and Sox2 have the ability to complex and stimulate the expression of the factor Nanog, which has a role in the acquisition of inner cell mass pluripotency (Chambers et al. 2003, 2007; Mitsui et al. 2003; Silva et al. 2009). Klf4 is an important factor for the self-renewal of embryonic stem cells, it is also involved in embryonic development, proliferation, differentiation and cellular apoptosis (Dang et al. 2000). Klf4 interacts with the Oct3/4-Sox2 complex to regulate the expression of other factors

involved in the self-renewal and differentiation of embryonic stem cells such as Lefty1 (Nakatake et al. 2006). C-myc is a proto-oncogene involved in cell cycle regulation, proliferation and apoptosis (Bretones et al. 2015). Oct3/4, Sox 2 and Nanog are the core factors in pluripotency gene network necessary for induction, maintenance and loss of pluripotency during cell reprogramming (Chen et al. 2017; Li and Belmonte 2017). They act together as an interconnected network to regulate pluripotency gene expression (Boyer et al. 2005). Nanog is not necessary to initiate the reprogramming process but is essential to maintain the pluripotency of the reprogrammed cells (Mitsui et al. 2003; Chambers et al. 2007) and is activated by the Oct3/4-Sox2 complex. Klf4 promote reprogramming via a direct interaction Oct3/4-Sox2 complex (Wei et al. 2009).

Alternatives to retroviruses have been developed in order to decrease the risk of insertional mutagenesis as they randomly integrate into the host genome and the risk of reactivation of the reprogramming factor. Reprogramming can be done using an integrative or a non-integrative method, their advantages and disadvantages are described in table 4.

Table 4: Summary of advantages and disadvantages of published transcription factors delivery methods used for cellular reprogramming (Brouwer et al. 2016; Takahashi and Yamanaka 2016; Karagiannis et al. 2019).

	Delivery method	Advantages	Disadvantages	References
Integrative	Retrovirus	Efficient +	Genomic integration, requires cell division	(Takahashi et al. 2007; Aasen et al. 2008)
	Lentivirus	Efficient + No cell division required, inducible/excisable, infects wide range of cell types	Genomic integration	(Hockemeyer et al. 2008; Maherali et al. 2008)
	Transposon	Efficient, Xeno-free, excisable	Genomic integration, risk of reintegration	(Woltjen et al. 2009; Grabundzija et al. 2013)
	Bacteriophage	Integrates in intergenic regions	Genomic integration	(Ye et al. 2010)
	Zinc finger nucleases	Targeted integration, excisable	Genomic integration	(Ramalingam et al. 2013)
Non-integrative	mRNA	No genomic integration, efficient	Requires multiple transfections,	(Warren et al. 2010, 2012; Mandal and

			triggers immune response	Rossi 2013; Yoshioka et al. 2013)
	Plasmid	No genomic integration, easy to use	Inefficient, requires multiple transfections, risk of genomic integration	(Okita et al. 2008, 2011; Yu et al. 2009; Jia et al. 2010)
	Protein	No genomic integration	Inefficient, requires multiple transfections, requires high levels of proteins	(Kim et al. 2009a)
	Adenovirus	No genomic integration	Inefficient, Requires multiple infections	(Zhou and Freed 2009)
	Sendai virus	No genomic integration, infects wide range of cell types, easily removable	Requires multiple viruses containing one factor each	(Fusaki et al. 2009; Ban et al. 2011)
	Minicircle DNA	No genomic integration, easy to use, small constructs, xeno-free	Inefficient, Requires multiple transfections	(Narsinh et al. 2011)

The reprogramming efficiency of the Yamanaka's cocktail was quite low. In the last year the reprogramming outcome was significantly improved by alternatives at the original reprogramming cocktail (Table 5).

Table 5: Evaluation of reprogramming factors capable of reprogramming human cells. EMT: epithelial to mesenchymal transition. MET: mesenchymal to epithelial transition. (Brouwer et al. 2016; Omole and Fakoya 2018).

Reprogramming factors	Function	Affected pathway	Effect on pluripotency	References
Oct4	Maintenance of pluripotency and self-renewal	Core transcriptional circuitry	+	(Takahashi et al. 2007; Okita et al. 2011)
Sox2	Maintenance of pluripotency and self-renewal	Core transcriptional circuitry	+	(Takahashi et al. 2007)
Klf4	Maintenance of pluripotency and self-renewal	Core transcriptional circuitry	+	(Jiang et al. 2008; Zhang et al. 2010)
c-Myc	Maintenance of pluripotency and self-renewal	Core transcriptional circuitry	+	(Takahashi et al. 2007)
Lin28	Maintenance of pluripotency, translational enhancer, inhibits let7	Core transcriptional circuitry	+	(Yu et al. 2007)

Nanog	Maintenance of pluripotency and self-renewal	Core transcriptional circuitry	+	(Yu et al. 2007)
Salf4	Maintenance of pluripotency and self-renewal	Core transcriptional circuitry	+	(Tsubooka et al. 2009)
Utf1	Maintenance of pluripotency	Core transcriptional circuitry	+	(Zhao et al. 2008)
p53	Induces senescence, tumor suppressor	Apoptosis/cell cycle	-	(Zhao et al. 2008; Banito et al. 2009; Chou et al. 2011)
p21	Induces senescence, tumor suppressor	Apoptosis/cell cycle	-	(Banito et al. 2009)
p16 ^{Ink4a}	Induces senescence, tumor suppressor	Apoptosis/cell cycle	-	(Banito et al. 2009; Li et al. 2009a)
GLIS1	Activates multiple pro-pluripotency pathways	Core transcriptional circuitry; Wnt/b-catenin; PI3K; TGFb core transcriptional circuitry	+	(Maekawa et al. 2011)
L-Myc	Suppresses differentiation associated genes	TGFb	+	(Okita et al. 2011)
TGFb	Facilitates EMT	TGFb	+	(Liu et al. 2013)
MDM2	p53 inhibitor	Apoptosis/cell cycle	+	(Hong et al. 2009)
REM2	p53 inhibitor	Apoptosis/cell cycle	+	(Edel et al. 2010)
Cyclin D1	Stimulateds E2F/G1-S cell cycle	Apoptosis/cell cycle	+	(Edel et al. 2010)
SV40 large T antigen	Inhibits p53 tumor suppression	Apoptosis/cell cycle	+	(Mali et al. 2008; Chou et al. 2011)
DOT1L	Histone H3K79 methyltransferase	Chromatin remodeling	-	(Onder et al. 2012)
Cx43	Promotes MET transition	E-cadherin/b-cat	+	(Ke et al. 2013)
MBD3	Histone deacetylation, chromatine remodeling	Chromatin remodeling	-	(Rais et al. 2013)
Sirt6	Chromatine remodeling/ telomere maintenance	Chromatin remodeling	+	(Sharma et al. 2013)
TCL1a	Stimulates akt pathway	PI3k	+	(Picanço-Castro et al. 2011)
RARy	Binds RAREoct, promotes Oct4 expression	Core transcriptional circuitry	+	(Wang et al. 2011b)
SNAIL	Promotes EMT transition	Core transcriptional circuitry/TGFb	+	(Unternaehrer et al. 2014)
Lrh-1	Binds RAREoct, promotes Oct4 expression	Core transcriptional circuitry	+	(Wang et al. 2011b)
RCOR2	Facilitates histone demethylation	Chromatin remodeling	+	(Yang et al. 2011)
Non-coding RNA				
miR367	Inhibits EMT	TGFb	+	(Anokye-Danso et al. 2011)
LincRNA-ROR	Regulates expression of core transcriptional factors	Core transcriptional circuitry	+	(Loewer et al. 2010; Wang et al. 2013)
miR302	Inhibits EMT/stimulates oct4 expression	TGFb; core transcriptional circuitry, apoptosis	+	(Lin et al. 2010, 2011; Anokye-Danso et al. 2011)

miR766	Inhibits Sirt6	Chromatin remodeling	-	(Sharma et al. 2013)
miR200c miR369 miR372	Inhibits EMT/TGFb pathway	TGFb	+	(Miyoshi et al. 2011)
Let7	Regulates expression of core transcriptional factors and transcriptional genes	Core transcriptional circuitry/TGFb	-	(Worringer et al. 2014)
miR 19a/b	Inhibits PTEN	PI3k	+	(He et al. 2014)
Small molecules				
Vitamin C	Alleviates cell senescence/antioxyadant	Hypoxia response	+	(Esteban et al. 2010)
Valproic acid	Inhibits histone deacetylases	Chromatin remodeling	+	(Huangfu et al. 2008)
CHIR99021	GSK3-inhibitor	PI3k, Wnt/b-catenin	+	(Li et al. 2009b)
Pamate	Lysine-specific demethylase 1 inhibitor	Chromatin remodeling	+	(Li et al. 2009b)
SB431542	ALK5/TGFb receptor inhibitor	TGFb	+	(Lin et al. 2009)
PD0325901	MEK inhibitor	MAPK/ERK	+	(Lin et al. 2009)
BIX-01294	Methyltransferase G9a inhibitor	Chromatine remodeling	+	(Medvedev et al. 2011)
Lithium	GSK3-inhibitor	PI3k; Wnt/b-catenin	+	(Wang et al. 2011a)
Maxadilan	Downregulates Caspase 3 and 9, anti-apoptotic	Apoptose	+	(Zhao et al. 2012)
8-Br-cAMP	Protein kinase A activator	cAMP	+	(Wang and Adjaye 2011)
A-83-01	ALK5/TGFb receptor inhibitor	TGFb	+	(Zhu et al. 2010)
Tiazovivin	Promotes survival, ROCK inhibitor	PI3k	+	(Lin et al. 2009)
Y-27632	Promotes survival, ROCK inhibitor	PI3k	+	(Gharechahi et al. 2014)
EPZ004777	DOT1L inhibitor	Chromatin remodeling	+	(Onder et al. 2012)
DAPT	Inhibits Notch/ increases core transcription factor expression/ inhibits p53 pathway	Core transcriptional circuitry/apoptosis	+	(Ichida et al. 2014)
Trichostatin A	Inhibits histone deacetylases	Chromatin remodeling	+	(Huangfu et al. 2008)

3) Pluripotent stem cell applications

Pluripotent stem cells are a promising tool for therapeutic applications and also for the study of embryonic development, to model human diseases and for drug discovery (Figure 17).

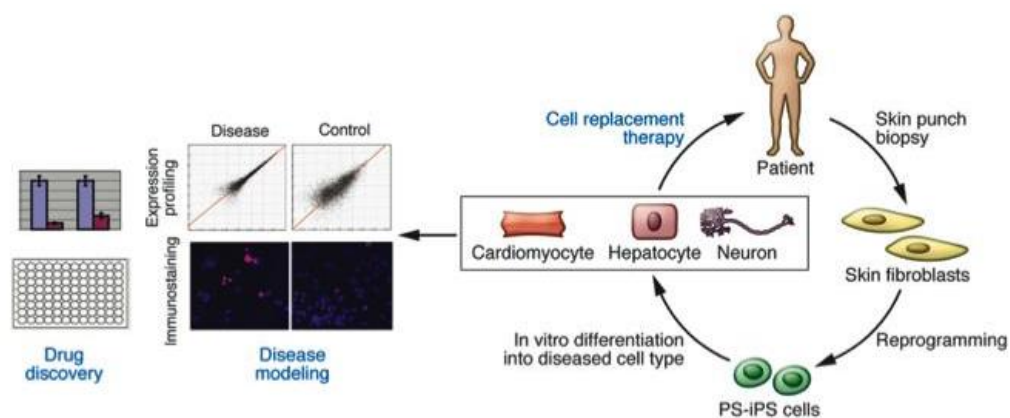


Figure 17: Possible application for pluripotent stem cells in research and for clinical treatment strategy (Kiskinis and Eggen 2010).

In vitro model of development

Most embryonic development studies are based on work done in rodents hence the *in vitro* differentiation of human pluripotent stem cells allows the study of the molecular mechanisms involved during human embryonic development. Although most molecular mechanisms are well preserved between species, recent studies have shown that there may also be differences. For instance, in human, GATA 6 is essential for pancreatic organogenesis (Fisher et al. 2017; Shi et al. 2017b; Tiyaboonchai et al. 2017), while both GATA 4 and GATA6 control mouse pancreatic organogenesis (Carrasco et al. 2012; Xuan et al. 2012). A recent study, used human iPSC technology to model human hepato-biliary-pancreatic organogenesis in order to observe interactions between neighboring components (Koike et al. 2019). Using single-cell expression analysis on β -like cells differentiated from human ESC, a study uncovered distinct subpopulations over the endocrine differentiation process and an early lineage bifurcation toward polyhormonal cells or monohormonal β -like cells (Petersen et al. 2017). Another single-cell transcriptome analysis of pancreatic progenitors and endocrine cells derived from mice and human ESC cells, provided comparative data on biological development in mouse and human available on https://lynnlab.shinyapps.io/embryonic_pancreas (Krentz et al. 2018). These data will provide a better understanding of the underlying molecular mechanisms of embryonic development, and also to improve differentiation protocols.

Disease modeling / drug screening application

The development of differentiation protocols allows the use of the patient derived cells to identify the underlying pathological mechanisms of a disease. To this end, iPSC cells have many advantages, in particular that of providing an unlimited differentiated-cell source from patients suffering from

diseases as T1D, T2D, MODY (Maturity Onset Diabetes of the young) or pancreatic agenesis (Park et al. 2008; Maehr et al. 2009; Thatava et al. 2013; Chan et al. 2015; El Khatib et al. 2016; Millman et al. 2016; Griscelli et al. 2017, 2018; Rajaei et al. 2017; Kondo et al. 2018).

Although pluripotent stem cell-based modeling has shown its tremendous value to model early onset diseases such as Progeria (Lo Cicero et al. 2018) or long QT syndrome (Moretti et al. 2010; Bellin et al. 2013), most cells derived from pluripotent stem cells show poor maturity and functionality making it more challenging to model late-onset diseases such as type 2 diabetes, or neurodegenerative diseases like Alzheimers disease or Parkinsons.

CRISPR/Cas9 technology can be used to induce disease-mutations in wild type iPS and to correct mutations in patient specific iPS to create isogenic controls. CRISPR/Cas 9 technology has been used to mutate specific genes, previously identified by GWAS involved in T2D, to study their effect on β cell function (Zeng et al. 2016).

Pluripotent stem cell technology can also be used for efficacy and toxicity drug screening. The first large-scale drug screening identified 1 compound among 6912 to improve aberrant splicing responsible for dysautonomia, on neural crest precursors derived from family dysautonomia by the iPSC (Lee et al. 2012). Such technology was also used for drug screening for Progeria disease (Blondel et al. 2016; Lo Cicero et al. 2016).

Clinical application of pluripotent stem cells

The discovery of iPSC has provided a great interest for regenerative medicine to replace the patient's damaged cells or regenerate them. Clinical trials with embryonic stem cell-derived cells are currently underway for the treatment of various diseases (Table 6) however, ethical concerns limit the utilization of these cells. On the other hand, iPSC cells are independent of ethical concerns and might be used for both autologous and allogeneic applications (Table 7) (Trounson and DeWitt 2016). Autologous transplants are assumed to be safer to avoid immune rejection. Nevertheless, currently, this strategy does not appear feasible as a general treatment option due to the time required to generate patient derived iPS cell line and excessive cost.

An accepted strategy currently under evaluation is to produce differentiate cells from HLA (Human Leukocyte Antigen) homozygous donor iPS cells. Indeed, using HLA compatible cells will a reduce the risk of rejection and the time needed to provide HLA-matched iPSC products to significant numbers of patients. Although, the benefit of HLA matching to minimize rejection has been demonstrated, an immunosuppressive treatment may be required (Turner et al. 2013; Wilmut

et al. 2015; Lee et al. 2018). For this purpose, HLA haplobanks has been envisaged (Okita et al. 2011; Gourraud et al. 2012; Taylor et al. 2012; Jacquet et al. 2013) and a Global Alliance for iPSC Therapies (GAiT) developed to achieve a consensus on clinical-grade pluripotent stem cells.

Table 6: Clinical trials with embryonic stem cell-derived cells

Disease	Cell type	NCT	Investigator	References
Ischemic Heart Disease	hESC-derived CD15+ Isl-1 progenitors	NCT02057900	APHP- France	(Menasché et al. 2018)
Dry Age-related Macular Degeneration	hESC-derived retinal pigment epithelium	NCT01344993	Astellas	(Schwartz et al. 2015)
Spinal Cord Injury	hESC-derived oligodendrocyte progenitors	NCT02302157	Asterias Biotherapeutics	
Parkinson disease	hESC-derived neural precursor cells	NCT03119636	Chinese Academy of Sciences	(Wang et al. 2018)
Type 1 Diabetes	hESC-derived pancreatic endoderm cells	NCT03163511	Viacyte	

Table 7: Clinical trials with induced pluripotent stem cell-derived cells

Disease	Cell type	Clinical Trial Number	Investigator	References
Exudative Age-related Macular Degenerescence	Autologous iPSC-derived retinal pigment epithelial	UMIN000011929	Riken	(Mandai et al. 2017)
Graft-versus-host-disease (GvHD)	Allogenic iPSC-derived mesenchymal stem cells	NCT02923375	Cynata Therapeutics	

6. Stem-cell derived pancreatic endocrine cells

In 2001, Assady et al. (Assady et al. 2001) reported for the first time, the generation of insulin producing cells generated by spontaneous differentiation of human embryonic stem cells (hESC). A major step forward was the efficient differentiation of hESC to definitive endoderm (Kubo et al. 2004; D'Amour et al. 2005) (stage 1), a prerequisite for subsequent differentiation to pancreatic progenitors. From 2006-2009 protocols were published to guide definitive endoderm cells to primitive gut tube (stage 2) by vitamin C and FGF7 activation and further to posterior foregut (stage 3) by inhibiting BMP and SHH while maintaining FGF7 signaling pathway. The next stage (stage 4) was a breakthrough in mimicking pancreas organogenesis, which leads to the generation of multipotent pancreatic progenitors (PP). The cells can be generated with high efficiency by inhibition of BMP signaling pathway and tankyrases and the activation of EGF. Once transplanted *in vivo*, the multipotent PPs differentiate into all pancreatic cell types including the insulin producing β cells (D'Amour et al. 2006; Kroon et al. 2008). This protocol was further optimized (Schulz et al. 2012) and it is currently used in clinical trials in USA and Canada by ViaCyte as a regenerative approach for the treatment of T1D (NCT02239354, NCT03163511, NCT03162926). These publications were obtained with specific embryonic stem cell lines (CyT49 and CyT203) not readily available. Since then, many modified and improved protocols have been published using several cell lines (Table 8) (Chen et al. 2009; Ameri et al. 2010; Mfopou et al. 2010; Nostro et al. 2011, 2015; Xu et al. 2011; Rezania et al. 2012, 2013). Although there has been no direct comparisons between the different protocols, differentiated cells were often polyhormonal (figure 18), poorly functional (not responsive to glucose) and resemble fetal cells (Hrvatin et al. 2014). While polyhormonal cells are rare in human adult pancreas ($1.34\% \pm 0.6\%$), they appear not to be an artifact of *in vitro* differentiation as they are frequent in human fetal pancreas (11-13 week-old: $28.79\% \pm 5.6\%$) (Riedel Kieffer Diabetologia 2012). It has been previously shown that polyhormonal insulin/glucagon positive cells have been shown to be NKX6.1 negative/ PDX-1 negative and ARX positive (Riedel Kieffer Diabetologia 2012). With time these cells become glucagon positive α cells (Figure 18).

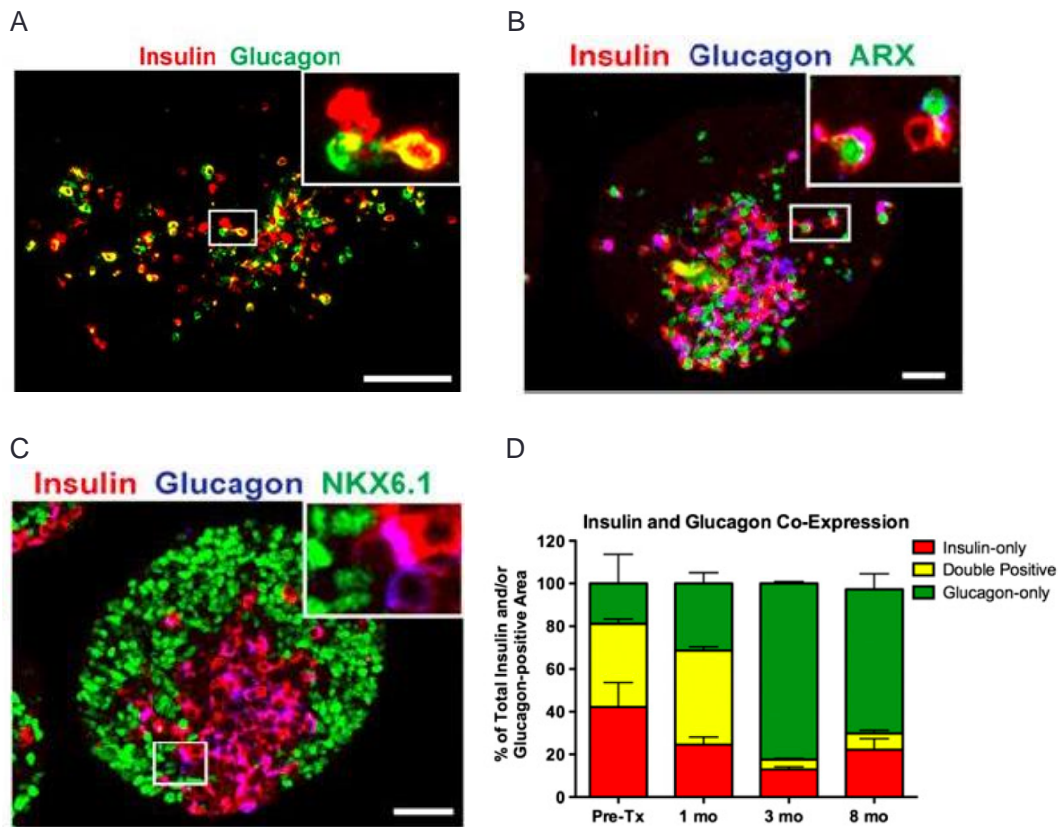


Figure 18: (A) Insulin and glucagon polyhormonal cells, pluripotent stem cell derived insulin and glucagon positive cells are ARX positive (B) and NKX6.1 negative (C). Proportion of insulin positive, glucagon positive and double positive cells in pre-transplanted clusters and in grafts at 1, 3 and 8 months post-transplantation showing that transplanted cells mainly convert into α cells. (Rezania et al. 2012).

Strategies to obtain monohormonal insulin positive cells became a priority. Cell progenitor cells positive for NKX6.1 have been shown to rather develop into insulin positive cells associated with improved *in vivo* function (Rezania et al. 2013). Another study identified key signaling pathways to generate NKX6.1 positive cells from various human pluripotent stem cell (hPSC) lines and demonstrated that NKX6.1 positive progenitors lead to mono-hormonal positive cells (Nostro et al. 2015). The NKX6.1 positive pancreatic progenitor cell should be c-peptide negative at S4. Russ *et al.* also demonstrated that NKX6.1+/PDX1+ progenitor cells generate mono-hormonal insulin positive cells (Russ et al. 2015).

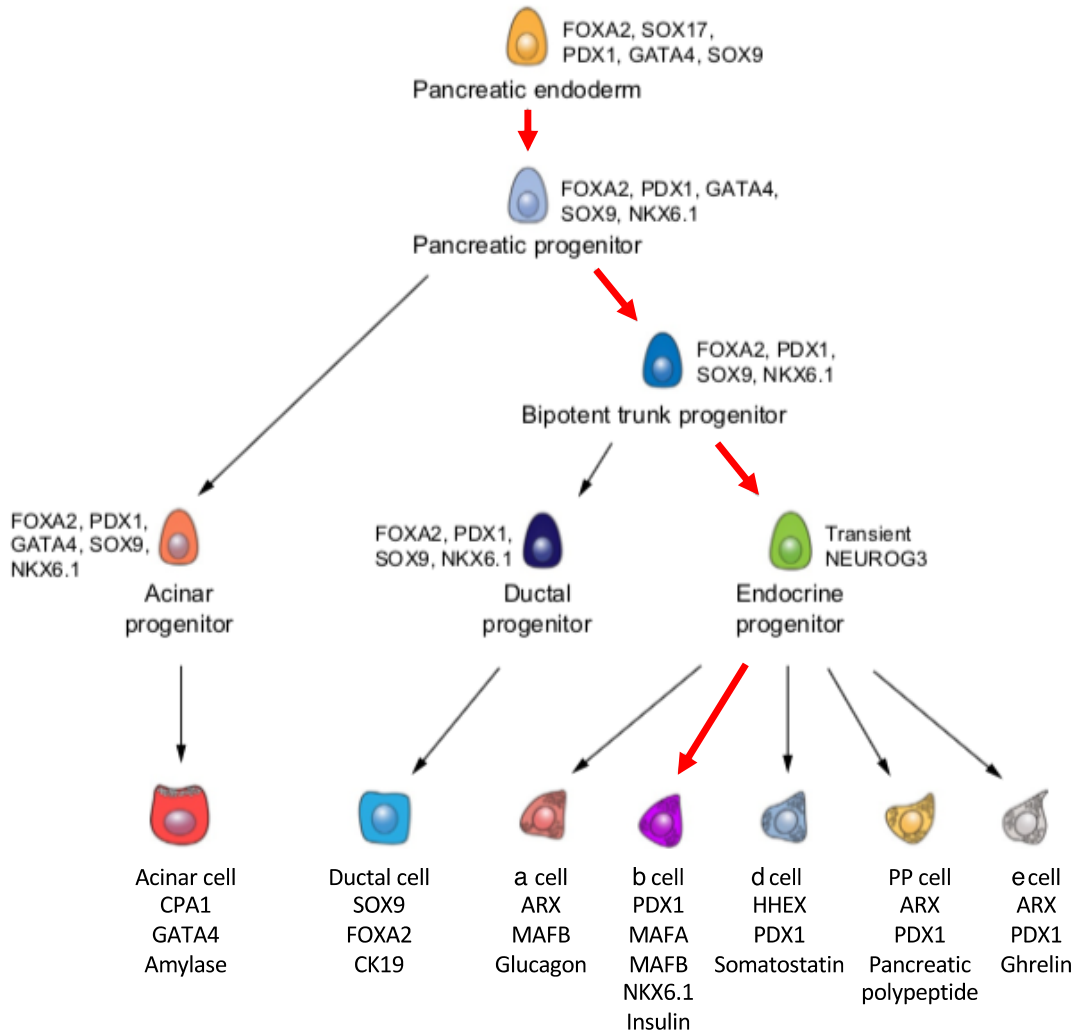


Figure 19: Overview of lineage segregation in human pancreatic development. Key transcription factors for each cell type at various developmental stages are shown in this graph. The differentiation pathway for β -like cells is highlighted by red arrows (adapted from Petersen et al. 2018).

β cell differentiation is a complex process that is orchestrated by the expression of key transcription factors (Figure 19 and 20). To study β cell commitment *in vitro*, differentiation protocols were prolonged to stage 5 including NGN3+ endocrine progenitors and stage 6 insulin+ β -like cells (BLCs) (Pagliuca et al. 2014; Rezanian et al. 2014; Russ et al. 2015). BLCs generated *in vitro* at stage 6 (or in some groups stage 7) were 50% insulin positive; these cells respond to static glucose-stimulated insulin secretion and restore normal glycemia in 8-12 weeks when transplanted in

immunodeficient diabetic mice (Rezania et al. 2014). However, those *in vitro* generated cells were still immature as they had major differences to native β cells, such as gene expression profiles (particularly high NGN3 and proinsulin and low urocortin 3 (UCN3) expression levels), calcium signaling and lack of response in dynamic GSIS (Pagliuca et al. 2014). UCN3 is a neuropeptide expressed in mature α and β cells (van der Meulen et al. 2012). It has been shown that only functional β cells express UCN3 and it is induced in hESC-derived β cells after *in vivo* maturation (Blum et al. 2012, 2014). Furthermore, Ghazizadeh et al. demonstrated that increased *in vitro* UCN3 expression is associated with increased static GSIS response (Ghazizadeh et al. 2017). More recently, two studies demonstrated the enhanced functional maturation of BLC *in vitro* by mimicking endogenous endocrine cell clustering comparable to human pancreatic islets (Nair et al. 2019; Velazco-Cruz et al. 2019). Nair *et al.* used an insulin-GFP labelled hPSC line and enrichment by FACS purification before reaggregating single cells into clusters generated 99% of chromogranin A positive cells. For the first time, generated cells showed, in dynamic GSIS (perfusion), a robust first phase response however insulin secretion was not sustained in the second phase. Velazco-cruz *et al.* published a differentiation protocol without selection or sorting allowing to obtain BLC with an enhanced functional maturation as they display both first and second phase response similar to the response of native human islets in a perfusion experiment. In addition, differentiated cells had an increase in their insulin expression and content. Both studies, show *in vivo* function of transplanted cells rapidly after grafting (10 days). These two studies represent a major technical advance in the differentiation of human pluripotent cells, although a difference in UCN3 and MAFA mRNA expression persists between the cells produced and human islets. Table 8 summarizes the characteristics of the key published protocols.

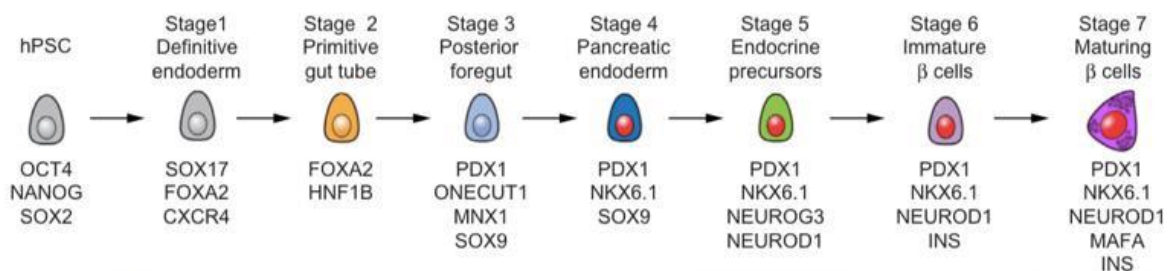


Figure 20: Overview of human pluripotent stem cells (hPSC) step-wise differentiation towards β cells. Different differentiation stages from pluripotent stem cell towards stage 7 (maturing β cell). Characteristic stage specific markers are shown below the corresponding stages (Petersen et al. 2018).

Table 8: Characteristics of published pancreatic β -like cell differentiation protocols.

References	Cell type used	Last differentiation stage	Cell type produced and % of insulin or c-peptide positive cell produced
(D'Amour et al. 2006)	CyT203 (ESC)	Hormone expressing endocrine cell secreting c-peptide and proinsulin	INS (7,3%), GCG, SST, PPY, GHRL
(Jiang et al. 2007a)	H1, H7, H9 (ESC)	Islet-like clusters	INS, GCG, SST
(Jiang et al. 2007b)	H1, H9 (ESC)	Insulin producing cell	INS, GCG, SST
(Kroon et al. 2008)	CyT49, CyT203 (ESC)	Pancreatic endoderm and endocrine precursor	INS+, GCG, SST, PPY, GHRL
(Rezania et al. 2012)	H1, ESI-49 (ESC)	Pancreatic endoderm and endocrine precursor	INS (10%), GCG, SST, PPY
(Schulz et al. 2012)	CyT49 (ESC)	Pancreatic progenitor and endocrine precursor	INS, GCG, SST
(Rezania et al. 2013)	H1 (ESC)	Pancreatic endoderm and endocrine precursor	INS, GCG, SST, PPY, GHRL
(Rezania et al. 2014)	H1 (ESC), episomal iPSC	Maturing β -like cell	INS (>40% mono) GCG (4% mono) INS+/GCG (11%)
(Pagliuca et al. 2014)	HUES8 (ESC), hiPSC1, hiPSC2 (iPSC)	Glucose-responsive β -like cell	C-pep>50%, GCG
(Russ et al. 2015)	MEL1 Ins ^{GFP/W} (hESC)	β -like cell	INS (>60%), GCG, SST
(Nostro et al. 2015)	H1, H9 NKX6-1 ^{GFP/W} , MEL-1, INS ^{GFP/W} (ESC), hiPSCs 38-2, MSC-iPSC1, BJ-iPSC1 (iPSC)	NKX6-1+ pancreatic progenitor	Mean 70% NKX6.1
(Millman et al. 2016)	T1D iPSC, hiPSC1, hiPSC2 (non-diabetic iPSC)	Glucose-responsive β -like cell	C-pep (40%), GCG

(Ghazizadeh et al. 2017)	H1, HUES8, 1005 iPSC, INS ^{GFP/W} HES 3 (ESC), 1018 iPSC	β -like cell	C-pep (30%), GCG (9%)
(Nair et al. 2019)	MEL-1 INS ^{GFP/W} (ESC)	GFP sort enriched β -like cell cluster	C-pep (87,4%), GCG (5%)
(Velazco-Cruz et al. 2019)	HUES8 (ESC), hiPSC-1, hiPSC2, T1D iPSC	Glucose-responsive β -like cell	C-pep (75%), C-pep/gcg (19%), C-pep/SST (12%), SST, GCG (4%)

The finding that hPSC derived cells are functionally immature has been reported for pancreatic β cells, hepatocytes, neurons, and hematopoietic cells (Miller et al. 2013). This is a major inconvenience for clinical applications, basic research, and drug screening. The production of fully functional cells with characteristics of mature cells is an essential goal in stem cell biology. Most of the *in vitro* differentiated cell types reach maturation only after prolonged culture or *in vivo* transplantation for long periods of time. Many research groups that use pluripotent stem cells and patient derived stem cells to model late onset neurodegenerative diseases such as Parkinson's disease and Alzheimer disease, or metabolic diseases associated with aging and obesity such as T2D, face with a particular challenge since pathological features may only arise upon aging.

The prolonged gestational period in humans compared to rodents may be in part responsible for the "fetal state" of differentiated hPSC. Indeed, Scharfmann *et al.* compared the endocrine development of early murine and human embryonic pancreas in the muscle of immunodeficient mice that (Castaing et al. 2001) and showed that the endocrine differentiation of early human embryonic pancreas occurs over 60 weeks (> 1 year) compared to only 2 weeks with murine embryonic E12.5 pancreas.

7. Factors associated with the maturation of pancreatic β cells

Adult endocrine cells are long-lasting cells like post-mitotic cortical neurons (Cnop et al. 2010; Arrojo E Drigo et al. 2019). Pancreatic islet cells undergo dramatic changes during life in terms of functionality and in terms of their proliferation capacity. Neonatal islet cells are highly proliferative and insulin secretion is at low levels and normally increases during development and with time. In contrast, islets from elderly people display low cell replication capacities (Hellerström and Swenne 1991; Bonner-Weir et al. 2016). Furthermore, few proteins have been linked to β cell maturation, among which MAFA, ERR γ (Estrogen-related receptor γ), NeuroD and UCN3 (Urocortin 3). MAFA is up-regulated by glucose and activates the insulin gene (Kataoka et al. 2002; Olbrot et al.

2002; Matsuoka et al. 2004), during rat development, MAFA gradually increases and shifts its cytoplasmic localization to a nuclear localization (Matsuoka et al. 2004; Artner et al. 2010; Aguayo-Mazzucato et al. 2011) and leads to a positive GSIS response. Increases of MAFA, p16 and improved GSIS have been induced by tri-iodothyronine hormone (T3) (Aguayo-Mazzucato et al. 2013, 2015, 2018). ER γ expression increased during pancreas development and is required for post-natal β cell maturation as well as metabolic maturation of β -like cells derived from human iPSC (Yoshihara et al. 2016).

UCN3 is highly expressed in adult human β cells and increases during *in vivo* maturation of insulin expressing cells derived from hPSC (Blum et al. 2012; van der Meulen et al. 2012). However, UCN3 is a passive maturation marker as UCN3 treatment does not promote maturation of stem cell-derived endocrine cells (Blum et al. 2012).

In terms of functionality, it has been shown that adult murine β cells show changes in methylation patterns which repress proliferation and activate genes involved in insulin secretion resulting in higher insulin secretion in β cells from older mice than β cells from young mice (Avrahami et al. 2015). However, this finding is controversial as others found no intrinsic functional difference between old and young islets and rather point to an aging extracellular matrix and vessels (Almaça et al. 2014). Similarly, insulin secretion in human islets from adult donors (>28 years old) was superior to human islets from young donors (<9 year old). Additionally, p16^{ink4a} (p16), which is expressed during normal aging of β cells and, transgenic mice in which p16^{ink4a} is activated both show increased insulin secretion (Helman et al. 2016).

Different methods have been tested to age *in vitro* hPSC-derived lineages, one of which includes overexpressing progerin.

8. Directing aging using progerin

Although human pluripotent stem cell differentiation is a useful tool to deciphering embryogenesis, physiopathology, model disease and also for cell replacement, lack of maturation and fetal-like properties of most of the PSC-differentiated cells types can be a challenge, particularly to model late-onset diseases. Indeed, from a development perspective there is a continuity between cell specification, maturation and aging. Cellular specification is characterized by the development of a specific transcriptional program and the expression of markers, maturation through the acquisition of a function and aging through the progressive decline of this function (Studer et al. 2015).

Indeed, iPS cells derived from old donors (as young donors) show rejuvenation patterns during reprogramming in particular an increase of telomer size (Marion et al. 2009) and loss of senescence markers (Prigione et al. 2010; Suhr et al. 2010), and months of post-differentiation maturation are necessary for the acquisition of a functionality (Saha and Jaenisch 2009; Liu et al. 2012a).

Several strategies have been developed in order to induce maturation or aging in differentiated iPSC cells, such as cellular stressors which target mitochondrial function or protein degradation (Nguyen et al. 2011; Cooper et al. 2012; Liu et al. 2012b; Shi et al. 2017a), overexpressing progerin (Miller et al. 2013), 3D co-culture which enhance cell-cell interaction (Giacomelli et al. 2017; Shi et al. 2017a; Correia et al. 2018; Doss and Sachinidis 2019; Yan et al. 2019), or the use of telomerase inhibitors (Vera et al. 2016) (Figure 21).

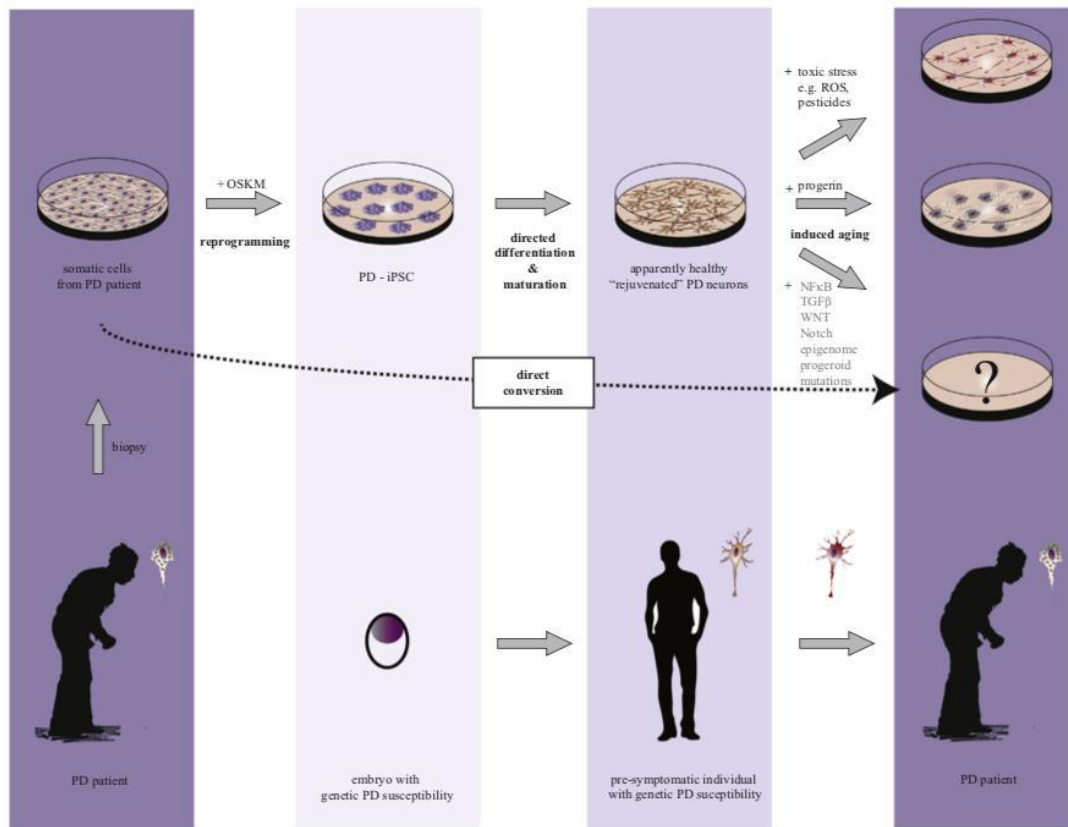


Figure 21: Inducing cellular aging in hPSC-derived lineages (Cornacchia and Studer 2017).

In 2011, Izpisua Belmonte group showed that iPSC-derived from progeria patients did not express aging markers and progerin, while after differentiation, the smooth muscle cells they expressed signs of premature senescence phenotypes (Liu et al. 2011). Studer et al. has used progerin as a tool to accelerate aging in neurons (which are not affected by progeria disease) to obtain a model of late-onset of Parkinson disease (Miller et al. 2013). Indeed, progerin overexpression induced age-associated changes in iPSC differentiated neurons including nuclear blebbing, increased accumulation of γ H2AX (DNA damage), dendrite shortening and global transcriptional changes (Figure 22).

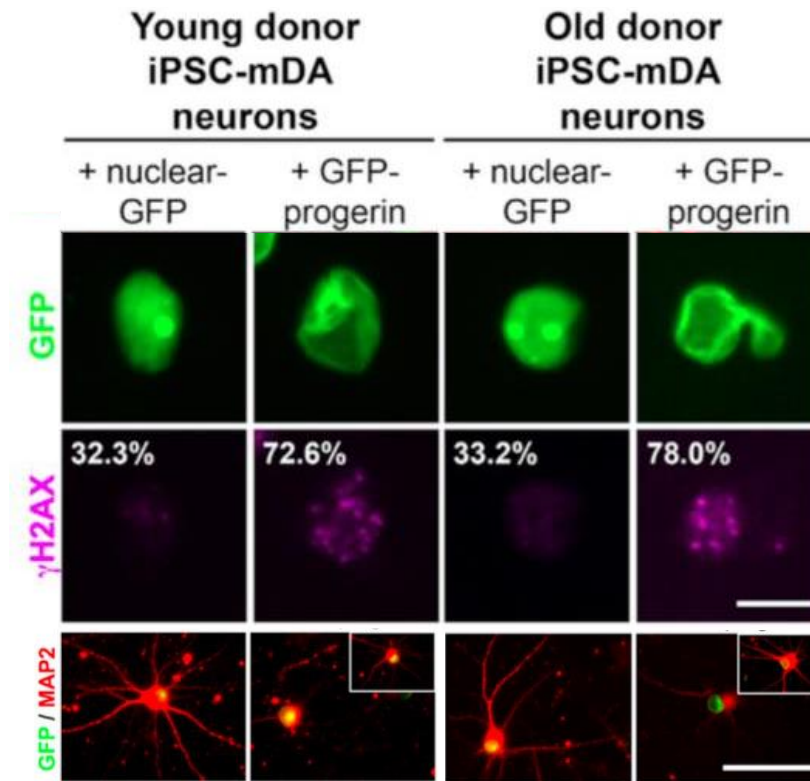


Figure 22: Age-associated changes induced by progerin overexpression in iPSC-mDA Neurons derived from young and old donors. γ H2AX (DNA-damage, pink) and MAP2 (dendritic marker, red) (Miller et al. 2013).

9. Hutchinson-Gilford Progeria Syndrome

Hutchinson-Gilford Progeria Syndrome (HGPS), also known as Progeria, is a very rare genetic disease which is part of laminopathies (heterogenous group of genetic disorders caused by mutations in LMNA gene encoding nuclear Lamin A/C). HGPS is characterized by a premature-aging like phenotype. It was first described by Hutchinson 1886 and Gilford 1887.

HGPS is caused by a single *de novo* point mutation on the LMNA gene, which is located on chromosome 1q22. The LMNA gene code for two different types of lamins: Lamin A and C and are produced through alternative splicing of exon 10. Indeed, exons 1 to 10 code for lamin C while exons 1 to 12 code for prelamin A (which requires post-translational modifications to form lamin A). These post-translational modifications are on the CaaX motif and are an isoprenylation by a farnesylase transferase, a cleavage of terminal amino acids by ZMPSTE24 (metalloprotease homologous to STE24), a methylation of cysteine by isoprenylcysteine carboxymethyl transferase and the cleavage of the 15 C-terminal amino acids by ZMPSTE24 (Figure 23).

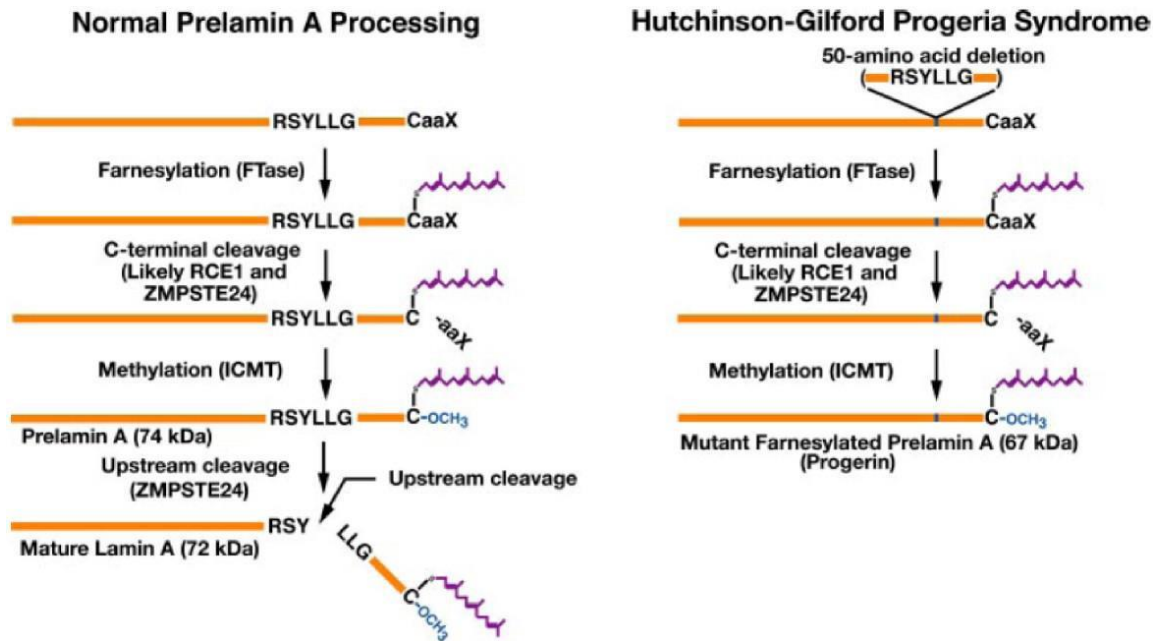


Figure 23: Schematic overview of the biogenesis of lamin A and progerin. Under physiological conditions, prelamin A is synthesized as precursor, and after 4 post-translational maturation steps, it becomes lamina A (left panel). In Progeria patients, prelamin A is deficient of 50 amino acids, which hinders the last stage of maturation. Progerin remains farnesylated and carboxymethylated in the C-terminal position (right panel) (Coutinho et al. 2009).

The onset of Progeria is due to a point mutation of the LMNA gene. There are more than 400 mutations associated with this disease reported to date (<http://www.umd.be/LMNA/>) but the most frequently observed is the replacement of a cytosine by a thymine in position 1824 (c.1824>T) (De Sandre-Giovannoli et al. 2003; Eriksson et al. 2003; Verstraeten et al. 2006; Moulson et al. 2007). This mutation activates a cryptic splicing site, responsible for the deletion of 150 base pairs in the lamin A transcript. Therefore, the protein produced, lamin A Δ 50 also called progerin, is truncated of 50 amino acids on its C-terminal region. The produced protein undergoes the same post-translational modifications as lamin A except for the last cleavage. Indeed, the deletion is responsible for the absence of the ZMPSTE24 (Zinc Metallopeptidase STE24) enzyme recognition site which allows the last proteolysis. Therefore, the protein produced (progerin) remains farnesylated and carboxymethylated.

Lamin A is one of the intermediate filaments of type V constituting the nuclear lamina. Nuclear lamina is the structural support of the nuclear envelope, and is also involved in many cellular mechanisms such as gene regulation and transcription, cell differentiation, DNA replication and

repair, and nuclear envelope assembly (Goldman et al. 2004; Capell and Collins 2006; Frock et al. 2006; Shumaker et al. 2006; Dechat et al. 2007; Young et al. 2013).

The mutation of the lamin A responsible for HGPS alters the structure and function of the nuclear lamin. As result, the nuclei of the cells have an abnormal shape (blebbing) (Figure 24).

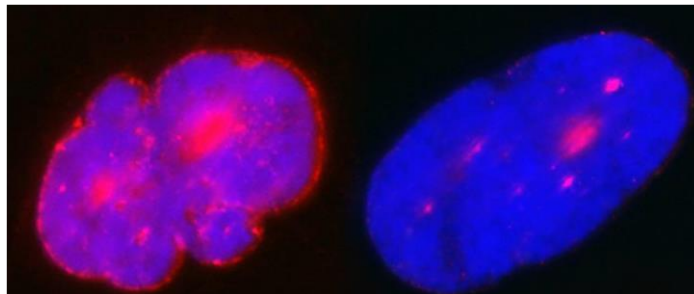


Figure 24: Representative immunofluorescent image of HGPS cells: progerin (red) and human DNA (blue) showing nuclei deformation with high level of progerin (left) compared to low level of progerin (right). From K Djabali / TUM

Progerin is responsible for the onset of nuclear and cellular defects commonly observed during physiological aging, such as telomere dysfunction (Cao et al. 2011), increased DNA damage, senescence (van Deursen 2014), epigenetic changes and cell cycle deregulation (Cao et al. 2007a; Carrero et al. 2016).

Children suffering from progeria show no evidence of the disease at birth, the first clinical signs appear in the early years of life: growth retardation, characteristic facial features (prominent forehead and scalp veins, pinched nose, thin lips and abnormal dentition), alopecia, loss of subcutaneous adipose tissue, skeletal dysplasia, diminished bone mineral density, skeletal muscle wasting, severe cardiovascular decline with progressive coronary atherosclerosis (Hennekam 2006; Merideth et al. 2008). HGPS is a “segmental ageing disease”, the main tissues affected are of mesodermal origin, in particular blood vessels, bones, heart, muscles, skin and dander, whereas organs such as liver, kidneys, lungs, gastrointestinal tract and brain are not affected (Gordon et al. 2007; Ullrich and Gordon 2015). A team using genome-scale expression profiling found that in patients with progeria, the most affected gene was MEOX2/GAX (Mesenchyme Homeobox 2/ Growth Arrest-specific Homeobox) which is a transcription factor that is a negative regulator of mesodermal tissue proliferation (Csoka et al. 2004). Indeed, abnormal oral glucose-tolerance test (OGTT) have been observed in only 2 out of 13 patients and an abnormal fasting glycemia over 100mg/dl was observed in only 1 out of 13 HGPS patients (Merideth et al. 2008).

Premature-aging features observed in HGPS are shared with normal aging although HGPS patients do not express all physiological aging features such as osteoporosis, cancer or dementia (Figure 25). The sparing of the cognitive functions may be attributed to the upregulation of miR-9. Indeed, it has been shown that miR9 microRNA expression in neural cells allows their preservation (Nissan et al. 2012). The similitude between HGPS and physiological aging can be explained by the implication of lamin A defects in normal aging. Indeed, fibroblasts from healthy aged individuals presented nuclear abnormalities comparable to HGPS fibroblasts as well as changes in histone modifications and increased DNA damage (Scaffidi and Misteli 2006). This discovery has been further confirmed by the detection of progerin in fibroblasts of healthy patients responsible for mitotic defects associated with HGPS (Cao et al. 2007b; McClintock et al. 2007). In addition, progerin accumulation has been detected in the adventitial layer of arteries from healthy aged donors (Olive et al. 2010).

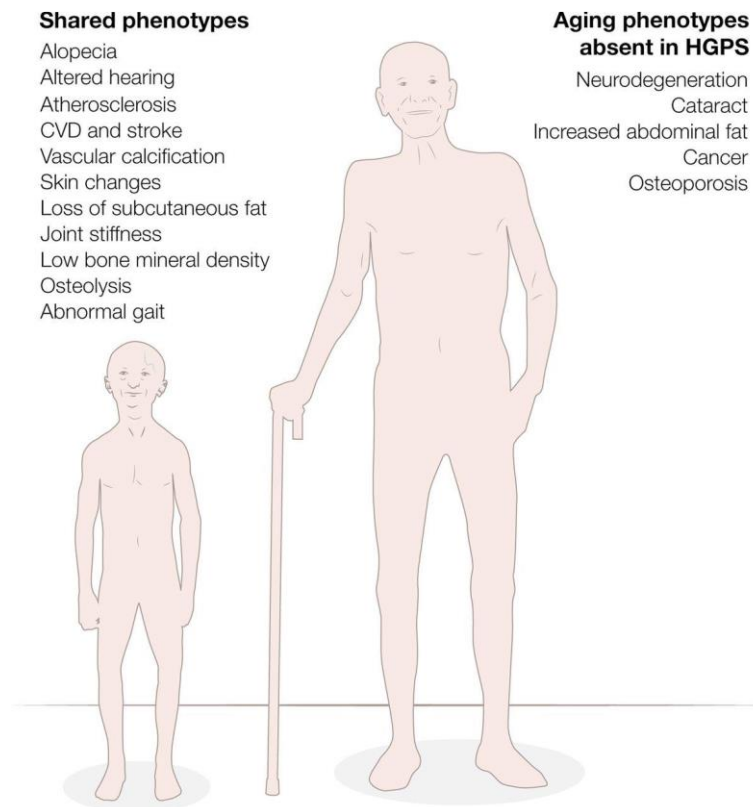


Figure 25: Similarities and differences between HGPS (left) and physiological aging (Strandgren et al. 2017).

10. Objectives

Our first objective (Chapter 3) was to test the feasibility and reproducibility of methods already published in the literature to produce pseudo-islets from human pancreas and to adapt them to clinical transplantation constraints (animal derived component free). Moreover, the objective was to compare the functionality of pseudo-islets with the native human islets, *in vitro* and *in vivo*, and to evaluate if the use of pseudo-islets could be a valid strategy to reduce the donor derived heterogeneity observed in native human islets. An important functional heterogeneity is observed between the different human islet preparations (Nasteska and Hodson 2018; Dybala and Hara 2019) and there are several explanations for this heterogeneity (Kayton et al. 2015; Lyon et al. 2016; Westacott et al. 2017; Henquin 2018).

Therefore, our laboratory was interested in testing the feasibility and reproducibility of this technology. By producing 80-100 μ m pseudo-islets and comparing their function *in vitro* and *in vivo* with their matched native human islet counterparts to evaluate whether inter-donor heterogeneity (donor's signature) persists or is abolished.

Our second objective (Chapter 4) was to produce endocrine cells from pluripotent stem cells and subsequently test if progerin could accelerate the maturation of the pancreatic endocrine cells of endodermal origin. To achieve this, we used several types of stem cells: the human embryonic stem cell H1 and induced pluripotent stem cells (iPS) DF19.9 from healthy individuals, and iPS HGPS 1972 from patients with progeria. We first aimed to optimize the differentiation protocol for each specific cell lines mainly stage 1 definitive endoderm and then S4 pancreatic progenitors, and then, to determine if progerin was expressed during the differentiation steps and to investigate if it had an effect on endocrine differentiation and maturation both *in vitro* and *in vivo*.

The production of functional cells from pluripotent stem cells remains an important issue. The majority of cells generated *in vitro* from human pluripotent stem cells are immature post differentiation which is, for instance, substantiated by the expression in iPS-generated hepatocytes of α fetoprotein and low albumin levels (Baxter et al. 2015). Beta cells generated from pluripotent stem cell technology are immature and do not typically respond to glucose (Hrvatin et al. 2014). Studer's laboratory recently presented a strategy to artificially induce aging *in vitro*, which is particularly interesting to obtain model of late-onset diseases as Parkinson or Alzheimer, and perhaps type 2 diabetes mellitus. In 2013, Studer's group exploited progerin, the protein involved

in Hutchinson-Gilford Progeria Syndrome. They demonstrated that after the differentiation of iPS cells into fibroblasts and neurons, progerin overexpression accelerated *in vitro* aging (Miller et al. 2013). The over-expression of progerin was sufficient to induce aging markers similar to elderly donor cells. Although progerin is a pathological protein, low levels of progerin expression have been found in healthy individuals (Scaffidi and Misteli 2005). Progerin has been implicated in the aging of skin induced by UV light (Takeuchi and Runger 2013).

Therefore, our third objective (Chapter 5) was to study the influence of the overexpression of progerin on pancreatic endocrine cell differentiation. To do this we used iPS cells derived from patients with the premature aging disease HGPS or Progeria. We compared these cells to H1 cells and in order to confirm the specific role of progerin, we planned to overexpress progerin in H1 cells during differentiation.

Chapter 2: Materiel & Methods

1. Materials

1) Human pluripotent cell lines

iPS DF19-9-7T (referred to herein as iPS DF19.9) were purchased from WiCell®. They were reprogrammed from foreskin fibroblasts from a male donor with no reported disease and using a non-integrating method Sendai virus (OCT4, SOX2, NANOG, LIN28, L-MYC, KLF4, SV40LT) by Dr. J. Thomson at University of Wisconsin (UW, USA) (Yu et al. 2009). WA01 cells (referred to herein as H1) were purchased from WiCell®. Dr. Julie Kerr-Conte is authorized to import, conserve and do research on H1 cell line by the ABM (Annexe 2). This embryonic stem cell line was derived from a human blastocyst by Dr. J. Thomson (UW, USA) (Thomson et al. 1998). iPS HGPS AG01972 cells (referred to herein as iPS HGPS) were kindly provided by Dr. X. Nissan and Dr. M. Peschanski (I-STEM, France). iPS HGPS AG01872 cells were reprogrammed from HGPS patient fibroblasts (Fibro HGPS Ag001972) using Yamanaka's method with OCT4, KLF4, SOX2, c-MYC (Takahashi et al. 2007).

2) Human islets

Human islets are isolated from pancreata obtained from brain dead donors by Prof. F. Pattou's team (Inserm U1190) using the Edmonton protocol (Shapiro et al. 2000). Islet isolation and evaluation was assessed by trained employees of the biotherapy platform.

To gauge the differentiation state of the *in vitro* stem cell-derived endocrine cells we used a pool of 10 human islets coming from 10 different donors for qPCR experiments. For "previous results", qPCR results were compared to a single donor.

The pseudo-islets generated from each donor were compared to native islets at Day 1 and to native islets at D8 from the same donor. Islet donor characteristics are described in the table 9.

Table 9: Islet donor characteristics for pseudo-islets experiments.

Lot	1063	1044	1037	1035
Age (years)	59	39	30	49
BMI	32	22	21	21
Sex	F	M	M	M
HbA1c (%)	5,7	5,8	5,1	5,5
Alcohol	no	no	yes	no
Tobacco	yes	no	yes	no
Cold ischemia time	6,4	5,8	5,1	5,5
Cardiorespiratory arrest (min)	0	15	30	0
Intensive Care Unit stay (days)	5	5	1	8

3) Human fibroblasts

Human fibroblasts were isolated in the laboratory from the human islet fraction or from Hutchinson Progeria patients, fibroblasts HGPS Coriell, HGPS Ag001972, HGPS 8243 (referred to herein as fibro HGPS) were kindly provided by Dr. X Nissan and Dr. M. Peschanski (I-STEM, France).

4) Cell culture

Cell culture reagents

Reagent	Company	Catalog #
1-Thioglycerol (MTG)	Sigma	M6145
Accutase	PAA Laboratories	L11-007
Agarose	Sigma	A9045
Ascorbic Acid	Sigma	A4544
B-27 (without vitamin A)	Gibco	12587010
β -Mercaptoethanol	Sigma	M3148
BSA	Sigma	A9647
CHIR99021	SelleckChem	S2924
CMRL 1066	Connaught Medical Research Laboratories	PM-C1051
DMEM High Glucose	Gibco	41966-029
DMEM/F-12	Gibco	31330-038
DMSO	Sigma	D8418

DNase I	Roche	Pulmozyme
Dorsopmorphin	Sigma	P5499
EGF	R&D system	236-EG
FBS	Eurobio	CVFSVF06-0U
FGF-10	R&D system	345-FG
Glutamine	Gibco	25030-024
Ham's F12	Gibco	21765-024
HEPES	Gibco	15630
IMDM	Gibco	21980-032
Insulin 100 UI/mL	Lilly	Umuline NPH
m-TeSR	STEMCELL Technologies	85851
m-FreSR	STEMCELL Technologies	05854
Matrigel	Corning	354277
MCDB 131	Gibco	10372-019
N2 supplement	Gibco	17502-048
Nicotinamide	Sigma	N0636
Noggin	R&D system	3344-NG
PBS (Without Ca ²⁺ & Mg ²⁺)	Gibco	12190-094
Penicilin/Streptomycin	Sigma	P0781
Retinoic Acid	Sigma	R2625
Rock inhibitor Y-27632	STEMCELL Technologies	72304
RPMI 1640	Gibco	21875-034
SANT-1	Tocris	1974
Sodium bicarbonate 7,5%	Gibco	25080-060
Sodium pyruvate solution	Gibco	11360-039
StemMACS iPS Brew	Miltenyi Biotec	130-104-368
TrypLE	Gibco	12604-021
Versène	Gibco	15040-033

Cell culture material

Material	Company
6 well plate	Falcon
Sphericalplate 5D	Kugelmeiers

Cell culture media

iPS DF19.9 and H1 cells:

m-TeSR

supplement 5X

iPS HGPS:

iPS Brew
 supplement 50X

Fibroblasts:

DMEM + glutamax
 SVF 20%
 Sodium Pyruvate 1%
 HEPES 1%
 P/S 1%

Human islets and pseudo-islets:

CMRL 1066
 HSA 0.0625%
 Insulin 80UI/L
 P/S 1%

5) Molecular biology

Materials for molecular biology

Lysis buffer (RNA): Qiagen

Extraction: RNeasy Mini kit (Qiagen)

RNA quality: Experion (Biorad)

RNA Dosage: Nanodrop (Thermo Scientific)

Retrotranscription: Reverse Transcriptase : iScript (64179970 – Biorad)

Quantitative real-time PCR:

- SYBR Green Supermix SSO Advanced (64225938 – Biorad)
- TAQMAN Gene Expression Assay (4453320)

Primers for Sybergreen qRT-PCR

Name	5' to 3' Sequence
CHGA	5' gagaaggcctgagtgaga 3' 3' agctccatccacagccagag 5'
INS	5' tgcacagaagaggccatca 3' 3' cgttccccgcactagga 5'

GCG	5' gtcccaagagggttgc 3' 3' gtctgcctgggaagctgaga 5'
SST	5' gctgtgtctgaaccaacc 3' 3' attctgcagcagctttgc 5'
NKX6.1	5' agaagcacgctgccgagatg 3' 3' tctcgtcctccagttggat 5'
PDX1	5' ctgccttccatggatgaa 3' 3' caacatgacagccagctcca 5'
ARX	5' cctcactgcatcgacagc 3' 3' ctcttagggagccttgac 5'
KRT19 (CK19)	5' ccagccggactgaagaattg 3' 3' tgggctcaataaccgctgat 5'
SSEA4	5' tggacgggcacaacttcac 3' 3' gggcaggttctggcactct 5'
CXCR4	5' ggaacctgtttcgtgaag 3' 3' aggacactgctgtagagtt 5'
FOXA2	5' tggacctcaaggcctacgaa 3' 3' cataatggccgggagtaca 5'
SOX17	5' gaacgcttcatggtgtggg 3' 3' gccgtactttagtgggg 5'
NGN3	5' ccaggcagtctggctttct 3' 3' gggagaagcagaaggaacaa 5'
MAFA	5' caaagagcgggacctgtaca 3' 3' ctacaggaagaagtcggccg 5'
RPL27	5' tctggtggtggaattgacc 3' 3' cctgtgggcattaggtgattg 5'

Taqman probes

Name	Probe
LAM A	6-FAM-actgcagctaccg-MGB
LAM C	6-FAM-atgcgaagctggtg-MGB
PROGERIN	6-FAM-cgctgagtacaacct-MGB
RPLP0	Hs9999902_m1

6) Immunohistochemistry

Antibody	Host / Specification	Dilution	Manufacturer
α -Chromo A	Rabbit	1/200	Abcam (ab15160)
α -CK19	Mouse	1/100	Dako (M0888)

α -CXCR4	Mouse	1/50	Thermo (PA3305)
DAPI	Vectashield Mounting Medium		Vector (H-1200)
α -FOXA2	Rabbit	1/50	Thermo (PA535033)
α -Glucagon	Rabbit	1/500	Abcam (ab92517)
α -Human nuclei	Mouse	1/100	Genetex (gtx82634)
α -Insulin	Guinea Pig	1/500	Dako (A0564)
α -LamA/C	Mouse	1/100	Santacruz (sc376248)
α -NKX6.1	Mouse	1/100	Biosciences (5630221)
α -Prelamin A	Rabbit	1/100	Diatheva (ANT0045)
α -Progerin	Mouse	1/100	Santacruz (sc81611)
α -P16	Mouse	1/100	Santacruz (377412)
α - γ H2AX	Mouse	1/100	Santacruz (sc517336)
α -53BP1	Mouse	1/100	Santacruz (sc515841)
α -ATG12	Mouse	1/100	Santacruz (sc271688)
α -IGF1r	Mouse	1/100	Santacruz (sc390130)

7) Flow cytometry (FCM)

Buffers:

FACS Buffer: PBS (w/o Ca²⁺ Mg²⁺) + 10% BSA

BD Cytotfix™ (BD, 554714)

BD Cytoperm™ (BD, 554714) (1/10 dilution)

Antibodies:

Antibody	Host / Specification	Dilution	Manufacturer
α -CXCR4-PE	Rat IgG2b	1:50	BD (551966)
α -cKit-APC	Mouse IgG1k	1:100	Life (CD11705)
α -NKX6.1-AF647	Mouse IgG1k	5 μ L/test	BD (563338)
α -PDX-PE	Mouse IgG1k	5 μ L/test	BD (562161)
α -c-peptide	Rat IgG2a	2-5 μ g/mL	DSHB(GN-ID4)

8) Fluorescence activated cell sorting (FACS)

Antibodies:

Antibody	Host / Specification	Dilution	Manufacturer
α -GP2	Mouse IgG1k	1/10 000	MBL (D277-3)
α -CXCR4-PE	Rat IgG2b	1:50	BD (551966)
α -c-Kit-APC	Mouse IgG1k	1:100	Life (CD11705)

9) Perifusion

Materials:

2110 fraction collector, Bio-Rad

Miniplus 3, Gilson

10) Mice

CB17 SCID from Charles River Laboratories (L'Arbresle – France)

Nude mice from Charles River Laboratories (L'Arbresle – France)

11) ELISA

Material:

Ultrasensitive c-peptide ELISA, Mercodia (10-1141-01).

12) Software

Software	Application	Manufacturer
CFX Manager	PCR	Bio-Rad
Amersham Imager 680 on-board software	Western-Blot	GE Healthcare
Zen Black	Confocal	Zeiss
Flow-Jo	Cytometry	LLC
Prism 7	Statistics	GraphPad
BD FACS sorter software	Cell Sorting	BD Biosciences

13) Microscopes and devices

Device	Manufacturer
BD Influx cell sorter	BD Biosciences
BD LSR Fortessa X-20 Cytometer	BD Biosciences
Incubator	Binder
Centrifuge 5702R	Eppendorff
Centrifuge Allegra X12R	Beckhman
CFX Connect RT-PCR	Bio-Rad
LSM710 Confocal microscope	Zeiss
Microscope Eclipse TS1000	Nikon
Amersham Imager 680	GE Healthcare
Verriti	Applied Biosystem

2. Methods

1. Cell culture

Cell culture conditions

All cells were cultured at 37°C and 5% CO₂.

Thawing and freezing

Vials with cryopreserved cells were thawed and transferred to a 15mL falcon tube to which DMEM media was added dropwise. Cell suspension was centrifuged at 200g during 5 minutes. Supernatant was removed and the cell pellet was resuspended in specific media for each cell line as detailed in materials – cell culture section.

For freezing of pluripotent stem cells, EDTA (Versene™) treatment during 3 to 5 minutes was used to remove pluripotent stem cells. Cells were detached using 2mL of DMEM media 3 times; cell suspension was centrifuged at 300g for 5 minutes. Supernatant was removed and the cell pellet was resuspended in mFreSR™ media. Cells were stored in Mr. Frosty™ Freezing Containers (Thermo Fisher) with isopropyl alcohol during 24 hours at -80°C before storage in liquid nitrogen.

Cell maintenance

Pluripotent stem cells were grown in 6-well plates coated with Matrigel™ diluted to 1:60. After 3 to 5 days cells reached approximately 70-80% confluence and their passage was done by adding

1mL EDTA per well for 3 to 5 min. Cells were detached using 2mL of culture media with 10uM of rock inhibitor, three times. Cell suspension was then centrifuged at 200g for 5 minutes.

Fibroblasts were cultivated in T75 flasks. Media was changed every other day.

Human islets and human pseudo-islets were cultivated in T150 flasks. Media was changed every other day. For native human islets and pseudo islets groups, cells were kept for up to 8 days post-isolation.

Cell differentiation

Cell differentiation was done without antibiotics, on Matrigel™ and according to:

- Odorico protocol (confidential agreement, adapted from (Xu et al. 2011))
- (Rezania et al. 2012)
- (Rezania et al. 2014)
- (Korytnikov and Nostro 2016)

STEMdiff™ Definitive endoderm kit and STEMdiff™ pancreatic progenitor kit (StemCell Technologies, Canada) were used and mixed with other protocols.

Acronyms are described in Table 10.

		Stage 1 Definitive Endoderm	Stage 2 Primitive Gut Tube	Stage 3 Posterior Foregut	Stage 4 Pancreatic Endoderm & Endocrine Precursors
Rezania 2012	60-70% confluence; H1 cells; 1:30 matrigel	1 day : RPMI1640 + 0,2% FBS + 100ng/ml Act A +20ng/ml Wnt3A 2 days : RPMI1640 + 0,5% FBS + 100ng/ml ActA	3 days : DMEM-F12 + 2% FBS + 50ng/ml FGF7	4 days : DMEM-HG + 0,25umol SANT-1 + 2umol/L retinoic acid + 100ng/ml Noggin + 1%B27	3 to 4 days : DMEM-HG + 1umol ALK5i II + 100ng/ml Noggin + 50nmol/L TPB + 1%B27

		Stage 1 Definitive Endoderm	Stage 2 Foregut	Stage 3 Pancreatic Endoderm	Stage 4 Endocrine Progenitors
SD Kit + Nostro 2016	50- 60 % confluence for iPS HGPS Single Cells + Rock inh for H1 cells	1day : SD Kit (10uL/mL supp CJ and 10uL/mL supp MR) 2-3 days : SD Kit (10uL/mL supp CJ)	3 days : RPMI +1% Gln + 1%B27(w/o vitA) + 50ng/mL hFGF10 + 0,75uM Dorsomorphin + 3ng/mL mWnt3a	2 days : DMEM + 1% Gln + 1% B27 + 50 ug/ml ascorbic acid + 50ng/mL hNoggin + 50ng/mL hFGF10 + 0,25uM SANT1 + 2uM ATRA	5 days : H1 + 1% Gln + 1% B27 + 50ug/ml ascorbic acid + 50ng/mL noggin + 100ng/ml hEGF + 10mM nicotinamide

		Stage 1	Stage 2	Stage 3	Stage 4
		Definitive Endoderm	Primitive Gut Tube	Posterior Foregut	Pancreatic Endoderm
Rezania 2014	70-80% confluence H1 & iPS 1:30 matrigel	1 day : MCDB131 +1,5g/L NaHCO3+ 1X glx + 10mM Glc + 0,5%BSA + 100ng/ml GDF8 +1uM CHIR	2 days : MCDB131 + 1,5g/L NaHCO3+1XGlx + 10mM Glc+ 0,25%BSA + 0,25mM Ascorbic acid + 50ng/mL FGF7	2 days : MCDB131 + 2,5g/L NaHCO3 + 1XGlx + 10mM Glc + 2%BSA+ 0,25mM ascorbic acid + 50ng/ml FGF7 + 0,25uM SANT1 + 1uM Retinoic acid+ 100nM LDN+1/200 ITS-X + 200nM TPB MCDB131 could be substituted for BLAR medium	3 days : MCDB131 + 2,5g/l NaHCO3 + 1xGlx + 10mM Glc + 2%BSA + 0,25mM ascorbic acid+ 2ng/ml FGF7 + 0,25uM SANT1 + 0,1uM retinoic acid + 200nM LDN + 1/200 ITS-X + 100nM TPB
		1day : MCDB +0,5%BSA + 1,5g/L NaHCO3 +1x Glx +10mM Glc + 100ng/ml GDF8 + 0,1uM CHIR			
		1day : MCDB +0,5%BSA + 1,5g/L NaHCO3 +1x Glx +10mM Glc + 100ng/ml GDF8			
	Air-Liquide Interface	Stage 5 Pancreatic Endocrine Progenitors	Stage 6 Immature Beta Cells	Stage 7 Maturing Beta Cells	
		MCDB131 +1,5g/L NaHCO3 + 1X Glx + 20mM Glc + 2%BSA + 0,25um SANT-1 + 0,005uM retinoic acid + 100nM LDN + 1/200 ITS-X + 1uM T3 + 10uM ALK5i II + 10uM ZnSO4 + 10ug/mL heparin	7 days : MCDB131 + 1,5g/L NaHCO3 + 1X Glx + 20mM Glc + 2% BSA + 100nM LDN + 1/200 ITS-X + 1uM T3 + 10uM ALK5i II + 10uM ZnSO4 + 10nM gamma secretase inhibitor XX	7 days : MCDB131 + 1,5g/L NaHCO3 + 1X Glx + 20mM Glc + 2% BSA + 1/200 ITS-X + 1uM T3 + 10uM ALK5i II + 10uM ZnSO4 + 1mM Nacetyl cysteine + 10uM trolox + 2uM R428	
			7 days : MCDB131 + 1,5g/L NaHCO3 + 1X Glx + 20mM Glc + 2% BSA + 100nM LDN + 1/200 ITS-X + 1uM T3 + 10uM ALK5i II + 10uM ZnSO4 + 10nM gamma secretase inhibitor XX + 10ug/mL heparin	7 days : MCDB131 + 1,5g/L NaHCO3 + 1X Glx + 20mM Glc + 2% BSA + 1/200 ITS-X + 1uM T3 + 10uM ALK5i II + 10uM ZnSO4 + 1mM Nacetyl cysteine + 10uM trolox + 2uM R428 + 10ug/ml heparin	

Table 10: Acronyms used in differentiation protocols

Acronyms	Name
Act A	Activine A
ALK5i II	TGF- β RI Kinase Inhibitor II
ATRA	All-trans-retinoic acid
B27	Vitamin B27
BSA	Bovin serum albumin
CHIR	Aminopyrimidine derivative Inhibitor of GSK3
DMEM-F12	Dulbecco's Modified Eagle Medium: Nutrient Mixture F-12
DMEM-HG	Dulbecco's Modified Eagle Medium high glucose
Dorsomorphin	BMP and AMPK pathway inhibitor
FBS	Fetal bovin serum
hFGF10	Human fibroblast growth factor
FGF7	Fibroblast growth factor 7
ySec Inh XX	Gamma secretase inhibitor XX
GDF8	Growth Differentiation Factor 8
Glc	Glucose
Gln / Glx	Glutamine / glutamate
hEGF	Human Epidermal Growth Factor
ITS-X	Insulin-Tranferrin-Selenium-Ethanolamine
NaHCO ₃	Sodium bicarbonate
Nicotamide	Amide form of vitamin B3
hNoggin or Noggin	Human NOG protein
R428	Bemcentinib
Retinoic acid	Retinoic acid receptor (RAR) agonist
RPMI1640	Roswell Park Memorial Institute 1640
SD kit	Stem cell technology kit stage 1
Supp CJ	Stem cell technology supplement kit stage 1
Supp MR	Stem cell technology supplement kit stage 1
T3	Triiodothyronine
Wnt3A	Wnt3 protein
ZnSO ₄	Zinc Sulphate

Pseudo-islet formation:

One day after isolation, human islets were dissociated using Accutase (1mL/1000IEQ). Dissociation was done alternately by 1 minute cycles of pipetting (P1000) up and down and water

bath incubation at 37°C; the number of cycles was islet preparation dependent. The enzymatic reaction was stopped by adding 2 volumes of culture media (Lukowiak et al. 2001).

Single cells were counted and 187 500 cells were seeded per well of a 24-well sphericalplate (Kugelmeiers, Switzerland) making that 250 cells per microwell. Media was changed every other day.

2. Perifusion of human islets

As previously described, 300 IEQ were placed in the perifusion chamber (Henquin et al. 2006). Equilibration in Krebs solution with BSA (1mg/mL) at low glucose (3mM) for 50 min was done prior to starting. The islets were then perfused 3 min at 3mM glucose, 40 min at 15mM glucose and 20 min at 3mM glucose. During the experiments, samples were collected every 2 min. Outflow, pressure, temperature and oxygen were kept stable during the process. After perifusion, islets and pseudo-islets were lysed in ethanol acid and collected for intracellular insulin measurements (DxI Access Immunoassay System, Beckman Coulter) and insulin secretion measurements.

The reading range is between 0.3 and 300 IUU/ml. The samples are supplemented with albumin at 1mg/ml to promote insulin detection. Intracellular insulin was extracted from the cells after ultrasonication in ethanol-acid (1.5% concentrated HCl; 70% pure ethanol; 28.5% H₂O) on ice. Each intracellular insulin sample is diluted in 3 different concentrations (1/2114; 1/3844; 1/5761).

3. Molecular biology

RNA isolation

Cells were removed from culture and lysed in RLT buffer (Qiagen) complemented with 2-mercaptoethanol (10µL/mL). RNeasy mini Kit (Qiagen) was used according to the manufacturer's recommendations to extract RNA. RNA quality was controlled using a Biorad Experion chip, RQI > 7 were considered of sufficient quality to perform retrotranscription. RNA dosage was done using Nanodrop (Thermofisher).

Retrotranscription

RNA was reversely transcribed using the iScript cDNA Synthesis Kit (Bio-Rad) as follows:

iScript reaction mix	4 µL
iScript Reverse Transcriptase	1 µL
RNA	<i>qs</i> 300ng

Nuclease free water *qs* 20 μ L

The cDNA synthethis was performed in a 3-step cycler program on the Veriti (Applied Biosystem) using the following protocol: 5 min at 25°C, 20 min at 46°C and 1 min at 95°C.

The cDNA was stored at -80°C.

Quantitative Real Time PCR (qRT-PCR)

To normalize our results, we used as the house-keeping genes RPL27 for SYBR Green Q-PCRs and GAPDH for Taqman experiments. Experiments were done in duplicate and the $2^{-\Delta\Delta C_t}$ method was used for calculations in accordance with the MIQE guidelines (Bustin et al. 2009). Reactions were conducted on the CFX Connect RT-PCR Detection System (Bio-Rad) as follows:

For SYBR Green experiments:

SsoAdvanced Universal SYBR Green Supermix (Bio-Rad)	5 μ L
Forward primer (100 μ M)	0,25 μ L
Reverse primer (100 μ M)	0,25 μ L
cDNA	1 μ L
Nuclease free water <i>qs</i> 10 μ L	3,5 μ L

Reaction:

3 min at 95°C

40 cycles:

10 sec at 95°C for denaturation

30 sec at 60°C for annealing

Melt curve analysis was performed

For Taqman experiments:

Taqman Gene expression assay	5 μ L
Forward primer (1mM)	0,25 μ L
Reverse primer (1mM)	0,25 μ L
Taqman probes	0,25 μ L
cDNA	1 μ L
Nuclease free water <i>qs</i> 10 μ L	3,25 μ L

Reaction:

10 min at 95°C

40 cycles:

30 sec at 95°C for denaturation

min at 60°C for annealing

4. Immunohistochemistry

Pancreatic sections and mouse kidneys transplanted with human cells were fixed overnight in 4% PFA and embedded in paraffin. Sections of 10 µm thick sections were cut. Samples were deparaffinized in xylene, followed by a decreasing ethanol row of 100%, 90%, 70%, 50% and rehydrated in water and PBS. Antigen retrieval was performed in citrate buffer (pH6), 9 minutes at 750 watts in the microwave. When needed, sections were permeabilized in 0,1% Triton-X100. Protein block (Dako) was applied for 15 min to avoid unspecific binding. Primary antibody was incubated overnight at 4°C. The next day, slices were washed 3 times in PBS under agitation. Then, secondary antibody was incubated for 1 hour at room temperature in the dark. Finally, slices were then washed 3 times in PBS and DAPI was added before mounting.

5. Flow Cytometry and Fluorescence Activated Cell Separation

One well during differentiation experiments was taken for flow cytometry. TrypLE was used to obtain single cells. The cells were collected with FACS Buffer (PBS (w/o Ca²⁺ and Mg²⁺) + 10%FBS) and put in wells of a 96-well round bottom plate and centrifuged at 1400 rpm during 5 minutes.

For surface antigen:

One wash with FACS Buffer was done before adding antibodies and isotypes. After 20 min at room temperature, two washes were done before resuspension in FACS Buffer and prior to the flow cytometry run.

For intracellular antigen:

Cells were resuspended in CytoFix Solution (BD Biosciences) for 20-30 min at room temperature in the dark and washed twice with Wash/Perm Solution (BD Biosciences) at 2000 rpm during 2 minutes. Cells were incubated with antibody or isotypes overnight at 4°C. The following day, cells were washed once with Wash/Perm Solution prior to adding secondary antibodies for 30 min in the dark and at room temperature. After incubation, cells were washed twice before resuspension in FACS buffer for flow cytometry run.

Gating strategy:

First, we gated our population using forward and side scatters for size and granularity, debris were excluded. From the previous population, we used height (H) and width (W) for FSC and SSC scatters in order to gate single cells. From that single population, we gated the population of interest on isotypes sample (Figure 26).

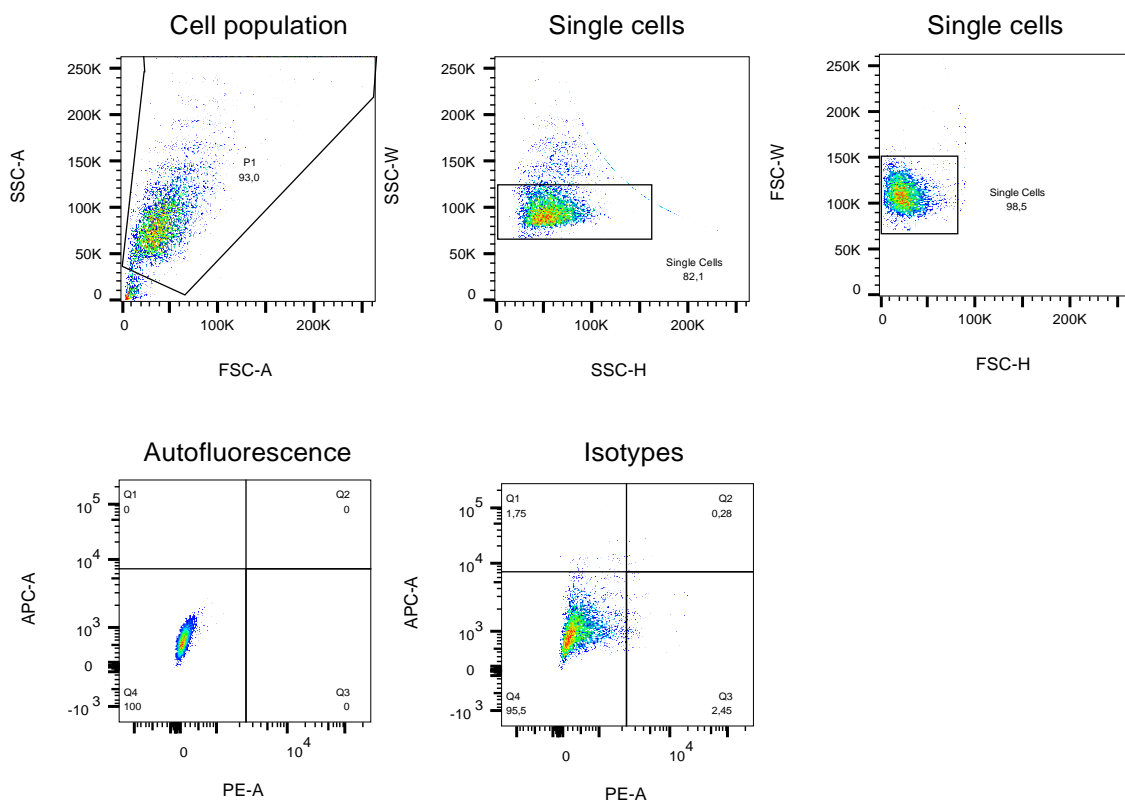


Figure 26: Strategy gating flowchart. FSC: Forward Scatter. SSC: Side Scatter. A: Area. W: Width. H: Height.

6. Mice

All animal experimentations were approved by our local animal ethical committee (CEEA75 - Lille). Under anesthesia and local analgesia, left kidney was exposed to proceed to the transplantation under the kidney capsule as previously described (Caiazzo et al. 2008).

Mice were housed in a SOPF facility with an *ad libitum* access to water and food, on a 12 hour dark/light cycle. Each animal was followed each 2 weeks for body weight, glycemia and blood sampling for c-peptide measurements.

Preliminary studies in our laboratory using human islets transplanted in normoglycemic nude mice (n=4) compared glucose stimulated insulin secretion (3g/Kg) with an oral glucose tolerance test (OGTT) vs intraperitoneal tolerance test (IPGTT) showing the highest secretion at 30 minutes with ipGTT (Figure 27).

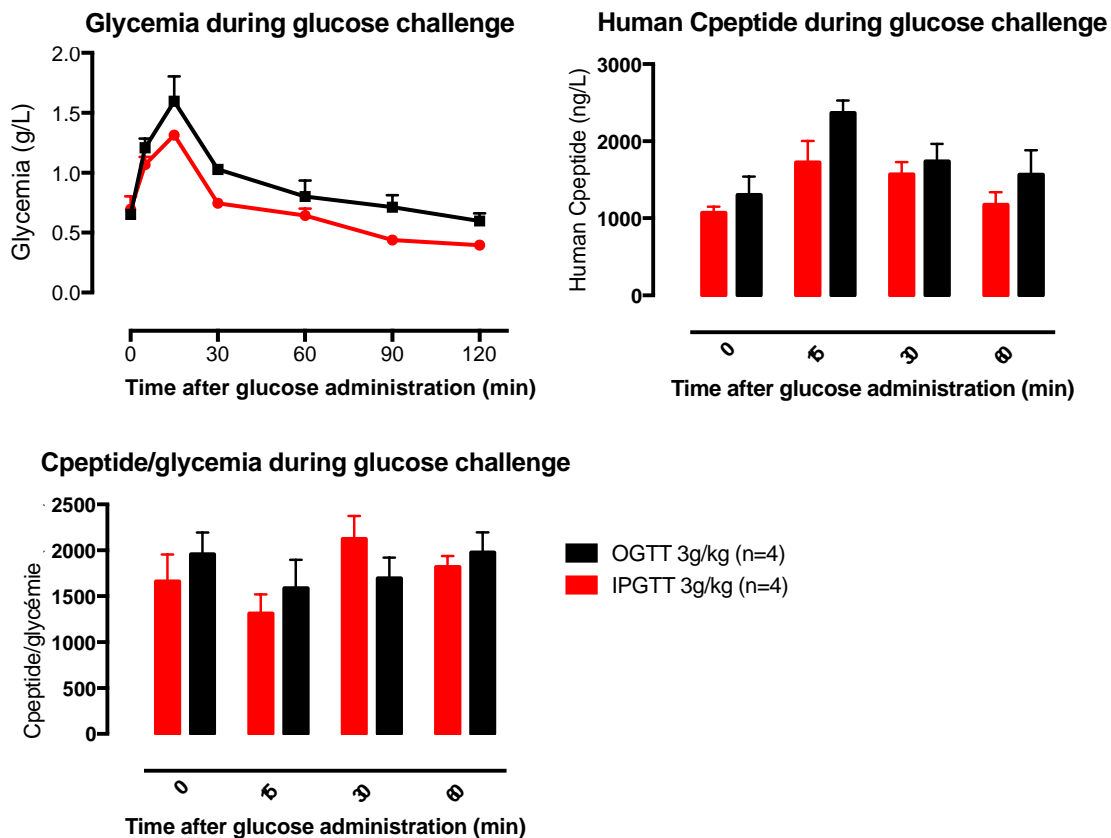


Figure 27: Glycemia, human c-peptide and human c-peptide divided by glycemia during glucose challenge (3g/kg) in normoglycemic nude mice with a human islet transplant under the kidney capsule. OGTT: Oral Glucose Tolerance Test; IPGTT: Intra-Peritoneal Glucose Tolerance Test.

7. ELISA

Plasma was obtained from blood sampling using heparinized micro tubes which were centrifugation (2000 rpm 5 min) and stored at -80°C until the assay. The detection limit is < 2,5 pmol/L (0,0076ug/L).

8. Statistics

All values are shown as mean \pm SEM. Prism 7 (GraphPad, USA) software was used for statistical analysis. The non-parametric Kruskal Wallis test was used to analyze the statistical significance in the pseudo-islet part.

Chapter 3: Pseudo-islets

The objective here was first to test the feasibility and reproducibility of pseudo-islet technology in clinically approved culture media and to compare their function *in vitro* and *in vivo* with their matched native human islet counterparts at D1 (day of dissociation) and D7 (day required for reaggregation). Secondly, we attempted to evaluate whether donor heterogeneity or the donor's signature in human intact islets persisted in pseudo-islets or was abolished.

Figure 28 gives an overview of the pseudo-islet experiments. The viability before dissociation of all four human islet preparations used in this experiment which was assessed by trypan blue staining and it was always above 90%. One day after isolation, the native D1 islets (red) were compared to donor matched pseudo-islets formed from dissociated single cells of native islets that were reaggregated for one week (pseudo-islets D7, blue) and to the native islets cultured for one week (Native islets D7, grey) (Figure 28). The islet functionality of the three groups was evaluated *in vitro* by a dynamic perfusion technique to study the insulin secretion capacity of 300 islet equivalents (IEQ) in response to glucose (Henquin et al. 2006). The secreted insulin was normalized to the intracellular insulin content. For the *in vivo* evaluation, 500 IEQs were grafted under the renal capsule of non-diabetic immunodeficient mice and, over a month, glycemia and fasting human c-peptide secretion were measured (Caiazzo et al. 2008). Afterwards, the animals were sacrificed and the insulin and glucagon positive area within the grafts was morphometrically evaluated.

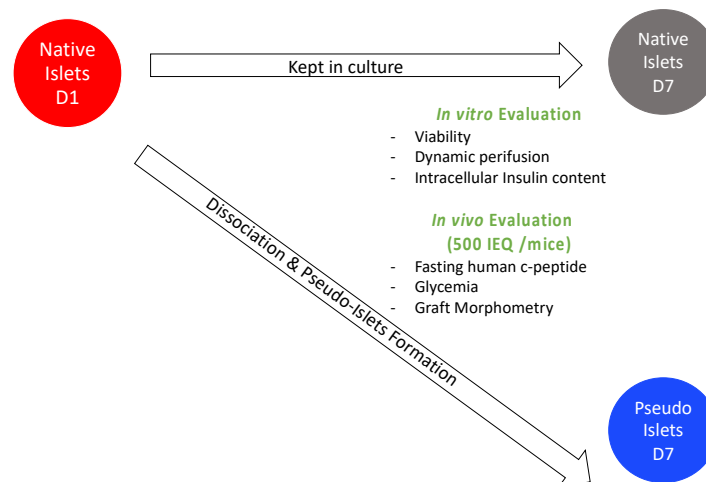


Figure 28: Overview of pseudo-islets experiments. Donor matched pseudo-islets (blue) were generated from dissociated single cells obtained from human islet donors one day after isolation and compared to intact native islets at day 1 (red) or day 7 (grey). Islet functionality was evaluated *in vitro* and *in vivo* (n=3-4 donors).

1. *In vitro* results

The islet donors had very diverse characteristics and medical histories (age, BMI, sex, alcohol, tobacco, cardiorespiratory arrest or time spent in intensive care unit). The phenotypic and clinical characteristics of human islet donors used in the present study are reported in Table 9 (see Material and Method). None of the islet preparations used were from diabetic donors. Pseudo-islets were successfully formed from 4/5 human islet preparation tested. For the *in vitro* evaluation of pseudo-islets vs. islets at D1 or D7, 300IEQ of each group were perfused with basal glucose (3mM), followed by high glucose (15mM) and finally again with basal levels (Figure 29). As expected, in all groups the insulin secretion profiles showed a negligible release of insulin at basal glucose (G3), and a secretion peak (first phase) at 15mM glucose (G15) followed by a stable plateau (second phase) until the glucose concentration was decreased to basal glucose (Figure 29). While the insulin secretion pattern of native human islets at D1 was rather heterogenous between donors (Figure 29A), the insulin release of native islets at D7 (Figure 29B) and pseudo-islets at D7 (Figure 29C) showed less variability. However, the total amount of secreted insulin was significantly higher for native islets at D1 compared to native islets at D7 (** $p < 0,01$) and pseudo-islets at D7 (**** $p < 0,0001$) (Figure 29D).

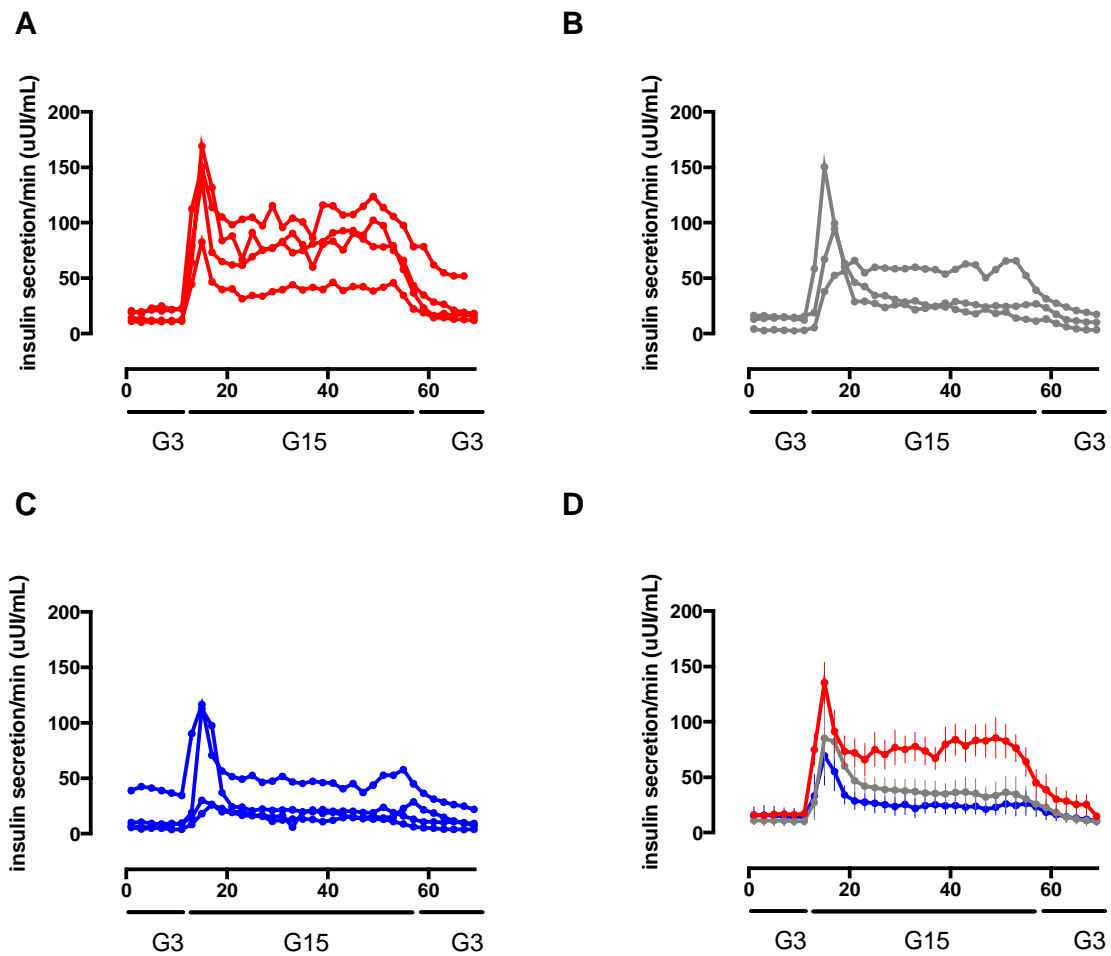


Figure 29: Dynamic insulin secretion by perfusion in response to glucose variations. (A) native islets one day after isolation (n=4) (B) native islets one week after isolation (n=3) (C) pseudo-islets one week after isolation (n=4) (D) average of donors from each group. Data are expressed as uUI/mL. One-way Anova and Kruskal-Wallis multiple comparison test were used. G3: glucose 3mM. G15: glucose 15mM.

Insulin content was drastically reduced (75%) upon culture in our clinical grade culture medium (CMRL 1066 with 0,0625% human serum albumin and recombinant insulin), both in pseudo-islets and intact native islets at D7 groups compared to native islets D1 insulin content (Figure 30). For this reason, insulin secretion levels between D1, D7 native islets and pseudo-islets were not expressed in percent of insulin content.

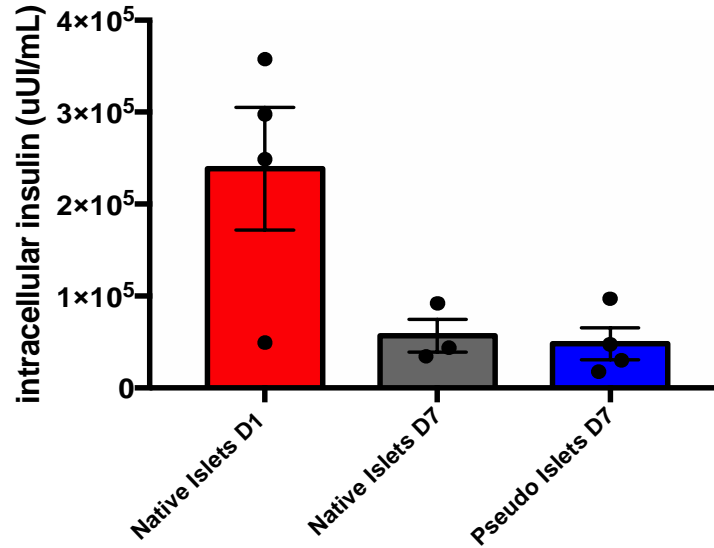


Figure 30: Insulin content of native human islets at D1 and D7 and pseudo-islets at D7. Native islets and pseudo-islets were cultured in clinical grade islet medium (CMRL 1066 with 0,0625% human serum albumin).

2. *In vivo* results

To evaluate the functionality of the three different groups *in vivo*, we performed grafts in an immunodeficient mouse model (Caiazzo et al. 2008). Islets were manually counted prior to transplantation and 500 IEQ (IEQ = islet at 150 μ m in diameter) were transplanted under the kidney capsule of mice. The *in vivo* function of pseudo-islets was evaluated as human c-peptide secretion in response to glucose (c-peptide/glycemia) and it was compared to native D1 human islets from the same donor and to native human islets cultured 7 days. The kinetic results over one month showed a tendency for native human islets at D1 to secrete higher levels of human c-peptide than pseudo-islets D7 (Figure 31A, pseudo-islets vs. native islets D1 p=0,2327) and native islets cultured 7 days, albeit only the later was statistically significant (Figure 31A, native islets D7 vs. native islets D1 p=0,0098). Mean of the c-peptide/glycemia ratio over one month was calculated and confirmed the superiority of intact native islets D1 over D7 islets and pseudo-islets (Figure 31B p=0,0038 and p=0,0294 respectively).

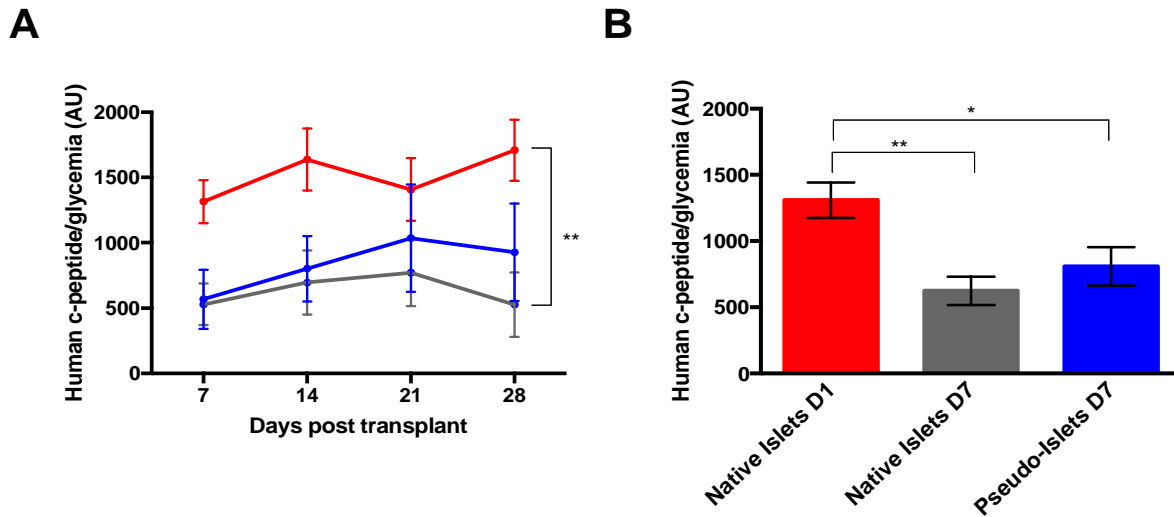


Figure 31: In vivo function of D1 native human islets, D7 native islets and pseudo-islets. Fasting human c-peptide / glycemia ratio measured from immunodeficient mice transplanted with D1 native human islets (red), D7 native islets (grey) and pseudo-islets (blue). (A) secretion profiles each 7 days and (B) mean of secretion over one month. AU: Arbitrary units. Data are expressed as mean \pm SEM.

Next, we quantified by morphometry, the distribution of endocrine cells in the 3 different groups, one month after transplantation under the kidney capsule of nondiabetic immunodeficient mice. The surface of insulin or glucagon positive cells was similar between D1 and D7 native islets, but a trend towards an increase in the glucagon surface area was observed in the pseudo-islet group, compared to the other two groups (Figure 32).

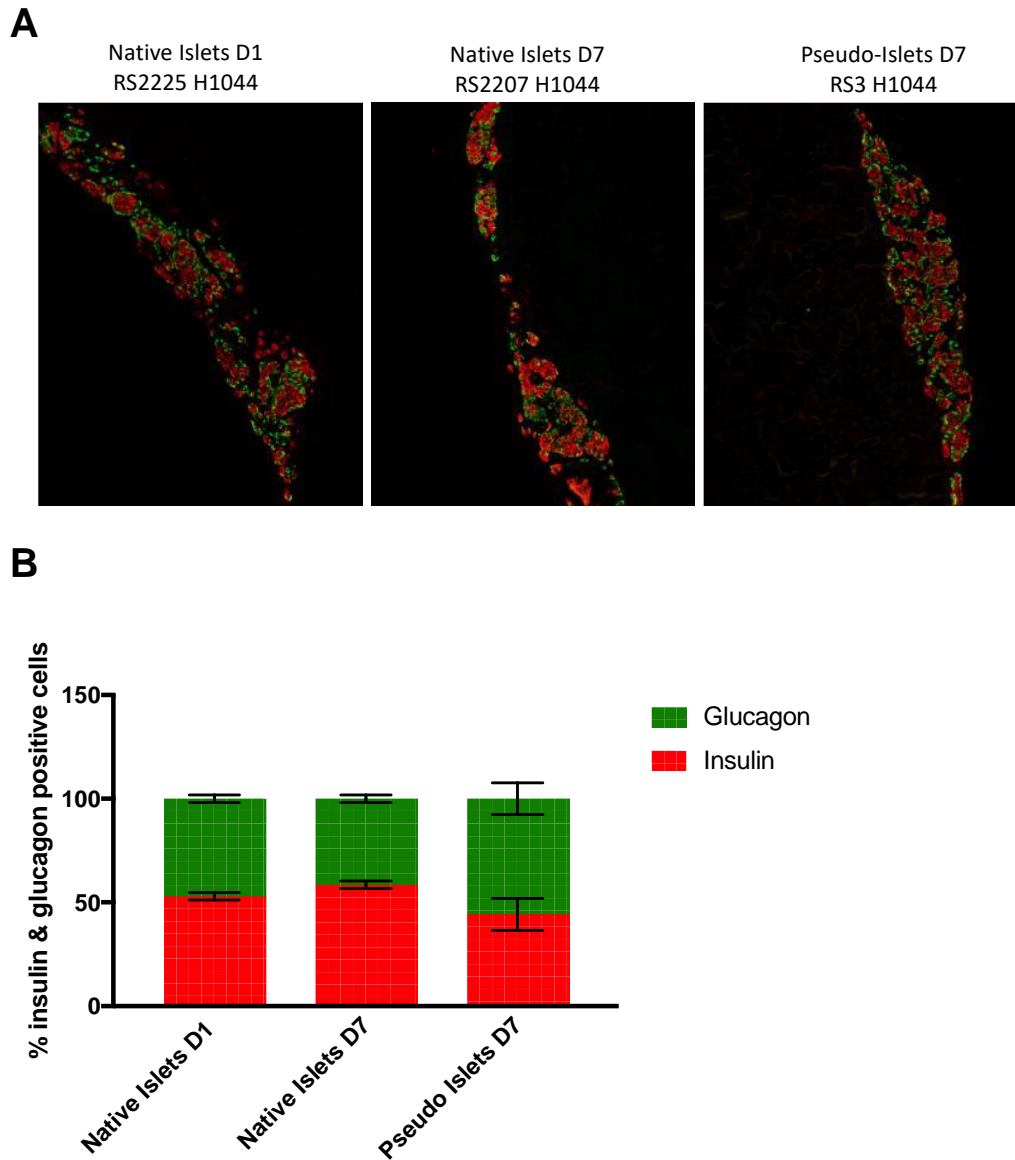


Figure 32: Morphometric analysis of grafted native human islets D1, D7 and pseudo-islets. (A) Representative images of the distribution of insulin (red) and glucagon (green) positive cells in grafts of native islets D1, D7 and pseudo-islets one month after transplantation. (B) Percentage of insulin and glucagon positive cells from graft of native islets D1, D7 and pseudo-islets in n=3 mice per group.

Finally, preliminary results on 4 islet preparations suggest that the donor heterogeneity persisted after pseudo-islet formation *in vitro* (Figure 33) both in the first and second phase of insulin secretion.

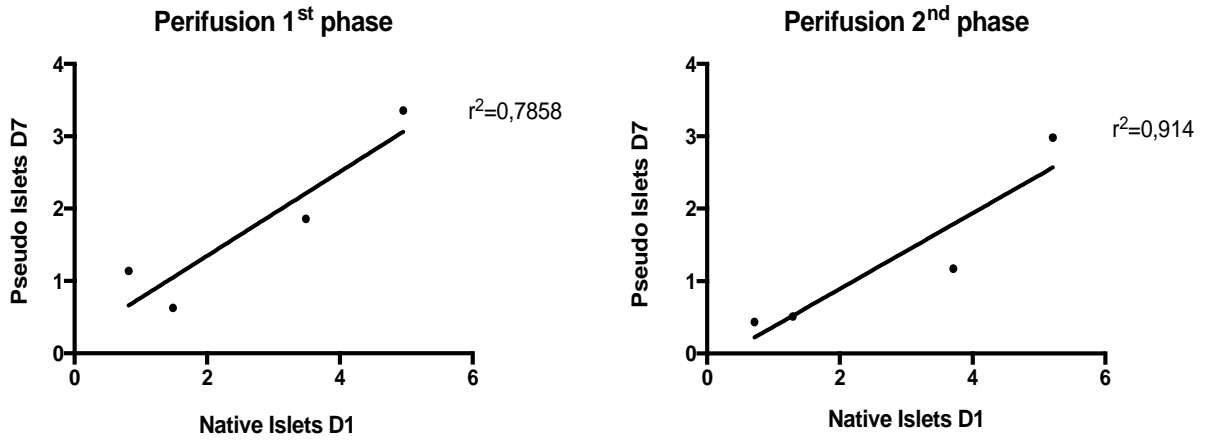


Figure 33: Correlation of glucose-stimulated insulin secretion between native human islets and pseudo-islets. Insulin secretion in response to high glucose was assessed by perifusion and the correlation between the native human islets and pseudo-islets insulin secretory response during first (left panel) and second phase (right panel) of stimulation was calculated.

Chapter 4: Human pluripotent stem cell differentiation
Reproduction of published protocols and optimization of two cell lines

The timeline of stem cell differentiation at U1190, Lille is shown in Figure 34. Before my arrival in the laboratory, in 2012 & 2013, Prof. J. Kerr-Conte visited the laboratory of Prof. J. Odorico at the University of Wisconsin, for training in stem cell differentiation. Our laboratory obtained authorization from the French Biomedical Agency (Agence de Biomédecine: ABM) to work with embryonic stem cells for research in July 2013. During the first 2 years, H1 and iPS DF19.9 cells were used for differentiation studies using the Odorico protocol. Of note, the most favorable results were obtained with H1 cells. The U1190 laboratory was successfully audited for the H1 activity by the ABM in 2015. At this stage, the French Jérôme-Lejeune Foundation who routinely takes the ABM to court to revoke authorizations for research on human embryonic stem cells contested Lille's authorization to work with human embryonic stem cells. The Tribunal Administrative in Paris pronounced the cancellation of Lille's authorization in Dec 2015, one month after the start of my PhD. Thus, the subsequent studies focused on optimizing induced pluripotent stem (iPS) cell differentiation using the Rezanian 2014 protocol (Rezanian et al. 2014) and the StemCell Differentiation Kit from by StemCell Technologies.

In 2017, a new authorization by the ABM for research on H1 (<https://www.legifrance.gouv.fr/affichTexte.do?cidTexte=JORFTEXT000036589951&categorieLien=id>) was granted and we were back to work two years later with H1 cells to test cell differentiation protocols. Finally, with the help of Dr. C Nostro from University of Toronto (Canada), we were able to optimize S1 and S4 stages for H1 cells and the iPS HGPS/Progeria cells.

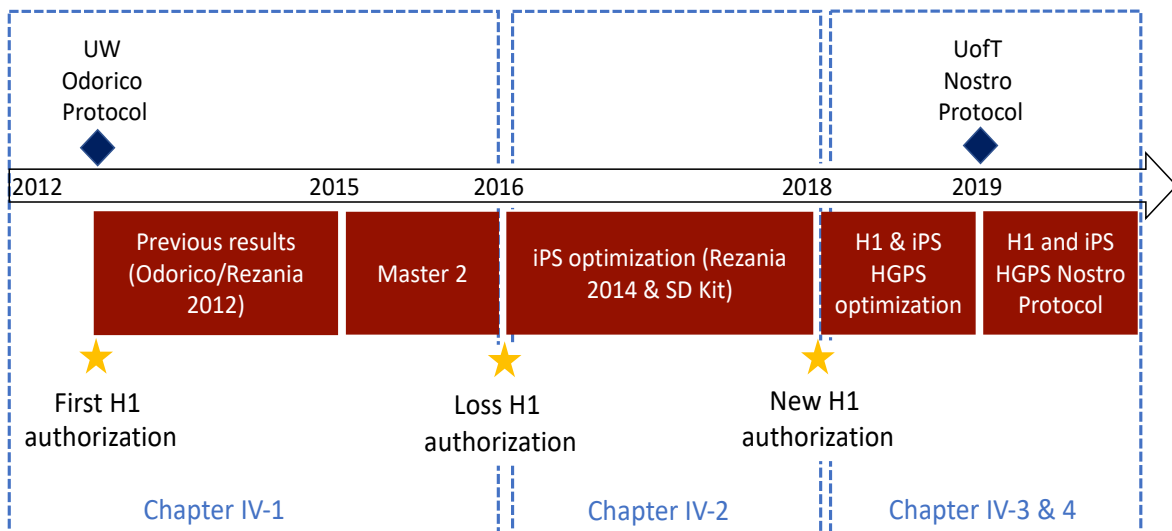


Figure 34: Timeline of stem cell differentiation at U1190, Lille. Stars indicate the timeframe of approval for the use of embryonic stem cell research in our laboratory by the French Biomedical Agency (ABM). The blue diamonds indicate the time spent as visiting scientist/professor at both the University of Wisconsin (UW) and University of Toronto (U of T). The blue dotted line indicates in which chapter the corresponding results are shown.

1. First generation differentiation protocol according to the Odorico 2012 protocol

Prior to my arrival in November 2015, twenty-seven differentiation experiments were carried out in the laboratory (G. Pasquetti and Prof. J. Kerr-Conte). Stem cells were differentiated using the “first generation” protocols according to the confidential protocol provided from Prof. Odorico that was adapted from the Xu protocol (Xu et al. 2011) or the Rezania 2012 protocol (Rezania et al. 2012) (Figure 35).

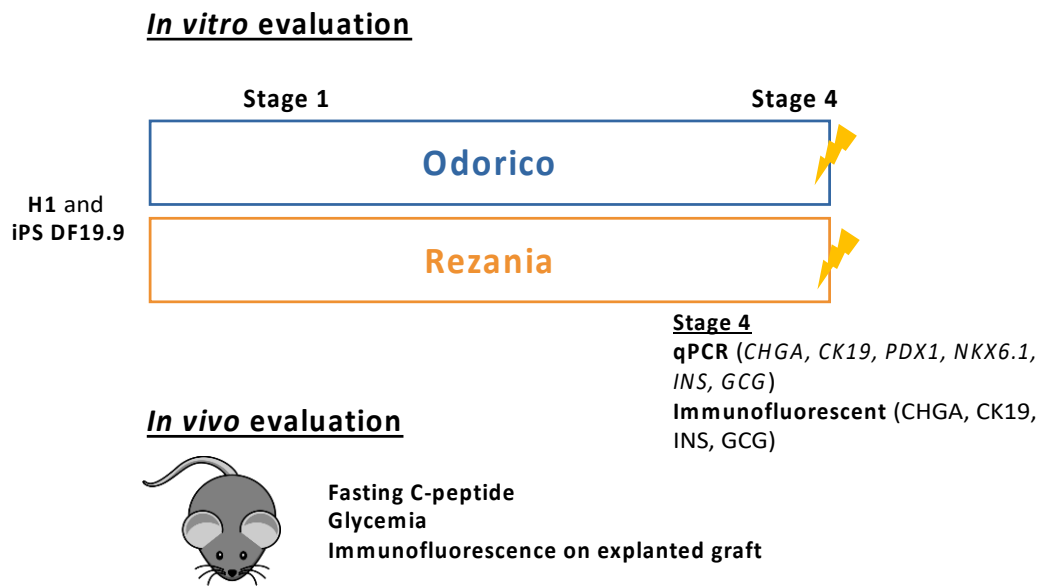


Figure 35: Overview of applied differentiation protocols from 2012 to 2015. H1 or iPS DF19.9 cell lines were differentiated towards stage 4 pancreatic progenitor cells according to Rezania 2012 protocol (Rezania et al. 2012) or an adapted protocol from Prof. Odorico’s laboratory (Xu et al. 2011). Stage 4 cells were analyzed *in vitro* by qPCR and immunofluorescent staining prior to transplantation under the kidney capsule of immunodeficient mice. Mice were followed for 3 months to evaluate human fasting c-peptide and glycaemia *in vivo*. Grafts were analyzed by various immunofluorescent stainings. Hereafter, only the experiments with H1 cells and J. Odorico’s protocol will be mentioned. Arrows represent timepoint of cell engraftment.

In this paragraph, only results obtained with the Odorico protocol are shown due to difficulties in reproducing the Rezania 2012 protocol.

To quantify the progress of stem cell differentiation from stage 1 to stage 4, we used real time qPCR techniques to determine the transcription levels of key endocrine differentiation markers genes, such as chromogranin A (*CHGA*), cytokeratin 19 (*CK19*), Pancreatic and Duodenal

Homeobox 1 (*PDX1*), *NKX6.1*, Insulin (*INS*) and Glucagon (*GCG*) during several differentiation stages (stage 1, stage 3, stage 3 and stage 4).

As controls, both undifferentiated H1 cells (white bar) and human islets isolated from one donor (red bar) were used and compared to differentiated H1 cells (grey bars). As expected, these key pancreatic genes were highly and progressively induced in human islets compared to undifferentiated H1 cells, to which the expression was normalized. Although non-significant, a gradual increase in *CHGA*, a pan-endocrine marker (Travis et al. 1998) was observed (Figure 36A). This coincided with a slight increase in *CK19* mRNA levels, a known ductal marker (Kerr-Conte et al. 1996). Of note, two key transcription factors crucial for β cell specification (Nelson et al. 2007), *PDX1* and *NKX6.1*, the pancreatic homeodomain transcription factor and a homeobox transcription factor, were also upregulated in stage 4 differentiated cells compared to undifferentiated cells (Figure 36A). Stage 4 cells expressed the same *PDX1* levels as human islets, however, *NKX6.1* expression remained one log apart from human islet expression. We then verified if the differentiated cells expressed *INS* and *GCG*. In comparison with human islets from one donor, the differentiated cells expressed *chromogranin A*, *CK19* and *PDX1* at the same magnitude, but one log less for *NKX6.1* and *INS* and 1,5 log less for *GCG*.

We then verified protein expression for Chromo A (pan-endocrine marker), CK19, Insulin and Glucagon by immunofluorescence techniques. Figure 36B (experiment 4) shows chromogranin A and CK19 positive cells in the 3D structure “budding” of. In addition, double positive cells for insulin and glucagon were observed (Figure 36B, yellow square) as previously reported (Hrvatin et al. 2014).

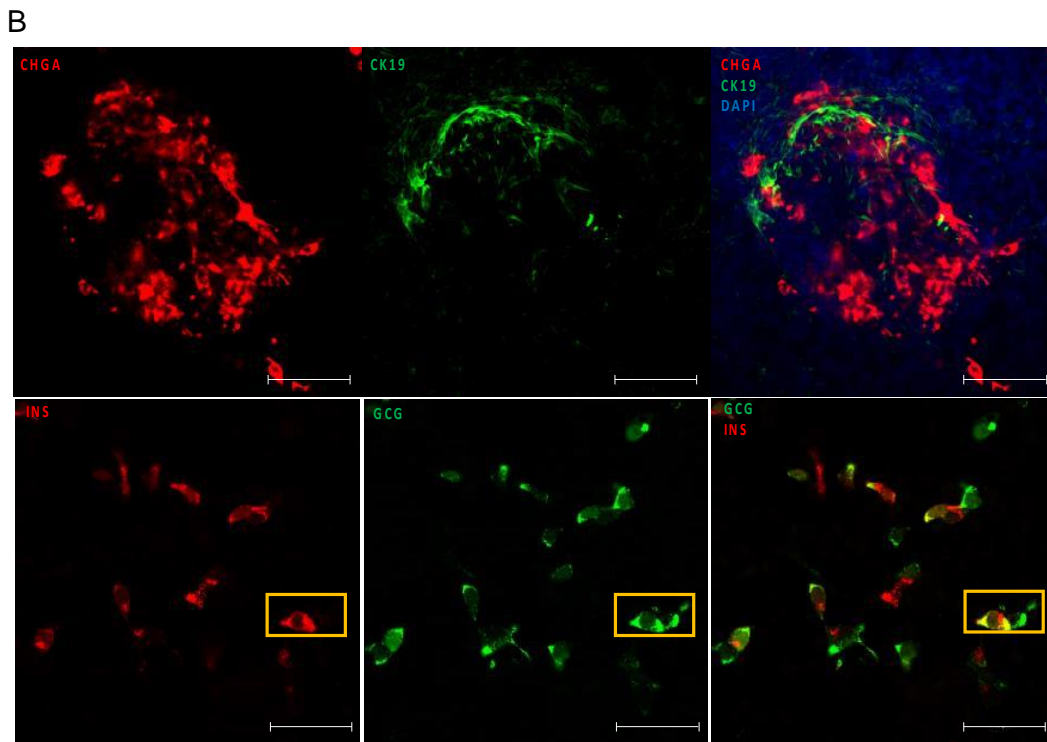
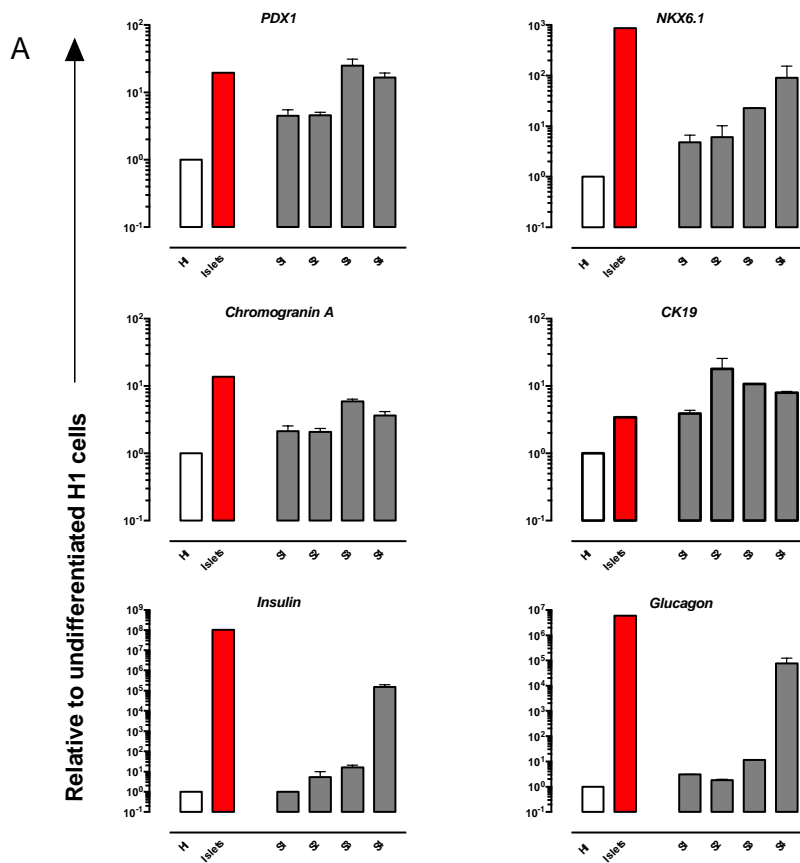


Figure 36: Phenotype of H1 cells stage 1-4 during differentiation with the Odorico protocol.
 (A) Gene expression of differentiated H1 cells at stage 4 compared to undifferentiated H1 cells (n=2).

Human islets were used as positive control (red bar, n=1). RPL27 was used as house-keeping gene and results are expressed as fold change relative to undifferentiated H1 cells. Data are shown on a logarithmic scale. (B) Immunofluorescent staining of stage 4 cells (Expt 4 - with H1 cells). Images in the upper panels show chromogranin A (CHGA) in red, cytokeratin (CK19) in green and the merge, while the lower panels show insulin (INS) in red and glucagon (GCG) in green and the merge. Yellow squares indicate polyhormonal cells. Scale bar = 50 μ m.

After *in vitro* differentiation, S4 cells were grafted under the kidney capsule of nondiabetic immunodeficient mice for *in vivo* maturation (Caiazzo et al. 2008). All mice were followed over a period of 3 months. In 9 mice out of a total of 29, fasting c-peptide secretion was detectable with the ultrasensitive human c-peptide kit (Mercoxia, Sweden). The maximum secretion did not exceed 200 ng/L in non-fasted animals, while the average range of fasting c-peptide of 500 human islet equivalents (IEQ) was 500 - 1000 ng/L (represented by the red dot in Figure 37A). However, with time the amount of detected human c-peptide was decreased in all grafted mice (Figure 37A). Immunofluorescent staining from a graft of cells from experiment 9, at 12 weeks after transplantation, showed positive cells for chromogranin A or CK19 (Figure 37B). In addition, insulin or glucagon positive cells were also identified by immunofluorescent staining (Figure 37B). Furthermore, identical to pancreatic islet neogenesis in the adult and fetal human islet a budding of chromogranin A positive endocrine cells was detected next to a Cytokeratin 19 positive duct, what resembles pancreatic islet neogenesis human islet (Figure 37C) (Swartz and Carstens 1986; Kerr-Conte et al. 1996). A typical adverse event of stem cell transplantation in animals is the formation of teratomas, it occurs when undifferentiated cells persist in the transplanted cells. Therefore, we analyzed the animals and identified 13% (4 mice from a total of 29) teratoma formation (Figure 37D). The frequency of observed teratomas in transplanted animals is in line with observations from other groups (Kroon et al. 2008).

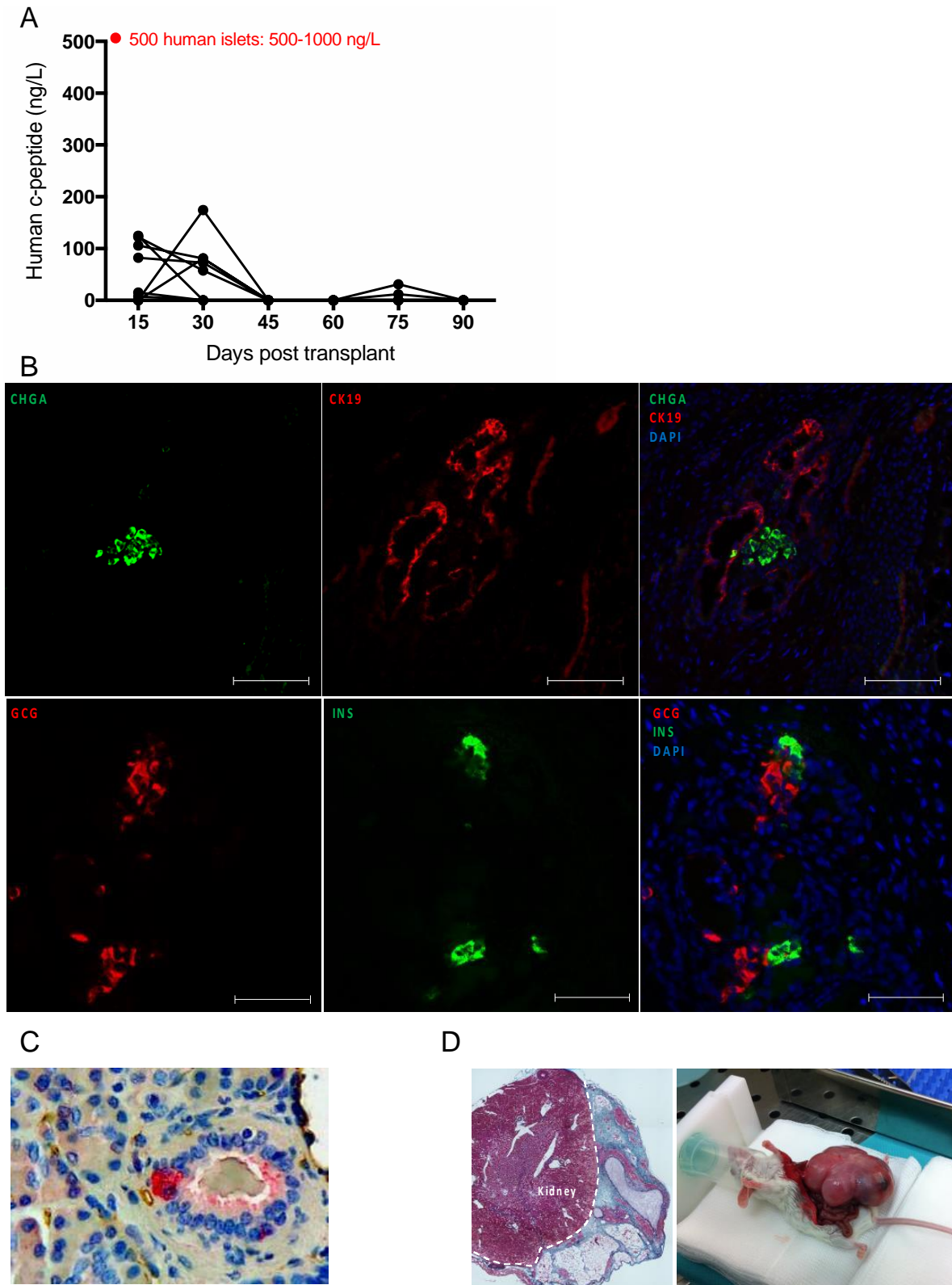


Figure 37: In vivo evaluation of engrafted stage 4-H1 cells differentiated according to the Odorico protocol. (A) Human c-peptide levels (ng/L) were measured under random fed conditions over 3 months.

Human c-peptide was detected in 9 mice out of a total of 29. Normal range of c-peptide secretion from 500 human islets is in red (500-100ng/L). (B) Immunofluorescent staining of graft of stage 4 cells, harvested 12 weeks after transplantation (Expt 9 – obtained with H1 cells) for chromogranin A (CHGA, panendocrine marker) in green, cytokeratin 19 (CK19, ductal marker) in red in the upper panels, and glucagon (GCG) in red and insulin (INS) in green in the lower panels. Scale bar = 100 μ m. (C) Human islet neogenesis from ducts in a human pancreatic section. (D) Hematoxylin and eosin staining of a teratoma (left image), mouse developing a teratoma at 4 weeks after transplantation (right image).

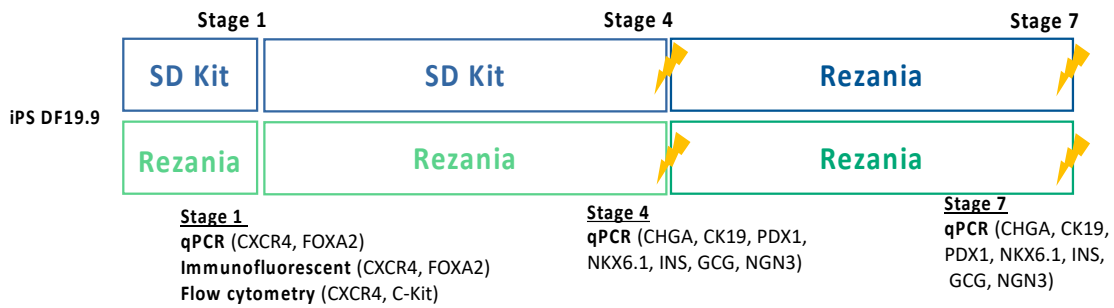
In conclusion, by using H1 cells differentiated according to the Odorico 2012 protocol and subsequently transplanted in immunodeficient mice, it was possible to obtain endocrine and ductal cells *in vivo*. Although these results were very encouraging, polyhormonal cells were observed as well as important teratoma formation *in vivo* suggesting that both, the differentiation efficiency toward endoderm and pancreatic progenitor were insufficient. Therefore, more emphasis was put on optimizing the efficiency of definitive endoderm (stage 1) and “second generation” protocols which generate large number of stage 4 PDX1+/NKX6.1+ cells with low expression of NGN3, thus optimizing S1 and S4 differentiation and lowering the teratoma formation.

2. Future strategies for the generation of pancreatic progenitors with iPS DF19.9 cells using second generation protocols following cancellation of H1 authorization.

As mentioned above, the most favorable results were obtained with H1 cells, however due to the loss of our authorization to work with embryonic stem cells we focused on the optimization of the differentiation of iPS DF19.9 cells, since this was the cell line used in Prof. Odorico’s laboratory in 2012 (Xu et al. 2011). In general, differentiation protocols were less efficient with the DF19.9 cell line than with H1 cells.

Subsequent studies focused on iPS DF19.9 cell differentiation using “second generation” protocols, either the SD Kit (STEMDiff Pancreatic Progenitor Kit) from stage 1 to 4 and Reznia 2014 for stage 4 to 7, or Reznia 2014 alone for stage 1 to 7 (adaptation of the protocol: no single cells at stage 4 and no transition to the air/liquid interface for stages 5 to 7 as described by Reznia) (Figure 38). We evaluated the differentiated cells *in vitro* at stage 1, stage 4 and stage 7. In some experiments we grafted cells at stage 4 and in others at stage 7, all animals were assessed for glycemia and c-peptide secretion.

In vitro evaluation



In vivo evaluation



Fasting C-peptide
Glycemia
Immunofluorescence on explanted graft

Figure 38: Overview of differentiation protocol applied with iPS DF19.9 cells. iPS DF19.9 cell line was differentiated towards stage 4 pancreatic progenitor cells or stage 7 maturing β cell according to Rezia 2012 or STEMdiff Pancreatic Progenitor Kit (SD KIT). Stage 1 cells were analyzed *in vitro* by qPCR, immunofluorescent staining and flow cytometry. Stage 4 and 7 cells were analyzed by qPCR and immunofluorescent staining prior to transplantation under the kidney capsule of immunodeficient mice. Mice were followed up to 3 months to assess human fasting c-peptide and glycemia *in vivo*. Grafts were analyzed by immunofluorescent staining. Arrows represent timepoint of cell engraftment. SD Kit: STEMdiff Kit.

- 1) Making definitive endoderm with the Rezia 2014 protocol and SD Kit (stage 1 cells)

We first focused on definitive endoderm (DE) differentiation to reduce the abundance of teratoma formation. We used real time qPCR techniques to investigate the expression of two key DE markers, *CXCR4* (C-X-C chemokine receptor type 4) and *FOXA2* (Forkhead box A2 also known as HNF3b) (D'Amour et al. 2005). Gene expression analysis at stage 1 (black) using the Rezia protocol (3 days) showed an increase in *CXCR4* and *FOXA2* mRNA expression in comparison to undifferentiated iPS DF19.9 cells (Figure 39A white bar). Then, quantification of their expression by immunofluorescent staining was performed. For each experiment, 100 cells were identified by DAPI, and both *CXCR4* and *FOXA2* positive cells were counted (Figure 39B). In total, 90% double positive cells were detected (Figure 39B). Because this method is time consuming and not accurate, a quantification method by flow cytometry was performed (Figure 39C) which was recommended in my 2nd PhD progress meeting by the jury members. For endoderm cytometry

analysis, we quantified endoderm formation by CXCR4 and c-Kit (tyrosine-protein kinase kit, also known as CD117) (Korytnikov and Nostro 2016). First, dead cells and debris were excluded. In a second step, the isotype controls were used to define the gates for each marker and channel (Figure 26). With the iPS DF19.9 we compared 2 protocols, either the Rezia 2014 protocol or the kit commercialized by StemCell Technologies (SD Kit). First CXCR4 expression reached in some experiments 79-91% of the cells however, only 21-25% of cells were double positive for CXCR4 and C-Kit with the Rezia protocol while with the SD Kit more than 34-58% of all differentiated cells were double positive (Figure 39C-D). It should be mentioned that for these experiments working banks were not yet made so the passage number between runs was not always constant.

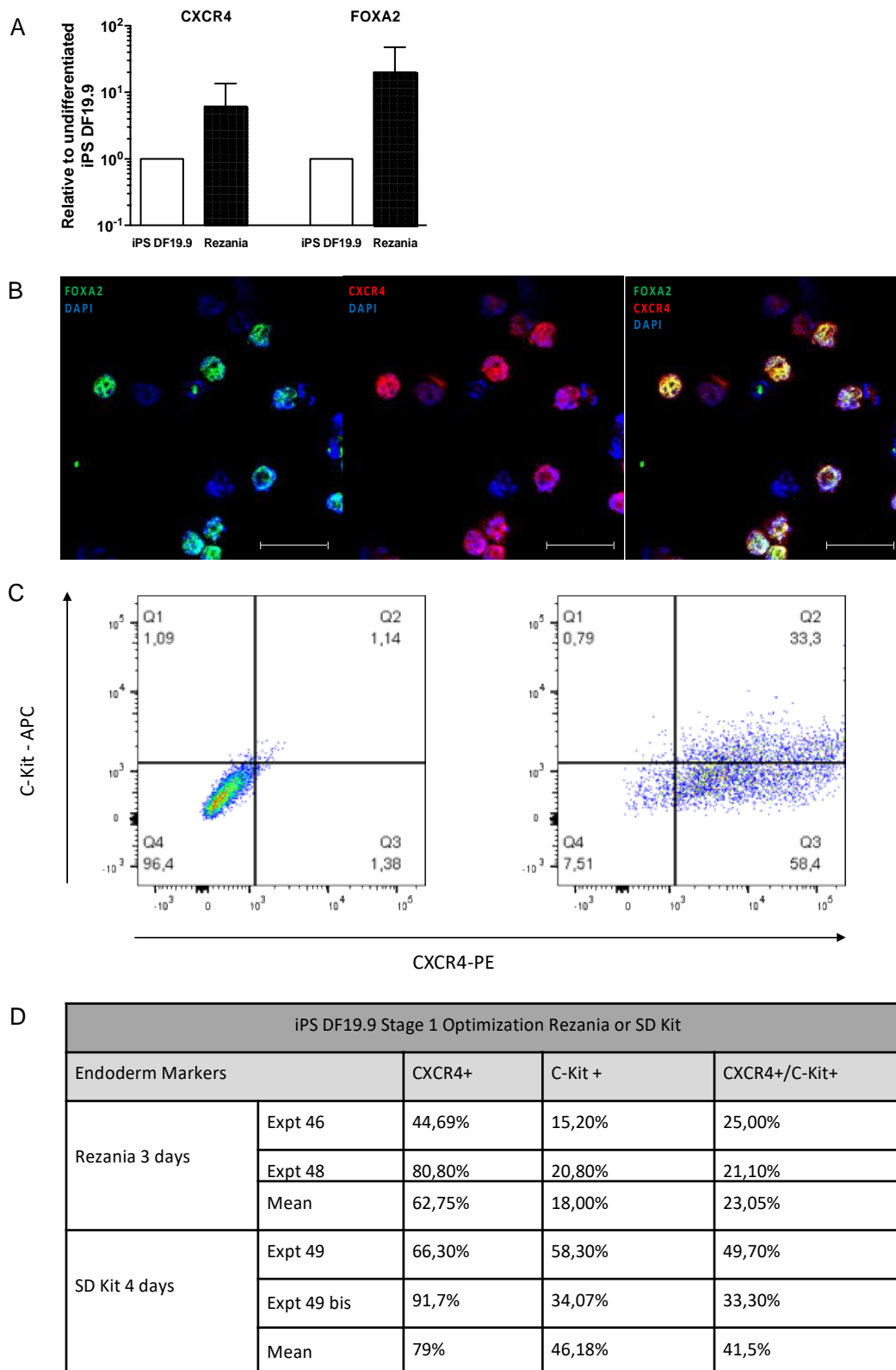


Figure 39: CXCR4 and FOXA2 gene and protein expression from iPS DF19.9-derived cells at differentiation stage 1 with SD Kit compared to the Rezania protocol. (A) Gene expression of *CXCR4* and *FOXA2* from iPS DF19.9-derived cells at differentiation stage 1 normalized to undifferentiated iPS DF19.9. *RPL27* was used as house-keeping gene. Gene expression is shown on a logarithmic scale. **(B)**

Immunofluorescent quantification of endoderm differentiation at stage 1 using CXCR4 and FOXA2 staining showing more than 90% endoderm formation (Expt 28). Scale bar = 30µm. (C) Representative image of FACS plots illustrating protein expression of CXCR4 and C-Kit in populations of iPS DF19.9-derived stage 1 cells (Expt 49) (D) FACS quantification of endoderm formation - Table shows percentage of stage 1 cells expressing CXCR4 and C-Kit with Rezia protocol and SD Kit. SD Kit: STEMdiff Kit.

2) Evaluation of stage 4 pancreatic progenitors using the Rezia 2014 protocol and STEMdiff Pancreatic Progenitor Kit (stage 4 cells)

For gene expression comparison, a pool of 10 human islet donors was systematically used in order to reduce heterogeneity and ensure consistency. Also, contrary to our previous results, endocrine marker expression was reported as a fold change relative to human islets, since our goal was to differentiate towards pancreatic endocrine cells. Gene expression levels of stage 4 cells generated with the Rezia 2014 protocol or SD Kit were compared to human islets (red). We observed, for all genes, that cells produced with the SD Kit had a higher mRNA expression than those obtained with the Rezia protocol (Figure 40).

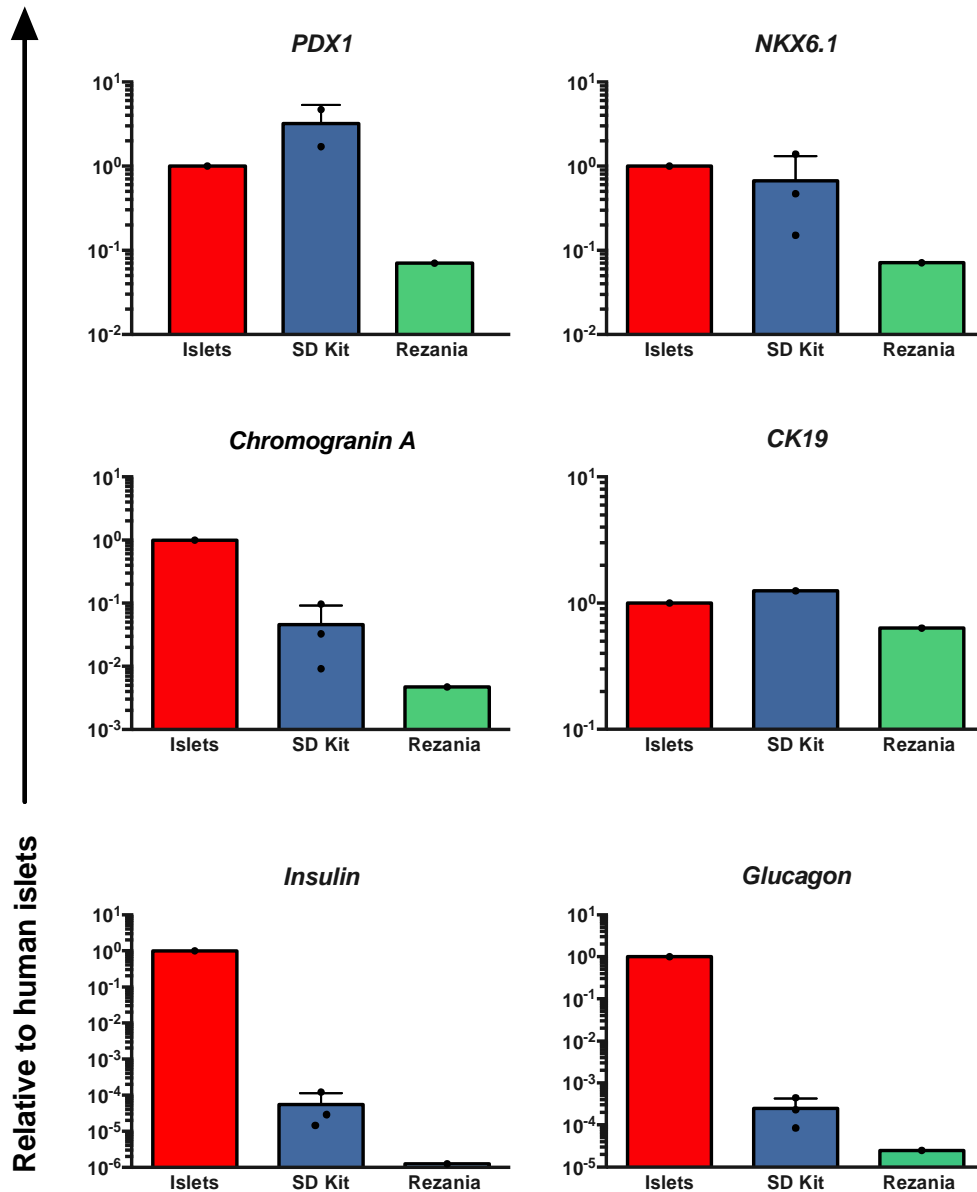


Figure 40: Stage 4 cells generated using the Reziaia protocol or SD Kit with iPS DF19.9 cells – in vitro evaluation. Gene expression of *PDX1*, *NKX6.1*, *Chromogranin A*, *CK19*, *Insulin* and *Glucagon* from iPS DF19.9-derived cells at differentiation stage 4. *RPL27* was used as house-keeping gene; results are expressed as a fold change relative to a pool of 10 human islet donors (red). Gene expression is shown on a logarithmic scale. SD Kit: STEMdiff Kit.

After *in vitro* differentiation, 5 million cells were grafted in mice for *in vivo* maturation over 3 months. In 33% of grafted animals (3 out of 9) we were able to detect human fasting c-peptide (Figure 41). As for previous results, the c-peptide secretion was below 200 ng/mL while normal secretion range for 500 IEQ is between 500 and 1000 ng/L (Figure 41 red dot).

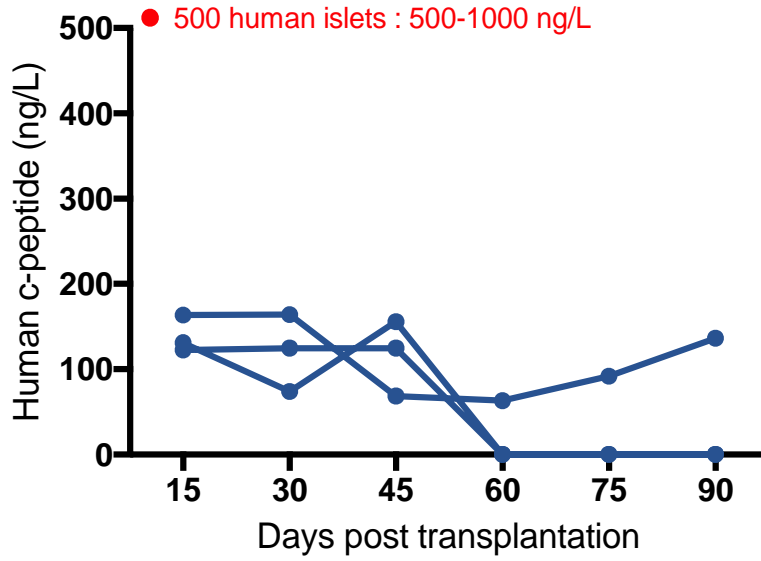


Figure 41: Stage 4 cells generated with iPS DF19.9 cells using SD Kit - In vivo evaluation. Fasting human c-peptide (ng/L) levels were measured over 3 months. Normal range of c-peptide secretion from 500 human islets is 500-100ng/L (red dot). SD Kit: STEMdiff Kit.

- 3) Evaluation of stage 4 cells compared to stage 7 β -like cell using the Reznicek 2014 protocol alone or and STEMDiff Pancreatic Progenitor Kit (S1-S4) followed by Reznicek to S7

Recently, several groups published β -like cell differentiation protocols in which the generated cells resemble a rather mature phenotype and *in vivo* maturation time to acquire functional properties is significantly reduced (Pagliuca et al. 2014; Reznicek et al. 2014; Russ et al. 2015).

For this thesis, either the Reznicek protocol was used to generate stage 1 to stage 7 cells or the STEMDiff Pancreatic Progenitor Kit (SD Kit) for the production of stage 1 to stage 4 (S4) followed by the Reznicek protocol to complete stages 5 to 7 (Figure 38).

Gene expression of the differentiation markers chromogranin A, CK19, PDX1 and NKX6.1 was increased between stage 4 and stage 7 in cells differentiated with the Reznicek protocol but not in cells differentiated with the SD Kit + Reznicek protocol (Figure 26). This increase allows the S7 cells of the Reznicek protocol to achieve the gene expression of the S4 cells produced with the SD Kit. Despite this increase, insulin and glucagon expression remained 4 log apart from the expression levels in a pool of human islets from 10 donors (Figure 42).

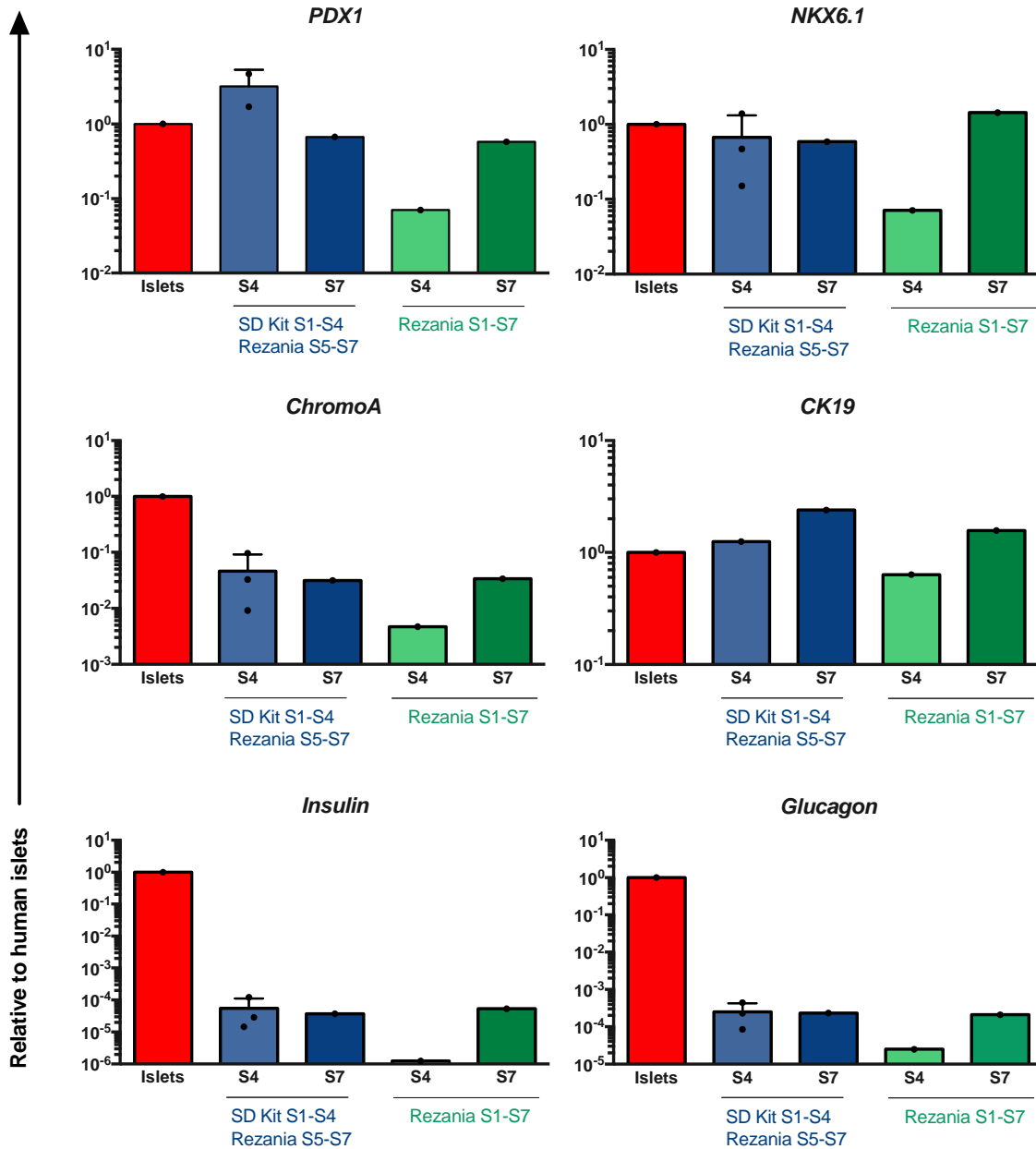


Figure 42: iPS DF19.9 cells at stage 7 using SD Kit + Rezania or Rezania alone - in vitro evaluation. Gene expression of *PDX1*, *NKX6.1*, *Chromogranin A*, *CK19*, *Insulin* and *Glucagon* from iPS DF19.9-derived cells at differentiation stage 4 and 7. *RPL27* was used as house-keeping gene and results are expressed as a fold change relative to a pool of 10 human islet donors. Gene expression is shown on a logarithmic scale. SD Kit: STEMdiff Kit.

After more than 2 months of *in vivo* maturation, we observed a significant increase in fasting human c-peptide, almost reaching the reference level of c-peptide secreted by 500 human islets. This finding indicates that “second generation” protocol generated cells showed advanced β -like cell maturation. In 3 mice out of 5 (1 mouse grafted with cells from the Rezania protocol and 2 mice

grafted with SD Kit + Rezia protocol) we observed a human c-peptide secretion higher than 200ng/L (Figure 43A). In a graft with cells differentiated with the Rezia protocol we detected a significant number of insulin positive cells (Figure 43B).

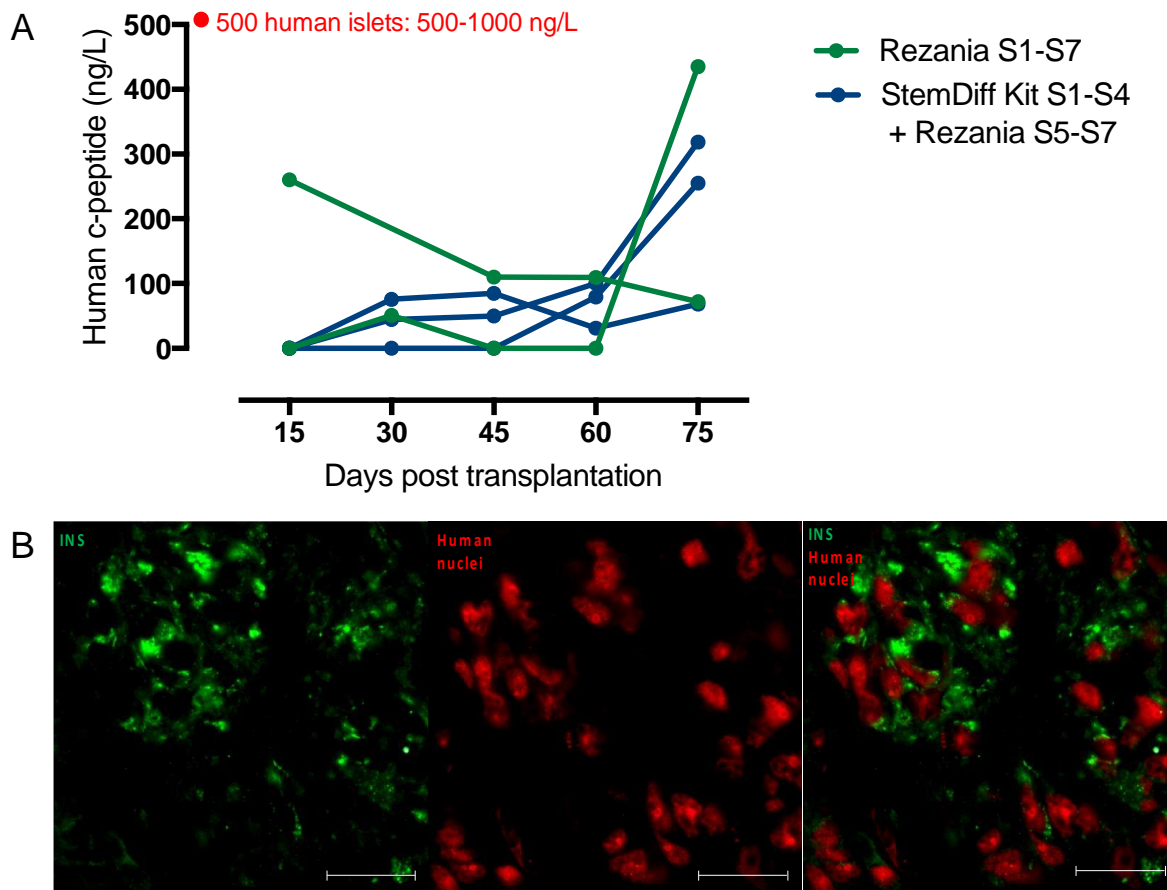


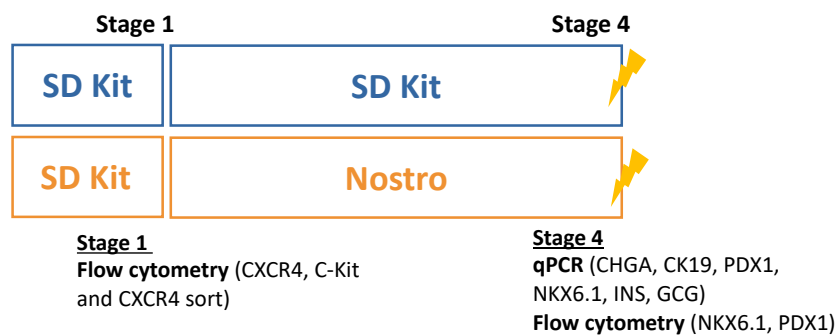
Figure 43: Stage 7 cells generated using the Rezia protocol or SD Kit with iPS DF19.9 cells engrafted under the kidney capsule – in vivo evaluation. (A) Fasting human c-peptide (ng/L) levels were measured over 3 months. Normal range of c-peptide secretion from 500 human islets (red dot) is 500-100ng/L. Stage 7 cells were obtained from either the Rezia 2014 protocol or with SD Kit (from stage 1 to 4) followed by Rezia 2014 (stage 5 to 7). (B) Immunofluorescent staining of stage 7 cells engrafted under the kidney capsule and harvested at 3 months post-transplant for insulin (green) and human nuclei (red) (Expt 31 – Rezia stage 1 to stage 7 protocol). Scale bar = 50 μ m. SD Kit: STEMdiff Kit.

In conclusion, although the same levels of expression of the pancreatic progenitor genes (*NKX6.1* and *PDX1*) were detected by q-PCR after differentiation were high and identical to levels expressed in human islets, efficiency of endoderm differentiation was low when taking into account double positive CXCR4/c-kit cells. In the following chapters, our objective was to obtain more than 80% endoderm evaluated by flow cytometry.

3. New authorization for H1 granted – December 2017.

Embryonic stem cells remain the gold standard for most published differentiation protocols. By the end of December 2017, we obtained a new authorization for embryonic stem cell research from the French ABM. Two months were required to re-establish the MTA and to import the cells again and finally in February 2018, we were able to start differentiation experiments using H1 cells. Just as for the iPS DF19.9 cell line, we first focused on endoderm differentiation optimization and then, on pancreatic progenitor differentiation. Visiting the laboratory of Dr. Nostro was a game changer in our goal of optimizing pancreatic differentiation as we learned to generate high rates of pancreatic progenitor cells for several cell lines. For the next differentiation experiments, we compared the newly learned protocol from Dr. Nostro laboratory to the STEMdiff Kit (Figure 44). For definitive endoderm quantification, the flow cytometry-based method analysis used in Toronto was adopted, standardized and used as a new gold standard of evaluating differentiation efficiencies.

In vitro evaluation



In vivo evaluation

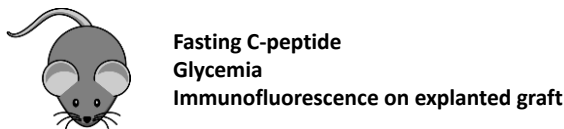


Figure 44: Overview of applied differentiation protocols with H1 cells. H1 cell line was differentiated towards stage 4 pancreatic progenitor cells according to the SD Kit from stage 1 to stage 4 or the SD Kit for stage 1 and the Nostro protocol for stages 2 to 4. Stage 1 cells were analyzed *in vitro* by flow cytometry. Stage 4 cells were analyzed *in vitro* by qPCR and flow cytometry prior to transplantation under the kidney capsule of immunodeficient mice. Mice were followed for 3 months to assess human fasting c-peptide and glycemia *in vivo*. Grafts were analyzed by immunofluorescent staining. Arrows represent timepoint of cell engraftment. SD Kit: STEMdiff Kit.

1) Optimization of definitive endoderm differentiation after Toronto visit

H1 cells were differentiated into stage 1 cells using the SD Kit. In experiment 53, the generation of stage 1 cells was optimized and lasted either 3 vs 4 days where 87,5% or 95,6% double positive cells for CXCR4 and C-Kit were obtained, respectively (Figure 45A). For additional experiments in Lille, the 4 days differentiation protocol was applied and resulted in 93,13% double positive cells on an average for CXCR4/C-Kit (Figure 45A). The evaluation of the 6 experiments included in this thesis revealed a similar dot plot pattern (as reported in Figure 45B), representing all achieved flow cytometry results for stage 4 determination.

A

H1 Optimization SD Kit				
Endoderm markers		CXCR4	C-Kit	CXCR4/C-Kit
H1 SDKit 3d	Expt 53	86%	91,70%	87,50%
H1 SDKit 4d	Expt 53	97,40%	97,10%	95,60%
	Expt 54	92,90%	97,40%	92,70%
	Expt 60	95,20%	96,17%	94,40%
	Expt 61	82,64%	86,81%	81,70%
	Expt 67	99,70%	99%	99,40%
	Expt 70	96,68%	98,06%	95%
	Mean	94,09%	95,76%	93,13%

B

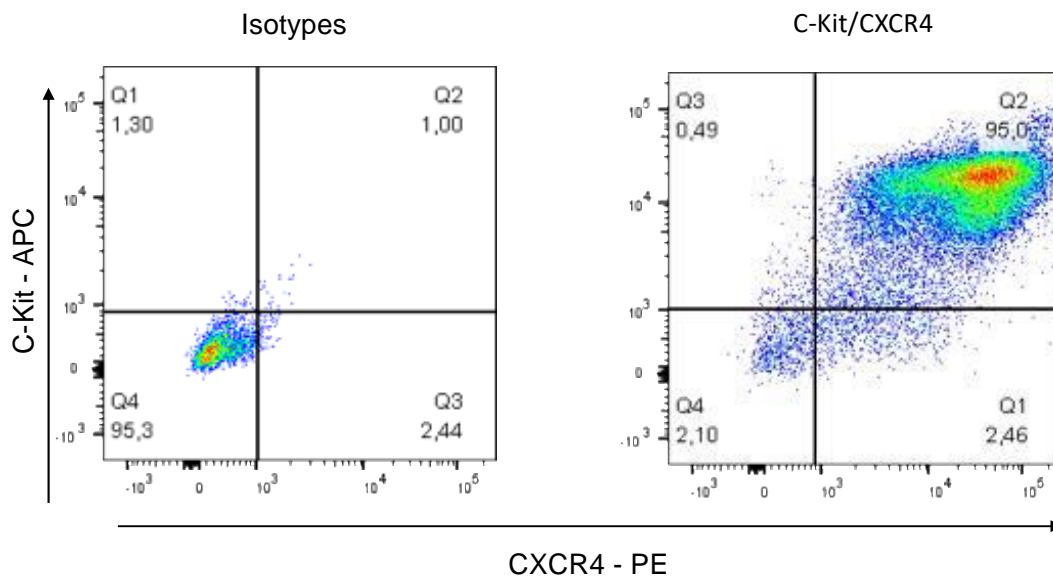


Figure 45: Stage 1 cells generated using SD Kit with H1 cells optimized in Toronto. FACS quantification of endoderm formation. (A) Table of percentage of stage 1 cells expressing CXCR4 and C-Kit that were differentiated with SD Kit. (B) Representative FACS dot plots of experiment 70 illustrating protein expression of CXCR4 and C-Kit in populations of H1-derived stage 1 cells. SD Kit: STEMdiff Kit.

2) Optimization of pancreatic progenitor differentiation

Using SD Kit:

Differentiation into pancreatic progenitors using the SD Kit was heterogeneous and not efficient enough. The best percentage of NKX6.1/PDX1 double positive cells was less than 25% (Figure 46A). Hence, as an attempt to improve differentiation efficiency before evaluation, we decided to

FACS sort the cells for GP2 (Glycoprotein 2), which is a specific cell surface maker for pancreatic progenitor cells (Ameri et al. 2017; Cogger et al. 2017). After FACS purification for GP2, we were able to obtain 48,30% of NKX6.1 positive cells. However, only 0,40 % of pre-sort cells were positive for GP2 (Figure 46B-C), indicating that the differentiation protocol was highly inefficient.

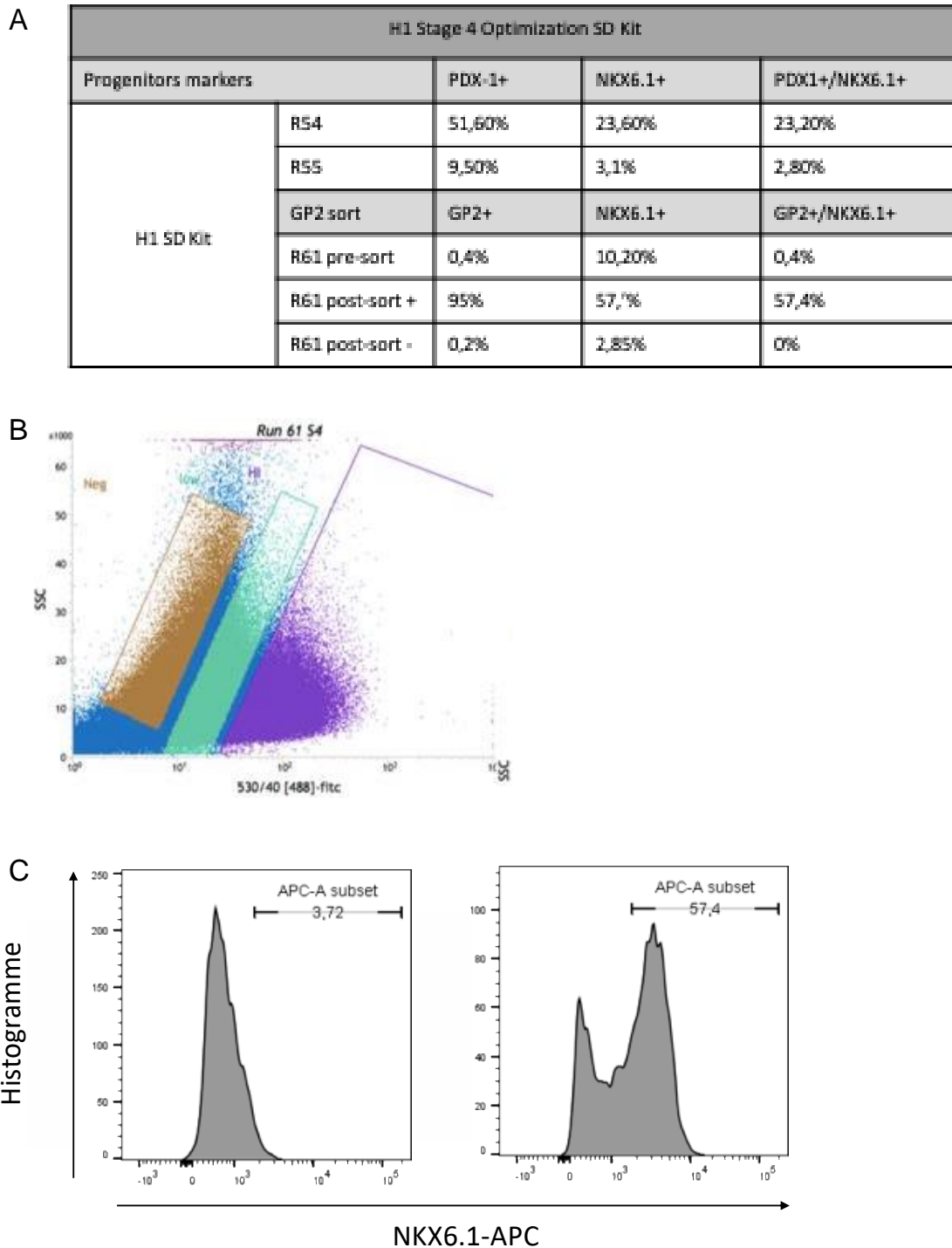


Figure 46: Stage 4 cells generated using SD Kit with H1 cells – FACS quantification of pancreatic progenitors. (A) Table of percentage of stage 4 cells expressing PDX1 and NKX6.1 with SD Kit and GP2

and NKX6.1 before and after sort on GP2 (experiment 61). (B) Representative FACS plot illustrating GP2 sort of experiment 61. (C) Representative FACS plots of protein expression of NKX6.1 in populations of H1- derived stage 4 cells in experiment 61 after GP2 sort (57,4% NKX6.1 expression). SD Kit: STEMdiff Kit.

Using the Nostro protocol:

After applying Dr Nostro’s differentiation protocol to H1 cells, we obtained a reproducible number of more than 95% of double positive cells for NKX6.1 and PDX1 (Figure 47A). In addition, more than 88% of cells were positive for GP2. In figure 47B we reported the flow cytometry plots for the isotype controls and PDX1 / NKX6.1 for stage 4 cells.

A

H1 Stage 4 Optimization SD Kit + Nostro					
Progenitors markers		PDX-1+	NKX6.1+	PDX1+/NKX6.1+	GP2+
H1 SD Kit + Nostro	Expt 70	96 %	97,3%	96%	
	Expt 73	96,9%	98%	96,9%	88,4%
	Expt 74	98,33%	95,27%	95,1	

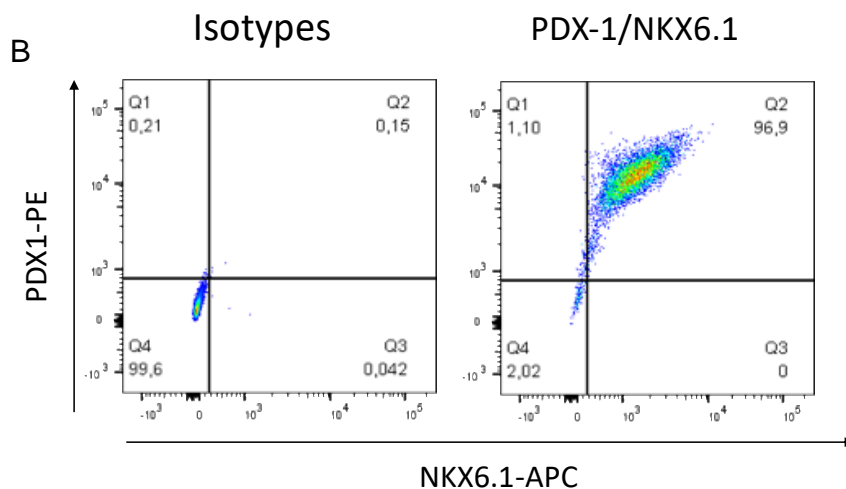


Figure 47: Stage 4 cells generated using the Nostro protocol with H1 cells – FACS quantification of endoderm formation. (A) Table of percentage of stage 4 cells expressing NKX6.1, PDX1 and GP2 with the Nostro protocol. (B) Representative FACS plots illustrating protein expression of NKX6.1 and PDX1 in populations of H1- derived stage 4 cells (Expt 73: 96,9% co-expression of NKX6.1 and PDX1). SD Kit: STEM diff Kit.

Gene expression analysis at stage 4 for the differentiation markers chromogranin A, CK19, PDX1, NKX6.1, insulin and glucagon compared to a pool of 10 human islets donors (red bar) revealed

that cells produced with SD Kit + Nostro's protocol had higher mRNA expression of chromogranin A, CK19 and PDX1 than the pool of 10 human islet donors. By contrast, they had lower expression of insulin and glucagon (2,5 and 1,5 log difference respectively) and identical NKX6.1 expression (Figure 48).

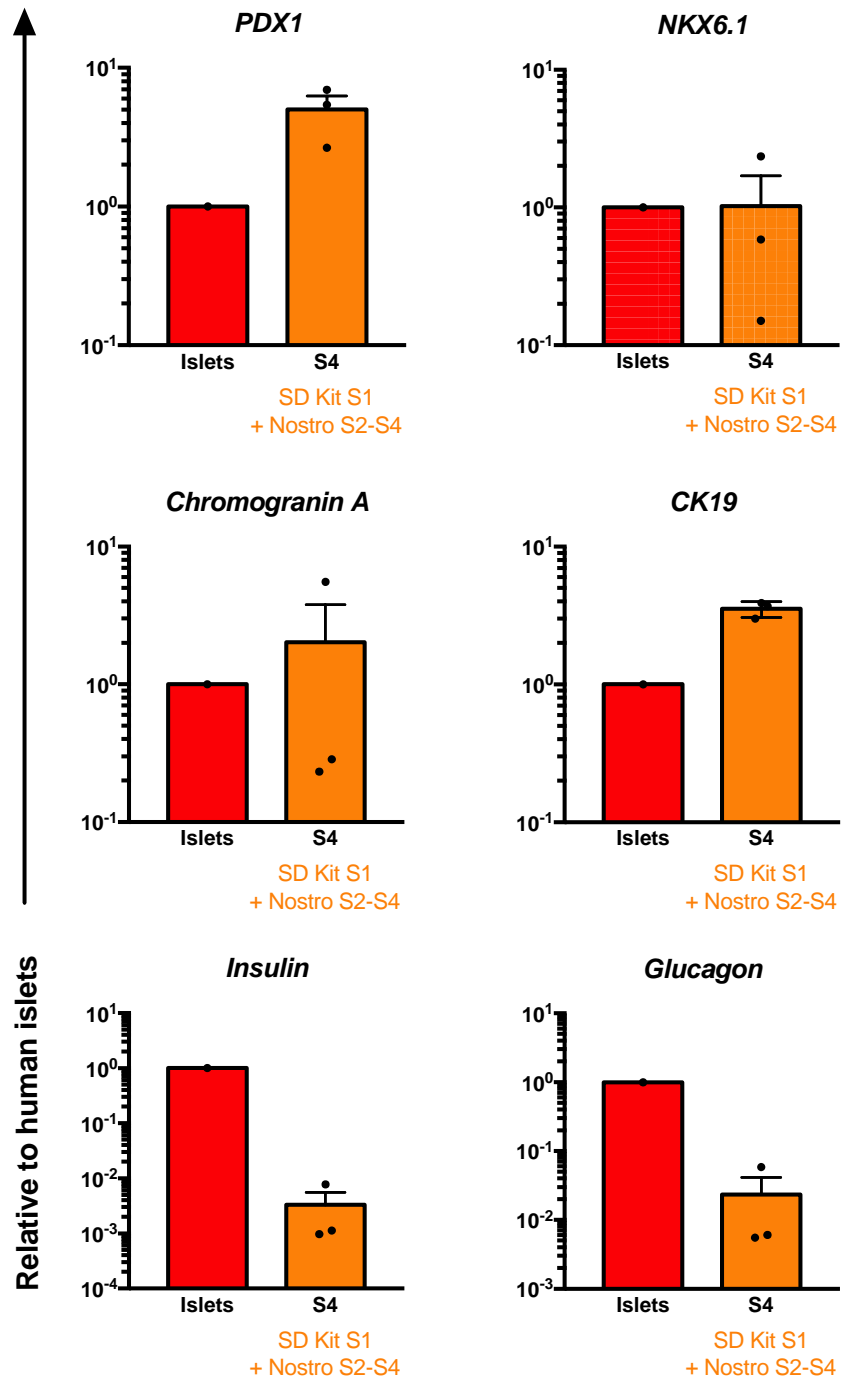


Figure 48: Stage 4 cells generated by using the Nostro protocol with H1 cells – in vitro evaluation. Gene expression of *PDX1*, *NKX6.1*, *Chromogranin A*, *CK19*, *Insulin* and *Glucagon* from H1-derived cells at differentiation stage 4. *RPL27* was used as house-keeping gene and results are expressed as a fold change

relative to a pool of 10 human islet donors (red bar). Data are expressed as mean \pm SEM. Gene expression is on logarithmic scale. SD Kit: STEMdiff Kit.

Finally, we considered that the differentiation of H1 cells into pancreatic progenitor cells was sufficiently optimized when using the Endoderm Kit for stage 1 followed by the Nostro protocol to obtain S4 pancreatic progenitors. Mean endoderm efficiency was 93%. Subsequently, at the end of the differentiation process, we obtain more than 95% double positive cells for NKX6.1 and PDX1.

To assess final maturation of pancreatic progenitor cells *in vivo*, 5 million double positive PDX+/NKX6.1 cells were grafted under the kidney capsule of immunodeficient mice. We obtained reproducibly, a fasting c-peptide secretion close to 100ng/L (the lower limit of the ultra-sensitive human c-peptide assay is 7,6ng/L). The red dot indicates human c-peptide secretion levels from 500-1000 IEQ (Figure 49).

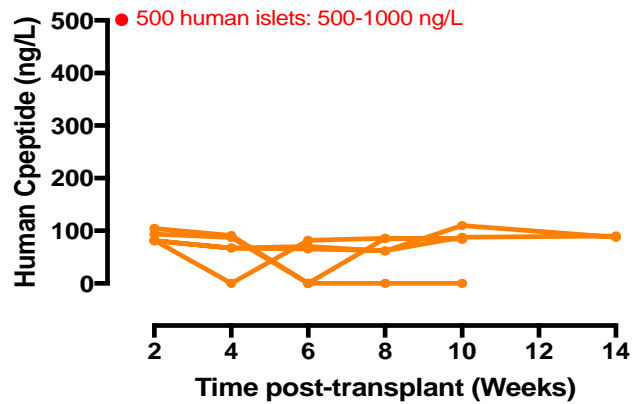


Figure 49: In vivo evaluation of stage 4 cells generated with H1 cells using SD Kit and the Nostro protocol over 4 months (n=8 mice). Normal range of c-peptide secretion from 500 human islets (red dot) is 500-1000 ng/L. Stage 4 cells were obtained using SD Kit (S1) and the Nostro protocol (S2-S4) from H1 cells. SD Kit: STEMdiff Kit.

After 6 months *in vivo*, two kidneys transplanted with 5 million H1 derived S4 cells were harvested and the graft was submitted to perfusion, a dynamic GSIS assay (low glucose, high glucose, high glucose + arginine (10mM) and low glucose). The pluripotent stem cells derived grafted S4 cells were compared to a 2000 IEQ human islets graft (Figure 50). While the human islet transplant (Figure 50, red dot) depicted a 1st phase response to both high glucose and high glucose + arginine stimulation, the H1 graft (figure 50, black square) only responded to high glucose + arginine albeit

at a lower level. When glucose levels were returned to basal levels, insulin secretion in the H1 graft decreased to pre-stimulation levels, demonstrating the specificity of the insulin secretion.

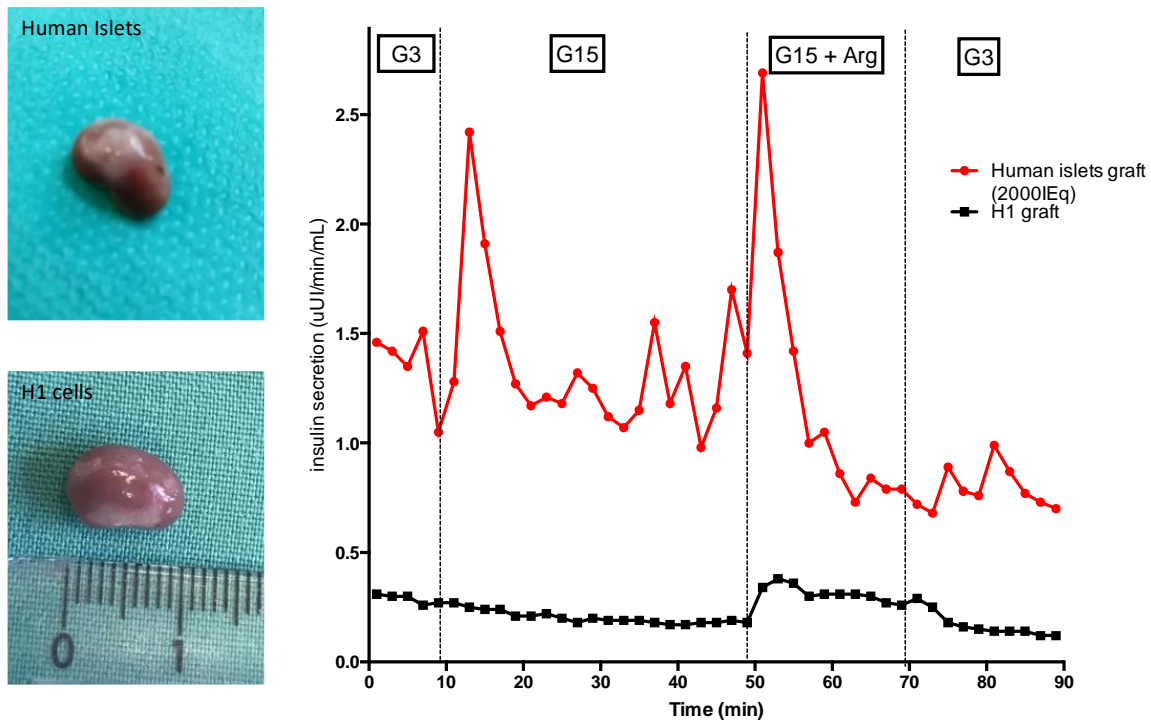
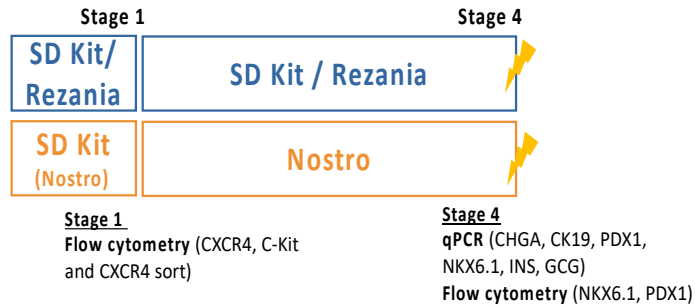


Figure 50: Dynamic GSIS by perfusion of explanted H1-derived S4 cells grafts, 6 months after transplant (black) and an explant human islet graft (control, red). G3: low glucose, G15: high glucose, G15+Arg: high glucose + 10mM arginine. Results are expressed in $\mu\text{U}/\text{minutes}/\text{mL}$.

4. iPS Progeria.

As an approach to accelerate the maturation and aging of differentiated cells, an iPS cell line from patients with Progeria was first tested for its capacity to differentiate into definitive endoderm and then pancreatic progenitors. Indeed, it has been shown that overexpression of progerin is sufficient to induce markers of aging in fetal-like neurons differentiated from pluripotent stem cells (Miller et al. 2013). The optimization of iPS cell line differentiation into pancreatic progenitor cells was the prerequisite to study the maturation and aging of differentiated cells (Figure 51).

In vitro evaluation



In vivo evaluation



Fasting C-peptide
Glycemia
Immuno on graft

Figure 51: Overview of the differentiation protocols applied with patient specific iPS HGPS cells. iPS HGPS AG1972 cell line was differentiated towards stage 1 and stage 4 pancreatic progenitor cells. Stage 1 differentiation was achieved with the Rezia protocol or SD Kit and stage 4 differentiation with the Rezia protocol, SD Kit or the Nostro protocol. Stage 1 cells were analyzed *in vitro* by flow cytometry. Stage 4 cells were analyzed *in vitro* by qPCR and flow cytometry prior to transplantation under the kidney capsule of immunodeficient mice. Mice were followed over 3 months to assess human fasting c-peptide and glycemia. Grafts were analyzed by immunofluorescent staining. Arrows represent timepoint of cell engraftment. SD Kit: STEMdiff Kit.

1) Optimization of definitive endoderm differentiation

Using Rezia and SD Kit:

Differentiation to stage 1 with iPS HGPS cells was performed with either the Rezia protocol or SD Kit at respectively 70/80% and 90% confluence. Endoderm quantification was performed by flow cytometry analysis. With the Rezia protocol we tried different S1 durations (3 days to 6 days), and different dosages of CHIR (1X or 2X) to improve S1 differentiation. CHIR is an inhibitor of GSK3 and functions as a WNT activator. Wnt signaling pathways are affected in Progeria disease. Indeed, Zmpste24 mutation interferes with Notch and Wnt pathways (Meshorer and Gruenbaum 2008; Sola-Carvajal et al. 2019). As Wnt increases Nodal plateaus during endoderm formation (Zorn and Wells 2009), we investigated if differentiation yields were increased using twice the concentration of CHIR in the Rezia protocol. Our best result, with the Rezia protocol, was obtained within 6 days of differentiation, 71,5% double positive cells for CXCR4 and C-Kit, with a mean of 54,3% of double positive cells (Figure 52A). With the SD Kit

our best result was obtained within 5 days (Figure 52B-C), 61,9% of CXCR4 and C-Kit double positive cells. Nevertheless, the endoderm differentiation yields were not sufficient to allow differentiation into pancreatic progenitors.

A

iPS HGPS Stage 1 Optimization Rezanía				
Endoderm Markers		CXCR4+	C-Kit +	CXCR4+/C-Kit+
Rezanía 3 days	Expt 45	72,66%	61,35%	56,65%
	Expt 47	46,30%	27,90%	18,70%
	Expt 52	44,80%	30,70%	25,80%
	Expt 57	66,70%	75,20%	52,90%
	Mean	57,61%	48,79%	38,51%
Rezanía 4 days	Expt 52	44,20%	33,40%	22,00 %
	Expt 57	76,40%	68,10%	57,50%
	Mean	60,3%	50,75%	39,75%
Rezanía 5 days	Expt 52	72,20%	63,00 %	51,30%
	Expt 57	82,90%	74,90%	61,80%
	Expt 58	68,30%	74,20%	57,30
	Expt 62	44,20%	58,40%	24%
	Expt 63	53,60%	57%	36,80%
	Mean	64,24%	65,5%	46,24%
Rezanía 5 days + CHIR	Expt 58	64,70%	53,90%	47,90%
Rezanía 6 days	Expt 57	87,90%	78,50%	71,50%
	Expt 58	47,60%	70,70%	37,10%
	Mean	67,75%	74,6%	54,3%
Rezanía 6 days + CHIR	Expt 58	60,10%	58,10%	40,90%

B

iPS HGPS Stage 1 Optimization SD Kit				
Endoderm Markers		CXCR4+	C-Kit +	CXCR4+/C-Kit+
SD Kit 3 days	Expt 56	68,1%	67,77%	55,6%
SD Kit 4 days	Expt 49	49,20%	56,10%	35,10%
	Expt 56	76,41%	67,75%	50,60%
	Mean	49,15%	48,95%	32,65%
SD Kit 5 days	Expt 56	57,69%	82,31%	61,9%

C

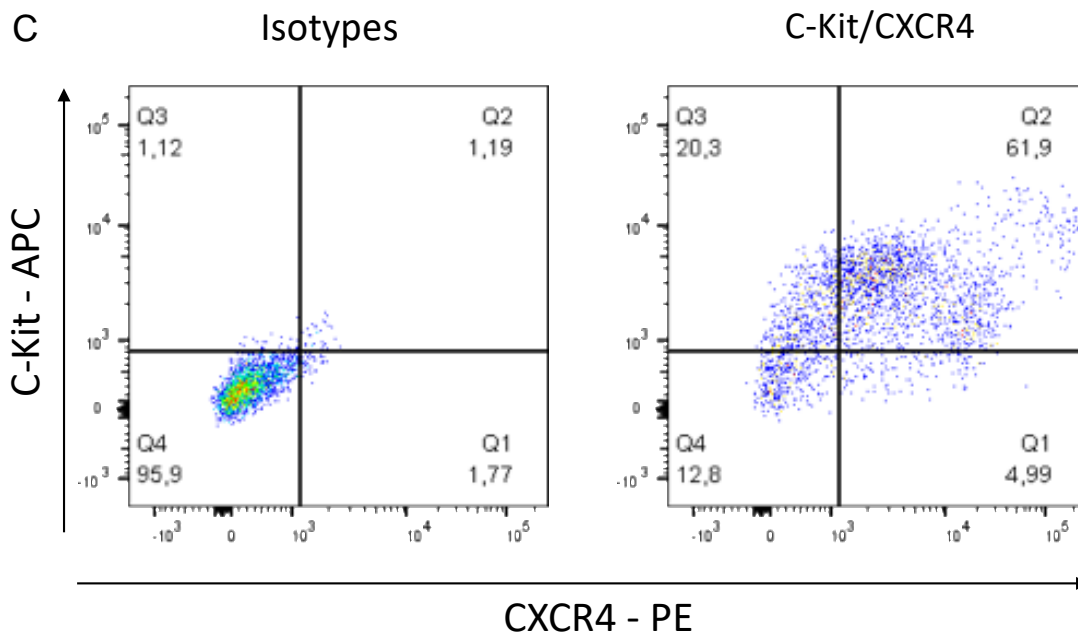
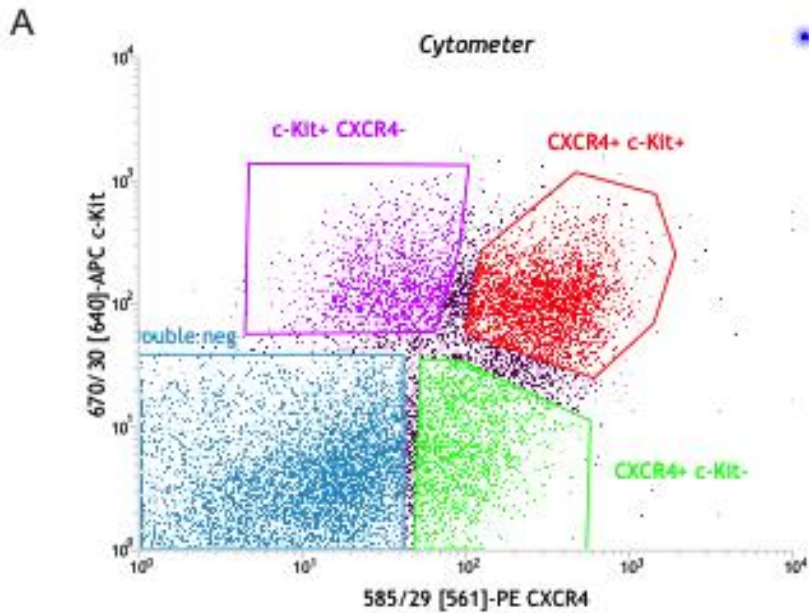


Figure 52: Stage 1 cells generated using SD Kit or the Rezia protocol with patient specific iPS HGPS cells – Definitive endoderm quantification. (A) Table of percentage of stage 1 cells expressing CXCR4 and C-Kit with the Rezia protocol. (B) Table of percentage of stage 1 cells expressing CXCR4 and C-Kit with SD Kit. (C) Representative FACS plots illustrating protein expression of CXCR4 and C-Kit in populations of iPS HGPS- derived stage 1 cells (Expt 56: 61,9% co-expression of CXCR4 and C-Kit). SD Kit: STEMdiff Kit.

To improve endoderm differentiation efficiency of the iPS HGPS, we sorted the cells by FACS for CXCR4 and C-Kit. The percentage of double positive cells after sorting was 94%, demonstrating the feasibility of the strategy (Figure 53). This strategy also allowed us to obtain comparable S1 efficiencies to subsequently compare the H1 cells directly to CXCR4/c-kit FAC purified iPS-HGPS cells. However, the cells were contaminated 1 day after culturing the sorted cell.



B

iPS HGPS Stage 1 Sort				
Endoderm Markers		CXCR4	C-Kit	CXCR4/C-Kit
Expt 63	Pre-sort	77,4%	63,1%	50,6%
	Post-sort	98%	94,17%	94%

Figure 53: Stage 1 cells generated using the Reznia protocol with patient specific iPS HGPS cells – FACS sorting on CXCR4/C-Kit. (A) Representative FACS plot illustrating CXCR4/C-Kit sort of experiment 63. (B) Table of percentage of stage 1 cells expressing CXCR4 and C-Kit before and after CXCR4/C-Kit sort.

Trouble shooting in Dr. Nostro's laboratory: importance of confluency.

For all cell lines and protocols the confluence status the day prior to differentiation is an important factor for differentiation efficiency (Korytnikov and Nostro 2016). In the laboratory of Dr. Nostro in Toronto, we optimized endoderm differentiation using the SD Kit for the H1 and iPS cell lines. We tried differentiation with cells that were confluent at 50% or 70%. The lowest confluence gave the best results at day 4 (data not shown). Back in Lille we reproduced the same conditions for the stage 1 differentiation experiments with the SD kit, as well as trying again on D3 and D5 (Figure

54A). The mean of CXCR4/C-Kit double positive cells was 80,35% at D4. Representative FACS plots of experiment 71 are shown in Figure 55B.

A

iPS HGPS Stage 1 Optimization Nostro				
Endoderm Markers		CXCR4+	C-Kit +	CXCR4+/C-Kit+
Expt 66	3 days	52,66%	98,14%	48,6%
	4 days	89,80%	85,90%	84%
	5 days	85,40%	91%	85,10%
Expt 68	4 days	93,71%	77,02%	78,20%
Expt 69	4 days	76,57%	96,98%	75,90%
Expt 71	4 days	83,82%	86,60%	82,20%
Mean		85,97%	86,625%	80,35%

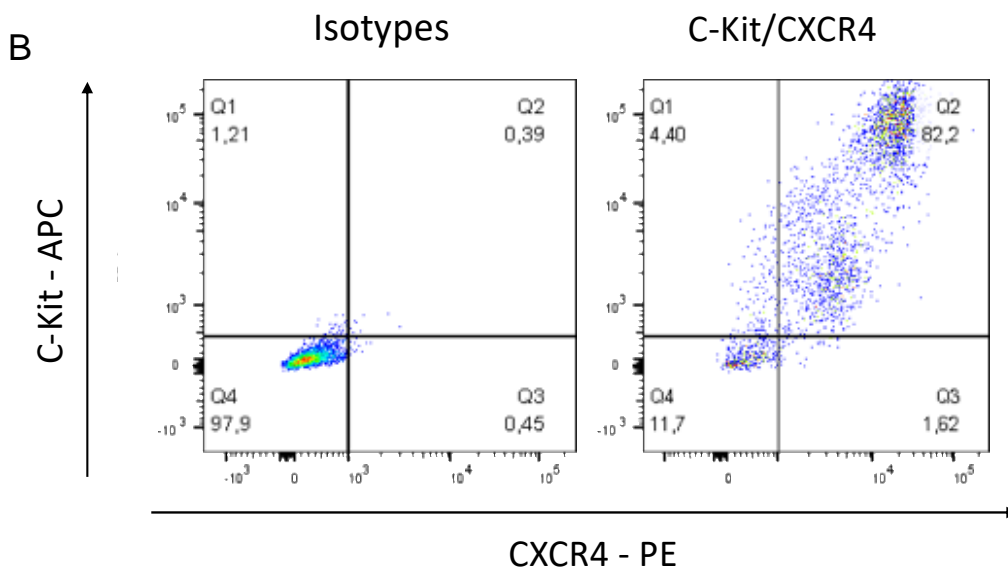


Figure 54: Stage 1 cells generated using a SD Kit (Nostro adaptation) with patient specific iPS HGPS AG1972– Definitive endoderm quantification. (A) Table of percentage of stage 1 cells expressing CXCR4 and C-Kit with a SD Kit. (B) Representative FACS plots illustrating protein expression of CXCR4 and C-Kit in populations of iPS HGPS- derived stage 1 cells (Expt 71: 82,2% co-expression of CXCR4 and C-Kit). SD Kit: STEMdiff Kit

2) Optimization of pancreatic progenitor differentiation

Using the Nostro protocol, we obtained a mean of 95% of double positive cells for NKX6.1 and PDX1 (Figure 55A). Flow cytometry plots from the experiment performed in Toronto are shown in Figure 55B.

A

iPS HGPS Stage 4 Optimization SD KIT (S1) + Nostro (S2-S4)				
Progenitors markers		PDX-1+	NKX6.1+	PDX1+/NKX6.1+
iPS HGPS SD Kit + Nostro	Expt Toronto	99,38%	97,91%	97,8%
	Expt 70	99,40%	95,2%	95%
	Expt 73	99,23%	96%	95,8%
	Expt 74	97,32%	91,7%	90,9%
	Mean	98,81%	95,03%	94,88%

B

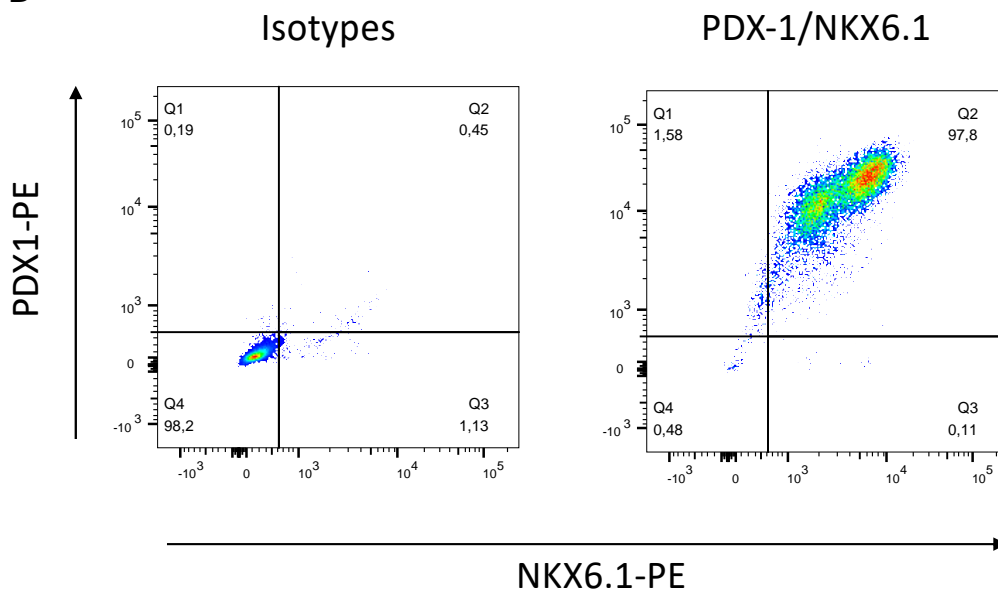


Figure 55: Stage 4 cells generated using the Nostro protocol with patient specific iPS HGPS AG1972 cells – FACS quantification of pancreatic progenitor. (A) Table of percentage of expression of NKX6.1, PDX1 and GP2 stage from at stage 4 of differentiation with the Nostro protocol. (B) Representative FACS plots illustrating protein expression of NKX6.1 and PDX1 in populations of iPS HGPS- derived stage 4 cells (Expt TORONTO: 97,8% co-expression of NKX6.1 and PDX1). SD Kit: STEMdiff kit.

Gene expression analysis at stage 4 for the differentiation markers chromogranin A, CK19, PDX1, NKX6.1, insulin and glucagon compared to a pool of 10 human islets donors (red bar) revealed that, cells produced with SD Kit + Nostro's protocol had higher mRNA expression levels of

chromogranin A, CK19 and PDX1 compared to human islets, a similar NKX6.1 expression and lower expression of insulin and glucagon (3 log difference) (Figure 56).

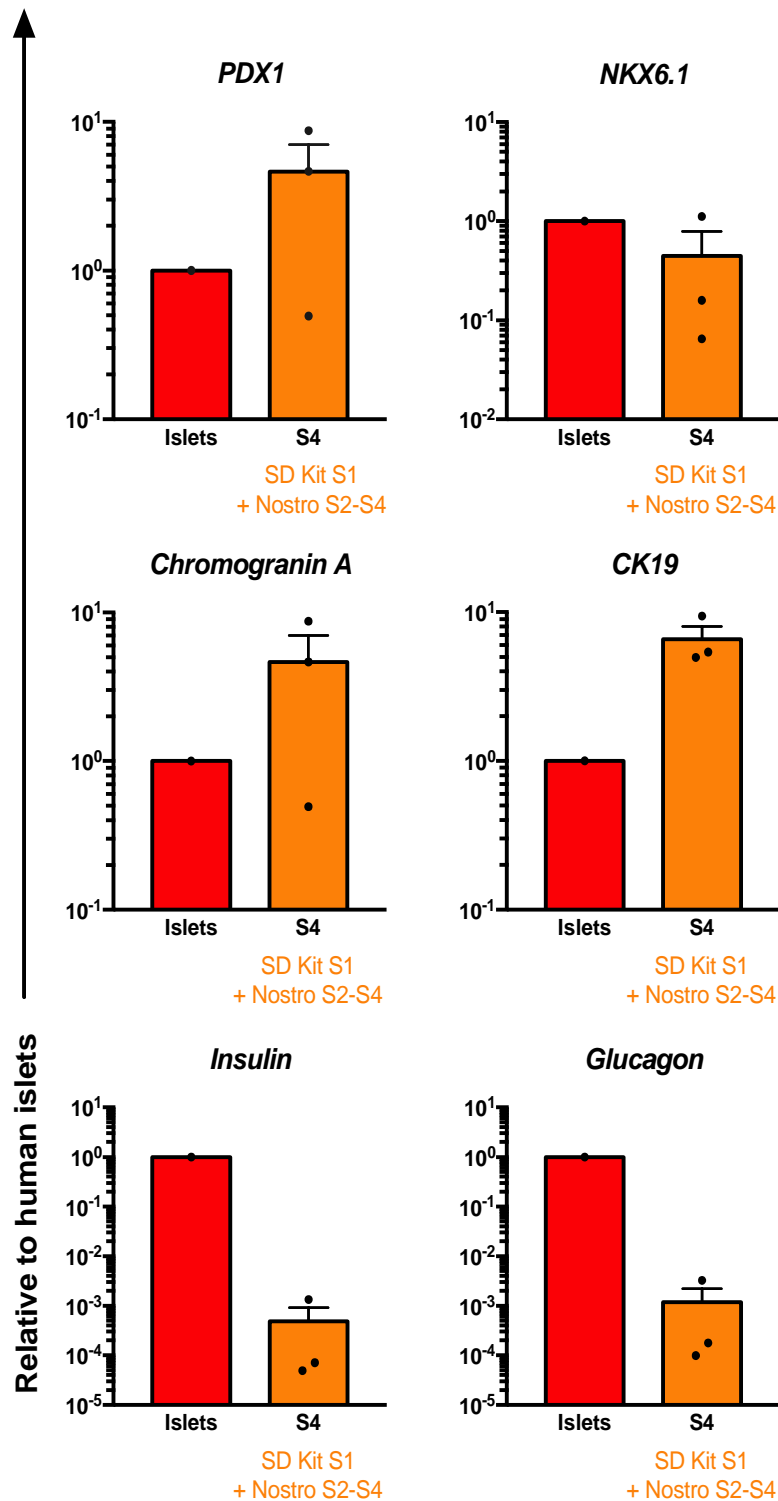


Figure 56: Stage 4 cells generated using the Nostro protocol with patient specific iPS HGPS AG1972 cells – in vitro evaluation. Gene expression of *PDX1*, *NKX6.1*, *Chromogranin A*, *CK19*, *Insulin* and

Glucagon from iPS HGPS cells at differentiation stage 4. *RPL27* is used as house-keeping gene and results are expressed as a fold change relative to a pool of 10 human islet donors (red bar). Gene expression is on logarithmic scale. SD Kit: STEMdiff Kit.

After trying several differentiation techniques, we finally succeeded with the help of Dr Nostro's group in obtaining more than 80% of definitive endoderm at stage 1 and more than 90% of PDX/NKX6.1 double positive cells at the end of differentiation with iPS-HGPS cell line.

Stage 4 pancreatic progenitor cells were then grafted under the kidney capsule of non-diabetic immunodeficient mice for *in vivo* maturation. Human fasting c-peptide was around 100ng/L for all mice (Figure 57).

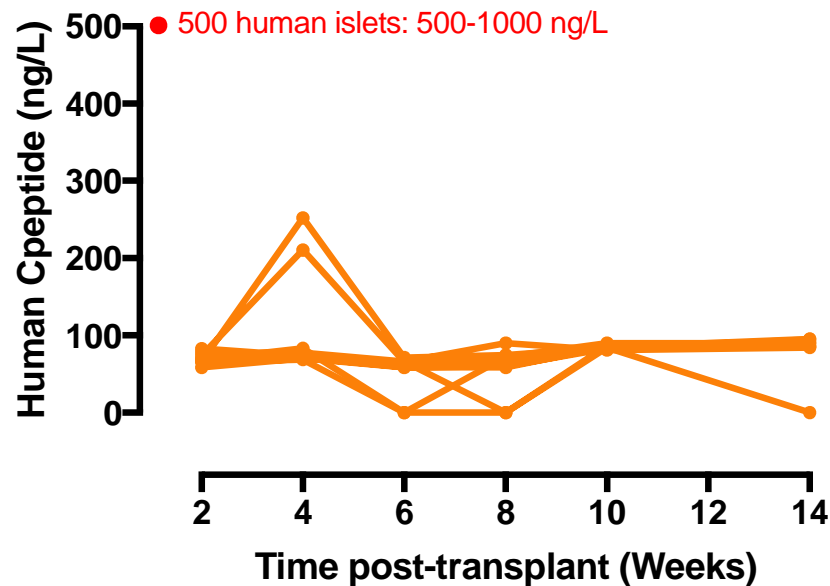


Figure 57: Fasting human c-peptide levels (ng/L) measured over 4 months (n=8 mice). Normal range of c-peptide secretion from 500 human islets is 500-1000 ng/L (red dot). Stage 4 cells were obtained using the SD Kit (S1) and the Nostro protocol (S2-S4) from iPS-HGPS AG1972 cells. SD Kit: STEMdiff Kit.

Chapter 5: Using progerin to induce aging in cells derived from pluripotent stem cells

The objective here was to study the influence of the expression of progerin on pancreatic endocrine cell differentiation *in vitro* and *in vivo* using the previous optimized experiments (Table 11 and Figure 58).

Table 11: Summary of optimized experiments with H1 and IPS HGPS cells both *in vitro* and *in vivo*.

Experiment	Transplantation date	Cell line	Stage	Transplantation site	Number of mice transplanted	<i>In vivo</i> maturation time	S1 (CXCR4+/C-kit+)	S4 (NKX6.1+/PDX-1+)	Use
Expt 68	29/03/2019	IPS HGPS	S4	Kidney capsule	2	6 or 7 months	95,7	95,1	IHC/IF, RNA
Expt 69	02/04/2019	IPS HGPS	S4	Kidney capsule	2	6,5 months	89,4	97,8	Perifusion, IHC/IF, RNA
Expt 70	05/04/2019	H1	S4	Kidney capsule	2	6 or 7 months	78,2	95	IHC/IF, RNA
Expt 71	09/04/2019	IPS HGPS	S4	Subcutaneous	4	6 or 7 months	75,9	95,8	IHC/IF, RNA, protein
Expt 73	16/05/2019	H1	S4	Kidney capsule	3	6,5 months	95	95	IHC/IF, perfusion, RNA
Expt 74	29/05/2019	H1	S4	Kidney capsule	3	6,5 months	87,5	90,9	IHC/IF, RNA, protein

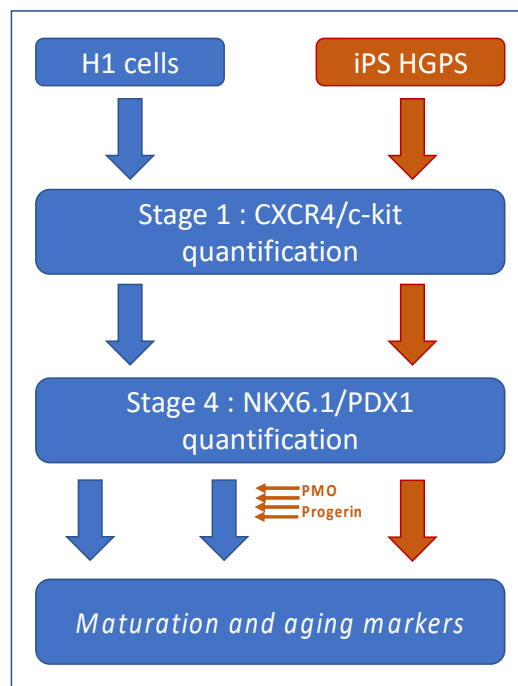


Figure 58: Overview of the objectives of using progeria to induce aging in cells derived from pluripotent cells.

1. Progerin expression during differentiation of pluripotent stem cells

In the undifferentiated state, the iPS HGPS cells derived from patients with progeria have been shown to no longer express the features of aging cells such as shortening of telomeres, mitochondrial fitness and loss of senescence markers (Agarwal 2010, Marion 2009, Prigione 2010, Suhr 2010, Lapasset 2011). First, we confirmed this finding and we questioned if pancreatic progenitor cells expressed *Progerin*. For this purpose, we performed Taqman qPCR gene expression analysis for *Progerin*, *Lamin A* and *Lamin C*, which are all encoded by the same gene. We compared human HGPS fibroblasts AG1972 obtained in collaboration with Dr. Nissan (iSTEM, France), undifferentiated iPS HGPS cells (dedifferentiated from iPS HGPS AG1972), S4 cells generated with iPS HGPS and H1 cells and human pancreatic islets (Figure 43). In mature cells, human islets and human HGPS fibroblasts expressed equivalent levels of *Lamin A* and *Lamin C*, however these two genes and *Progerin* were undetectable in undifferentiated iPS HGPS samples in accordance with Constantinescu et al. (Constantinescu Stem cells 2006). As expected, human HGPS fibroblasts expressed *Progerin* (Taqman q-PCR) while levels in human pancreatic islets were undetectable. We next asked the question what happens during differentiation of iPS HGPS cells. After differentiation, S4 cells expressed *Lamin A* and *Lamin C* at lower levels than mature cells, and differentiated iPS-HGPS expressed around 30% less of *Progerin* than their HGPS patient derived fibroblast counterpart (Fibroblast AG1972) (Figure 59).

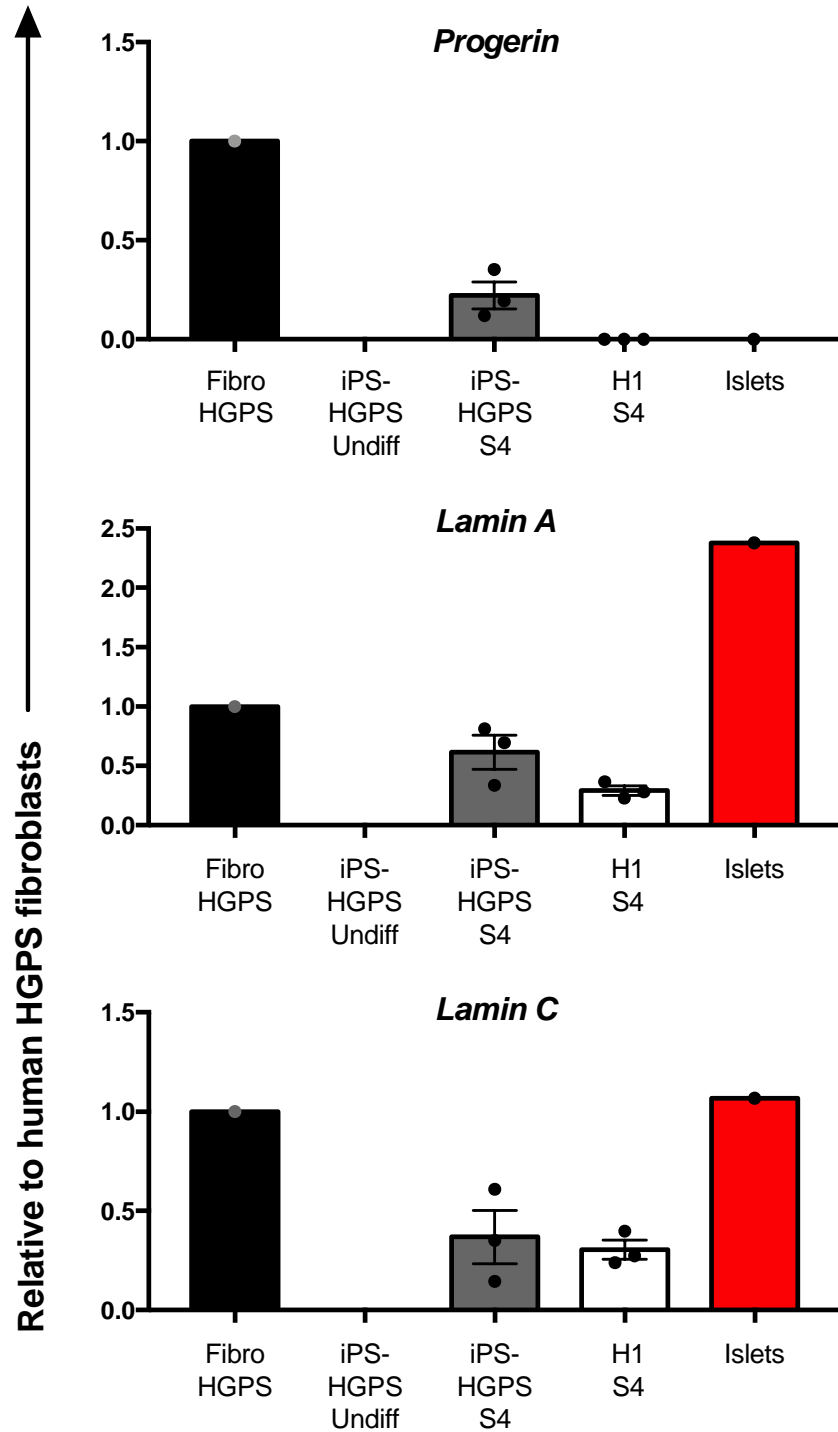


Figure 59: Gene expression profile of Progerin, Lamin A and Lamin C was determined in fibroblasts from patients with HGPS-Progeria (Fibro HGPS – AG1972), undifferentiated iPS HGPS cells (dedifferentiated from Fibro HGPS – AG1972), S4 cells generated from iPS HGPS or H1 cells and human islets by Taqman qPCR. GAPDH was used as house-keeping gene and results are expressed as fold change relative to Fibro HGPS AG1972.

2. Role of Progerin on inducing maturation

To assess the influence of progerin on the endocrine maturation of the produced cells, we aimed to determine if there was a difference in the expression of the 4 maturation genes (*MafA*, *MafB*, *NeuroD1* and *Urocortin 3*), in cells produced with H1 cells compared to cells produced with the iPS HGPS cells. *MafA* (Musculoaponeurotic fibrosarcoma oncogene family A) and *MafB* are required for pancreatic β cell development. It has been previously reported that they control β cell function in rodents (Artner et al. 2007, 2010; Aguayo-Mazzucato et al. 2011) and more recently that *MafA* and *Mafb* have an age-dependent expression in human (Arda et al. 2016). In addition, others have shown that *NeuroD1* (Neuronal Differentiation 1) is necessary for the maturation of β cells as well as the acquisition of their glucose response (Gu et al. 2010). Furthermore, it has been shown that cells differentiated from stem cells that exhibit glucose responsiveness after *in vivo* maturation also display an increase of *Urocortin 3* gene expression (Blum et al. 2012).

We compared the expression of these 4 genes in human pancreatic islets and H1 or iPS-HGPS derived cells at stage 4. While for *MafB* and *NeuroD1* the gene expression levels were lower than in human islets, for *MafA* and *Urocortin 3* the expressions were comparable in all groups. For all analyzed genes, a trend for higher expression in the HGPS group was observed compared to H1 differentiated cells (Figure 60).

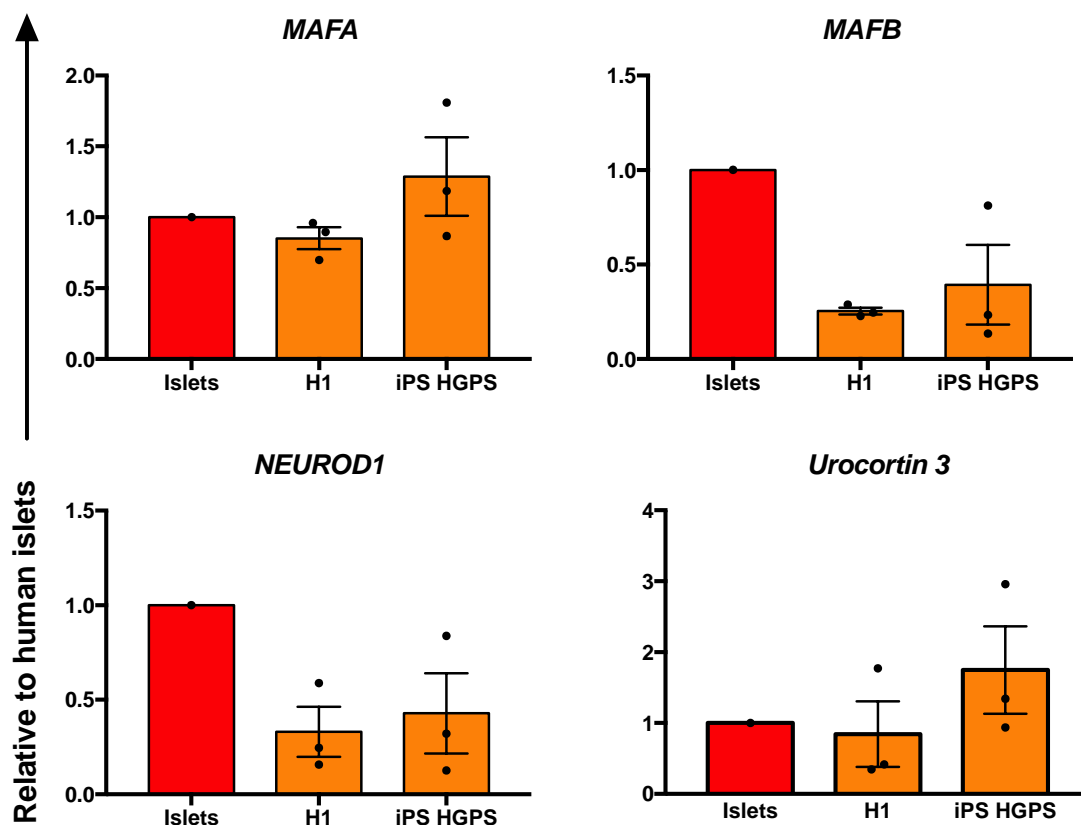


Figure 60: MAFA, MAFb, NeuroD1 and Urocortin 3 expression in iPS HGPS (AG1972) and H1-derived cells at stage 4 and human islets. *RPL27* was used as house-keeping gene and results are expressed as a fold change relative to a pool of 10 human islet donors (red).

As described above, 5 million double-positive PDX1/NKX6.1 cells generated from H1 or HGPS cells were grafted under the kidney capsule of immunodeficient mice. The functionality of the grafts was assessed by measuring glycemia and human fasting c-peptide. At 4 months, an intra-peritoneal glucose tolerance test (ipGTT) was performed to evaluate cells responsiveness to glucose.

Mice grafted with cells differentiated from H1 cells (n=5) secrete the same levels of fasting human c-peptide as mice grafted with HGPS cells (n=8) except for the timepoint of 4 weeks (Figure 60A). Of note, these values are above the detection limit of the Mercodia ultra-sensitive kit. When these values are expressed as an average, the values of the HGPS group were slightly increased compared to H1 group (Figure 60B). When the value of fasting c-peptide was normalized to blood glucose levels, similar secretion profiles over time were observed in both groups (Figure 60C). The average of the normalized values were about 20 arbitrary units higher in the HGPS group but no significance was reached (Figure 60D). After 4 months of *in vivo* maturation, in both groups, we were unable to detect any glucose stimulated human c-peptide secretion in response to an ipGTT

(Figure 60E), when expressed as c-peptide divided by glycemia ratio (Figure 60F). Out of the 7 grafts (Table 11) fixed for histology and immunohistochemistry, 2 showed few or no persistent grafted cells and a large infiltrate. Previous kinetic studies in the U1190 laboratory with human islets showed that ipGTT was superior to OGTT in our immunodeficient nondiabetic model where islets are grafted under the kidney capsule (see Material and Methods Figure 27).

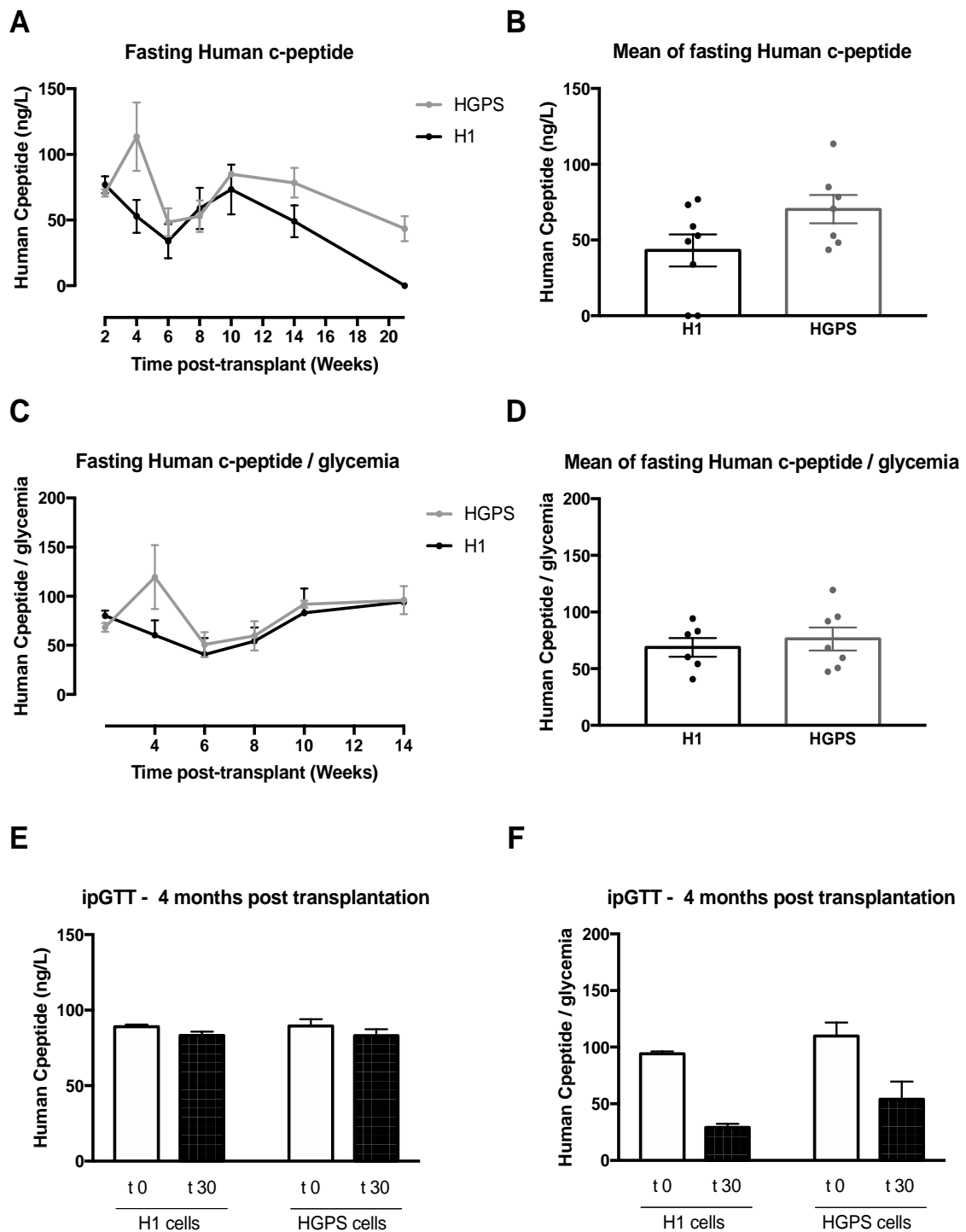


Figure 61: Human c-peptide secretion of differentiated H1 or iPS HGPS cells 4 months after transplantation. (A) Human c-peptide secretion measured each 2 weeks after transplantation. (B) Mean of human c-peptide secretion over 4 months. (C) Human c-peptide secretion/glycemia measured every 2 weeks after transplantation. (D) Mean of human c-peptide secretion/glycemia over 4 months. (E) Human c-peptide secretion after an overnight fast (t0) and after intraperitoneal injection of 3g/kg glucose (t30 min). (F) Human c-peptide secretion/glycemia after an overnight fast (t0) and after intraperitoneal injection of 3g/kg glucose (t30 min). For each group n=8 mice. Results are expressed as mean \pm SEM.

The figure 62 depicts ductal cells and endocrine like structures in iPS HGPS graft 5 months post-transplantation (right) which resemble structures in the human pancreas (left) after routine trichrome staining.

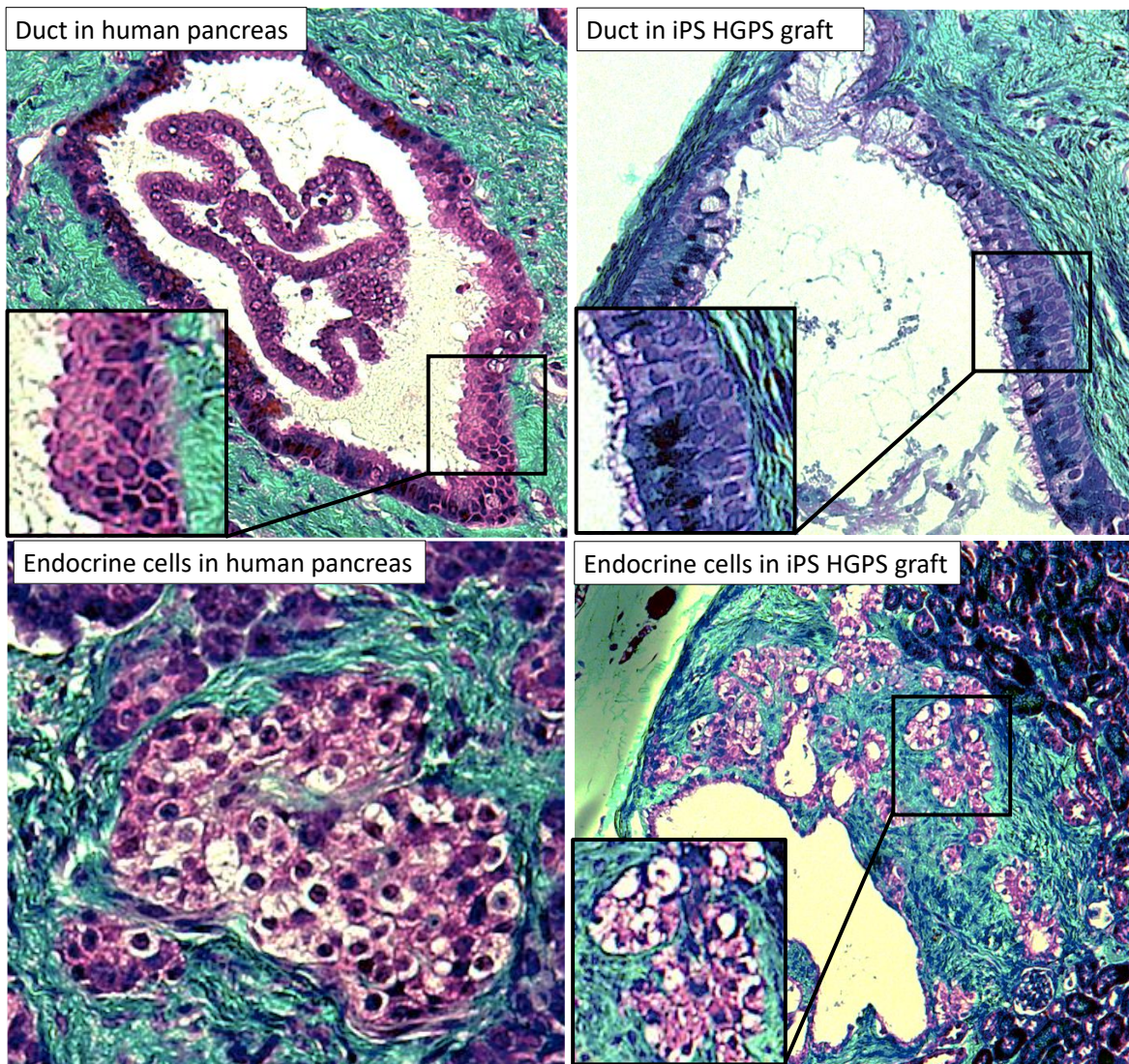


Figure 62: Representative image of a trichrome staining showing duct (top) and endocrine like structure (bottom) in human pancreas (left panel) and iPS HGPS graft 5 months post-transplantation (right panel).

Chromogranin A positive endocrine cells were intercalated in CK19 positive epithelium cells in iPS HGPS graft (Figure 63). Although CK19 epithelium was observed in grafts in our early experiments with H1 differentiated cells (Figure37), in optimized experiments only chromogranin A positive cells were detected in H1 cells (Figure 64). Cytokeratine 19 is a marker for ductal epithelium but we can not exclude the presence of other types of epithelium notably intestinal epithelium that contains neuroendocrine cells. Carbohydrate 19.9 (also known as sialyl-Lewis

antigen) labels human pancreatic ducts (Kerr-Conte et al. 1996) and its detected in blood as marker of pancreatic cancer showed specific labeling of the luminal side of the epithelium structures (results not shown).

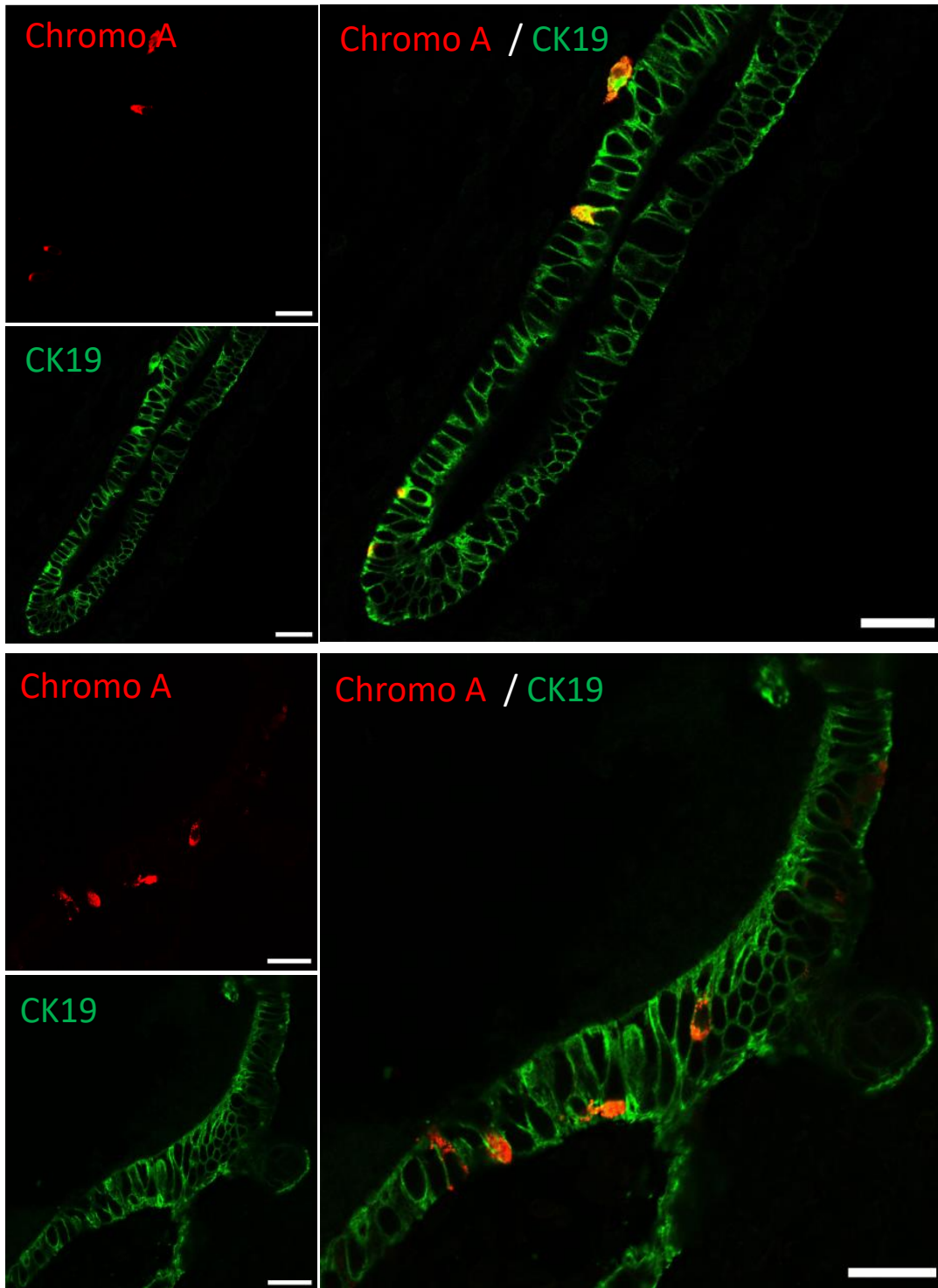


Figure 63: Immunofluorescent staining of graft of iPS HGPS-derived stage 4 cells, harvested 6 months after transplantation (Expt 68) for chromogranin A endocrine (Chromo A, red) and CK19 epithelium (green). Scale bar = 25 μ m.

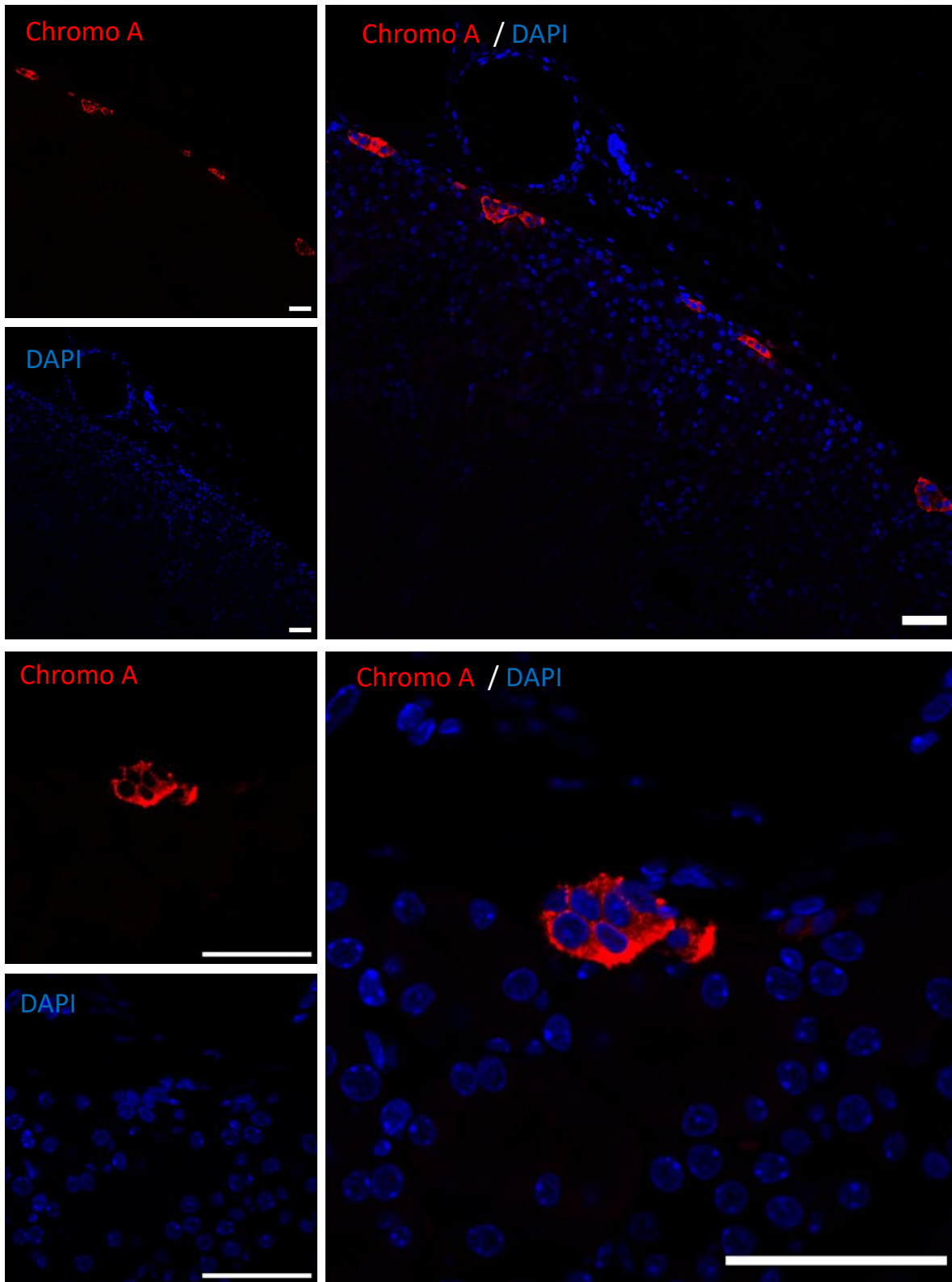


Figure 64: Immunofluorescent staining of graft of H1-derived stage 4 cells, harvested 6 months after transplantation (Expt 73) for chromogranin A (Chromo A, red) and DAPI (blue). Scale bar = 50 μ m

3. Progerin inducing aging

Before analyzing the impact of progerin on differentiated cell transplants, it was necessary to verify if progerin was expressed in grafts and more importantly in pancreatic endocrine cells. Interestingly, some patients with progeria may develop insulin resistance over time without the development of type 2 diabetes (Coppedè 2013). To our knowledge progerin has never been described in human pancreatic islets. In order to verify if progerin was expressed in islets, we performed costainings of progerin and chromogranin A in an old human pancreas (H1066) and on an insulinoma. An insulinoma is a benign tumor of the pancreas composed of immature cells. Progerin was detected in the cytoplasm of a subpopulation of endocrine cells from the old donor but not in the insulinoma cells (Figure 65A). As progerin is a mutated form of lamin A, we also stained the same samples for lamin A/C. Lamin A/C expression was detected in both the old pancreas and the insulinoma, although the lamin A/C signal was weak in endocrine islets cells from the old donor but positive in the neighboring exocrine pancreas (Figure 65A). The figure 65B depicts progerin immunofluorescent staining and nuclear deformation in human HGPS fibroblasts (positive control).

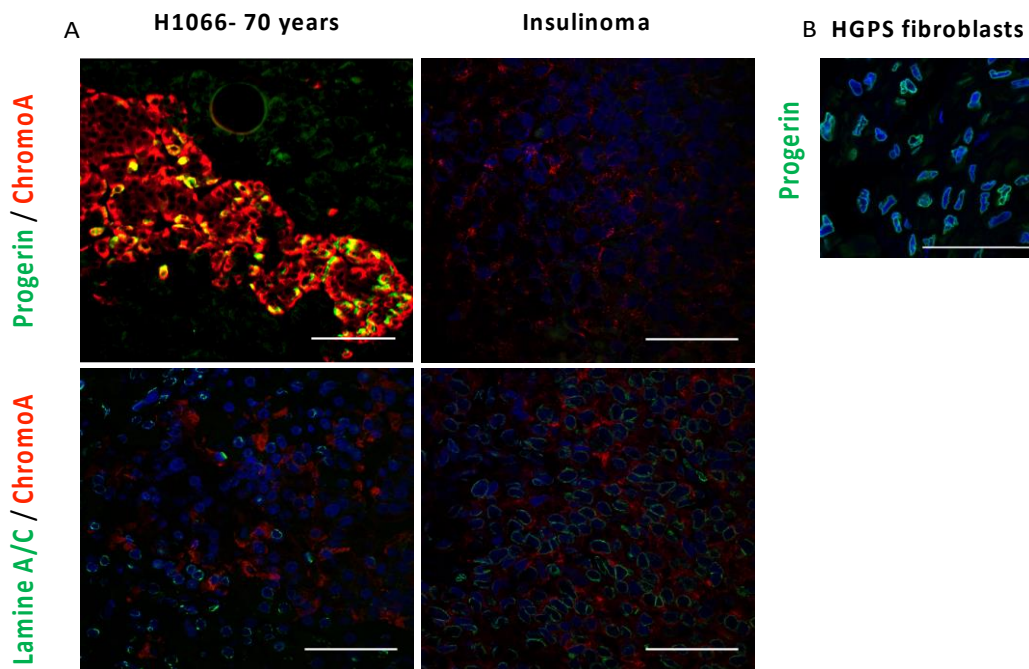


Figure 65: Representative immunofluorescent image for progerin, lamin A and chromogranin A. (A) Co-staining of chromogranin A (red) with progerin and lamin A/C (green) on a pancreas section from a 70 year-old donor (H1066) and an insulinoma. (B) Staining of progerin on HGPS fibroblasts (AG1972). Nuclei was stained with DAPI (blue). Scale bar = 60 μ m

During the early experiments with iPS HGPS cell line, both endoderm and pancreatic progenitor stages were not optimized and thus, few cells were positive for pancreatic progenitor markers after transplantation in mice and large teratomas were present. However, progerin was detected only in grafts of differentiated iPS HGPS cells and not in grafts from H1 cells (Figure 66). Endoderm and pancreatic progenitor stages have since been optimized. Similarly, progerin was detected in HGPS grafts but not in H1 grafts. All human nuclei were not progerin positive in iPS HGPS grafts (Figure 66). Endocrine positive cells were not progerin positive. However, progerin positive cells were detected in teratoma like structure in HGPS graft (Figure 67).

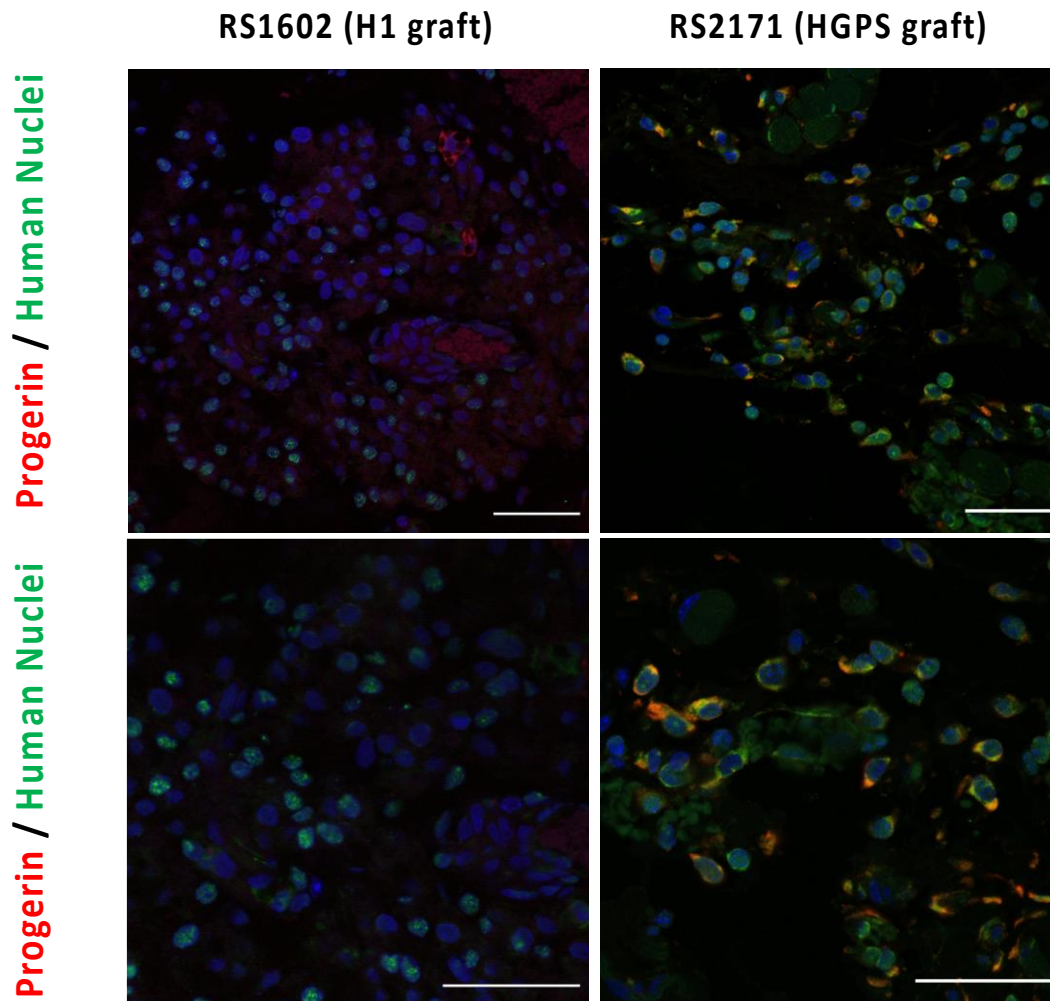


Figure 66: Progerin (red), human nuclei (green) and DAPI (blue) staining in iPS HGPS graft versus H1 graft. Scale bar = 40 μ m.

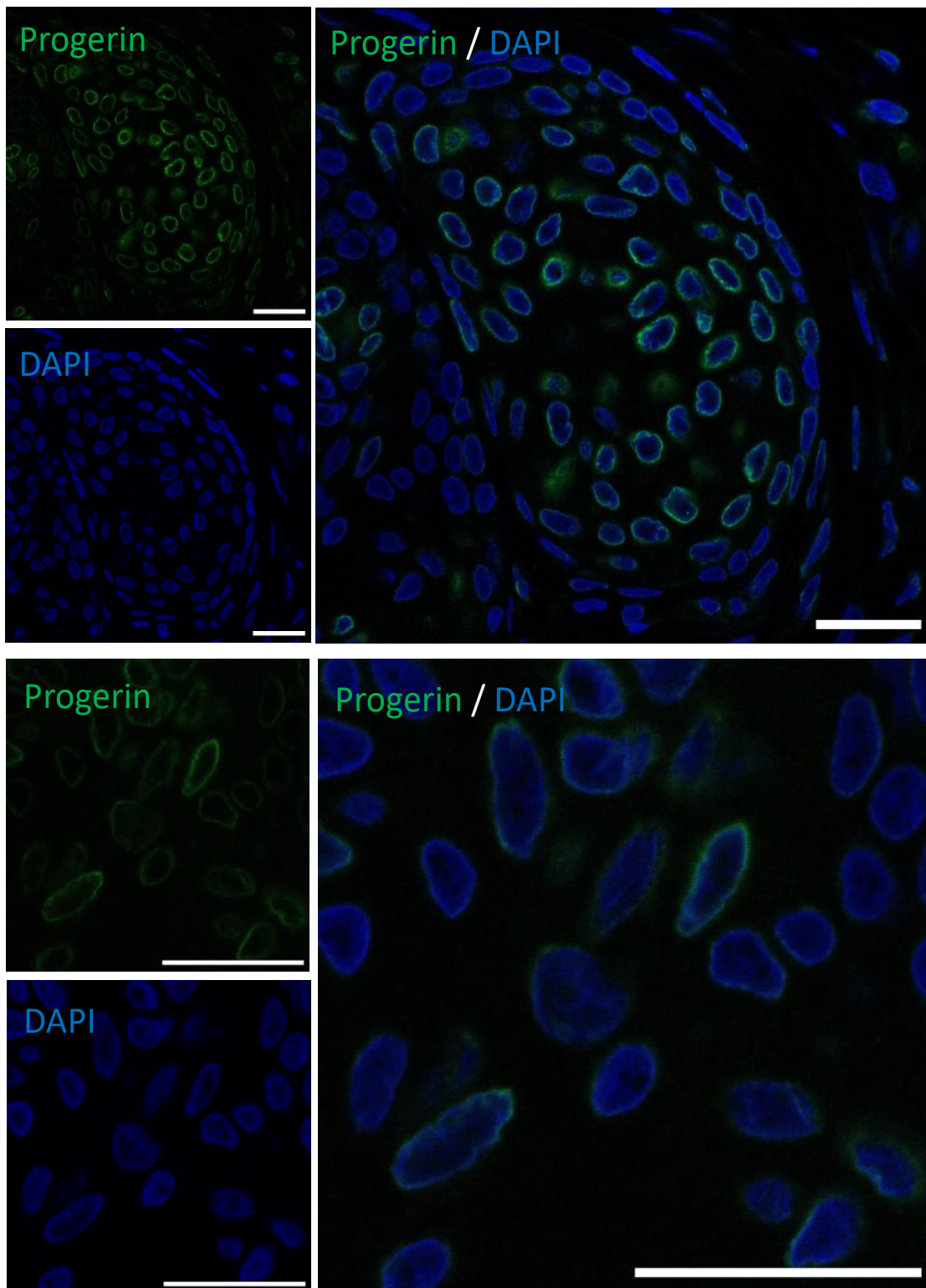


Figure 67: Representative immunofluorescent images for progerin in iPS HGPS-derived stage 4 cells graft, in a teratoma like structure harvested 6 months after transplantation (Expt 68). Scale bar=25 μ m.

In order to investigate the impact of progeria on differentiated cells in grafts, we evaluated several age-related markers, in particular 53BP1, γ H2AX, IGF1R and p16. The tumor suppressor p53 binding protein (53BP1) is a key transducer of DNA-damage signals and it plays a role in regulation or progression through the cell cycle, apoptosis, and genomic stability. P53BP1 is known as a senescence marker of β cells and was proven to be increased in β cells from aged-mice (1,5 years) compared to young mice (2 months) (Aguayo-mazzucato et al. 2017). Next, the H2A histone family member X (H2AX) is a type of histone protein from the H2A family. H2AX is γ -phosphorylated as a reaction on DNA double-strand breaks (DSB) which accumulate in senescent cell. Furthermore, it was shown that cells taken from five different tissues of older mice exhibited increased numbers of γ -foci (O. Sedelnikova et al. 2004). The insulin growth factor 1 receptor (IGF1r) is a membrane receptor which is activated by the IGF1. IGF1 is a growth factor and is involved in anabolic pathways in adults; it has been demonstrated that IGF1r expression is increased in β cell from old mice (1,5 year) compared to young animals of 2 months of age (Aguayo Mazzucato 2012). The same group also showed that IGF1r expression is absent in fetal pancreas and increases during the course of life (C. Aguayo-Mazzucato et al. 2017). Furthermore, enhanced expression of IGF1r can be correlated to p16^{ink4a} (p16) expression, which is a well-known aging marker (Aguayo-Mazzucato et al. 2017).

To further confirm if the above-mentioned markers are also expressed on protein levels, immunofluorescent stainings were performed on paraffin sections of pancreas from a 70-year-old donor (H1066) and a human insulinoma (Figure 68). All markers were co-stained for chromogranin A to identify endocrine cells. Positive staining for 53BP1 was observed in the nuclei of positive chromogranin A cells of the elderly pancreas donor while no signal was detected in the chromogranin A positive cells of the insulinoma. For γ H2AX a positive nuclear labelling in the pancreas H1066 was observed while the endocrine cells of the insulinoma were negative. Of note, the γ H2AX staining in the pancreas of the old donor was stronger in non-endocrine cells than in chromogranin A positive endocrine cells. IGF1r labelling was detected in the exocrine pancreas of the elderly donors but was absent in pancreatic islets whereas in the insulinoma no staining was detected. Previous results in the laboratory showed p16 is negative in young islets (5 year old donor pancreas) but positive in islets of a 20 and 60 year old donor (not shown). Results on grafts are in progress.

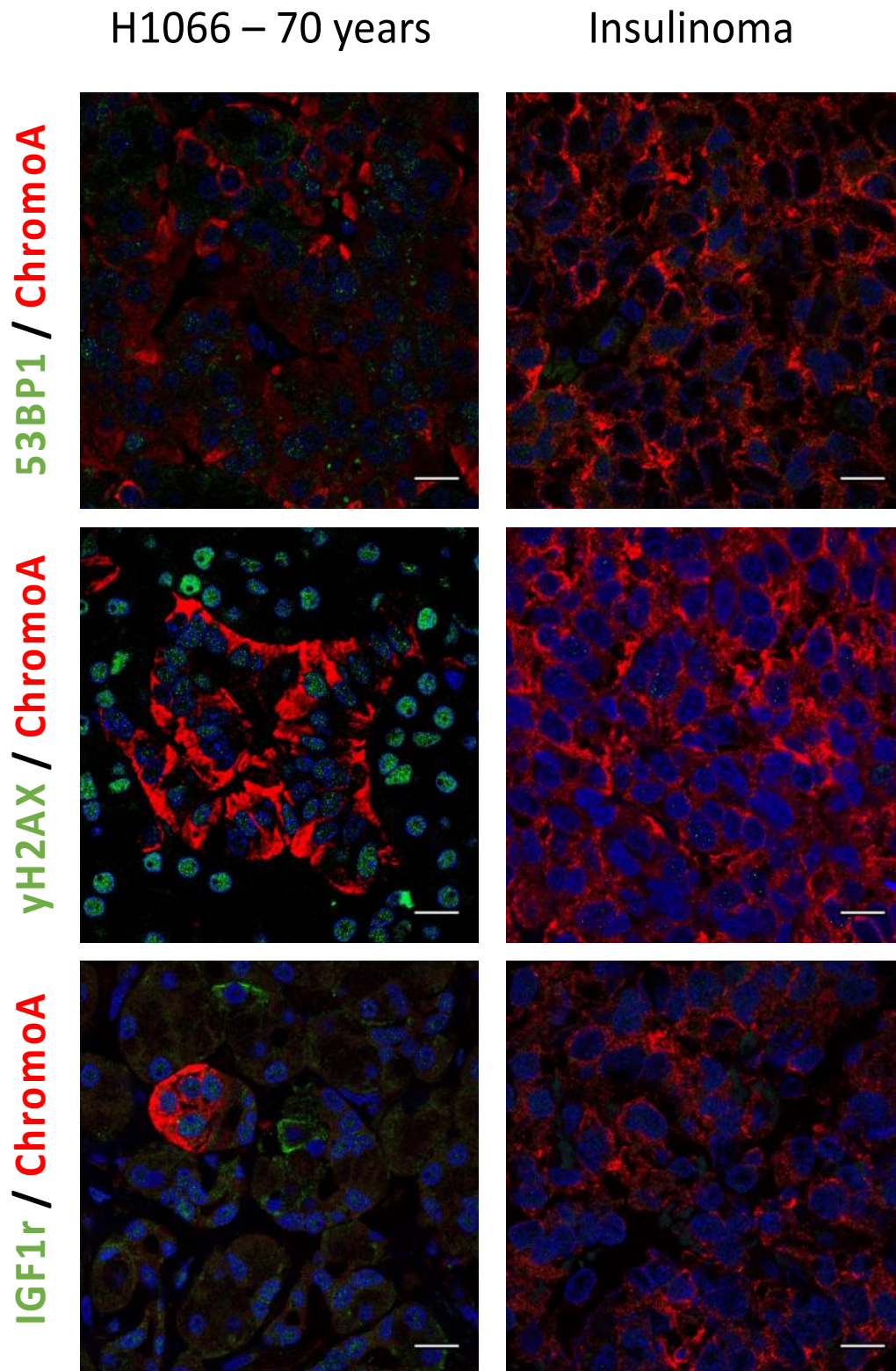


Figure 68: Validation of aging markers on 70-year-old pancreas (H1066) and an insulinoma. 53BP1, yH2AX, IGF1r (green) were co-stained with pan-endocrine marker chromogranin A (red) in the pancreas of a 70-year-old donor (H1066) and in an insulinoma (benign tumor composed of immature cells). Scale bar = 15µm.

yH2AX appeared to be one of the most sensitive markers since the expression was positive in the 70 year old pancreas but not in the more immature insulinoma. Immunofluorescent labeling of yH2AX did not show foci in endocrine cells of human fetal pancreas or young donor (<10 year old pancreas) but showed visible foci in an adult pancreas 20 year old pancreas (not shown). Figure 69 shows yH2AX after 6 months transplantation of H1-grafts in endocrine and non-endocrine cells, while the expression in iPS HGPS-grafts appeared in the majority of cells, which had various shape of nuclei. Furthermore, 53BP1 or IGF1r positive cells were not identify in both type of grafts.

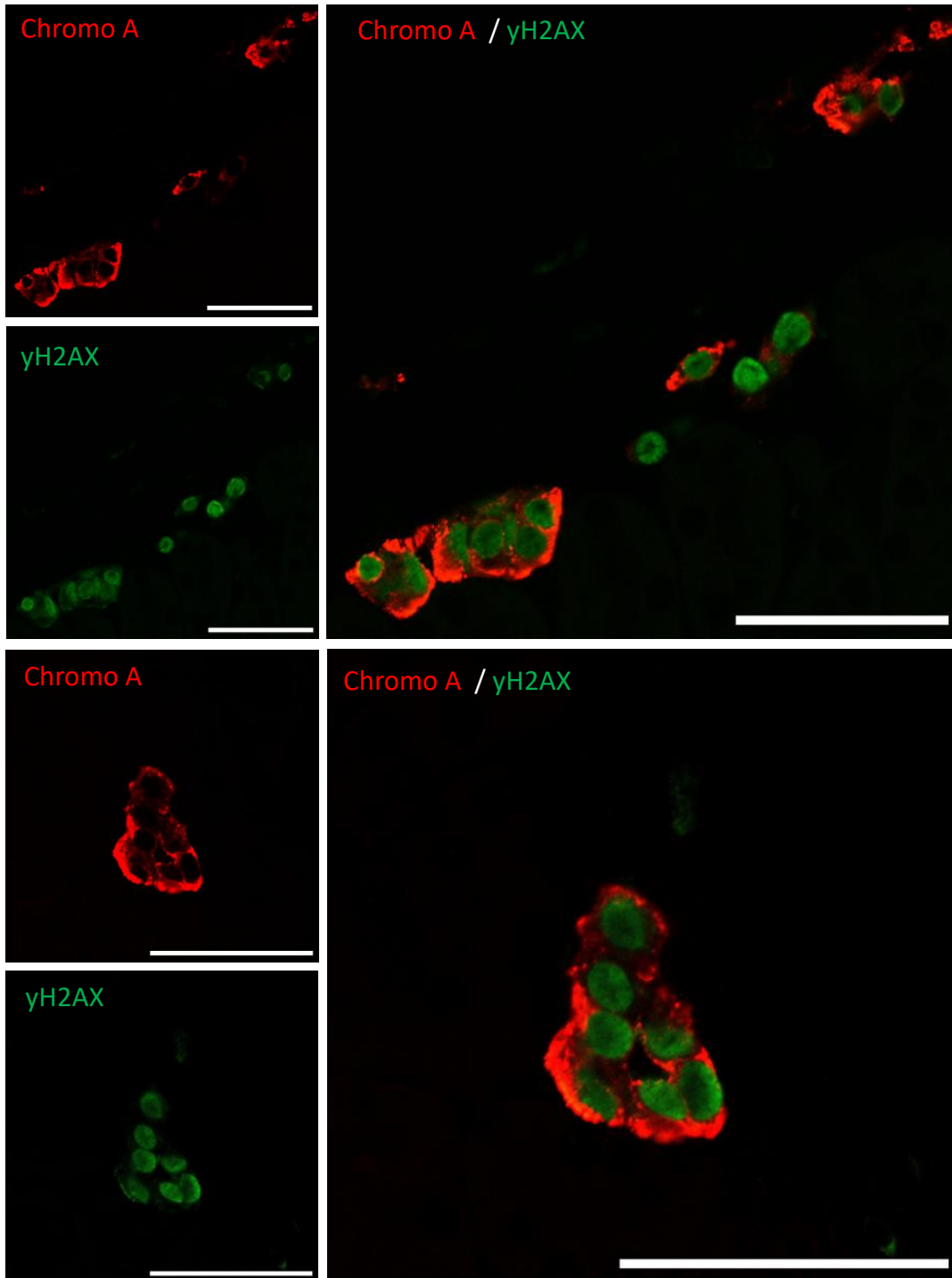


Figure 69: Immunofluorescent staining of graft of H1-derived stage 4 cells, harvested 6 months after transplantation (Expt 73) for chromogranin A (Chromo A, red) and γH2AX (green). Scale bar = 25 μm

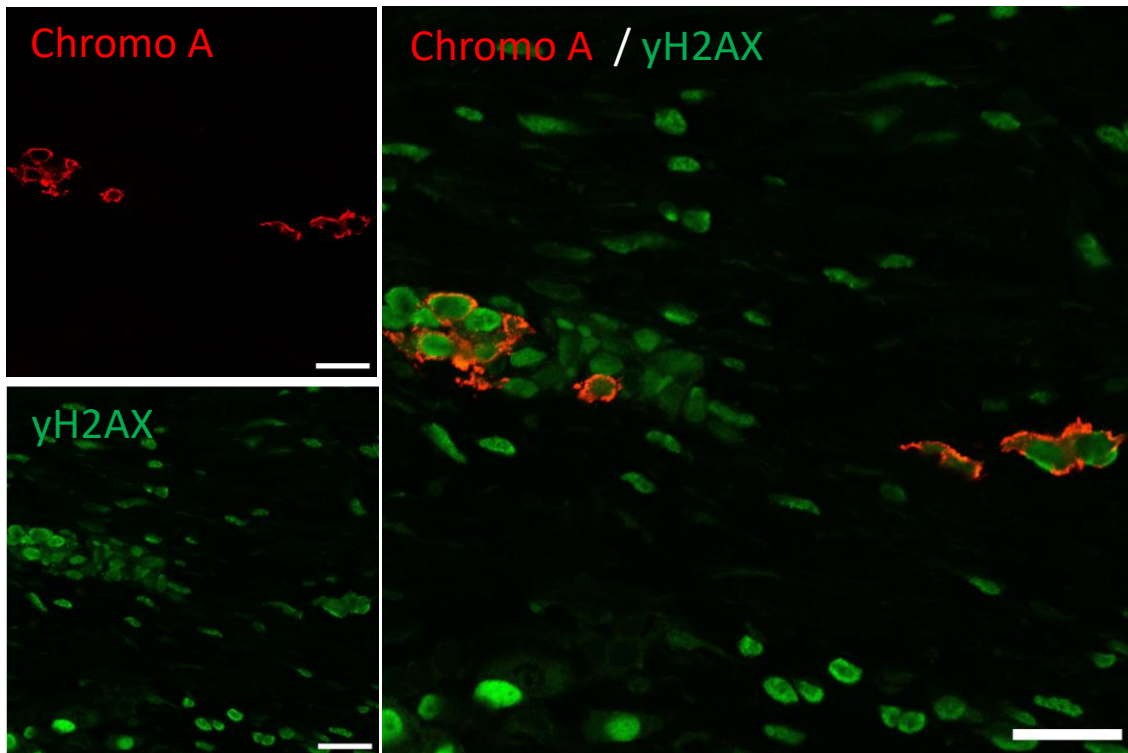


Figure 70: Immunofluorescent staining of graft of iPS HGPS-derived stage 4 cells, harvested 6 months after transplantation (Expt 68) for chromogranin A (Chromo A, red) and γ H2AX (green). Scale bar = 25 μ m

To convincingly prove the role of progerin in the maturation of pluripotent pancreatic endocrine derived cells, we planned to over express progerin using PMO in pancreatic progenitors derived from the H1 cell line. In preparation for this study we optimized both the concentration, and the duration of the transfection of adult human fibroblasts derived from the human islet fraction. As others have previously shown (Egesipe et al. 2016) we could increase the expression of progerin determined by Taqman probes after 48h at 10 μ M with PMOs to levels at 25% or 80% of expression levels detected in HGPS-patient derived fibroblasts respectively from HGPS AG1972 or HGPS Coriell. In our hands, western blots of patient derived fibroblasts required immunoprecipitation with a progerin specific antibody prior to western blotting (Annexe 3).

Chapter 6: Discussion

Pseudo-islets

Pseudo-islets and liver cell 3D microtissues outperform intact native human cells and provide a human cell source that remains functional for 1 month in culture which may hence lead to reduced animal experimentation (September 21, 2016 – InSphero, US Congressional Leaders Discuss Technologies to Reduce Animal Research). In addition to the interest of pseudo-islets for experimentation, our lab was contacted to participate in a clinical trial in the near future in collaboration with Dr. R. Lehmann & R. Zuellig (University of Zurich), Dr. E de Koning (Leiden University), Dr. T Berney (Geneva University) and the Kugelmeier company (AG, Switzerland). In preparation for this clinical trial, we explored the hypothesis that the standardization of human islets into pseudo-islets of a controlled diameter may be superior both *in vitro* and *in vivo* to native human islets. This work is based on the well described capacity of dissociated pancreatic epithelial cells to self-assemble into 3D structures that conserve the architecture of native islets (Halban et al. 1987). In preparation for clinical application of pseudo-islets, we purposely reaggregated pancreatic cells in culture media that was authorized in several past and ongoing clinical trials in Lille, even though most published experimental studies used media supplemented with fetal calf serum. Our clinical culture media consists of CMRL 1066 culture media containing human serum albumin (0.0626%), human recombinant insulin and antibiotics (penicillin / streptomycin).

In our experience, the formation of pseudo-islets was a reproducible technique in 80% of preparations (4/5) and the pseudo-islets were formed after 7 days. The failed islet preparation had a high percentage of dead cells after culture in both native islets and pseudo-islets groups potentially due to the long digestion of the pancreas during islet isolation (more than 20 minutes). Aggregates of 80 µm diameter were formed where the majority of cells were endocrine but exocrine cells were visible in the aggregates in contrast to reports by InSphero (<https://insphero.com/products/islet/>). InSphero reports that remaining exocrine cells rarely integrate the newly formed pseudoislet (InSphero whitepaper) and the nonincorporated exocrine cells eventually die. For their InSphero 3D InSight™ Islet Microtissues, they developed refined post isolation procedures to optimize the formation of uniform 3D pseudo-islets from “qualified donor islet preparations” received from different centers. They use a mild optimized dissociation and patented recovery and preconditioning technology that is able to eliminate the contaminating exocrine fraction and improve recovery followed by their patented GravityPlus plate technology (US2011306122) and media supplements that enhance reaggregation. However, no information was found on the latter technology. Evaluation by *in vitro* perfusion revealed that native islets at

D1 were superior than both groups at D7 which can be attributed to the insulin content drop observed in both D7 groups since glucose stimulated insulin secretion is expressed as percent of content. This decrease has also been observed in 5-6 days pseudo-islets cultured in fetal calf serum supplemented media (Halban et al. 1987). The decrease in intracellular insulin content might be due to the long culture time or the use of human serum albumin since other groups use fetal calf or bovine serum. Indeed, Yu et al reported no change in insulin content between native islets and D3 pseudo-islets using fetal bovine serum supplemented media (Yu et al. 2018) while InSphero reported an increase of insulin content after pseudo-islet formation. We previously published that native human islets can be cultured up to 5 days in CMRL 1066 supplemented with nicotinamide, pyruvate, 5% human AB serum, and antioxidant N-acetyl cysteine media without any change of insulin content (Kerr-Conte et al. 2010). We are currently repeating the pseudo-islet experiments with the human AB serum and antioxidants to confirm if this medium improves our results. Surprisingly if the raw insulin secretion profiles of pseudo-islets were compared to native islets the conclusion would have been different that if insulin secretion was expressed as percentage of content.

Other improvements planned in Lille include testing new molds to reduce the time required to form pseudo-islets (collaboration with Dr. Aart van Apeldoorn, University of Maastricht) in particular as this may then prevent this cell therapy procedure from being regulated by the EMA as an ATMP (Advanced Therapy Medicinal Product – Regulation 1394), which requires GMP production of cells.

Although preliminary (4 preparations), the donor derived heterogeneity of islet preparations including the *in vitro* GSIS was not abolished by the pseudo-islet formation technique. This is in contrast to InSphero's claims albeit they do show that pseudo-islets show persistent "donor dependent GLP-1 responsiveness" (InSphero whitepaper). Lisa Stehno-Bittel's group showed that there was no statistically significant difference in the stimulation index in reaggregated donors. Secondly, she consistently showed that re-aggregated human pseudo-islets respond better than native islets to drugs but that assay variability was decreased with re-aggregated pseudo-islets in 23 human donors (Ramachandran et al. 2014).

In Lille, we were unable to confirm if smaller diameter islets have improved function *in vitro* and *in vivo* as claimed by Lehmann and colleagues (Lehmann et al. 2007). Concerning Oxford's finding that islet number correlates with clinical function and not islet size (Hughes et al. 2018), we must

first mention that in Lille, islet count before culture does not correlate with graft function in our series of islet transplant patients (Mikael Chetboun, U1190, personal communication). However, we will verify if post culture counts correlate with graft function. It should be pointed out that Lehmann's original observation was based on human islet preparations that were immediately transplanted without culture. Oxford could not confirm Lehmann's findings but they used cultured islets and they hypothesized that if the large islets survive culture, then they will function well in vivo post transplantation and this was responsible for their finding that islet number correlated with clinical islet function.

Morphological comparisons between native human islets and donor matched pseudo-islets allowed us to confirm an increase of the glucagon positive surface area in pseudo-islets in the graft compared to grafted native islets, which has been confirmed in humans by Zuellig et al. and in rat by Ichihara et al. (Ichihara et al. 2016; Zuellig et al. 2017)

Several foreseeable limitations exist to current pseudo-islet technology. First pseudo-islet technology should allow formation and transplantation within 72 hours, in agreement with current islet transplantation phase 3 clinical trials authorized by national regulatory authorities. The technique used herein requires a 7 day culture with the Kugelmeier plates which may not be accepted by the French FDA. The Edmonton group is currently upscaling their 3 day centrifugal-forced-aggregation pseudo-islet technology in bioreactors (Yu et al. 2018) for clinical transplantation. In Europe the status and thus regulations of human pseudo-islet production for clinical allografts must be submitted to the CAT (Committee of Advanced Technologies) at the EMA. Extended culture time (more than 72h) and major modifications may result in an ATMP (and not a cell therapy product) status which will require that islet centers have GMP compliance. Another foreseeable limitation of scaling up of pseudo-islet technology for the clinics is the inefficiency of current human islet isolation techniques. The multiple steps before islet transplantation result in a sequential loss of functional β cell mass relative to the number of cells initially present in the pancreas. On average, less than 85% of the pancreas is digested in our center, where 1080 human pancreases have been processed, and subsequent purification steps with density gradients recover only 50-60% of isolated human islets. The current technology to form pseudo-islets involves two enzymatic digestions in two separate steps: enzymatic isolation of pancreatic islets and enzymatic dissociation of islets into isolated cells after several days of culture and before the production of pseudo-islets. We plan to substantially increase human endocrine cell yields for pseudo-islet technology with a single enzymatic digestion step and standardize procedures capable

of recovering more than 80% of human endocrine cells from the entire pancreas. This technology may also allow us to obtain uniform “standardized islets” regardless of the status of donors, including young donors, but also marginal donors including obese and aged donors. Indeed, islets isolated from young donors (under 40 years of age) appear ideal for transplantation but are notoriously difficult to purify, due to surrounding exocrine tissue that increases their density making their separation from the heavy exocrine layer a challenge (less than 40% recovery). In addition, in our center, 30% of human organs come from obese donors, which is linked with a high islet mass and a larger diameter of each islet. It is known that large islets survive poorly in culture (central necrosis). Lastly, the age of donors proposed for organ harvesting is increasing throughout the world. In Lille, 30% of donors are over 55 years of age (15% are over 60 years old). Islets of aging donors show signs of inflammation and fibrosis of the islet blood vessels, but glucose detection and insulin secretion are intact (Almaça et al. 2014). Eliminating the aging vascularization of islets during single cell production could broaden the scope of donors to older donors.

Islet vascular network is necessary for the preservation of the transplanted islet mass (Coronel and Stabler 2013; Vlahos et al. 2017; Weaver et al. 2017; Citro and Ott 2018). Recent ingenious integration of human amniotic epithelial cells with anti-inflammatory, angiogenic, and regenerative properties during pseudo-islet reaggregation appears to be a solution to improve pseudo-islet survival in culture, viability and resistance to hypoxia, grafted pseudo-islet vascularization, insulin content and function, as very recently demonstrated (Lebreton et al. 2019).

Lastly, one key advantage of pseudo-islets is the possibility of cryopreserving the single cells before reaggregation into pseudo-islets (Rawal et al. 2017). This may allow us to freeze cell preparations directly after single cell isolation from several pancreata and subsequently prepare pseudo-islets for a single transplantation. Current procedures involve 2 to 3 transplant procedures per islet transplant recipient. The ultimate long-term goal in the laboratory is to optimize and automate the technology for pancreatic endocrine cell culture and the renewal of culture media as well as digestion, purification and culture steps. The laboratory participates in a consortium (Zurich, Leiden, Geneva, Lille, Kugelmeier, AG Switzerland) to bring pseudo-islets to clinical transplantation.

Pluripotent Stem cells and the role of progerin in pancreatic cell differentiation and maturation:

The goal of this section was to investigate if the expression of a truncated form of lamin A progerin, associated with cellular aging and exploited to accelerate aging in neurons, could improve islet cell maturation. First of all, the differentiation of the H1 human embryonic stem cell line was compared to the differentiation both in vitro and in vivo of an iPS cell line derived from patients with progeria (cell line iPS HGPS 1972 obtained from iSTEM). Although our laboratory had some experience with the differentiation of H1 and the iPS DF19.9 cell line, the huge amount (20 %) of teratomas, the low human c-peptide level secretion post maturation in vivo and the low number of neuroendocrine and hormone positive cells post differentiation suggested that the efficiency of the definitive endoderm (Stage 1) and subsequent pancreatic progenitors (S4) was insufficient. By reading different publications we attempted to improve the differentiation of the cell lines. We tried several differentiation protocols (Odorico, Rezania, SD Kit, Nostro), conditions (2D and 3D) with two healthy (iPS DF19.9 and H1) and one HGPS (iPS HGPS AG1972) stem cell lines in order to obtain endocrine pancreatic cells. Our attempt with the iPS DF19.9 will not be further commented here as we discontinued use with it. Since our early differentiation efficiencies were variable between the 2 cell lines that we wanted to compare, we envisaged to standardize S1 cell purity by FAC purifying with CXCR4 and c-kit and then further enriching S4 pancreatic progenitors by FACs purifying for GP2 (Cogger et al. 2017). After a PhD progress meeting with Dr Nostro in 2018 it appeared that this may be a useful approach but that the efficiencies of both S1 and S4 were too low and needed to be significantly improved. Indeed, each stem cell line has an intrinsic propensity for differentiation in certain lineages (Osafune et al. 2008; Bock et al. 2011; Singec et al. 2016; Southard et al. 2018). Most of the protocols have been published with a limited number of cell lines. Furthermore, there has never been a direct comparison of the different protocols, using the same cell line under the same conditions (on feeder, feeder-free or 3D).

Optimization was done for each cell line during a visit to Dr Nostro's lab in Toronto. The Nostro protocol was the best to obtain sufficient levels of definitive endoderm (>90% CXCR4+/c-kit+) and pancreatic progenitor (>97% CXCR4+/c-kit+) cells for both H1 and iPS HGPS cells which was what was previously published (Nostro et al. 2015). This appears to be the first report of *in vitro* differentiation in definitive endoderm from an iPS HGPS cell line, which is not the major afflicted lineage in the progeria disease. Pancreatic progenitor efficiency was high (>90%

NKX6.1+/PDX-1+) for both cell lines. We learned during this PhD thesis that flow cytometry, which was used in the final years of the thesis is a more stringent and informative technique than following cell differentiation with Q-PCR, which was used in the first 2 years.

When comparing pancreatic progenitors generated from iPS HGPS AG1972 compared to H1 by Q-PCR, it did not allow us to document any differences in *PDX1*, *NKX6.1*, *INS*, *GCG*, *ChromoA*, *CK10* mRNA expression. However, *MAFA* and *UCN3* expression were slightly increased in iPS HGPS generated S4 cells compared to H1 generated S4 cells. Indeed, *MAFA* and *UCN3* expression have been shown to be expressed in mature α and β cells (van der Meulen et al. 2012) and linked to an improvement in static GSIS function (Ghazizadeh et al. 2017). However, they appear non-essential for insulin glucose response as published recently (Nair et al. 2019; Velazco-Cruz et al. 2019). We did not perform *in vitro* glucose stimulation before grafting since S4 cells have been notoriously shown to be insensitive to glucose and we were expecting increased *in vivo* function. However, in the 6 runs performed here with optimized S1 and S4 efficiencies, we were not able to observe any significant difference *in vivo* in human c-peptide secretion between the two groups and mostly the grafts were poorly responsive to glucose stimulation. One explanation may be that grafts were rejected by the mice. Indeed, we were not able to find most of the graft after sacrifice. For these studies, we used SCID beige mice as published (Viacyte) while other groups used NSG mice (Pagliuca et al. 2014; Rezanian et al. 2014; Nostro et al. 2015; Nair et al. 2019; Velazco-Cruz et al. 2019). SCID beige mice have dendritic, macrophage and NK activity which may have contributed to the graft loss. Infiltration of several grafts was observed suggesting rejection, or contamination of cells post transplantation. We did not formally determine the cell type at this time but in future studies, we will take a sample of culture supernatant for microbiological assessment, to validate the sterility of the preparation, just as it is routinely performed prior to clinical islet transplantation.

Hebrok's group showed with elegant imaging studies that more than 50% of differentiated human pluripotent stem cell derived insulin producing cells die shortly after transplantation in mice (Faleo et al. 2017). Furthermore, they verified that cell death was attributed to nutrient deprivation and hypoxia. Amino acid supplementation to prevent nutrient deprivation together with hypoxia preconditioning improved post transplantation survival. This was optimized to successfully culture and graft human islets under the kidney capsule and further supplementation was not done. Identical to the problematic for pseudo-islets (Furuyama et al. 2019), stem cell engraftment was improved by adding mesenchymal stem cells, endothelial cells (Takahashi et al. 2018), or amniotic

epithelial cells (Lebreton et al. 2019) to the graft. This could be easy to test to improve the survival of the highly enriched pancreatic progenitors (>95%).

By using Taqman probes we were able to detect that progerin was expressed during maturation of iPS HGPS AG1972 cell line but not the H1 line, where we expected to see progerin positive nuclei. After transplantation progerin positive nuclei were readily detectable in iPS grafts but again were not seen in the H1 derived grafts. It was unexpected was that not all human nuclei in the iPS grafts expressed progerin and notably the endocrine cells were indeed human in origin (positive for the human nuclear antigen antibody) but negative for progerin (further slides will be process to definitively confirm this finding). We could infer from this that perhaps since the major cell lineage afflicted in progeria patients is the mesoderm, that the endoderm lineage was not affected. Identification of mesoderm teratoma tissue with progerin positive human nuclei could confirm this hypothesis. We did not explore the expression of progerin in the ectoderm lineage.

No major differences were observed in the function of pancreatic progenitors between the H1 and iPS HGPS AG1972 cell lines, both measured for fasting human c-peptide, a quantitative measure of human islet mass. Levels reached 200 ng/L (0.2ng/ml) of human c-peptide but with time the levels dropped down to about 100 ng/ml or below the level of detection. Furthermore, early studies from Novocell describe proinsulin producing pancreatic progenitors (Kroon et al. 2008). Therefore, for future experiments, we aim to dose human proinsulin in serum from the different grafts. Perfusion of explanted grafts showed that H1-derived cells after 6 months *in vivo* were insensitive to glucose but displayed increased insulin secretion in response to high glucose and arginine. We hypothesize that arginine could elevate cAMP levels what is a known mechanism that increases the secretion capacity of both insulin and glucagon.

We then turned to quality differences between H1 grafts and iPS HGPS AG1972 grafts (3-6 months post transplantation) with aging markers previously published in the literature. First, we showed differential expression in insulinoma (immature cells) and human pancreas from an old donor. For example, for the γ H2AX marker, we planned to enumerate the number of foci per nuclei was calculated to gauge cell aging, however although nuclei were positive for this marker no foci were visible. In our hands the autophagy marker ATG 12 did not appear to be informative as the differences in expression between different ages of islets was not discriminatory.

This work is still in progress and will be important in confirming the positive role of progerin in accelerating the maturation of pancreatic endocrine cells. Another elegant proof would have been to correct, using CRISPR-Cas9 technology, the mutation in the iPS HGPS AG1972 cell line and then to compare the mutated line and its corrected isogenic control as it is routinely done. This was not in the scope of this thesis but may be required for publication of our results.

In summary, this work allowed us to generate endocrine positive cells from H1 and iPS HGPS AG1972 cell lines that were detectable after *in vivo* transplantation (3-6 months) in immunodeficient mice. Prior to transplantation the iPS HGPS derived S4 pancreatic progenitors expressing higher levels of maturation markers MafA and urocortin 3 but this did not translate into high human c-peptide levels nor higher GSIS *in vivo*. In grafts 6-7 months post transplantation, the lack of progerin in endocrine cells derived from H1 was logical, but the lack in iPS HGPS AG1972-derived endocrine cells in immunofluorescence in contrast to a strong expression in neighboring human cells in teratoma-like structures was a surprise in particular since a high percentage of pancreatic progenitors cells was observed by flowcytometry at S4. We can only infer from these results that the endoderm may not be sufficiently affected in the time frame explored in this study. More fine aging markers like p16 may allow us to better characterize the cells to determine if there are any differences between the H1 and iPS HGPS derived grafts. We also must admit that these results are based on only one HGPS cell line derived from AG1972 fibroblasts and that multiple iPS cell lines are available.

Perspective studies include overexpression of progerin with PMO technology in S4 pancreatic progenitors, since the expression is irreversible or at later stages, and improving early graft outcome by using pre-vascularized sites or by adding feeder cells like human amniotic epithelial cells with regenerative and angiogenic properties to increase the mass of pancreatic progenitors that survive initial grafting.

We were intrigued by the finding (Nissan et al. 2012) that the unaltered cognitive capacity of patients with Progeria syndrome may be explained by the protection of neural cells in progeria syndrome patients from progerin-induced damage (premature senescence, loss of proliferation, blebbing) by Mir-9, which decreases lamin A and progerin expression in these cells to provide protection. Terminally differentiated neurons including motor neurons, and neural stem cells appear to be negative for lamin A/C but express high levels of lamin B1. Overexpression of Mir9 decreased progerin and lamin A expression and damage (nuclear blebbing).

Indeed, islets are neuroendocrine cells and the old APUD (Amine Precursor Uptake Decarboxylase) system erroneously attributed these cells to be of ectodermal origin. In the literature, indeed Mir-9 has been reported to be expressed at high levels during human pancreatic development (Joglekar et al. 2009; Rosero et al. 2010). More recent work documents Mir-9-5p and miR-9-3p upregulation during the differentiation of human iPS cells to insulin producing cells (Sebastiani et al. 2017). Thus, neuroendocrine pancreatic islet cells may also be protected by Mir-9 expression. We will explore this pathway further. This could explain why progerin was only detected in a subpopulation of endocrine cells in the islet and was localized in the cytoplasm. Studer was able to accelerate aging in terminal dopaminergic neurons by overexpressing progerin and thus to better model late onset neurological diseases and thus perhaps this aging approach could work for human islets cells derived from pluripotent stem cells however Mir-9 expression must be taken into account in our system.

Chapter 7: General conclusion

Pseudo-islet technology has taken off both for drug testing and more recently for clinical transplantation. Human islet transplantation for severe forms of diabetes is under evaluation in France for reimbursement which should be approved in 2020. The clinical activity will increase access to human islets for research. Mastering pseudo-islet technology will allow our laboratory to more efficiently use human islets for research and reduce donor derived heterogeneity which is a major disadvantage when working with native human islets. Tweaking this approach to further improve each step will remain a priority of our laboratory. Our laboratory has excellent long-term clinical islet results and is well situated to test pseudo-islets in the clinics to confirm or disprove their advantage this will be done within a consortium. Partnering up for this clinical trial with InSphero who has years of experience and numerous patented technologies on the subject should be the direction to take.

Human pluripotent stem cell derived islets will one day be the future for both research and clinical transplantation for diabetes. In particular type 2 diabetic iPS cell lines are available and they would provide an excellent and unlimited source of cells to do research for comparison between healthy and diabetic cell lines. The complexity of stem cells and their differentiation to pancreatic islets, especially in terms of aging, requires profound know-how and resources. During this thesis, we had frequent contact with external expert (Dr. Nostro) which helped and guided us throughout our stem cell experiments. As a trained pharmacist, this PhD thesis however allowed me to become an expert in human stem cell culture and aseptic work, flow cytometry, confocal microscopy, and immunofluorescence to cite only a few techniques. My future work project is to work in a rather clinically environment with the pharmacy and clinicians in bringing ATMP cell therapy to the clinics, and in particular CAR-T cells. This thesis prepared me well for my future professional project.

Annexes

Annexe 1: Checklist for reporting human islet preparations used in research (Hart and Powers 2019)

Islet preparation	1	2	3	4	5	6	7	8
Donor demographics								
Unique identifier								
Age (years)								
Sex (M/F)								
BMI (kg/m ²)								
Ethnicity								
HbA _{1c}								
Cause of death								
Diabetes? (Y/N)								
Type of diabetes								
Diabetes duration								
Glucose-lowering therapy (outpatient)								
HbA _{1c}								
Additional donor information								
Pancreas								
Origin/source								
Warm ischaemia time (h)								
Cold ischaemia time (h)								
Islet handling and use								
Origin/source								
Isolation centre								
Estimated purity (%)								
Estimated viability (%)								
Total culture time (h)								
Functional measurement								
Description of purification and quantification								
Experimental islet use (including in which experiment each islet preparation was used)								

Additional notes								
------------------	--	--	--	--	--	--	--	--

Décrets, arrêtés, circulaires

TEXTES GÉNÉRAUX

MINISTÈRE DES SOLIDARITÉS ET DE LA SANTÉ

Décision du 20 décembre 2017 portant autorisation de protocole de recherche sur les cellules souches embryonnaires humaines en application des dispositions de l'article L. 2151-5 du code de la santé publique

NOR : SSAB1803354S

La directrice générale de l'Agence de la biomédecine,

Vu le code de la santé publique, et notamment les articles L. 2151-5 et R. 2151-1 à R. 2151-12 ;

Vu la décision du 8 septembre 2015 modifiant la décision 2013-11 du 17 septembre 2013 fixant le modèle de dossier de demande des autorisations mentionnées à l'article R. 2151-6 du code de la santé publique ;

Vu la demande présentée le 30 septembre 2017 par l'Institut national de la santé et de la recherche médicale (UMR 1190, Lille) aux fins d'obtenir une autorisation de protocole de recherche sur les cellules souches embryonnaires humaines ;

Vu l'avis émis par le conseil d'orientation de l'Agence de la biomédecine le 7 décembre 2017 ;

Vu les informations complémentaires apportées par le demandeur ;

Vu le rapport de la mission d'inspection de l'Agence de la biomédecine en date du 11 octobre 2017 ;

Vu les rapports d'expertise en date du 19 et 30 novembre 2017 ;

Considérant que le projet de recherche utilise une lignée de cellules souches embryonnaires humaines (H1 - WA-01) provenant du WiCell Research Institute (Etats-Unis) ; qu'elle fait l'objet d'une demande d'autorisation d'importation annexée à la présente demande d'autorisation de protocole de recherche sur les cellules souches embryonnaires humaines ; que le conseil d'orientation a rendu un avis favorable sur cette demande ; qu'à l'appui de la demande d'autorisation d'importation, le respect des exigences posées par les articles 16 à 16-8 du code civil et de celles relatives à l'information et au recueil du consentement des couples a été vérifié et la demande d'autorisation présente l'ensemble des documents permettant de s'assurer du respect des conditions législatives et réglementaires ; que la lignée est par ailleurs inscrite au registre du NIH, garantissant le respect des principes éthiques fondamentaux de consentement des donneurs, de gratuité du don et d'anonymat prévus par le droit français ;

Considérant que les locaux, matériels, équipements, procédés et techniques sont adaptés à l'activité de recherche envisagée ; que cette recherche sera effectuée dans des conditions permettant de garantir la sécurité des personnes exerçant une activité professionnelle sur le site, le respect des dispositions applicables en matière de protection de l'environnement, le respect des règles de sécurité sanitaire ainsi que la sécurité, la qualité et la traçabilité des cellules embryonnaires ; que les conditions matérielles de sécurité, de conservation, d'accès, de transferts, de locaux dédiés, de sécurisation desdits locaux, de désinfection, la qualité de l'ensemble des plateaux techniques sont parfaitement décrits et n'ont fait l'objet d'aucune réserve de la part de la mission d'inspection ; que le laboratoire dispose des équipements nécessaires à la mise en œuvre de ce protocole de recherche dans des conditions optimales ;

Considérant que l'équipe de Julie Kerr-Conte est installée à Lille, un site majeur dans l'étude et le traitement du diabète ; que le site regroupe des équipes de notoriété internationale, notamment sur la génétique du diabète (Pr Froguel, U1019) et les approches de biothérapies (transplantation îlots pancréatiques, F. Pattou, J Kerr-Conte) ; que ces équipes se sont regroupées avec d'autres pour créer l'Institut projet EGID (European genomic Institute for diabetes) dédié spécifiquement au diabète et ses complications ;

Considérant que les titres, diplômes, expérience et travaux scientifiques fournis à l'appui de la demande permettent de s'assurer des compétences du responsable de la recherche et des membres de l'équipe en la matière ; que l'équipe est pérenne et les financements sont assurés ; que Julie Kerr-Conte possède une excellente notoriété internationale sur le sujet, et cette équipe est la seule en France à développer ce type de protocole en ayant une très longue expérience de la thérapie cellulaire du diabète ; qu'elle dispose de toute la légitimité à développer ce programme de recherche ;

Considérant que le diabète concerne actuellement plus de 200 millions de personnes dans le monde et est d'ores et déjà une des 5 premières causes de mortalité et de handicap (cécité, amputation...) ; que d'ici à 2030 les études démontrent que le nombre de personnes diabétiques va doubler ; que 90-95 % sont atteintes par sa forme la plus commune, le diabète de type 2 (DT2), dont le risque croît avec le degré d'obésité, le manque d'activité physique et

l'alimentation, et atteint aujourd'hui une dimension épidémique ; qu'une partie importante de la variabilité interindividuelle observée pour le DT2 et les maladies qui lui sont associées est régie par des facteurs génétiques, et l'héritabilité du DT2 est supérieure à 30 % ; que le diabète de type 2 résulte d'une inadaptation de la production d'insuline (qui régule le taux de glucose sanguin), ou de son action inefficace sur les tissus devenus résistants à cette hormone ;

Considérant que l'objectif principal est de dériver des précurseurs pancréatiques des îlots de Langerhans, dont les cellules bêta pancréatiques sécrétant de l'insuline et du glucagon, à partir de cellules souches pluripotentes ; qu'à terme, l'équipe souhaite utiliser des cellules souches pluripotentes induites (dites cellules iPS), car sa stratégie est de modéliser les conséquences des différents variants génotypiques décrits chez les patients diabétiques, afin de mieux comprendre la diversité des facteurs sous-tendant l'émergence du DT2 ;

Considérant que le résultat escompté ne peut être obtenu par d'autres moyens, notamment par le recours exclusif à d'autres types de cellules souches ; que l'équipe a tenté de mener des expériences de différenciation directement à partir de cellules iPS, qui ont permis d'obtenir une sécrétion d'insuline et de glucagon, mais qui reste très nettement inférieure à celle d'îlots humains ; qu'avant de concevoir et d'exploiter cette banque d'iPS-modèles, l'équipe souhaite donc mettre au point un protocole de différenciation robuste et reproductible à partir de cellules de la lignée H1, lignée de référence mondiale dans beaucoup de protocoles de différenciation de CSEh en cellules pancréatiques ;

Considérant que l'équipe a décidé de suivre un protocole proposé par une équipe canadienne, toujours à partir des lignées H1 ou H9 (Kieffer, 2013) ; que ce protocole comprend 7 étapes, mimant les étapes de spécification embryonnaire, en endoderme primitif, en intestin primitif, puis postérieur, pour aboutir à l'ébauche pancréatique puis la spécification en cellules endocrines, et la maturation en cellules sécrétrices d'insuline ; que ces étapes sont délicates, et la maîtrise des multiples paramètres intervenant dans ce processus ne peut s'acquérir en quelques mois seulement ; que pour assurer au mieux le succès de leur projet, Julie Kerr-Conte a établi une collaboration avec l'équipe de Kieffer ;

Considérant que la finalité médicale du projet et l'objectif thérapeutique est évidente à la fois en termes de modélisation du DT2 et de production de cellules pancréatiques de bonne qualité, homogènes, et en nombre suffisant, pour une recherche compétitive à visée médicale sur le diabète ; que les aspects techniques sont parfaitement maîtrisés et le projet est parfaitement intégré dans le contexte de l'institut EGID consacré au diabète ; que le conseil d'orientation souligne qu'un essai clinique utilisant des précurseurs pancréatiques dérivés de CSEh est en cours aux Etats-Unis « ViaCyte's VC-01™ Investigational Stem Cell-Derived Islet Replacement Therapy Successfully Implanted into First Patient » ;

Considérant que le demandeur apporte les éléments suffisants concernant la pertinence scientifique du projet de recherche d'une part, et ses conditions de mise en œuvre au regard des principes éthiques d'autre part ; qu'il justifie en particulier que le projet sera mené dans le respect des principes éthiques relatifs à la recherche sur l'embryon et les cellules souches embryonnaires humaines et que ces cellules ont été obtenues conformément aux conditions législatives et réglementaires,

Décide :

Art. 1^{er}. – L'Institut national de la santé et de la recherche médicale (UMR 1190, Lille) est autorisé à mettre en œuvre, dans les conditions décrites dans le dossier de demande d'autorisation, le protocole de recherche sur les cellules souches embryonnaires humaines ayant pour finalité l'étude de la production *in vitro* d'îlots (cellules β , α , δ) de Langerhans humains pour la recherche. Ces recherches sont placées sous la responsabilité de Mme Julie Kerr-Conte.

Art. 2. – La présente autorisation est accordée pour une durée de cinq ans. Elle peut être suspendue à tout moment pour une durée maximale de trois mois, en cas de violation des dispositions législatives ou réglementaires, par le directeur général de l'Agence de la biomédecine. L'autorisation peut également être retirée, selon les modalités prévues par les dispositions du code de la santé publique susvisées.

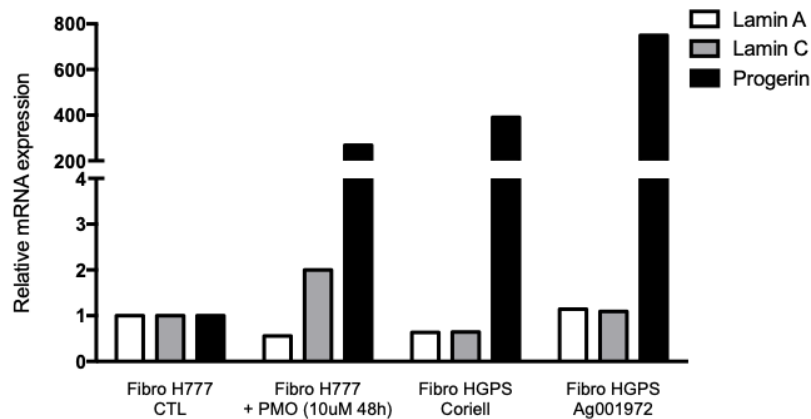
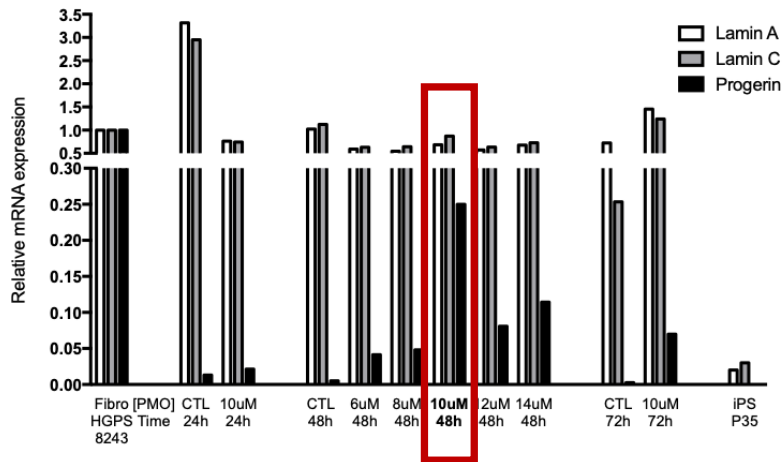
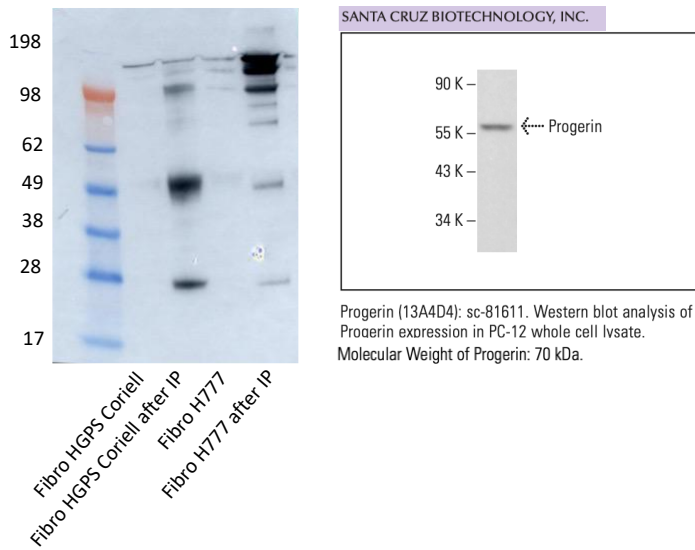
Art. 3. – Toute modification des éléments figurant dans le dossier de demande d'autorisation doit être portée à la connaissance du directeur général de l'Agence de la biomédecine.

Art. 4. – Le directeur général adjoint chargé des ressources de l'Agence de la biomédecine est chargé de l'exécution de la présente décision, qui sera publiée au *Journal officiel* de la République française.

Fait le 20 décembre 2017.

A. COURRÈGES

Annexe 3: Characterization of progerin by western-blot and progerin, lamin A and lamin C by Taqman qPCR after PMO treatments.



Bibliography

Aasen T, Raya A, Barrero MJ, Garreta E, Consiglio A, Gonzalez F, et al. Efficient and rapid generation of induced pluripotent stem cells from human keratinocytes. *Nat Biotechnol*. 2008 Nov;26(11):1276–84.

Aguayo-Mazzucato C, DiIenno A, Hollister-Lock J, Cahill C, Sharma A, Weir G, et al. MAFA and T3 Drive Maturation of Both Fetal Human Islets and Insulin-Producing Cells Differentiated From hESC. *J Clin Endocrinol Metab*. 2015 Oct;100(10):3651–9.

Aguayo-Mazzucato C, van Haaren M, Mruk M, Lee TB, Crawford C, Hollister-Lock J, et al. β Cell Aging Markers Have Heterogeneous Distribution and Are Induced by Insulin Resistance. *Cell Metab*. 2017 Apr 4;25(4):898-910.e5.

Aguayo-Mazzucato C, Koh A, El Khattabi I, Li W-C, Toschi E, Jermendy A, et al. Mafa expression enhances glucose-responsive insulin secretion in neonatal rat beta cells. *Diabetologia*. 2011 Mar;54(3):583–93.

Aguayo-Mazzucato C, Lee TB, Matzko M, DiIenno A, Rezanejad H, Ramadoss P, et al. T3 Induces Both Markers of Maturation and Aging in Pancreatic β -Cells. *Diabetes*. 2018;67(7):1322–31.

Aguayo-Mazzucato C, Zavacki AM, Marinelarena A, Hollister-Lock J, El Khattabi I, Marsili A, et al. Thyroid hormone promotes postnatal rat pancreatic β -cell development and glucose-responsive insulin secretion through MAFA. *Diabetes*. 2013 May;62(5):1569–80.

Akberdin IR, Omelyanchuk NA, Fadeev SI, Leskova NE, Oschepkova EA, Kazantsev FV, et al. Pluripotency gene network dynamics: System views from parametric analysis. *PLOS ONE*. 2018 Mar 29;13(3):e0194464.

Allen N, Gupta A. *Current Diabetes Technology: Striving for the Artificial Pancreas*. Diagnostics (Basel). 2019 Mar 15;9(1).

Almaça J, Molina J, Arrojo E, Drigo R, Abdulreda MH, Jeon WB, Berggren P-O, et al. Young capillary vessels rejuvenate aged pancreatic islets. *Proc Natl Acad Sci USA*. 2014 Dec 9;111(49):17612–7.

Ameri J, Borup R, Prawiro C, Ramond C, Schachter KA, Scharfmann R, et al. Efficient Generation of Glucose-Responsive Beta Cells from Isolated GP2+ Human Pancreatic Progenitors. *Cell Rep*. 2017 04;19(1):36–49.

Ameri J, Ståhlberg A, Pedersen J, Johansson JK, Johannesson MM, Artner I, et al. FGF2 specifies hESC-derived definitive endoderm into foregut/midgut cell lineages in a concentration-dependent manner. *Stem Cells*. 2010 Jan;28(1):45–56.

American Diabetes Association. 2. Classification and Diagnosis of Diabetes: Standards of Medical

Care in Diabetes-2019. *Diabetes Care*. 2019 Jan;42(Suppl 1):S13–28.

Anokye-Danso F, Trivedi CM, Juhr D, Gupta M, Cui Z, Tian Y, et al. Highly efficient miRNA-mediated reprogramming of mouse and human somatic cells to pluripotency. *Cell Stem Cell*. 2011 Apr 8;8(4):376–88.

Arda HE, Li L, Tsai J, Torre EA, Rosli Y, Peiris H, et al. Age-Dependent Pancreatic Gene Regulation Reveals Mechanisms Governing Human β Cell Function. *Cell Metabolism*. 2016 May 10;23(5):909–20.

Arrojo E, Drigo R, Lev-Ram V, Tyagi S, Ramachandra R, Deerinck T, Bushong E, et al. Age Mosaicism across Multiple Scales in Adult Tissues. *Cell Metab*. 2019 Aug 6;30(2):343-351.e3.

Artner I, Bianchi B, Raum JC, Guo M, Kaneko T, Cordes S, et al. MafB is required for islet beta cell maturation. *Proc Natl Acad Sci USA*. 2007 Mar 6;104(10):3853–8.

Artner I, Hang Y, Mazur M, Yamamoto T, Guo M, Lindner J, et al. MafA and MafB regulate genes critical to beta-cells in a unique temporal manner. *Diabetes*. 2010 Oct;59(10):2530–9.

Assady S, Maor G, Amit M, Itskovitz-Eldor J, Skorecki KL, Tzukerman M. Insulin production by human embryonic stem cells. *Diabetes*. 2001 Aug;50(8):1691–7.

Atkinson MA, Bluestone JA, Eisenbarth GS, Hebrok M, Herold KC, Accili D, et al. How does type 1 diabetes develop?: the notion of homicide or β -cell suicide revisited. *Diabetes*. 2011 May;60(5):1370–9.

Avilion AA, Nicolis SK, Pevny LH, Perez L, Vivian N, Lovell-Badge R. Multipotent cell lineages in early mouse development depend on SOX2 function. *Genes Dev*. 2003 Jan 1;17(1):126–40.

Avrahami D, Li C, Zhang J, Schug J, Avrahami R, Rao S, et al. Aging-Dependent Demethylation of Regulatory Elements Correlates with Chromatin State and Improved β Cell Function. *Cell Metab*. 2015 Oct 6;22(4):619–32.

Ban H, Nishishita N, Fusaki N, Tabata T, Saeki K, Shikamura M, et al. Efficient generation of transgene-free human induced pluripotent stem cells (iPSCs) by temperature-sensitive Sendai virus vectors. *Proc Natl Acad Sci USA*. 2011 Aug 23;108(34):14234–9.

Banito A, Rashid ST, Acosta JC, Li S, Pereira CF, Geti I, et al. Senescence impairs successful reprogramming to pluripotent stem cells. *Genes Dev*. 2009 Sep 15;23(18):2134–9.

Bar-Nur O, Russ HA, Efrat S, Benvenisty N. Epigenetic memory and preferential lineage-specific differentiation in induced pluripotent stem cells derived from human pancreatic islet beta cells. *Cell Stem Cell*. 2011 Jul 8;9(1):17–23.

Basu A, Dube S, Slama M, Errazuriz I, Amezcua JC, Kudva YC, et al. Time lag of glucose from

intravascular to interstitial compartment in humans. *Diabetes*. 2013 Dec;62(12):4083–7.

Baxter M, Withey S, Harrison S, Segeritz C-P, Zhang F, Atkinson-Dell R, et al. Phenotypic and functional analyses show stem cell-derived hepatocyte-like cells better mimic fetal rather than adult hepatocytes. *J Hepatol*. 2015 Mar;62(3):581–9.

Bayha E, Jørgensen MC, Serup P, Grapin-Botton A. Retinoic acid signaling organizes endodermal organ specification along the entire antero-posterior axis. *PLoS ONE*. 2009 Jun 10;4(6):e5845.

Bellin M, Casini S, Davis RP, D’Aniello C, Haas J, Ward-van Oostwaard D, et al. Isogenic human pluripotent stem cell pairs reveal the role of a KCNH2 mutation in long-QT syndrome. *EMBO J*. 2013 Dec 11;32(24):3161–75.

Blondel S, Egesipe A-L, Picardi P, Jaskowiak A-L, Notarnicola M, Ragot J, et al. Drug screening on Hutchinson Gilford progeria pluripotent stem cells reveals aminopyrimidines as new modulators of farnesylation. *Cell Death Dis*. 2016 Feb 18;7:e2105.

Blum B, Hrvatin S, Schuetz C, Bonal C, Rezanja A, Melton DA. Functional beta-cell maturation is marked by an increased glucose threshold and by expression of urocortin 3. *Nat Biotechnol*. 2012 26;30(3):261–4.

Blum B, Roose AN, Barrandon O, Maehr R, Arvanites AC, Davidow LS, et al. Reversal of β cell de-differentiation by a small molecule inhibitor of the TGF β pathway. *Elife*. 2014 Sep 16;3:e02809.

Bock C, Kiskinis E, Verstappen G, Gu H, Boulting G, Smith ZD, et al. Reference Maps of human ES and iPS cell variation enable high-throughput characterization of pluripotent cell lines. *Cell*. 2011 Feb 4;144(3):439–52.

Bonner C, Kerr-Conte J, Gmyr V, Queniat G, Moerman E, Thévenet J, et al. Inhibition of the glucose transporter SGLT2 with dapagliflozin in pancreatic alpha cells triggers glucagon secretion. *Nat Med*. 2015 May;21(5):512–7.

Bonner-Weir S, Aguayo-Mazzucato C, Weir GC. Dynamic development of the pancreas from birth to adulthood. *Ups J Med Sci*. 2016 May;121(2):155–8.

Boyer LA, Lee TI, Cole MF, Johnstone SE, Levine SS, Zucker JP, et al. Core transcriptional regulatory circuitry in human embryonic stem cells. *Cell*. 2005 Sep 23;122(6):947–56.

Bretones G, Delgado MD, León J. Myc and cell cycle control. *Biochim Biophys Acta*. 2015 May;1849(5):506–16.

Britt LD, Stojeba PC, Scharp CR, Greider MH, Scharp DW. Neonatal pig pseudo-islets. A product of selective aggregation. *Diabetes*. 1981 Jul;30(7):580–3.

Brouwer M, Zhou H, Nadif Kasri N. Choices for Induction of Pluripotency: Recent Developments

in Human Induced Pluripotent Stem Cell Reprogramming Strategies. *Stem Cell Rev Rep*. 2016 Feb;12(1):54–72.

Bustin SA, Benes V, Garson JA, Hellems J, Huggett J, Kubista M, et al. The MIQE guidelines: minimum information for publication of quantitative real-time PCR experiments. *Clin Chem*. 2009 Apr;55(4):611–22.

Caiazzo R, Gmyr V, Kremer B, Hubert T, Soudan B, Lukowiak B, et al. Quantitative in vivo islet potency assay in normoglycemic nude mice correlates with primary graft function after clinical transplantation. *Transplantation*. 2008 Jul 27;86(2):360–3.

Cao K, Blair CD, Faddah DA, Kieckhafer JE, Olive M, Erdos MR, et al. Progerin and telomere dysfunction collaborate to trigger cellular senescence in normal human fibroblasts. *J Clin Invest*. 2011 Jul;121(7):2833–44.

Cao K, Capell BC, Erdos MR, Djabali K, Collins FS. A lamin A protein isoform overexpressed in Hutchinson-Gilford progeria syndrome interferes with mitosis in progeria and normal cells. *Proc Natl Acad Sci USA*. 2007a Mar 20;104(12):4949–54.

Cao K, Capell BC, Erdos MR, Djabali K, Collins FS. A lamin A protein isoform overexpressed in Hutchinson-Gilford progeria syndrome interferes with mitosis in progeria and normal cells. *Proc Natl Acad Sci USA*. 2007b Mar 20;104(12):4949–54.

Capell BC, Collins FS. Human laminopathies: nuclei gone genetically awry. *Nat Rev Genet*. 2006 Dec;7(12):940–52.

Carrasco M, Delgado I, Soria B, Martín F, Rojas A. GATA4 and GATA6 control mouse pancreas organogenesis. *J Clin Invest*. 2012 Oct;122(10):3504–15.

Carrero D, Soria-Valles C, López-Otín C. Hallmarks of progeroid syndromes: lessons from mice and reprogrammed cells. *Dis Model Mech*. 2016 01;9(7):719–35.

Castaing M, Péault B, Basmaciogullari A, Casal I, Czernichow P, Scharfmann R. Blood glucose normalization upon transplantation of human embryonic pancreas into beta-cell-deficient SCID mice. *Diabetologia*. 2001 Nov;44(11):2066–76.

Cavallari G, Zuellig RA, Lehmann R, Weber M, Moritz W. Rat pancreatic islet size standardization by the “hanging drop” technique. *Transplant Proc*. 2007 Aug;39(6):2018–20.

Chambers I, Colby D, Robertson M, Nichols J, Lee S, Tweedie S, et al. Functional expression cloning of Nanog, a pluripotency sustaining factor in embryonic stem cells. *Cell*. 2003 May 30;113(5):643–55.

Chambers I, Silva J, Colby D, Nichols J, Nijmeijer B, Robertson M, et al. Nanog safeguards

pluripotency and mediates germline development. *Nature*. 2007 Dec 20;450(7173):1230–4.

Chan XY, Black R, Dickerman K, Federico J, Lévesque M, Mumm J, et al. Three-Dimensional Vascular Network Assembly From Diabetic Patient-Derived Induced Pluripotent Stem Cells. *Arterioscler Thromb Vasc Biol*. 2015 Dec;35(12):2677–85.

Chen B, Dodge ME, Tang W, Lu J, Ma Z, Fan C-W, et al. Small molecule-mediated disruption of Wnt-dependent signaling in tissue regeneration and cancer. *Nat Chem Biol*. 2009 Feb;5(2):100–7.

Chen C-Y, Cheng Y-Y, Yen CYT, Hsieh PCH. Mechanisms of pluripotency maintenance in mouse embryonic stem cells. *Cell Mol Life Sci*. 2017;74(10):1805–17.

Cho NH, Shaw JE, Karuranga S, Huang Y, da Rocha Fernandes JD, Ohlrogge AW, et al. IDF Diabetes Atlas: Global estimates of diabetes prevalence for 2017 and projections for 2045. *Diabetes Res Clin Pract*. 2018 Apr;138:271–81.

Chou B-K, Mali P, Huang X, Ye Z, Dowey SN, Resar LM, et al. Efficient human iPSC cell derivation by a non-integrating plasmid from blood cells with unique epigenetic and gene expression signatures. *Cell Res*. 2011 Mar;21(3):518–29.

Citro A, Ott HC. Can We Re-Engineer the Endocrine Pancreas? *Curr Diab Rep*. 2018 02;18(11):122.

Cnop M, Hughes SJ, Igoillo-Esteve M, Hoppa MB, Sayyed F, van de Laar L, et al. The long lifespan and low turnover of human islet beta cells estimated by mathematical modelling of lipofuscin accumulation. *Diabetologia*. 2010 Feb;53(2):321–30.

Cogger KF, Sinha A, Sarangi F, McGaugh EC, Saunders D, Dorrell C, et al. Glycoprotein 2 is a specific cell surface marker of human pancreatic progenitors. *Nat Commun*. 2017 24;8(1):331.

Cooper O, Seo H, Andrabi S, Guardia-Laguarta C, Graziotto J, Sundberg M, et al. Pharmacological rescue of mitochondrial deficits in iPSC-derived neural cells from patients with familial Parkinson's disease. *Sci Transl Med*. 2012 Jul 4;4(141):141ra90.

Coppedè F. The epidemiology of premature aging and associated comorbidities. *Clin Interv Aging*. 2013;8:1023–32.

Cornacchia D, Studer L. Back and forth in time: Directing age in iPSC-derived lineages. *Brain Res*. 2017 01;1656:14–26.

Coronel MM, Stabler CL. Engineering a local microenvironment for pancreatic islet replacement. *Curr Opin Biotechnol*. 2013 Oct;24(5):900–8.

Correia C, Koshkin A, Duarte P, Hu D, Carido M, Sebastião MJ, et al. 3D aggregate culture improves metabolic maturation of human pluripotent stem cell derived cardiomyocytes. *Biotechnol*

Bioeng. 2018;115(3):630–44.

Coutinho HDM, Falcão-Silva VS, Gonçalves GF, da Nóbrega RB. Molecular ageing in progeroid syndromes: Hutchinson–Gilford progeria syndrome as a model. *Immun Ageing*. 2009 Apr 20;6:4.

Csoka AB, English SB, Simkevich CP, Ginzinger DG, Butte AJ, Schatten GP, et al. Genome-scale expression profiling of Hutchinson–Gilford progeria syndrome reveals widespread transcriptional misregulation leading to mesodermal/mesenchymal defects and accelerated atherosclerosis. *Aging Cell*. 2004;3(4):235–43.

D’Amour KA, Agulnick AD, Eliazer S, Kelly OG, Kroon E, Baetge EE. Efficient differentiation of human embryonic stem cells to definitive endoderm. *Nat Biotechnol*. 2005 Dec;23(12):1534–41.

D’Amour KA, Bang AG, Eliazer S, Kelly OG, Agulnick AD, Smart NG, et al. Production of pancreatic hormone-expressing endocrine cells from human embryonic stem cells. *Nat Biotechnol*. 2006 Nov;24(11):1392–401.

Dang DT, Pevsner J, Yang VW. The biology of the mammalian Krüppel-like family of transcription factors. *Int J Biochem Cell Biol*. 2000 Dec;32(11–12):1103–21.

De Sandre-Giovannoli A, Bernard R, Cau P, Navarro C, Amiel J, Boccaccio I, et al. Lamin A truncation in Hutchinson–Gilford progeria. *Science*. 2003 Jun 27;300(5628):2055.

Dechat T, Shimi T, Adam SA, Rusinol AE, Andres DA, Spielmann HP, et al. Alterations in mitosis and cell cycle progression caused by a mutant lamin A known to accelerate human aging. *Proc Natl Acad Sci USA*. 2007 Mar 20;104(12):4955–60.

Dessimoz J, Opoka R, Kordich JJ, Grapin-Botton A, Wells JM. FGF signaling is necessary for establishing gut tube domains along the anterior-posterior axis in vivo. *Mech Dev*. 2006 Jan;123(1):42–55.

van Deursen JM. The role of senescent cells in ageing. *Nature*. 2014 May 22;509(7501):439–46.

Diabetes Control and Complications Trial (DCCT)/Epidemiology of Diabetes Interventions and Complications (EDIC) Study Research Group. Intensive Diabetes Treatment and Cardiovascular Outcomes in Type 1 Diabetes: The DCCT/EDIC Study 30-Year Follow-up. *Diabetes Care*. 2016 May;39(5):686–93.

Diabetes Control and Complications Trial Research Group, Nathan DM, Genuth S, Lachin J, Cleary P, Crofford O, et al. The effect of intensive treatment of diabetes on the development and progression of long-term complications in insulin-dependent diabetes mellitus. *N Engl J Med*. 1993 30;329(14):977–86.

Dittrich R, Beckmann MW, Würfel W. Non-embryo-destructive Extraction of Pluripotent Embryonic Stem Cells: Implications for Regenerative Medicine and Reproductive Medicine. *Geburtshilfe Frauenheilkd.* 2015 Dec;75(12):1239–42.

Dominguez-Gutierrez G, Xin Y, Gromada J. Heterogeneity of human pancreatic β -cells. *Mol Metab.* 2019 Sep;27S:S7–14.

Doss MX, Sachinidis A. Current Challenges of iPSC-Based Disease Modeling and Therapeutic Implications. *Cells.* 2019 30;8(5).

Dybala MP, Hara M. Heterogeneity of the Human Pancreatic Islet. *Diabetes.* 2019 Jun;68(6):1230–9.

Edel MJ, Menchon C, Menendez S, Consiglio A, Raya A, Izpisua Belmonte JC. Rem2 GTPase maintains survival of human embryonic stem cells as well as enhancing reprogramming by regulating p53 and cyclin D1. *Genes Dev.* 2010 Mar 15;24(6):561–73.

Egesipe A-L, Blondel S, Lo Cicero A, Jaskowiak A-L, Navarro C, Sandre-Giovannoli AD, et al. Metformin decreases progerin expression and alleviates pathological defects of Hutchinson–Gilford progeria syndrome cells. *NPJ Aging Mech Dis.* 2016 Nov 10;2:16026.

El Khatib MM, Ohmine S, Jacobus EJ, Tonne JM, Morsy SG, Holditch SJ, et al. Tumor-Free Transplantation of Patient-Derived Induced Pluripotent Stem Cell Progeny for Customized Islet Regeneration. *Stem Cells Transl Med.* 2016 May;5(5):694–702.

Eriksson M, Brown WT, Gordon LB, Glynn MW, Singer J, Scott L, et al. Recurrent de novo point mutations in lamin A cause Hutchinson-Gilford progeria syndrome. *Nature.* 2003 May 15;423(6937):293–8.

Esteban MA, Wang T, Qin B, Yang J, Qin D, Cai J, et al. Vitamin C enhances the generation of mouse and human induced pluripotent stem cells. *Cell Stem Cell.* 2010 Jan 8;6(1):71–9.

Evans MJ, Kaufman MH. Establishment in culture of pluripotential cells from mouse embryos. *Nature.* 1981 Jul 9;292(5819):154–6.

Faleo G, Russ HA, Wisel S, Parent AV, Nguyen V, Nair GG, et al. Mitigating Ischemic Injury of Stem Cell-Derived Insulin-Producing Cells after Transplant. *Stem Cell Reports.* 2017 12;9(3):807–19.

Fisher JB, Pulakanti K, Rao S, Duncan SA. GATA6 is essential for endoderm formation from human pluripotent stem cells. *Biol Open.* 2017 Jul 15;6(7):1084–95.

Frock RL, Kudlow BA, Evans AM, Jameson SA, Hauschka SD, Kennedy BK. Lamin A/C and emerin are critical for skeletal muscle satellite cell differentiation. *Genes Dev.* 2006 Feb

15;20(4):486–500.

Furuyama K, Chera S, van Gurp L, Oropeza D, Ghila L, Damond N, et al. Diabetes relief in mice by glucose-sensing insulin-secreting human α -cells. *Nature*. 2019;567(7746):43–8.

Fusaki N, Ban H, Nishiyama A, Saeki K, Hasegawa M. Efficient induction of transgene-free human pluripotent stem cells using a vector based on Sendai virus, an RNA virus that does not integrate into the host genome. *Proc Jpn Acad, Ser B, Phys Biol Sci*. 2009;85(8):348–62.

Gargani S, Thévenet J, Yuan JE, Lefebvre B, Delalleau N, Gmyr V, et al. Adaptive changes of human islets to an obesogenic environment in the mouse. *Diabetologia*. 2013 Feb;56(2):350–8.

Gharechahi J, Pakzad M, Mirshavaladi S, Sharifitabar M, Baharvand H, Salekdeh GH. The effect of Rho-associated kinase inhibition on the proteome pattern of dissociated human embryonic stem cells. *Mol Biosyst*. 2014 Mar 4;10(3):640–52.

Ghazizadeh Z, Kao D-I, Amin S, Cook B, Rao S, Zhou T, et al. ROCKII inhibition promotes the maturation of human pancreatic beta-like cells. *Nat Commun [Internet]*. 2017 Aug 21 [cited 2019 Oct 23];8. Available from: <https://www.ncbi.nlm.nih.gov/pmc/articles/PMC5563509/>

Giacomelli E, Bellin M, Sala L, van Meer BJ, Tertoolen LGJ, Orlova VV, et al. Three-dimensional cardiac microtissues composed of cardiomyocytes and endothelial cells co-differentiated from human pluripotent stem cells. *Development*. 2017 15;144(6):1008–17.

Giorgetti A, Montserrat N, Aasen T, Gonzalez F, Rodríguez-Pizà I, Vassena R, et al. Generation of induced pluripotent stem cells from human cord blood using OCT4 and SOX2. *Cell Stem Cell*. 2009 Oct 2;5(4):353–7.

Goldman RD, Shumaker DK, Erdos MR, Eriksson M, Goldman AE, Gordon LB, et al. Accumulation of mutant lamin A causes progressive changes in nuclear architecture in Hutchinson-Gilford progeria syndrome. *Proc Natl Acad Sci USA*. 2004 Jun 15;101(24):8963–8.

Gordon LB, McCarten KM, Giobbie-Hurder A, Machan JT, Campbell SE, Berns SD, et al. Disease progression in Hutchinson-Gilford progeria syndrome: impact on growth and development. *Pediatrics*. 2007 Oct;120(4):824–33.

Gourraud P-A, Gilson L, Girard M, Peschanski M. The role of human leukocyte antigen matching in the development of multiethnic “haplobank” of induced pluripotent stem cell lines. *Stem Cells*. 2012 Feb;30(2):180–6.

Grabundzija I, Wang J, Sebe A, Erdei Z, Kajdi R, Devaraj A, et al. Sleeping Beauty transposon-based system for cellular reprogramming and targeted gene insertion in induced pluripotent stem cells. *Nucleic Acids Res*. 2013 Feb 1;41(3):1829–47.

Grandy R, Tomaz RA, Vallier L. Modeling Disease with Human Inducible Pluripotent Stem Cells. *Annu Rev Pathol.* 2019 Jan 24;14:449–68.

Griscelli F, Ezanno H, Soubeyrand M, Feraud O, Oudrhiri N, Bonnefond A, et al. Generation of an induced pluripotent stem cell (iPSC) line from a patient with maturity-onset diabetes of the young type 3 (MODY3) carrying a hepatocyte nuclear factor 1-alpha (HNF1A) mutation. *Stem Cell Res.* 2018;29:56–9.

Griscelli F, Feraud O, Ernault T, Oudrhiri N, Turhan AG, Bonnefond A, et al. Generation of an induced pluripotent stem cell (iPSC) line from a patient with maturity-onset diabetes of the young type 13 (MODY13) with a the potassium inwardly-rectifying channel, subfamily J, member 11 (KCNJ11) mutation. *Stem Cell Res.* 2017;23:178–81.

Gruessner AC, Gruessner RWG. Pancreas transplant outcomes for United States and non United States cases as reported to the United Network for Organ Sharing and the International Pancreas Transplant Registry as of December 2011. *Clin Transpl.* 2012;23–40.

Gu C, Stein GH, Pan N, Goebbels S, Hörnberg H, Nave K-A, et al. Pancreatic beta cells require NeuroD to achieve and maintain functional maturity. *Cell Metab.* 2010 Apr 7;11(4):298–310.

Gu G, Dubauskaite J, Melton DA. Direct evidence for the pancreatic lineage: NGN3+ cells are islet progenitors and are distinct from duct progenitors. *Development.* 2002 May;129(10):2447–57.

Halban PA, Powers SL, George KL, Bonner-Weir S. Spontaneous reassociation of dispersed adult rat pancreatic islet cells into aggregates with three-dimensional architecture typical of native islets. *Diabetes.* 1987 Jul;36(7):783–90.

Hart NJ, Powers AC. Use of human islets to understand islet biology and diabetes: progress, challenges and suggestions. *Diabetologia.* 2019;62(2):212–22.

He X, Cao Y, Wang L, Han Y, Zhong X, Zhou G, et al. Human fibroblast reprogramming to pluripotent stem cells regulated by the miR19a/b-PTEN axis. *PLoS ONE.* 2014;9(4):e95213.

Hellerström C, Swenne I. Functional maturation and proliferation of fetal pancreatic beta-cells. *Diabetes.* 1991 Dec;40 Suppl 2:89–93.

Helman A, Klochendler A, Azazmeh N, Gabai Y, Horwitz E, Anzi S, et al. p16(Ink4a)-induced senescence of pancreatic beta cells enhances insulin secretion. *Nat Med.* 2016 Apr;22(4):412–20.

Hennekam RCM. Hutchinson-Gilford progeria syndrome: review of the phenotype. *Am J Med Genet A.* 2006 Dec 1;140(23):2603–24.

Henquin J-C. Influence of organ donor attributes and preparation characteristics on the dynamics of insulin secretion in isolated human islets. *Physiol Rep.* 2018;6(5).

Henquin J-C, Nenquin M, Stiernet P, Ahren B. In vivo and in vitro glucose-induced biphasic insulin secretion in the mouse: pattern and role of cytoplasmic Ca²⁺ and amplification signals in beta-cells. *Diabetes*. 2006 Feb;55(2):441–51.

Hilderink J, Spijker S, Carlotti F, Lange L, Engelse M, van Blitterswijk C, et al. Controlled aggregation of primary human pancreatic islet cells leads to glucose-responsive pseudoislets comparable to native islets. *J Cell Mol Med*. 2015 Aug;19(8):1836–46.

Hockemeyer D, Soldner F, Cook EG, Gao Q, Mitalipova M, Jaenisch R. A drug-inducible system for direct reprogramming of human somatic cells to pluripotency. *Cell Stem Cell*. 2008 Sep 11;3(3):346–53.

Holman N, Young B, Gadsby R. Current prevalence of Type 1 and Type 2 diabetes in adults and children in the UK. *Diabet Med*. 2015 Sep;32(9):1119–20.

Holman RR, Paul SK, Bethel MA, Matthews DR, Neil HAW. 10-year follow-up of intensive glucose control in type 2 diabetes. *N Engl J Med*. 2008 Oct 9;359(15):1577–89.

Hong H, Takahashi K, Ichisaka T, Aoi T, Kanagawa O, Nakagawa M, et al. Suppression of induced pluripotent stem cell generation by the p53-p21 pathway. *Nature*. 2009 Aug 27;460(7259):1132–5.

Hopcroft DW, Mason DR, Scott RS. Structure-function relationships in pancreatic islets: support for intraislet modulation of insulin secretion. *Endocrinology*. 1985 Nov;117(5):2073–80.

Hrvatin S, O'Donnell CW, Deng F, Millman JR, Pagliuca FW, DiIorio P, et al. Differentiated human stem cells resemble fetal, not adult, β cells. *Proc Natl Acad Sci USA*. 2014 Feb 25;111(8):3038–43.

Huangfu D, Maehr R, Guo W, Eijkelenboom A, Snitow M, Chen AE, et al. Induction of pluripotent stem cells by defined factors is greatly improved by small-molecule compounds. *Nat Biotechnol*. 2008 Jul;26(7):795–7.

Hughes SJ, Bateman PA, Cross SE, Brandhorst D, Brandhorst H, Spiliotis I, et al. Does Islet Size Really Influence Graft Function After Clinical Islet Transplantation? *Transplantation*. 2018 Nov;102(11):1857–63.

Ichida JK, Tcw J, Williams LA, Carter AC, Shi Y, Moura MT, et al. Notch inhibition allows oncogene-independent generation of iPS cells. *Nat Chem Biol*. 2014 Aug;10(8):632–9.

Ichihara Y, Utoh R, Yamada M, Shimizu T, Uchigata Y. Size effect of engineered islets prepared using microfabricated wells on islet cell function and arrangement. *Heliyon*. 2016 Jun 1;2(6):e00129.

Jacquet L, Stephenson E, Collins R, Patel H, Trussler J, Al-Bedaery R, et al. Strategy for the creation of clinical grade hESC line banks that HLA-match a target population. *EMBO Mol Med*. 2013;5(1):10–7.

Jaenisch R, Young R. Stem cells, the molecular circuitry of pluripotency and nuclear reprogramming. *Cell*. 2008 Feb 22;132(4):567–82.

Jennings RE, Berry AA, Gerrard DT, Wearne SJ, Strutt J, Withey S, et al. Laser Capture and Deep Sequencing Reveals the Transcriptomic Programmes Regulating the Onset of Pancreas and Liver Differentiation in Human Embryos. *Stem Cell Reports*. 2017 14;9(5):1387–94.

Jennings RE, Berry AA, Kirkwood-Wilson R, Roberts NA, Hearn T, Salisbury RJ, et al. Development of the human pancreas from foregut to endocrine commitment. *Diabetes*. 2013 Oct;62(10):3514–22.

Jeon J, Correa-Medina M, Ricordi C, Edlund H, Diez JA. Endocrine cell clustering during human pancreas development. *J Histochem Cytochem*. 2009 Sep;57(9):811–24.

Jia F, Wilson KD, Sun N, Gupta DM, Huang M, Li Z, et al. A nonviral minicircle vector for deriving human iPS cells. *Nat Methods*. 2010 Mar;7(3):197–9.

Jiang J, Au M, Lu K, Eshpeter A, Korbitt G, Fisk G, et al. Generation of insulin-producing islet-like clusters from human embryonic stem cells. *Stem Cells*. 2007a Aug;25(8):1940–53.

Jiang J, Chan Y-S, Loh Y-H, Cai J, Tong G-Q, Lim C-A, et al. A core Klf circuitry regulates self-renewal of embryonic stem cells. *Nat Cell Biol*. 2008 Mar;10(3):353–60.

Jiang W, Shi Y, Zhao D, Chen S, Yong J, Zhang J, et al. In vitro derivation of functional insulin-producing cells from human embryonic stem cells. *Cell Res*. 2007b Apr;17(4):333–44.

Joglekar MV, Joglekar VM, Hardikar AA. Expression of islet-specific microRNAs during human pancreatic development. *Gene Expr Patterns*. 2009 Feb;9(2):109–13.

Johansson KA, Dursun U, Jordan N, Gu G, Beermann F, Gradwohl G, et al. Temporal control of neurogenin3 activity in pancreas progenitors reveals competence windows for the generation of different endocrine cell types. *Dev Cell*. 2007 Mar;12(3):457–65.

Ju MK, Jeong JH, Lee JI, Kim YS, Kim MS. Proliferation and functional assessment of pseudo-islets with the use of pancreatic endocrine cells. *Transplant Proc*. 2013 Jun;45(5):1885–8.

Karagiannis P, Takahashi K, Saito M, Yoshida Y, Okita K, Watanabe A, et al. Induced Pluripotent Stem Cells and Their Use in Human Models of Disease and Development. *Physiol Rev*. 2019 01;99(1):79–114.

Kataoka K, Han S, Shioda S, Hirai M, Nishizawa M, Handa H. MafA is a glucose-regulated and

pancreatic beta-cell-specific transcriptional activator for the insulin gene. *J Biol Chem*. 2002 Dec 20;277(51):49903–10.

Kayton NS, Poffenberger G, Henske J, Dai C, Thompson C, Aramandla R, et al. Human islet preparations distributed for research exhibit a variety of insulin-secretory profiles. *Am J Physiol Endocrinol Metab*. 2015 Apr 1;308(7):E592-602.

Ke Q, Li L, Cai B, Liu C, Yang Y, Gao Y, et al. Connexin 43 is involved in the generation of human-induced pluripotent stem cells. *Hum Mol Genet*. 2013 Jun 1;22(11):2221–33.

Kerr-Conte J, Pattou F, Lecomte-Houcke M, Xia Y, Boilly B, Proye C, et al. Ductal cyst formation in collagen-embedded adult human islet preparations. A means to the reproduction of nesidioblastosis in vitro. *Diabetes*. 1996 Aug;45(8):1108–14.

Kerr-Conte J, Vandewalle B, Moerman E, Lukowiak B, Gmyr V, Arnalsteen L, et al. Upgrading pretransplant human islet culture technology requires human serum combined with media renewal. *Transplantation*. 2010 May 15;89(9):1154–60.

Kim D, Kim C-H, Moon J-I, Chung Y-G, Chang M-Y, Han B-S, et al. Generation of human induced pluripotent stem cells by direct delivery of reprogramming proteins. *Cell Stem Cell*. 2009a Jun 5;4(6):472–6.

Kim JB, Greber B, Araúzo-Bravo MJ, Meyer J, Park KI, Zaehres H, et al. Direct reprogramming of human neural stem cells by OCT4. *Nature*. 2009b Oct 1;461(7264):649–643.

Kiskinis E, Eggan K. Progress toward the clinical application of patient-specific pluripotent stem cells. *J Clin Invest*. 2010 Jan;120(1):51–9.

Koike H, Iwasawa K, Ouchi R, Maezawa M, Giesbrecht K, Saiki N, et al. Modelling human hepatobiliary-pancreatic organogenesis from the foregut-midgut boundary. *Nature*. 2019;574(7776):112–6.

Kondo Y, Toyoda T, Inagaki N, Osafune K. iPSC technology-based regenerative therapy for diabetes. *J Diabetes Investig*. 2018 Mar;9(2):234–43.

Korytnikov R, Nostro MC. Generation of polyhormonal and multipotent pancreatic progenitor lineages from human pluripotent stem cells. *Methods*. 2016 15;101:56–64.

Krentz NAJ, Lee MYY, Xu EE, Sproul SLJ, Maslova A, Sasaki S, et al. Single-Cell Transcriptome Profiling of Mouse and hESC-Derived Pancreatic Progenitors. *Stem Cell Reports*. 2018 11;11(6):1551–64.

Kroon E, Martinson LA, Kadoya K, Bang AG, Kelly OG, Eliazar S, et al. Pancreatic endoderm derived from human embryonic stem cells generates glucose-responsive insulin-secreting cells in

vivo. *Nat Biotechnol.* 2008 Apr;26(4):443–52.

Kubo A, Shinozaki K, Shannon JM, Kouskoff V, Kennedy M, Woo S, et al. Development of definitive endoderm from embryonic stem cells in culture. *Development.* 2004 Apr;131(7):1651–62.

Kulkarni RN, Stewart AF. Summary of the Keystone islet workshop (April 2014): the increasing demand for human islet availability in diabetes research. *Diabetes.* 2014 Dec;63(12):3979–81.

Kunisato A, Wakatsuki M, Shinba H, Ota T, Ishida I, Nagao K. Direct generation of induced pluripotent stem cells from human nonmobilized blood. *Stem Cells Dev.* 2011 Jan;20(1):159–68.

Larsen HL, Grapin-Botton A. The molecular and morphogenetic basis of pancreas organogenesis. *Semin Cell Dev Biol.* 2017;66:51–68.

Latres E, Finan DA, Greenstein JL, Kowalski A, Kieffer TJ. Navigating Two Roads to Glucose Normalization in Diabetes: Automated Insulin Delivery Devices and Cell Therapy. *Cell Metab.* 2019 Mar 5;29(3):545–63.

Lawlor N, Márquez EJ, Orchard P, Narisu N, Shamim MS, Thibodeau A, et al. Multiomic Profiling Identifies cis-Regulatory Networks Underlying Human Pancreatic β Cell Identity and Function. *Cell Rep.* 2019 Jan 15;26(3):788-801.e6.

Lawson KA, Meneses JJ, Pedersen RA. Cell fate and cell lineage in the endoderm of the presomite mouse embryo, studied with an intracellular tracer. *Dev Biol.* 1986 Jun;115(2):325–39.

Lebreton F, Lavallard V, Bellofatto K, Bonnet R, Wassmer CH, Perez L, et al. Insulin-producing organoids engineered from islet and amniotic epithelial cells to treat diabetes. *Nat Commun [Internet].* 2019 Oct 3 [cited 2019 Nov 3];10. Available from: <https://www.ncbi.nlm.nih.gov/pmc/articles/PMC6776618/>

Lee G, Ramirez CN, Kim H, Zeltner N, Liu B, Radu C, et al. Large-scale screening using familial dysautonomia induced pluripotent stem cells identifies compounds that rescue IKBKAP expression. *Nat Biotechnol.* 2012 Dec;30(12):1244–8.

Lee S, Huh JY, Turner DM, Lee S, Robinson J, Stein JE, et al. Repurposing the Cord Blood Bank for Haplobanking of HLA-Homozygous iPSCs and Their Usefulness to Multiple Populations. *Stem Cells.* 2018;36(10):1552–66.

Lehmann R, Zuellig RA, Kugelmeier P, Baenninger PB, Moritz W, Perren A, et al. Superiority of small islets in human islet transplantation. *Diabetes.* 2007 Mar;56(3):594–603.

Li H, Collado M, Villasante A, Strati K, Ortega S, Cañamero M, et al. The Ink4/Arf locus is a barrier for iPSC cell reprogramming. *Nature.* 2009a Aug 27;460(7259):1136–9.

Li M, Belmonte JCI. Ground rules of the pluripotency gene regulatory network. *Nat Rev Genet.* 2017;18(3):180–91.

Li W, Wei W, Zhu S, Zhu J, Shi Y, Lin T, et al. Generation of rat and human induced pluripotent stem cells by combining genetic reprogramming and chemical inhibitors. *Cell Stem Cell.* 2009b Jan 9;4(1):16–9.

Lin S-L, Chang DC, Lin C-H, Ying S-Y, Leu D, Wu DTS. Regulation of somatic cell reprogramming through inducible mir-302 expression. *Nucleic Acids Res.* 2011 Feb;39(3):1054–65.

Lin S-L, Chang DC, Ying S-Y, Leu D, Wu DTS. MicroRNA miR-302 inhibits the tumorigenicity of human pluripotent stem cells by coordinate suppression of the CDK2 and CDK4/6 cell cycle pathways. *Cancer Res.* 2010 Nov 15;70(22):9473–82.

Lin T, Ambasudhan R, Yuan X, Li W, Hilcove S, Abujarour R, et al. A chemical platform for improved induction of human iPSCs. *Nat Methods.* 2009 Nov;6(11):805–8.

Liu G-H, Barkho BZ, Ruiz S, Diep D, Qu J, Yang S-L, et al. Recapitulation of premature ageing with iPSCs from Hutchinson-Gilford progeria syndrome. *Nature.* 2011 Apr 14;472(7342):221–5.

Liu G-H, Ding Z, Izpisua Belmonte JC. iPSC technology to study human aging and aging-related disorders. *Curr Opin Cell Biol.* 2012a Dec;24(6):765–74.

Liu G-H, Qu J, Suzuki K, Nivet E, Li M, Montserrat N, et al. Progressive degeneration of human neural stem cells caused by pathogenic LRRK2. *Nature.* 2012b Nov 22;491(7425):603–7.

Liu H, Ye Z, Kim Y, Sharkis S, Jang Y-Y. Generation of endoderm-derived human induced pluripotent stem cells from primary hepatocytes. *Hepatology.* 2010 May;51(5):1810–9.

Liu X, Sun H, Qi J, Wang L, He S, Liu J, et al. Sequential introduction of reprogramming factors reveals a time-sensitive requirement for individual factors and a sequential EMT-MET mechanism for optimal reprogramming. *Nat Cell Biol.* 2013 Jul;15(7):829–38.

Lo Cicero A, Jaskowiak A-L, Egesipe A-L, Tournois J, Brinon B, Pitrez PR, et al. A High Throughput Phenotypic Screening reveals compounds that counteract premature osteogenic differentiation of HGPS iPS-derived mesenchymal stem cells. *Sci Rep.* 2016 14;6:34798.

Lo Cicero A, Saidani M, Allouche J, Egesipe AL, Hoch L, Bruge C, et al. Pathological modelling of pigmentation disorders associated with Hutchinson-Gilford Progeria Syndrome (HGPS) revealed an impaired melanogenesis pathway in iPS-derived melanocytes. *Sci Rep.* 2018 14;8(1):9112.

Loewer S, Cabili MN, Guttman M, Loh Y-H, Thomas K, Park IH, et al. Large intergenic non-

coding RNA-RoR modulates reprogramming of human induced pluripotent stem cells. *Nat Genet.* 2010 Dec;42(12):1113–7.

Loh Y-H, Agarwal S, Park I-H, Urbach A, Huo H, Heffner GC, et al. Generation of induced pluripotent stem cells from human blood. *Blood.* 2009 May 28;113(22):5476–9.

Lombardo C, Baronti W, Amorese G, Vistoli F, Marchetti P, Boggi U. Transplantation of the Pancreas [Internet]. MDText.com, Inc.; 2017 [cited 2019 Nov 3]. Available from: <https://www.ncbi.nlm.nih.gov/sites/books/NBK278979/>

Lu CC, Brennan J, Robertson EJ. From fertilization to gastrulation: axis formation in the mouse embryo. *Curr Opin Genet Dev.* 2001 Aug;11(4):384–92.

Lukowiak B, Vandewalle B, Riachy R, Kerr-Conte J, Gmyr V, Belaich S, et al. Identification and purification of functional human beta-cells by a new specific zinc-fluorescent probe. *J Histochem Cytochem.* 2001 Apr;49(4):519–28.

Lyon J, Manning Fox JE, Spigelman AF, Kim R, Smith N, O’Gorman D, et al. Research-Focused Isolation of Human Islets From Donors With and Without Diabetes at the Alberta Diabetes Institute IsletCore. *Endocrinology.* 2016 Feb;157(2):560–9.

Maehr R, Chen S, Snitow M, Ludwig T, Yagasaki L, Goland R, et al. Generation of pluripotent stem cells from patients with type 1 diabetes. *Proc Natl Acad Sci USA.* 2009 Sep 15;106(37):15768–73.

Maekawa M, Yamaguchi K, Nakamura T, Shibukawa R, Kodanaka I, Ichisaka T, et al. Direct reprogramming of somatic cells is promoted by maternal transcription factor Glis1. *Nature.* 2011 Jun 8;474(7350):225–9.

Maherali N, Ahfeldt T, Rigamonti A, Utikal J, Cowan C, Hochedlinger K. A high-efficiency system for the generation and study of human induced pluripotent stem cells. *Cell Stem Cell.* 2008 Sep 11;3(3):340–5.

Mali P, Ye Z, Hommond HH, Yu X, Lin J, Chen G, et al. Improved efficiency and pace of generating induced pluripotent stem cells from human adult and fetal fibroblasts. *Stem Cells.* 2008 Aug;26(8):1998–2005.

Mandai M, Watanabe A, Kurimoto Y, Hirami Y, Morinaga C, Daimon T, et al. Autologous Induced Stem-Cell-Derived Retinal Cells for Macular Degeneration. *N Engl J Med.* 2017 16;376(11):1038–46.

Mandal PK, Rossi DJ. Reprogramming human fibroblasts to pluripotency using modified mRNA. *Nat Protoc.* 2013 Mar;8(3):568–82.

Marion RM, Strati K, Li H, Tejera A, Schoeftner S, Ortega S, et al. Telomeres acquire embryonic stem cell characteristics in induced pluripotent stem cells. *Cell Stem Cell*. 2009 Feb 6;4(2):141–54.

Martin GR. Isolation of a pluripotent cell line from early mouse embryos cultured in medium conditioned by teratocarcinoma stem cells. *Proc Natl Acad Sci U S A*. 1981 Dec;78(12):7634–8.

Masui S, Nakatake Y, Toyooka Y, Shimosato D, Yagi R, Takahashi K, et al. Pluripotency governed by Sox2 via regulation of Oct3/4 expression in mouse embryonic stem cells. *Nat Cell Biol*. 2007 Jun;9(6):625–35.

Mathieu C, Gillard P, Benhalima K. Insulin analogues in type 1 diabetes mellitus: getting better all the time. *Nat Rev Endocrinol*. 2017;13(7):385–99.

Matsuoka T, Artner I, Henderson E, Means A, Sander M, Stein R. The MafA transcription factor appears to be responsible for tissue-specific expression of insulin. *Proc Natl Acad Sci USA*. 2004 Mar 2;101(9):2930–3.

McClintock D, Ratner D, Lokuge M, Owens DM, Gordon LB, Collins FS, et al. The mutant form of lamin A that causes Hutchinson-Gilford progeria is a biomarker of cellular aging in human skin. *PLoS ONE*. 2007 Dec 5;2(12):e1269.

McCracken KW, Wells JM. Molecular pathways controlling pancreas induction. *Semin Cell Dev Biol*. 2012 Aug;23(6):656–62.

McLin VA, Rankin SA, Zorn AM. Repression of Wnt/beta-catenin signaling in the anterior endoderm is essential for liver and pancreas development. *Development*. 2007 Jun;134(12):2207–17.

Medvedev SP, Grigor'eva EV, Shevchenko AI, Malakhova AA, Dementyeva EV, Shilov AA, et al. Human induced pluripotent stem cells derived from fetal neural stem cells successfully undergo directed differentiation into cartilage. *Stem Cells Dev*. 2011 Jun;20(6):1099–112.

Menasché P, Vanneaux V, Hagège A, Bel A, Cholley B, Parouchev A, et al. Transplantation of Human Embryonic Stem Cell-Derived Cardiovascular Progenitors for Severe Ischemic Left Ventricular Dysfunction. *J Am Coll Cardiol*. 2018 30;71(4):429–38.

Merani S, Shapiro AMJ. Current status of pancreatic islet transplantation. *Clin Sci*. 2006 Jun;110(6):611–25.

Merideth MA, Gordon LB, Clauss S, Sachdev V, Smith ACM, Perry MB, et al. Phenotype and course of Hutchinson-Gilford progeria syndrome. *N Engl J Med*. 2008 Feb 7;358(6):592–604.

Meshorer E, Gruenbaum Y. Gone with the Wnt/Notch: stem cells in laminopathies, progeria, and

aging. *J Cell Biol.* 2008 Apr 7;181(1):9–13.

van der Meulen T, Xie R, Kelly OG, Vale WW, Sander M, Huisin MO. Urocortin 3 marks mature human primary and embryonic stem cell-derived pancreatic alpha and beta cells. *PLoS ONE.* 2012;7(12):e52181.

Mfopou JK, Chen B, Mateizel I, Sermon K, Bouwens L. Noggin, retinoids, and fibroblast growth factor regulate hepatic or pancreatic fate of human embryonic stem cells. *Gastroenterology.* 2010 Jun;138(7):2233–45, 2245.e1-14.

Miller JD, Ganat YM, Kishinevsky S, Bowman RL, Liu B, Tu EY, et al. Human iPSC-based modeling of late-onset disease via progerin-induced aging. *Cell Stem Cell.* 2013 Dec 5;13(6):691–705.

Millman JR, Xie C, Van Dervort A, Gürtler M, Pagliuca FW, Melton DA. Generation of stem cell-derived β -cells from patients with type 1 diabetes. *Nat Commun.* 2016 10;7:11463.

Mitsui K, Tokuzawa Y, Itoh H, Segawa K, Murakami M, Takahashi K, et al. The homeoprotein Nanog is required for maintenance of pluripotency in mouse epiblast and ES cells. *Cell.* 2003 May 30;113(5):631–42.

Miyoshi N, Ishii H, Nagano H, Haraguchi N, Dewi DL, Kano Y, et al. Reprogramming of mouse and human cells to pluripotency using mature microRNAs. *Cell Stem Cell.* 2011 Jun 3;8(6):633–8.

Moretti A, Bellin M, Welling A, Jung CB, Lam JT, Bott-Flügel L, et al. Patient-specific induced pluripotent stem-cell models for long-QT syndrome. *N Engl J Med.* 2010 Oct 7;363(15):1397–409.

Moulson CL, Fong LG, Gardner JM, Farber EA, Go G, Passariello A, et al. Increased progerin expression associated with unusual LMNA mutations causes severe progeroid syndromes. *Hum Mutat.* 2007 Sep;28(9):882–9.

Nair G, Hebrok M. Islet formation in mice and men: lessons for the generation of functional insulin-producing β -cells from human pluripotent stem cells. *Curr Opin Genet Dev.* 2015 Jun;32:171–80.

Nair GG, Liu JS, Russ HA, Tran S, Saxton MS, Chen R, et al. Recapitulating endocrine cell clustering in culture promotes maturation of human stem-cell-derived β cells. *Nat Cell Biol.* 2019;21(2):263–74.

Nakatake Y, Fukui N, Iwamatsu Y, Masui S, Takahashi K, Yagi R, et al. Klf4 cooperates with Oct3/4 and Sox2 to activate the Lefty1 core promoter in embryonic stem cells. *Mol Cell Biol.* 2006 Oct;26(20):7772–82.

Nano R, Bosco D, Kerr-Conte JA, Karlsson M, Charvier S, Melzi R, et al. Human islet distribution

programme for basic research: activity over the last 5 years. *Diabetologia*. 2015 May;58(5):1138–40.

Nano R, Kerr-Conte JA, Bosco D, Karlsson M, Lavallard V, Melzi R, et al. Islets for Research: Nothing Is Perfect, but We Can Do Better. *Diabetes*. 2019 Aug;68(8):1541–3.

Narsinh KH, Jia F, Robbins RC, Kay MA, Longaker MT, Wu JC. Generation of adult human induced pluripotent stem cells using nonviral minicircle DNA vectors. *Nat Protoc*. 2011 Jan;6(1):78–88.

Nasteska D, Hodson DJ. The role of beta cell heterogeneity in islet function and insulin release. *J Mol Endocrinol*. 2018 Jul;61(1):R43–60.

Nathan DM. The Diabetes Control and Complications Trial/Epidemiology of Diabetes Interventions and Complications Study at 30 Years: Overview. *Diabetes Care*. 2014 Jan;37(1):9–16.

Nathan DM, Cleary PA, Backlund J-YC, Genuth SM, Lachin JM, Orchard TJ, et al. Intensive diabetes treatment and cardiovascular disease in patients with type 1 diabetes. *N Engl J Med*. 2005 Dec 22;353(25):2643–53.

Nathan DM, Lachin J, Cleary P, Orchard T, Brillon DJ, Backlund J-Y, et al. Intensive diabetes therapy and carotid intima-media thickness in type 1 diabetes mellitus. *N Engl J Med*. 2003 Jun 5;348(23):2294–303.

Nelson SB, Schaffer AE, Sander M. The transcription factors Nkx6.1 and Nkx6.2 possess equivalent activities in promoting beta-cell fate specification in Pdx1+ pancreatic progenitor cells. *Development*. 2007 Jul;134(13):2491–500.

Nguyen HN, Byers B, Cord B, Shcheglovitov A, Byrne J, Gujar P, et al. LRRK2 mutant iPSC-derived DA neurons demonstrate increased susceptibility to oxidative stress. *Cell Stem Cell*. 2011 Mar 4;8(3):267–80.

Nichols J, Zevnik B, Anastassiadis K, Niwa H, Klewe-Nebenius D, Chambers I, et al. Formation of pluripotent stem cells in the mammalian embryo depends on the POU transcription factor Oct4. *Cell*. 1998 Oct 30;95(3):379–91.

Nissan X, Blondel S, Navarro C, Maury Y, Denis C, Girard M, et al. Unique preservation of neural cells in Hutchinson- Gilford progeria syndrome is due to the expression of the neural-specific miR-9 microRNA. *Cell Rep*. 2012 Jul 26;2(1):1–9.

Nostro MC, Sarangi F, Ogawa S, Holtzinger A, Corneo B, Li X, et al. Stage-specific signaling through TGFβ family members and WNT regulates patterning and pancreatic specification of

human pluripotent stem cells. *Development*. 2011 Mar;138(5):861–71.

Nostro MC, Sarangi F, Yang C, Holland A, Elefanty AG, Stanley EG, et al. Efficient generation of NKX6-1+ pancreatic progenitors from multiple human pluripotent stem cell lines. *Stem Cell Reports*. 2015 Apr 14;4(4):591–604.

Okita K, Matsumura Y, Sato Y, Okada A, Morizane A, Okamoto S, et al. A more efficient method to generate integration-free human iPS cells. *Nat Methods*. 2011 May;8(5):409–12.

Okita K, Nakagawa M, Hyenjong H, Ichisaka T, Yamanaka S. Generation of mouse induced pluripotent stem cells without viral vectors. *Science*. 2008 Nov 7;322(5903):949–53.

Olbrot M, Rud J, Moss LG, Sharma A. Identification of beta-cell-specific insulin gene transcription factor RIPE3b1 as mammalian MafA. *Proc Natl Acad Sci USA*. 2002 May 14;99(10):6737–42.

Olive M, Harten I, Mitchell R, Beers JK, Djabali K, Cao K, et al. Cardiovascular pathology in Hutchinson-Gilford progeria: correlation with the vascular pathology of aging. *Arterioscler Thromb Vasc Biol*. 2010 Nov;30(11):2301–9.

Omole AE, Fakoya AOJ. Ten years of progress and promise of induced pluripotent stem cells: historical origins, characteristics, mechanisms, limitations, and potential applications. *PeerJ*. 2018;6:e4370.

Onder TT, Kara N, Cherry A, Sinha AU, Zhu N, Bernt KM, et al. Chromatin-modifying enzymes as modulators of reprogramming. *Nature*. 2012 Mar 4;483(7391):598–602.

Osafune K, Caron L, Borowiak M, Martinez RJ, Fitz-Gerald CS, Sato Y, et al. Marked differences in differentiation propensity among human embryonic stem cell lines. *Nat Biotechnol*. 2008 Mar;26(3):313–5.

Pagliuca FW, Millman JR, Gürtler M, Segel M, Van Dervort A, Ryu JH, et al. Generation of functional human pancreatic β cells in vitro. *Cell*. 2014 Oct 9;159(2):428–39.

Park I-H, Arora N, Huo H, Maherali N, Ahfeldt T, Shimamura A, et al. Disease-specific induced pluripotent stem cells. *Cell*. 2008 Sep 5;134(5):877–86.

Pathak S, Regmi S, Gupta B, Pham TT, Yong CS, Kim JO, et al. Engineered islet cell clusters transplanted into subcutaneous space are superior to pancreatic islets in diabetes. *FASEB J*. 2017;31(11):5111–21.

Petersen MBK, Azad A, Ingvorsen C, Hess K, Hansson M, Grapin-Botton A, et al. Single-Cell Gene Expression Analysis of a Human ESC Model of Pancreatic Endocrine Development Reveals Different Paths to β -Cell Differentiation. *Stem Cell Reports*. 2017 10;9(4):1246–61.

Petersen MBK, Gonçalves CAC, Kim YH, Grapin-Botton A. Recapitulating and Deciphering

Human Pancreas Development From Human Pluripotent Stem Cells in a Dish. *Curr Top Dev Biol.* 2018;129:143–90.

Picanço-Castro V, Russo-Carbolante E, Reis LCJ, Fraga AM, de Magalhães DAR, Orellana MD, et al. Pluripotent reprogramming of fibroblasts by lentiviral mediated insertion of SOX2, C-MYC, and TCL-1A. *Stem Cells Dev.* 2011 Jan;20(1):169–80.

Polak M, Bouchareb-Banaei L, Scharfmann R, Czernichow P. Early pattern of differentiation in the human pancreas. *Diabetes.* 2000 Feb;49(2):225–32.

Polonsky KS, Given BD, Hirsch LJ, Tillil H, Shapiro ET, Beebe C, et al. Abnormal patterns of insulin secretion in non-insulin-dependent diabetes mellitus. *N Engl J Med.* 1988 May 12;318(19):1231–9.

Prigione A, Fauler B, Lurz R, Lehrach H, Adjaye J. The senescence-related mitochondrial/oxidative stress pathway is repressed in human induced pluripotent stem cells. *Stem Cells.* 2010 Apr;28(4):721–33.

Qu X, Liu T, Song K, Li X, Ge D. Induced Pluripotent Stem Cells Generated from Human Adipose-Derived Stem Cells Using a Non-Viral Polycistronic Plasmid in Feeder-Free Conditions. *PLOS ONE.* 2012 Oct 26;7(10):e48161.

Rais Y, Zviran A, Geula S, Gafni O, Chomsky E, Viukov S, et al. Deterministic direct reprogramming of somatic cells to pluripotency. *Nature.* 2013 Oct 3;502(7469):65–70.

Rajaei B, Shamsara M, Amirabad LM, Massumi M, Sanati MH. Pancreatic Endoderm-Derived From Diabetic Patient-Specific Induced Pluripotent Stem Cell Generates Glucose-Responsive Insulin-Secreting Cells. *J Cell Physiol.* 2017 Oct;232(10):2616–25.

Ramachandran K, Peng X, Bokvist K, Stehno-Bittel L. Assessment of re-aggregated human pancreatic islets for secondary drug screening. *Br J Pharmacol.* 2014 Jun;171(12):3010–22.

Ramalingam S, London V, Kandavelou K, Cebotaru L, Guggino W, Civin C, et al. Generation and genetic engineering of human induced pluripotent stem cells using designed zinc finger nucleases. *Stem Cells Dev.* 2013 Feb 15;22(4):595–610.

Ravassard P, Hazhouz Y, Pechberty S, Bricout-Neveu E, Armanet M, Czernichow P, et al. A genetically engineered human pancreatic β cell line exhibiting glucose-inducible insulin secretion. *J Clin Invest.* 2011 Sep 1;121(9):3589–97.

Rawal S, Harrington S, Williams SJ, Ramachandran K, Stehno-Bittel L. Long-term cryopreservation of reaggregated pancreatic islets resulting in successful transplantation in rats. *Cryobiology.* 2017;76:41–50.

Rezania A, Bruin JE, Arora P, Rubin A, Batushansky I, Asadi A, et al. Reversal of diabetes with insulin-producing cells derived in vitro from human pluripotent stem cells. *Nat Biotechnol.* 2014 Nov;32(11):1121–33.

Rezania A, Bruin JE, Riedel MJ, Mojibian M, Asadi A, Xu J, et al. Maturation of human embryonic stem cell-derived pancreatic progenitors into functional islets capable of treating pre-existing diabetes in mice. *Diabetes.* 2012 Aug;61(8):2016–29.

Rezania A, Bruin JE, Xu J, Narayan K, Fox JK, O’Neil JJ, et al. Enrichment of human embryonic stem cell-derived NKX6.1-expressing pancreatic progenitor cells accelerates the maturation of insulin-secreting cells in vivo. *Stem Cells.* 2013 Nov;31(11):2432–42.

Rooman I, Schuit F, Bouwens L. Effect of vascular endothelial growth factor on growth and differentiation of pancreatic ductal epithelium. *Lab Invest.* 1997 Feb;76(2):225–32.

Rosero S, Bravo-Egana V, Jiang Z, Khuri S, Tsinoremas N, Klein D, et al. MicroRNA signature of the human developing pancreas. *BMC Genomics.* 2010 Sep 22;11:509.

Rosler ES, Fisk GJ, Ares X, Irving J, Miura T, Rao MS, et al. Long-term culture of human embryonic stem cells in feeder-free conditions. *Dev Dyn.* 2004 Feb;229(2):259–74.

Russ HA, Parent AV, Ringler JJ, Hennings TG, Nair GG, Shveygert M, et al. Controlled induction of human pancreatic progenitors produces functional beta-like cells in vitro. *EMBO J.* 2015 Jul 2;34(13):1759–72.

Saha K, Jaenisch R. Technical challenges in using human induced pluripotent stem cells to model disease. *Cell Stem Cell.* 2009 Dec 4;5(6):584–95.

Salisbury RJ, Blaylock J, Berry AA, Jennings RE, De Krijger R, Piper Hanley K, et al. The window period of NEUROGENIN3 during human gestation. *Islets.* 2014;6(3):e954436.

Saponaro C, Gmyr V, Thévenet J, Moerman E, Delalleau N, Pasquetti G, et al. The GLP1R Agonist Liraglutide Reduces Hyperglucagonemia Induced by the SGLT2 Inhibitor Dapagliflozin via Somatostatin Release. *Cell Rep.* 2019 Aug 6;28(6):1447-1454.e4.

Scaffidi P, Misteli T. Reversal of the cellular phenotype in the premature aging disease Hutchinson-Gilford progeria syndrome. *Nat Med.* 2005 Apr;11(4):440–5.

Scaffidi P, Misteli T. Lamin A-dependent nuclear defects in human aging. *Science.* 2006 May 19;312(5776):1059–63.

Scharfmann R, Staels W, Albagli O. The supply chain of human pancreatic β cell lines. *J Clin Invest.* 2019 Sep 3;129(9):3511–20.

Schöler HR, Hatzopoulos AK, Balling R, Suzuki N, Gruss P. A family of octamer-specific proteins

present during mouse embryogenesis: evidence for germline-specific expression of an Oct factor. *EMBO J.* 1989 Sep;8(9):2543–50.

Schröder D, Wegner U, Besch W, Zühlke H. Characterization of pseudo-islets formed from pancreatic islet cell suspensions of neonatal rats. *Mol Cell Endocrinol.* 1983 Oct;32(2–3):179–93.

Schulz TC, Young HY, Agulnick AD, Babin MJ, Baetge EE, Bang AG, et al. A scalable system for production of functional pancreatic progenitors from human embryonic stem cells. *PLoS ONE.* 2012;7(5):e37004.

Schwartz SD, Regillo CD, Lam BL, Elliott D, Rosenfeld PJ, Gregori NZ, et al. Human embryonic stem cell-derived retinal pigment epithelium in patients with age-related macular degeneration and Stargardt's macular dystrophy: follow-up of two open-label phase 1/2 studies. *Lancet.* 2015 Feb 7;385(9967):509–16.

Sebastiani G, Valentini M, Grieco GE, Ventriglia G, Nigi L, Mancarella F, et al. MicroRNA expression profiles of human iPSCs differentiation into insulin-producing cells. *Acta Diabetol.* 2017 Mar;54(3):265–81.

Shapiro AM, Lakey JR, Ryan EA, Korbitt GS, Toth E, Warnock GL, et al. Islet transplantation in seven patients with type 1 diabetes mellitus using a glucocorticoid-free immunosuppressive regimen. *N Engl J Med.* 2000 Jul 27;343(4):230–8.

Sharma A, Diecke S, Zhang WY, Lan F, He C, Mordwinkin NM, et al. The role of SIRT6 protein in aging and reprogramming of human induced pluripotent stem cells. *J Biol Chem.* 2013 Jun 21;288(25):18439–47.

Shi Y, Inoue H, Wu JC, Yamanaka S. Induced pluripotent stem cell technology: a decade of progress. *Nat Rev Drug Discov.* 2017a;16(2):115–30.

Shi Z-D, Lee K, Yang D, Amin S, Verma N, Li QV, et al. Genome Editing in hPSCs Reveals GATA6 Haploinsufficiency and a Genetic Interaction with GATA4 in Human Pancreatic Development. *Cell Stem Cell.* 2017b 04;20(5):675-688.e6.

Shook D, Keller R. Mechanisms, mechanics and function of epithelial-mesenchymal transitions in early development. *Mech Dev.* 2003 Nov;120(11):1351–83.

Shumaker DK, Dechat T, Kohlmaier A, Adam SA, Bozovsky MR, Erdos MR, et al. Mutant nuclear lamin A leads to progressive alterations of epigenetic control in premature aging. *Proc Natl Acad Sci USA.* 2006 Jun 6;103(23):8703–8.

Silva J, Nichols J, Theunissen TW, Guo G, van Oosten AL, Barrandon O, et al. Nanog is the gateway to the pluripotent ground state. *Cell.* 2009 Aug 21;138(4):722–37.

Singec I, Crain AM, Hou J, Tobe BT, Talantova M, Winkquist AA, et al. Quantitative Analysis of Human Pluripotency and Neural Specification by In-Depth (Phospho)Proteomic Profiling. *Stem Cell Reports*. 2016 13;7(3):527–42.

Slack JM. Developmental biology of the pancreas. *Development*. 1995 Jun;121(6):1569–80.

Smith A. Formative pluripotency: the executive phase in a developmental continuum. *Development*. 2017 01;144(3):365–73.

Sola-Carvajal A, Revêchon G, Helgadóttir HT, Whisenant D, Hagblom R, Döhla J, et al. Accumulation of Progerin Affects the Symmetry of Cell Division and Is Associated with Impaired Wnt Signaling and the Mislocalization of Nuclear Envelope Proteins. *J Invest Dermatol*. 2019 May 23;

Southard SM, Kotipatruni RP, Rust WL. Generation and selection of pluripotent stem cells for robust differentiation to insulin-secreting cells capable of reversing diabetes in rodents. *PLoS ONE*. 2018;13(9):e0203126.

Strandgren C, Revêchon G, Sola-Carvajal A, Eriksson M. Emerging candidate treatment strategies for Hutchinson-Gilford progeria syndrome. *Biochem Soc Trans*. 2017 15;45(6):1279–93.

Studer L, Vera E, Cornacchia D. Programming and Reprogramming Cellular Age in the Era of Induced Pluripotency. *Cell Stem Cell*. 2015 Jun 4;16(6):591–600.

Suhr ST, Chang EA, Tjong J, Alcasid N, Perkins GA, Goissis MD, et al. Mitochondrial rejuvenation after induced pluripotency. *PLoS ONE*. 2010 Nov 23;5(11):e14095.

Swartz FJ, Carstens PH. An islet of Langerhans located within the epithelium of a human pancreatic duct. *Histol Histopathol*. 1986 Apr;1(2):111–7.

Tachibana M, Amato P, Sparman M, Gutierrez NM, Tippner-Hedges R, Ma H, et al. Human Embryonic Stem Cells Derived by Somatic Cell Nuclear Transfer. *Cell*. 2013 Jun 6;153(6):1228–38.

Takahashi K, Okita K, Nakagawa M, Yamanaka S. Induction of pluripotent stem cells from fibroblast cultures. *Nat Protoc*. 2007;2(12):3081–9.

Takahashi K, Yamanaka S. Induction of pluripotent stem cells from mouse embryonic and adult fibroblast cultures by defined factors. *Cell*. 2006 Aug 25;126(4):663–76.

Takahashi K, Yamanaka S. A decade of transcription factor-mediated reprogramming to pluripotency. *Nat Rev Mol Cell Biol*. 2016 Mar;17(3):183–93.

Takahashi Y, Sekine K, Kin T, Takebe T, Taniguchi H. Self-Condensation Culture Enables Vascularization of Tissue Fragments for Efficient Therapeutic Transplantation. *Cell Rep*. 2018

08;23(6):1620–9.

Takeuchi H, Rünger TM. Longwave UV light induces the aging-associated progerin. *J Invest Dermatol.* 2013 Jul;133(7):1857–62.

Taylor CJ, Peacock S, Chaudhry AN, Bradley JA, Bolton EM. Generating an iPSC bank for HLA-matched tissue transplantation based on known donor and recipient HLA types. *Cell Stem Cell.* 2012 Aug 3;11(2):147–52.

Teo AKK, Lim CS, Cheow LF, Kin T, Shapiro JA, Kang N-Y, et al. Single-cell analyses of human islet cells reveal de-differentiation signatures. *Cell Death Discov.* 2018 Dec;4:14.

Thatava T, Kudva YC, Edukulla R, Squillace K, De Lamo JG, Khan YK, et al. Inpatient variations in type 1 diabetes-specific iPSC cell differentiation into insulin-producing cells. *Mol Ther.* 2013 Jan;21(1):228–39.

Thomson JA, Itskovitz-Eldor J, Shapiro SS, Waknitz MA, Swiergiel JJ, Marshall VS, et al. Embryonic stem cell lines derived from human blastocysts. *Science.* 1998 Nov 6;282(5391):1145–7.

Tiso N, Filippi A, Pauls S, Bortolussi M, Argenton F. BMP signalling regulates anteroposterior endoderm patterning in zebrafish. *Mech Dev.* 2002 Oct;118(1–2):29–37.

Tiyaboonchai A, Cardenas-Diaz FL, Ying L, Maguire JA, Sim X, Jobaliya C, et al. GATA6 Plays an Important Role in the Induction of Human Definitive Endoderm, Development of the Pancreas, and Functionality of Pancreatic β Cells. *Stem Cell Reports.* 2017 14;8(3):589–604.

Travis WD, Rush W, Flieder DB, Falk R, Fleming MV, Gal AA, et al. Survival analysis of 200 pulmonary neuroendocrine tumors with clarification of criteria for atypical carcinoid and its separation from typical carcinoid. *Am J Surg Pathol.* 1998 Aug;22(8):934–44.

Tremblay KD, Zaret KS. Distinct populations of endoderm cells converge to generate the embryonic liver bud and ventral foregut tissues. *Dev Biol.* 2005 Apr 1;280(1):87–99.

Trounson A, DeWitt ND. Pluripotent stem cells progressing to the clinic. *Nat Rev Mol Cell Biol.* 2016 Mar;17(3):194–200.

Tsubooka N, Ichisaka T, Okita K, Takahashi K, Nakagawa M, Yamanaka S. Roles of Sall4 in the generation of pluripotent stem cells from blastocysts and fibroblasts. *Genes Cells.* 2009 Jun;14(6):683–94.

Turner M, Leslie S, Martin NG, Peschanski M, Rao M, Taylor CJ, et al. Toward the development of a global induced pluripotent stem cell library. *Cell Stem Cell.* 2013 Oct 3;13(4):382–4.

Ullrich NJ, Gordon LB. Hutchinson-Gilford progeria syndrome. *Handb Clin Neurol.*

2015;132:249–64.

Unternaehrer JJ, Zhao R, Kim K, Cesana M, Powers JT, Ratanasirintrao S, et al. The epithelial-mesenchymal transition factor SNAIL paradoxically enhances reprogramming. *Stem Cell Reports*. 2014 Nov 11;3(5):691–8.

Utikal J, Maherali N, Kulalert W, Hochedlinger K. Sox2 is dispensable for the reprogramming of melanocytes and melanoma cells into induced pluripotent stem cells. *J Cell Sci*. 2009 Oct 1;122(Pt 19):3502–10.

Vantyghem M-C, Chetboun M, Gmyr V, Jannin A, Espiard S, Le Mapihan K, et al. Ten-Year Outcome of Islet Alone or Islet After Kidney Transplantation in Type 1 Diabetes: A Prospective Parallel-Arm Cohort Study. *Diabetes Care*. 2019a Nov;42(11):2042–9.

Vantyghem M-C, de Koning EJP, Pattou F, Rickels MR. Advances in β -cell replacement therapy for the treatment of type 1 diabetes. *Lancet*. 2019b 05;394(10205):1274–85.

Velazco-Cruz L, Song J, Maxwell KG, Goedegebuure MM, Augsornworawat P, Hogrebe NJ, et al. Acquisition of Dynamic Function in Human Stem Cell-Derived β Cells. *Stem Cell Reports*. 2019 Feb 12;12(2):351–65.

Vera E, Bosco N, Studer L. Generating Late-Onset Human iPSC-Based Disease Models by Inducing Neuronal Age-Related Phenotypes through Telomerase Manipulation. *Cell Rep*. 2016 18;17(4):1184–92.

Verstraeten VLRM, Broers JLV, van Steensel MAM, Zinn-Justin S, Ramaekers FCS, Steijlen PM, et al. Compound heterozygosity for mutations in LMNA causes a progeria syndrome without prelamin A accumulation. *Hum Mol Genet*. 2006 Aug 15;15(16):2509–22.

Villasenor A, Chong DC, Cleaver O. Biphasic Ngn3 expression in the developing pancreas. *Dev Dyn*. 2008 Nov;237(11):3270–9.

Vlahos AE, Cober N, Sefton MV. Modular tissue engineering for the vascularization of subcutaneously transplanted pancreatic islets. *Proc Natl Acad Sci USA*. 2017 29;114(35):9337–42.

Wang Q, Xu X, Li J, Liu J, Gu H, Zhang R, et al. Lithium, an anti-psychotic drug, greatly enhances the generation of induced pluripotent stem cells. *Cell Res*. 2011a Oct;21(10):1424–35.

Wang W, Yang J, Liu H, Lu D, Chen X, Zenonos Z, et al. Rapid and efficient reprogramming of somatic cells to induced pluripotent stem cells by retinoic acid receptor gamma and liver receptor homolog 1. *Proc Natl Acad Sci USA*. 2011b Nov 8;108(45):18283–8.

Wang Y, Adjaye J. A cyclic AMP analog, 8-Br-cAMP, enhances the induction of pluripotency in

human fibroblast cells. *Stem Cell Rev Rep*. 2011 Jun;7(2):331–41.

Wang Y, Xu Z, Jiang J, Xu C, Kang J, Xiao L, et al. Endogenous miRNA sponge lincRNA-RoR regulates Oct4, Nanog, and Sox2 in human embryonic stem cell self-renewal. *Dev Cell*. 2013 Apr 15;25(1):69–80.

Wang Y-K, Zhu W-W, Wu M-H, Wu Y-H, Liu Z-X, Liang L-M, et al. Human Clinical-Grade Parthenogenetic ESC-Derived Dopaminergic Neurons Recover Locomotive Defects of Nonhuman Primate Models of Parkinson's Disease. *Stem Cell Reports*. 2018 10;11(1):171–82.

Warren L, Manos PD, Ahfeldt T, Loh Y-H, Li H, Lau F, et al. Highly efficient reprogramming to pluripotency and directed differentiation of human cells with synthetic modified mRNA. *Cell Stem Cell*. 2010 Nov 5;7(5):618–30.

Warren L, Ni Y, Wang J, Guo X. Feeder-free derivation of human induced pluripotent stem cells with messenger RNA. *Sci Rep*. 2012;2:657.

Weaver JD, Headen DM, Aquart J, Johnson CT, Shea LD, Shirwan H, et al. Vasculogenic hydrogel enhances islet survival, engraftment, and function in leading extrahepatic sites. *Science Advances*. 2017 Jun 1;3(6):e1700184.

Wei Z, Yang Y, Zhang P, Andrianakos R, Hasegawa K, Lyu J, et al. Klf4 interacts directly with Oct4 and Sox2 to promote reprogramming. *Stem Cells*. 2009 Dec;27(12):2969–78.

Wells JM, Melton DA. Early mouse endoderm is patterned by soluble factors from adjacent germ layers. *Development*. 2000 Apr;127(8):1563–72.

Westacott MJ, Farnsworth NL, St Clair JR, Poffenberger G, Heintz A, Ludin NW, et al. Age-Dependent Decline in the Coordinated [Ca²⁺] and Insulin Secretory Dynamics in Human Pancreatic Islets. *Diabetes*. 2017;66(9):2436–45.

Wilmut I, Leslie S, Martin NG, Peschanski M, Rao M, Trounson A, et al. Development of a global network of induced pluripotent stem cell haplobanks. *Regen Med*. 2015;10(3):235–8.

Woltjen K, Michael IP, Mohseni P, Desai R, Mileikovsky M, Hämäläinen R, et al. piggyBac transposition reprograms fibroblasts to induced pluripotent stem cells. *Nature*. 2009 Apr 9;458(7239):766–70.

Worringer KA, Rand TA, Hayashi Y, Sami S, Takahashi K, Tanabe K, et al. The let-7/LIN-41 pathway regulates reprogramming to human induced pluripotent stem cells by controlling expression of prodifferentiation genes. *Cell Stem Cell*. 2014 Jan 2;14(1):40–52.

Xu X, Browning VL, Odorico JS. Activin, BMP and FGF pathways cooperate to promote endoderm and pancreatic lineage cell differentiation from human embryonic stem cells. *Mech Dev*.

2011 Dec;128(7–10):412–27.

Xuan S, Borok MJ, Decker KJ, Battle MA, Duncan SA, Hale MA, et al. Pancreas-specific deletion of mouse Gata4 and Gata6 causes pancreatic agenesis. *J Clin Invest*. 2012 Oct;122(10):3516–28.

Yan Y, Bejoy J, Xia J, Griffin K, Guan J, Li Y. Cell population balance of cardiovascular spheroids derived from human induced pluripotent stem cells. *Sci Rep*. 2019 Feb 4;9(1):1295.

Yang P, Wang Y, Chen J, Li H, Kang L, Zhang Y, et al. RCOR2 is a subunit of the LSD1 complex that regulates ESC property and substitutes for SOX2 in reprogramming somatic cells to pluripotency. *Stem Cells*. 2011 May;29(5):791–801.

Ye L, Chang JC, Lin C, Qi Z, Yu J, Kan YW. Generation of induced pluripotent stem cells using site-specific integration with phage integrase. *Proc Natl Acad Sci USA*. 2010 Nov 9;107(45):19467–72.

Yoshihara E, Wei Z, Lin CS, Fang S, Ahmadian M, Kida Y, et al. ERR γ Is Required for the Metabolic Maturation of Therapeutically Functional Glucose-Responsive β Cells. *Cell Metab*. 2016 Apr 12;23(4):622–34.

Yoshioka N, Gros E, Li H-R, Kumar S, Deacon DC, Maron C, et al. Efficient generation of human iPSCs by a synthetic self-replicative RNA. *Cell Stem Cell*. 2013 Aug 1;13(2):246–54.

You W-P, Henneberg M. Type 1 diabetes prevalence increasing globally and regionally: the role of natural selection and life expectancy at birth. *BMJ Open Diabetes Res Care*. 2016;4(1):e000161.

Young HE, Duplaa C, Romero-Ramos M, Chesselet M-F, Vourc'h P, Yost MJ, et al. Adult reserve stem cells and their potential for tissue engineering. *Cell Biochem Biophys*. 2004;40(1):1–80.

Young SG, Yang SH, Davies BSJ, Jung H-J, Fong LG. Targeting protein prenylation in progeria. *Sci Transl Med*. 2013 Feb 6;5(171):171ps3.

Yu J, Hu K, Smuga-Otto K, Tian S, Stewart R, Slukvin II, et al. Human Induced Pluripotent Stem Cells Free of Vector and Transgene Sequences. *Science*. 2009 May 8;324(5928):797–801.

Yu J, Vodyanik MA, Smuga-Otto K, Antosiewicz-Bourget J, Frane JL, Tian S, et al. Induced pluripotent stem cell lines derived from human somatic cells. *Science*. 2007 Dec 21;318(5858):1917–20.

Yu Y, Gamble A, Pawlick R, Pepper AR, Salama B, Toms D, et al. Bioengineered human pseudoislets form efficiently from donated tissue, compare favourably with native islets in vitro and restore normoglycaemia in mice. *Diabetologia*. 2018;61(9):2016–29.

Zeng H, Guo M, Zhou T, Tan L, Chong CN, Zhang T, et al. An Isogenic Human ESC Platform for Functional Evaluation of Genome-wide-Association-Study-Identified Diabetes Genes and Drug

Discovery. *Cell Stem Cell*. 2016 01;19(3):326–40.

Zeng X. Human embryonic stem cells: mechanisms to escape replicative senescence? *Stem Cell Rev*. 2007 Dec;3(4):270–9.

Zeng X, Rao MS. Human embryonic stem cells: long term stability, absence of senescence and a potential cell source for neural replacement. *Neuroscience*. 2007 Apr 14;145(4):1348–58.

Zhang P, Andrianakos R, Yang Y, Liu C, Lu W. Kruppel-like factor 4 (Klf4) prevents embryonic stem (ES) cell differentiation by regulating Nanog gene expression. *J Biol Chem*. 2010 Mar 19;285(12):9180–9.

Zhao Y, Yin X, Qin H, Zhu F, Liu H, Yang W, et al. Two supporting factors greatly improve the efficiency of human iPSC generation. *Cell Stem Cell*. 2008 Nov 6;3(5):475–9.

Zhao Z, Yu R, Yang J, Liu X, Tan M, Li H, et al. Maxadilan prevents apoptosis in iPS cells and shows no effects on the pluripotent state or karyotype. *PLoS ONE*. 2012;7(3):e33953.

Zhou Q, Law AC, Rajagopal J, Anderson WJ, Gray PA, Melton DA. A multipotent progenitor domain guides pancreatic organogenesis. *Dev Cell*. 2007 Jul;13(1):103–14.

Zhou W, Freed CR. Adenoviral gene delivery can reprogram human fibroblasts to induced pluripotent stem cells. *Stem Cells*. 2009 Nov;27(11):2667–74.

Zhu S, Li W, Zhou H, Wei W, Ambasudhan R, Lin T, et al. Reprogramming of human primary somatic cells by OCT4 and chemical compounds. *Cell Stem Cell*. 2010 Dec 3;7(6):651–5.

Zorn AM, Wells JM. Vertebrate endoderm development and organ formation. *Annu Rev Cell Dev Biol*. 2009;25:221–51.

Zuellig RA, Cavallari G, Gerber P, Tschopp O, Spinass GA, Moritz W, et al. Improved physiological properties of gravity-enforced reassembled rat and human pancreatic pseudo-islets. *J Tissue Eng Regen Med*. 2017;11(1):109–20.